

ADSORPTION STUDIES OF DYEING  
NATURAL DYES FROM LOCAL RESOURCES  
ONTO BAMBOO YARN



TENGGU KHAMANUR AZMA BINTI TG.  
MOHD ZAMRI

Doctor of Philosophy

UNIVERSITI MALAYSIA PAHANG

## UNIVERSITI MALAYSIA PAHANG

### DECLARATION OF THESIS AND COPYRIGHT

Author's Full Name : Tengku Khamanur Azma Binti Tg. Mohd Zamri

Date of Birth : 20 July 1988

Title : Adsorption Studies of Dyeing Natural Dyes from Local Resources onto Bamboo Yarn

Academic Session : \_\_\_\_\_

I declare that this thesis is classified as:

- CONFIDENTIAL (Contains confidential information under the Official Secret Act 1997)\*
- RESTRICTED (Contains restricted information as specified by the organization where research was done)\*
- OPEN ACCESS I agree that my thesis to be published as online open access (Full Text)

I acknowledge that Universiti Malaysia Pahang reserve the right as follows:

1. The Thesis is the Property of Universiti Malaysia Pahang
2. The Library of Universiti Malaysia Pahang has the right to make copies for the purpose of research only.
3. The Library has the right to make copies of the thesis for academic exchange.

Certified by:

\_\_\_\_\_  
(Student's Signature)

\_\_\_\_\_  
(Supervisor's Signature)

880720-11-5470  
Date:

\_\_\_\_\_  
Prof. Dato' Dr. Zularisam Bin Abd Wahid  
Date:

NOTE : \* If the thesis is CONFIDENTIAL or RESTRICTED, please attach with the letter page 2 from the organization with the period and reasons for confidentiality or restriction.

## THESIS DECLARATION LETTER (OPTIONAL)

Librarian,  
Perpustakaan Universiti Malaysia Pahang,  
Universiti Malaysia Pahang,  
Lebuhraya Tun Razak,  
26300, Gambang, Kuantan.

Sir,

### CLASSIFICATION OF THESIS AS RESTRICTED

Please be informed that the following thesis is classified as RESTRICTED for a period of three (3) years from the date of this letter. The reasons for this classification are as listed below.

Author's Name	Tengku Khamanur Azma Binti Tg. Mohd Zamri
Thesis Title	Adsorption Studies of Dyeing Natural Dyes from Local Resources onto Bamboo Yarn
Reasons	(i)  (ii)  (iii)

Thank You.

Sincerely yours,

---

(Supervisor's Signature)

Date:

Stamp:

Notes : This letter should be written by the supervisor, addressed to Perpustakaan Universiti Malaysia Pahang and a copy attached to the thesis.

## SUPERVISOR'S DECLARATION

We hereby declare that We have checked this thesis and in our opinion, this thesis is adequate in terms of scope and quality for the award of the degree of Doctor of Philosophy in Chemical Engineering.

---

(Supervisor's Signature)

Full Name : Prof. Dato' Dr. Zularisam Bin Abd Wahid

Position : Dean of Faculty Engineering Technology

Date :

---

(Co-supervisor's Signature)

Full Name : Prof Datin Dr. Mimi Sakinah Binti Abd Munaim

Position : Lecturer

Date :

### **STUDENT'S DECLARATION**

I hereby declare that the work in this thesis is based on my original work except for quotations and citation which have been duly acknowledged. I also declare that it has not been previously or concurrently submitted for any other degree at Universiti Malaysia Pahang or any other institutions.

---

(Student's Signature)

Full Name : TENGKU KHAMANUR AZMA BINTI TG. MOHD ZAMRI ID

ID Number : PKC 13014

Date :



UMP

ADSORPTION STUDIES OF DYEING NATURAL DYES FROM LOCAL  
RESOURCES ONTO BAMBOO YARN



TENGGU KHAMANUR AZMA BINTI TG. MOHD ZAMRI

Thesis submitted in fulfillment of the requirements  
for the award of the degree of  
Doctor of Philosophy

Faculty of Engineering Technology

UNIVERSITI MALAYSIA PAHANG

DECEMBER 2017

## ACKNOWLEDGEMENT

Thanks to the Almighty Allah, for giving me the strength and the courage to finished this research. I would also like to thank my husband Mohamed Syukri Bin Abd Manaf, and my parents for their support and prayers throughout the process in completing this thesis.

I am grateful and would like to express my sincere gratitude to my supervisor Prof. Dr. Dato' Zularisam Bin Ab Wahid and Co-supervisor Prof. Dr. Datin Mimi Sakinah Bt Abdul Munaim for her germinal ideas, invaluable guidance, continuous encouragement and constant support in making this business plan possible. They have always impressed me with her outstanding professional conduct, strong conviction of science and belief that the Doctor of Philosophy in Chemical Engineering is only a start of a lifelong learning experience.

Last but not least, I would like to thank to all of the staff of the Chemical and Natural Resources Engineering Department, Technology and Engineering Department, UMP, who give a hand to me in many ways and giving me a pleasant and unforgettable experience in the UMP. Many special thanks go to my friends, especially Siti Norsita Binti Mohd Rawi for their excellent co-operation, inspirations and support during the completion of this research and thesis. Thank You.



UMP

## ABSTRAK

Sifat pewarna sintetik yang mengancam alam sekitar menyebabkan keperluan mendesak terhadap penggunaan pewarna semulajadi sebagai pengganti bagi pewarna sintetik semakin mendapat perhatian dalam industri tekstil masa kini. Dengan ini, penggunaan pewarna semulajadi memberi kepentingan kepada pelbagai industri seperti industri tekstil, kulit, kertas dan plastik bagi tujuan mewarnakan produk-produk keluaran mereka. Air sisa buangan daripada industri-industri ini adalah punca utama kepada pencemaran air. Oleh itu amatlah penting bagi industri-industri ini mencari alternatif kepada penggunaan pewarna sintetik dan fiber sintetik yang menyebabkan pencemaran sumber air dengan menggantikan penggunaan pewarna sintetik dan fiber sintetik kepada pewarna dan fiber semulajadi yang lebih mudah, efisien, dan murah dengan cara mengekstrak pewarna semulajadi kepada fiber semulajadi seperti Benang Buluh. Disebabkan itu penyelidikan ini tertumpu kepada empat objektif utama, yang mana objektif pertama dan kedua adalah untuk mengoptimumkan pengekstrakkan warna semulajadi daripada sumber semulajadi tempatan terpilih, dan mengoptimumkan proses mewarnakan Benang Buluh dengan pewarna semulajadi dengan menggunakan OFAT dan RSM. Dalam penyelidikan ini sumber warna semulajadi yang dipilih untuk diekstrak adalah Bunga Telang, Buah Naga Merah, dan Kunyit Hidup. Objektif ketiga pula adalah untuk menghuraikan tentang penyerapan pewarna secara kinetik dan penyerapan isoterma diantara pigmen warna yang diekstrak daripada pewarna semulajadi keatas Benang Buluh dengan mengaplikasikan kaedah isoterma Langmuir, Freundlich, Temkin dan Dubinin-Radushkevich. Manakala penyelidikan tentang kinetik penyerapan pewarna semulajadi ke atas Benang Buluh adalah dengan menggunakan kaedah Pseudo-first order dan kaedah Pseudo-second order. Objektif yang keempat adalah untuk membandingkan perbezaan ciri-ciri antara benang buluh yang telah diwarnakan dengan pewarna semula jadi dan yang tidak diwarnakan dengan menggunakan FTIR dan SEM. Keputusan keadaan yang optimum bagi tujuan pengekstrakkan warna pada Bunga Telang bagi faktor suhu, masa dan SLR adalah masing-masing adalah 55 °C, 15 minit, dan 0.10 g/mL; manakala bagi pengekstrakkan warna pada kunyit hidup adalah masing-masing pada 55 °C, 25 minit, dan 0.12 g/mL. Penyelidikan menemukan keadaan yang optimum bagi tujuan rendaman itu adalah seperti berikut; untuk Bunga Telang, Buah Naga dan kunyit masing-masing adalah kepekatan cecair rendaman, masa rendaman dan pH rendaman pewarna semulajadi masing-masing adalah 0.083 g/mL, 60 minit dan 6.5. 0.10 g/mL, 90 minit, pH 3 dan 70 °C, 0.101 g/mL, 60 minit, pH 4.1 dan 67 °C. Disamping itu, analisa untuk penyerapan kinetik bagi penyerapan pigmen berwarna iaitu Betasianin didalam Buah Naga Merah dan kurkumin didalam Kunyit Hidup keatas Benang Buluh adalah pseudo-second order kinetik model. Manakala Langmuir Isoterma hanya menunjukkan kesesuaian untuk penyerapan Betasianin keatas Benang Buluh, Freundlich Isoterma menunjukkan kesesuaian dengan penyerapan antosianin dan Temkin Isoterma untuk kurkumin ke atas Benang Buluh. Berdasarkan keputusan penyelidikan yang diperolehi dengan kiraan menggunakan kaedah isoterma dan kinetic model, pewarnaan Bunga Telang keatas Benang buluh adalah disebabkan oleh Penyerapan fizikal manakala pewarnaan keatas Benang Buluh oleh Buah Naga merah dan Kunyit Hidup adalah melalui Peyerapan Kimia. Analisa dengan menggunakan FTIR juga menunjukkan pewarna semulajadi yang dipilih juga membentuk ikatan kimia yang lemah dengan Benang buluh yang mana menyebabkan perubahan kimia yang amat sedikit antara pewarna dan Benang Buluh. Kesimpulan daripada penyelidikan ini kesemua objektif yang dinyatakan telah tercapai dan kesemua pewarna semulajadi yang dipilih sesuai digunakan keatas Benang Buluh.



## ABSTRACT

Recently, natural dyes play an important role in the textile industry due to the needs of substituting synthetic dyes that are deleterious to the environment. This means; the use of natural dyes does benefits their entire user which attribute in numerous industries, such as textiles, leather, paper, and plastics, to colour their final products. Effluents from such industries are major sources of water pollution. Hence, it is important to find alternative to replacing the synthetic dyes as well as synthetic fibers by promoting the simple, efficient, and inexpensive ways to extract the natural dyes and dyeing it onto bamboo yarn (BY). This research is navigated by four prime objectives, in which the first objective is to optimize the extraction of selected natural dyes from local resources. The second objective is to optimize the dyeing of natural dyes on the BY. These optimizations were done via OFAT and central composite design (CCD) in RSM with the aid of Design Expert Version 8.0.6. The selected natural dyes were extracted from Blue Butterfly Pea Flower (BBPF), Red Dragon Fruit Peel (RDFP), and Turmeric. Meanwhile, the third objective is to evaluate the dyeing adsorption kinetically and adsorption isotherm between colorant pigments extracted from selected natural dyes onto BY. The adsorption of natural dyes on BY had been studied with the application of Langmuir, Freundlich, Temkin, and Dubinin-Radushkevich isotherm models. The kinetic studies of dyeing natural dyes onto BY were investigated by using Pseudo-first order model and Pseudo-second order model. Finally, the last objective is to characterize the colorant pigments extracted from selected natural dyes, undyed and dyed yarns which are BY through the analyses of FTIR spectroscopy and SEM. As a result, this study had determined that the optimum extraction of BBPF dye for temperature, time, and SLR are 55 °C, 15 minutes and 0.10 g/mL, respectively; while turmeric dye extraction at 55 °C, 25 minutes and 0.12 g/mL, respectively. Other than that, the optimum conditions of dyeing BY with BBPF dye for dye bath concentration, dyeing time, and dye bath pH had been 0.083 g/mL, 60 minutes and 6.5, respectively. On the other hand, the optimized conditions of dyeing of RDFP dye and turmeric dye on BY for dye bath concentration, dyeing time, dye bath pH, and dyeing temperature were 0.10 g/mL and 0.101 g/mL, 90 minutes and 60 minutes, pH 3 and pH 4.1, 70 °C and 67 °C, respectively. In addition, the data retrieved from the experimental runs displayed a good linear fit, as reflected from the pseudo-first order kinetic model for adsorption of anthocyanin in BBPF dye onto BY. Furthermore, pseudo-second order kinetic model had been fit for the adsorption of the colorant pigments of betacyanin (RDFP) and curcumin (turmeric) onto BY. Meanwhile, Langmuir isotherm was fit only for betacyanin adsorption onto BY, whereas Freundlich isotherm and Temkin isotherm for anthocyanin and curcumin adsorption onto BY respectively. Based on the results of the best isotherm model and kinetic model, the dyeing of BBPF dye on BY was controlled by physical adsorption while dyeing of RDFP dye and turmeric dye on BY were both controlled by chemisorption. FTIR analysis showed that the selected natural dyes were formed weak bonds on BY, resulting in minimal chemical changes. As a conclusion, all the objectives outlined in this study have been successfully achieved and all natural dyes that were selected in this study were compatible with BY.

## TABLE OF CONTENT

<b>DECLARATION</b>	
<b>TITLE PAGE</b>	<b>i</b>
<b>ACKNOWLEDGEMENT</b>	<b>ii</b>
<b>ABSTRAK</b>	<b>iii</b>
<b>ABSTRACT</b>	<b>iv</b>
<b>TABLE OF CONTENT</b>	<b>v</b>
<b>LIST OF TABLES</b>	<b>xi</b>
<b>LIST OF FIGURES</b>	<b>xiii</b>
<b>LIST OF SYMBOLS</b>	<b>xvi</b>
<b>LIST OF ABBREVIATION</b>	<b>xvii</b>
<b>CHAPTER 1 INTRODUCTION</b>	<b>1</b>
1.1 Research Background	1
1.2 Problem Statement	2
1.3 Research Objectives	5
1.4 Research Roadmap	6
1.5 Scope of the Study	7
1.6 Significance of the Study	7
1.7 Thesis Outline	9
1.8 Summary	9
<b>CHAPTER 2 LITERATURE REVIEW</b>	<b>11</b>
2.1 Introduction	11

2.2	Extraction	11
2.2.1	Types of Extraction	12
2.2.2	Water Extraction	14
2.2.3	Natural Dye	15
2.2.4	Optimization Strategies	36
2.3	Dyeing	39
2.3.1	Fibre	40
2.3.2	Mordanting	47
2.3.3	Optimization Strategies	51
2.4	Adsorption	54
2.4.1	Principal of adsorption	57
2.4.2	Desorption	59
2.5	Characterization	60
2.6	Summary	60
<b>CHAPTER 3 MATERIALS AND METHODOLOGY</b>		<b>62</b>
3.1	Introduction	62
3.2	Materials	63
3.2.1	Chemicals and Reagents	63
3.2.2	Blue Butterfly Pea Flower (BBPF)	63
3.2.3	Red Dragon Fruit Peel (RDFP)	64
3.2.4	Turmeric	64
3.2.5	Bamboo Yarn (BY)	64
3.3	Operational Framework	64
3.3.1	Phase 1: Extraction of natural dyes	64
3.3.2	Phase 2: Dyeing of natural dyes on BY	65

3.3.3	Phase 3: Adsorption study of dyeing natural dyes onto BY	65
3.3.4	Phase 4: Characterization of samples	65
3.4	Extraction of Natural Dyes	68
3.4.1	Preparation of Anthocyanin Extract from BBPF	68
3.4.2	Preparation of Betacyanin Extract from RDFP	68
3.4.3	Preparation of Curcumin Extract from Turmeric	69
3.4.4	OFAT of Extraction Process	69
3.4.5	RSM of Extraction Process	70
3.5	Dyeing of Natural Dyes on Bamboo Yarn (BY)	71
3.5.1	Sample Preparation	71
3.5.2	Mordanting Process	72
3.5.3	OFAT of Dyeing Process	72
3.5.4	RSM of Dyeing Process	75
3.6	Adsorption Study of Dyeing Natural Dyes on Bamboo Yarn (BY)	76
3.6.1	Equilibrium time	76
3.6.2	Adsorption isotherm	76
3.6.3	Adsorption isotherm models	77
3.6.4	Kinetic study	81
3.6.5	Desorption Process	82
3.6.6	Calculations of anthocyanin pigments	82
3.6.7	Calculations of betacyanin pigments	83
3.6.8	Calculations of curcumin pigments	83
3.6.9	Adsorptive capacity	84
3.7	Characterization of the Samples	84
3.7.1	Fourier Transform Infra-Red (FTIR) Spectroscopy Analysis	84
3.7.2	Scanning Electron Microscope (SEM) Analysis	84

3.8	Summary	84
<b>CHAPTER 4 EXTRACTION OF NATURAL DYES</b>		<b>85</b>
4.1	Introduction	85
4.2	Design of Parameters for Natural Dye Extraction	85
4.2.1	Effect of solid liquid ratio (SLR)	86
4.2.2	Effect of extraction temperature	87
4.2.3	Effect of extraction time	90
4.3	Optimization of Natural Dyes Extraction by RSM	91
4.3.1	Extraction of BBPF dye	92
4.3.2	Extraction of turmeric dye	93
4.3.3	Diagnosis of model properties	94
4.3.4	Optimization of process condition	100
4.3.5	Interaction effect of variables	106
4.3.6	Model validation	115
4.3.7	Confirmation	117
<b>CHAPTER 5 DYEING OF NATURAL DYES ON BAMBOO YARN (BY)</b>		<b>119</b>
5.1	Introduction	119
5.2	Design of Parameter for Dyeing of Natural Dye on Bamboo Yarn(BY)	119
5.2.1	Effect of dyeing time	120
5.2.2	Effect of dyeing temperature	122
5.2.3	Effect of dye bath concentration	124
5.2.4	Effect of dye bath pH	125
5.3	Optimization of Natural Dyes Dyeing on Bamboo Yarn (BY) via RSM	128
5.3.1	Dyeing of BBPF dye on BY	129

5.3.2	Dyeing of RDFP dye on BY	131
5.3.3	Dyeing of turmeric dye on BY	133
5.3.4	Diagnosis of model properties	135
5.3.5	Optimization of process condition	142
5.3.6	Interaction effect of variable	151
5.3.7	Model validation	161
5.3.8	Confirmation	162
<b>CHAPTER 6 ADSORPTION STUDY ON DYEING OF NATURAL DYES ONTO BAMBOO YARN</b>		<b>164</b>
6.1	Introduction	164
6.2	Effect of Different Parameters of Adsorption Processes of Natural Dyes on BY	165
6.2.1	Effect of Time	165
6.2.2	Effect of Dye Bath Concentrations	166
6.3	Adsorption Kinetics Modelling	168
6.4	Adsorption Isotherm	174
6.4.1	Langmuir isotherm	174
6.4.2	Freundlich isotherm	176
6.4.3	Temkin isotherm	177
6.4.4	Dubinin-Radushkevich isotherm	178
6.5	Error Analysis	180
6.5.1	The Sum of the Squares of the Errors (SSE)	180
6.5.2	Residual Root Mean Square Error (RSME)	180
6.5.3	Chi-square ( $\chi^2$ ) Tests	180
6.5.4	Non-linear analysis	180
6.6	Desorption Study on Dyeing of Natural Dyes onto Bamboo Yarn (BY)	183

<b>CHAPTER 7 CHARACTERIZATION OF MATERIALS</b>	<b>184</b>
7.1 Introduction	184
7.2 Spectral Analysis of Extracted Natural Dyes	184
7.2.1 BBPF dye	184
7.2.2 RDFP dye	185
7.2.3 Turmeric dye	186
7.3 Spectral Analysis of Dyeing Natural Dyes on Bamboo Yarn (BY)	187
7.4 Morphology Analysis	198
<b>CHAPTER 8 GENERAL CONCLUSIONS AND RECOMMENDATIONS FOR FUTURE WORK</b>	<b>200</b>
8.1 INTRODUCTION	200
8.2 General Conclusions	200
8.3 Recommendations for Future Work	202
<b>REFERENCES</b>	<b>204</b>
<b>APPENDIX A LIST OF CHEMICALS AND REAGENTS</b>	<b>216</b>
<b>APPENDIX B CALIBRATION CURVE FOR STANDARD</b>	<b>217</b>
<b>APPENDIX C EXPERIMENTAL SET UP</b>	<b>220</b>

## LIST OF TABLES

Table 2.1	Literature for types of extraction and solvents used	13
Table 2.2	Natural sources for dye from various journals	20
Table 2.3	Types of fibres used in the dyeing process by various researchers	42
Table 2.4	Literature of mordanting methods and the types of mordants used for dyeing	51
Table 2.5	Literature on adsorption studies using various isotherms, adsorbents, and adsorbates	56
Table 3.1	OFAT for Extraction of BBPF and Turmeric	70
Table 3.2	Ranges and levels of independent variables involved in CCD for extraction of natural dyes	71
Table 3.3	OFAT for Dyeing of BBPF, RDFP, and Turmeric on BY	74
Table 3.4	Ranges and levels of independent variables involved in CCD for dyeing of natural dyes on BY	76
Table 3.5	Water and Dye ratio for Dilution Factor	77
Table 3.6	The linearized equation transformed and intercept for isotherms model	81
Table 4.1	Constraint for Extraction Conditions for BBPF	92
Table 4.2	The Actual Level of Independent Variables for BBPF	92
Table 4.3	Constraint for Extraction Conditions for Turmeric	93
Table 4.4	The Actual Level of Independent Variables for Turmeric	93
Table 4.5	Analysis of variance (ANOVA) for extraction of BBPF dye	102
Table 4.6	Analysis of variance (ANOVA) for extraction of turmeric dye	105
Table 4.7	The results of verification process of BBPF dye extraction	116
Table 4.8	The results of verification process of turmeric dye extraction	116
Table 4.9	The results of confirmation process of BBPF dye extraction	118
Table 4.10	The results of confirmation process of turmeric dye extraction	118
Table 5.1	Constraint for the dyeing of blue dye from BBPF on BY conditions	129
Table 5.2	The actual level of independent variables for the dyeing of blue dye from BBPF on BY	130
Table 5.3	Constraint for dyeing of red dye from RDFP on BY conditions	131
Table 5.4	The actual level of independent variables for dyeing of red dye from RDFP on BY	132
Table 5.5	Constraint for dyeing of yellow dye from turmeric on BY conditions	133



Table 5.6	The actual level of independent variables for dyeing of yellow dye from turmeric on BY	134
Table 5.7	Analysis of variance (ANOVA) for dyeing of BBPF dye on BY	144
Table 5.8	Analysis of variance (ANOVA) for dyeing of BBPF dye on BY	147
Table 5.9	Analysis of variance (ANOVA) for dyeing of turmeric dye on BY	150
Table 5.10	The results of verification process of dyeing of BBPF dye on BY	162
Table 5.11	The results of verification process of dyeing of RDFP dye on BY	162
Table 5.12	The results of verification process of dyeing of turmeric dye on BY	162
Table 5.13	The results of confirmation process of dyeing of BBPF dye on BY	163
Table 5.14	The results of confirmation process of dyeing of RDFP dye on BY	163
Table 5.15	The results of confirmation process of dyeing of turmeric dye on BY	163
Table 6.1	Kinetic parameters for colorant pigments adsorption onto BY	172
Table 6.2	Langmuir adsorption isotherm parameters for adsorption of colorant pigments onto BY	176
Table 6.3	Freundlich adsorption isotherm parameters for adsorption of colorant pigments onto BY	177
Table 6.4	Temkin adsorption isotherm parameters for adsorption of colorant pigments onto BY	178
Table 6.5	Dubin-Radushkevich adsorption isotherm parameters for adsorption of colorant pigments onto BY	179
Table 6.6	Comparison of non-linear regression of the Squares of the errors (SSE), Residual root mean square error (RMSE), Chi-square test, $\chi^2$ and coefficient of determination, $R^2$	182
Table 6.7	Anthocyanin, betacyanin, and curcumin contents in water after the desorption process	183

## LIST OF FIGURES

Figure 1.1	A roadmap of present research	6
Figure 2.1	Blue Butterfly Pea Flower (BBPF)	22
Figure 2.2	Common chemical structure of anthocyanin	26
Figure 2.3	Chemical structures of cyanidin 3-glucoside in BBPF	27
Figure 2.4	Red Dragon Fruit (RDF)	28
Figure 2.5	Chemical composition of betacyanin in RDFP	30
Figure 2.6	Rhizome of Turmeric	32
Figure 2.7	Chemical structure for curcumin in turmeric	36
Figure 2.8	Bamboo yarn (BY) produced from 100% of bamboo fibre	43
Figure 2.9	Chemical structure for cellulose BY	47
Figure 3.1	Experimental flowchart for dyeing of natural dyes from BBPF, RDFP and Turmeric on BY.	63
Figure 3.2	Schematic diagram of operational framework of this study	67
Figure 4.1	Effect of SLR on the extraction of the BBPF dye and turmeric dye at temperature (60 °C), time (10 minutes), and pH (4.2 and 8.5 respectively)	87
Figure 4.2	Effect of temperature on the extraction of the BBPF dye and turmeric dye at SLR at 0.050 g/mL, 10 minutes, and pH (4.2 and 8.5 respectively)	89
Figure 4.3	Degradation of anthocyanin mechanism at temperature higher than 70 °C	89
Figure 4.4	Effect of time on the extraction of BBPF dye and turmeric dye	91
Figure 4.5	Normal probability plot of for BBPF extraction	96
Figure 4.6	Plot of residuals versus predicted responses of BBPF extraction	97
Figure 4.7	Normal probability plot for turmeric extraction	98
Figure 4.8	Plot of residuals versus predicted responses of turmeric extraction	99
Figure 4.9	Effects of temperature and time on extraction of BBPF dye: (a) interaction and (b) response surface graph	109
Figure 4.10	Effects of temperature and SLR on extraction of BBPF dye: (a) interaction and (b) response surface graph	110
Figure 4.11	Effects of time and SLR on extraction of BBPF dye: (a) interaction and (b) response surface graph	111
Figure 4.12	Effects of temperature and time on extraction of turmeric dye: (a) interaction and (b) response surface graph	112
Figure 4.13	Effects of temperature and SLR on extraction of turmeric dye: (a) interaction and (b) response surface graph	113

Figure 4.14	Effects of time and SLR on extraction of turmeric dye: (a) interaction and (b) response surface graph	114
Figure 5.1	Effect of time on dyeing of BBPF, RDFP and turmeric dye on BY	122
Figure 5.2	Effect of temperature on dyeing of BBPF, RDFP and turmeric dye on BY	123
Figure 5.3	Effect of dyebath concentration on dyeing of BBPF, RDFP and turmeric dye on BY	125
Figure 5.4	Effect of BBPF, RDFP and turmeric dye bath pH on BY	128
Figure 5.5	Normal probability plots for dyeing of BBPF dye on BY	136
Figure 5.6	Normal probability plots for dyeing of RDFP dye on BY	137
Figure 5.7	Normal probability plots for dyeing of turmeric dye on BY	138
Figure 5.8	Residuals versus predicted plot for dyeing of BBPF dye on BY	139
Figure 5.9	Residuals versus predicted plots for dyeing of RDFP dye on BY	140
Figure 5.10	Residuals versus predicted plots for dyeing of turmeric dye on BY	141
Figure 5.11	Effects of dye bath concentration and time on dyeing of BBPF dye on BY: (a) interaction and (b) response surface graph	154
Figure 5.12	Effects of dye bath concentration and dye bath pH on dyeing of BBPF dye on BY: (a) interaction and (b) response surface graph	155
Figure 5.13	Effects of time and dye bath pH on dyeing of RDFP dye on BY: (a) interaction and (b) response surface graph	156
Figure 5.14	Effects of temperature and dye bath pH on dyeing of RDFP dye on BY: (a) interaction and (b) response surface graph	157
Figure 5.15	Effects of dye bath concentration and dyebath pH on dyeing of turmeric dye on BY: (a) interaction and (b) response surface graph	158
Figure 5.16	Effects of time and dye bath pH on dyeing of turmeric dye on BY: (a) interaction and (b) response surface graph	159
Figure 6.1	Amount of colorant pigments adsorbed onto BY at different time intervals	166
Figure 6.2	Amount of colorant pigments adsorbed onto BY at equilibrium time and various dilution factors	167
Figure 6.3	Pseudo-first order kinetic model for colorant pigments adsorption onto BY at 60 °C for both anthocyanin and curcumin, while 90 °C for betacyanin	170
Figure 6.4	Pseudo-second order kinetic model for colorant pigments adsorption onto BY at 60 °C for both anthocyanin and curcumin, while 90 °C for betacyanin.	171
Figure 6.5	Intraparticle diffusion model for colorant pigments adsorption onto BY	173

Figure 6.6	Langmuir isotherm on adsorption of colorant pigments onto BY	175
Figure 6.7	Freundlich isotherm for adsorption of colorant pigments onto BY	177
Figure 6.8	Temkin isotherm on adsorption of colorant pigments onto BY (a) Anthocyanin, (b) Betacyanin, and (c) Curcumin	178
Figure 6.9	Dubin- Radushkevich isotherm on adsorption of colorant pigments onto BY (a) Anthocyanin, (b) Betacyanin, and (c) Curcumin	179
Figure 7.1	FTIR spectra for BBPF dye	185
Figure 7.2	FTIR spectra for RDFP dye	186
Figure 7.3	FTIR spectra for turmeric dye	187
Figure 7.4	The FTIR spectra of untreated BY and treated BY using distilled water	189
Figure 7.5	The FTIR spectra of blue dyed BY and undyed BY	191
Figure 7.6	The FTIR spectra of pink dyed BY and undyed BY	192
Figure 7.7	The FTIR spectra of yellow dyed BY and undyed BY	193
Figure 7.8	The FTIR spectra of post-mordanted blue dyed BY and undyed BY	195
Figure 7.9	The FTIR spectra of post-mordanted pink dyed BY and undyed BY	196
Figure 7.10	The FTIR spectra of post-mordanted yellow dyed BY and undyed BY	197
Figure 7.11	SEM images of the samples (a) untreated BY and (b) treated BY	198
Figure 7.12	Optical images (column 1) and SEM micrographs (column 2) of BY (a) undyed BY, (b) BBPF dye-BY, (c) RDFP dye-BY and (d) Turmeric dye-BY	199

## LIST OF SYMBOLS

mg	milligram
g	gram
nm	nano metre
$\mu\text{m}$	micro metre
mL	millilitre
1/min	per minute
$\text{mg}/\text{m}^3$	milligram per cubic metre
mg/g	milligram per gram
mg/mL	milligram per millilitre
$\mu\text{g}/\text{g}$	microgram per gram
$\mu\text{g}/\text{mL}$	microgram per millilitre
kg	kilogram
g/mol	g per mol
$^{\circ}\text{C}$	Degree celcius
%	Percent
$q_e$	Adsorption capacity
$C_o$	Initial concentration dye adsorbed on BY
$C_e$	Equilibrium concentration dye adsorbed on BY
MW	Molecular weight
DF	Dilution factor
W	Weight of BY
$q_{\text{max}}$	Maximum adsorption capacity
V	Volume
A	Temperature
B	Time
C	Solid Liquid Ratio/Concentration
D	Dye bath pH
Y	Response
$K_F$	Freundlich constant
$K_L$	Langmuir constant
$K_T$	Temkin constant
$k_1$	Pseudo first order constant
$k_2$	Pseudo second order constant
$E_{\text{DR}}$	Mean free energy of D-R

## LIST OF ABBREVIATION

ANOVA	Analysis of Variance
ALUM	Aluminum Sulfate
BF	Bamboo Fibre
BY	Bamboo Yarn
BBPF	Blue Butterfly Pea Flower
CCD	Central Composite Design
DBY	Dyed Bamboo Yarn
FTIR	Fourier Transform Infra-Red
MBY	Mordanted Bamboo Yarn
OFAT	One-Factor-At-A-Time-
RDFP	Red Dragon Fruit Peel
RSM	Response Surface Method
RSME	Residual Root Mean Square Error
SEM	Scanning Electron Microscope
SLR	Solid Liquid Ratio
SSE	Squares of the Error
UV-VIS	Ultra Violet Visible



UMP

## CHAPTER 1

### INTRODUCTION

#### 1.1 Research Background

At present, colorants are widely used for a variety of applications, such as in food industry, textile industry, and pharmaceutical industry. Moreover, the use of natural dyes has been increasing with the growing demand for environmental-friendly products in the textile industry. Furthermore, the interest in the use of natural dye has been growing rapidly due to the result of stringent environmental standards imposed by many nations in response to toxic and allergic reactions associated with harmful synthetic dyes. On top of that, many studies concerning synthetic dyes have proven their deleterious chemical release as allergic, carcinogenic, and detrimental to human health (Grover and Patni, 2011). Hence, non-allergic, non-toxic, and eco-friendly natural dyes on textiles have been sought due to the increased environmental awareness in order to avoid the use of hazardous synthetic dyes (Samanta and Agarwal, 2009). In fact, the development activities in the textile industry have focused on the utilisation of renewable and biodegradable resources, as well as environmentally-sound manufacturing processes in textiles (Erdumlu and Ozipek, 2008). Natural dyes are obtained from any part of plants and they are eco-friendly as they do not create any environmental problems at the stage of production or use, maintain ecological balance, and have beautiful attractive shades. Thus, the use of natural dyes have replaced and minimized on a significant manner on the amount of toxic effluents resulting from the dye process (Samanta and Agarwal, 2009).

Moreover, the growing demand of natural dyes in the textile industry is parallel to the increment in the development of suitable efficient technique, optimum extraction conditions, and optimum dyeing conditions. In fact, a growing demand has spurred in developing suitable and efficient extraction techniques for natural dyes from plants materials

(Rahman et al., 2013). Besides, natural colorants are obtained from plant, animals or mineral sources with or without chemical treatment.

The most commonly available raw materials for natural dyes are extracted from various plant parts indispensable for survival. Flowers are dispensable and have the most colourful parts, but unfortunately, have not been used extensively (Sinha et al., 2012). One of the latest developments in new fibre researches is the use of bamboo fibre in various textile products that have found its way for usage in construction materials, decorating items, furniture, and high performance composite materials for years (Erdumlu and Ozipek, 2008). The demands related to textiles vary from year-to-year with the ever-changing fashion, especially when consumers dictate and demand for different types of fibres. With that, increase in the global demand for textile fibres has been expected to continue not only due to increase in the world population, but also due to the standards of living. Therefore, the focus of fibre research has shifted towards the exploration of new fibres and their combinations with the older ones (Ahmad et al., 2012). As such, the characteristics and the usage of bamboo fibre in various applications have been widely investigated; especially studies concerning regenerated bamboo fibre for textile applications, which are rather limited (Erdumlu and Ozipek, 2008).

As the production of natural dyes in the textile industry is a high value product with rapid growing market potential that can reduce operational and production costs of the industry, research for better extraction and dyeing processes of natural dyes is essential. As such, this study investigated the optimum conditions for extraction and dyeing processes in order to achieve optimum extraction of dyes and adsorption onto fibre.

## **1.2 Problem Statement**

Colours play an important role in influencing consumers, as they can tempt and attract one in purchasing goods, especially those with quality colours. Colours also can be one of the factors of marketing technique for manufacturers as they have been widely used in numerous industries, such as cosmetics, pharmaceutical, foods, and textile, to name a few. In the textile industry, colours are usually used in the dyeing process. Dyes can be divided into natural dye and synthetic dye, where the natural dye is obtained from extraction of any



part of plants, animals, and mineral sources. Moreover, the production of synthetic dyes is highly not recommended due to their harmful effects upon the environment, as well as one's health. There are two issues will be discussed in the problem statement where the first problem is the need to replace the synthetic dyes and the second problem is the need to find new alternative of natural fibre or yarn or fabrics.

Textile wastewater is complex and has highly variable mixture of many polluting substances, including dye (Boujaady et al., 2013). These dyes and pigments contain aromatic rings in their structures, thus turning them into toxic, non-biodegradable, carcinogenic, and mutagenic substances for both aquatic systems and human health (Boujaady et al., 2013). Although synthetic dyes are widely available at an economical price and come in a wide variety of colours; these dyes, however, cause skin allergy and toxic wastes that are harmful to the human (Samanta and Agarwal, 2009). As such, natural dyes and pigments have emerged as an important alternative to potentially harmful synthetic dyes (Tamil et al., 2013). Therefore, the production of natural dyes in the textile industry is definitely needed in order to overcome multiple environmental and consumer issues. Besides, natural dyes comprise of colorants that are mostly eco-friendly, biodegradable, non-toxic, and less allergenic, when compared to those synthetic (Tamil et al., 2013 and Sivakumar et al., 2009), hence emerging as a significant alternative to substitute harmful synthetic dyes (Tamil et al., 2013). In addition, natural dyes are comprised of colorants obtained from animal or vegetable substances without involving any chemical process, which is an important aspect for some sensitive applications. In fact, the release of harmful toxic chemicals from substrates during usage has attracted worldwide attention, such as EU and REACH (Sivakumar et al., 2009). Furthermore, the low availability and the high processing cost of natural colouring substances have surfaced as some reasons for the prevention of these products from becoming popular. Moreover, the attempts to overcome these problems have mainly focused on the discovery of newer sources, especially from by-products of farming and forestry, as well as valorisation of several wastes from the food and beverage industry, in order to extract the colouring substances to be used as natural dyes for textile dyeing. The idea of extracting colours from natural dyes is interesting because the raw materials are abundant, cheap and renewable (Haddar et al., 2014). Furthermore, since the advent of widely available and cheaper synthetic dyes in 1856 with moderate to excellent colour fastness properties; the use

of natural dyes with poor to moderate wash and light fastness declined largely. However, recently, a growing interest on the application of natural dyes on natural fibres has been noted due to worldwide environmental awareness (Samanta and Agarwal, 2009). Thus, in order to better control its quality, measurement, and appearance; colour stability needs to be observed and improved, especially on the aspect of natural colorant.

Additionally, researches to enhance the eco-friendliness of textile products have generally concentrated on wet processing of textile substrates to produce dyed and finished fabrics with minimal use of chemicals, water, and energy (Tausif et al., 2015). In fact, interest in renewable resource based on fibres has seen an increase in the world demand for textile fibres, thus directing towards exploration of new fibres (Ahmad et al., 2012). Moreover, the growing demand for more comfortable, healthier, and environmental-friendly products (Erdumlu and Ozipek, 2008) cannot be dismissed. Natural fibre has sparked immense interest due to their environmental-friendly and sustainable attributes (Kumar et al., 2016). In relation to that, bamboo has antibacterial and antifungal effects with ecologic and low cost production (Pinho et al., 2010). Furthermore, as bamboo fibre appears to be better, softer, has similar texture to silk, and dries quickly; the use of bamboo fibre as an alternative of other natural fibres benefits the environment due to the less dye used, thus consequently, limits the production of waste (Tausif et al., 2015).

In this study, the raw materials used to produce natural dyes are Blue Butterfly Pea Flower (BBPF), Red Dragon Fruit Peel (RDFP), and Turmeric. There is no doubt that BBPF, RDFP, and Turmeric do possess the ability of producing good quality natural dyes, but problem arises when the exact ratio of the concentration for each natural resource used in this study and water is unknown to ensure maximum adsorption process onto Bamboo Yarn (BY). The increment in the worldwide population seems to be parallel to the demand for textile production of apparel and interior textiles. In addition, the worldwide production of cotton has reached its limit due to land and productive constraints. Meanwhile, the production of polyester is bound to consumption of oil, thus its worldwide availability has decreased. Therefore, the interest in renewable resource based on fibres has been increasing. As such, Bamboo Yarn (BY) had been selected in this research because it is a new natural resource and studies in the area of BY dyeing properties are rather limited. Moreover, many

researchers only examined and improved several feature, for instance, characteristics and properties, structural variation, mechanical properties, extraction of fibres, chemical modification, and thermal properties (Lin et al., 2010; Tausif et al., 2015; Erdumlu and Ozipek, 2008; Demiroz et al., 2008; Majumdar and Pol, 2014 and Wang et al., 2015). Besides, although BY is relatively new, it is a very popular fibre that has been manufactured and applied worldwide.

Fundamental studies on adsorption kinetics and thermodynamics of dyeing processes are important for understanding the dyeing mechanisms and improving dyeing performance of natural dyes on various textile materials. Recently, lot of investigations have been undertaken on dyeing and functional finishing of textile materials along with the evaluations of adsorption studies in term of thermodynamics and kinetic parameters (Tayebi et al., 2015; Shen et al., 2014; Tayade and Adivarekar, 2013; Zhou et al., 2015 and Shabbir et al., 2016). Pathiraja, (2014) have been stated in their research, the kinetics and mechanisms are important for process control in the dye adsorption process because they lead to information and knowledge on the factors that affect the reaction rate and the interactions that occur between the adsorbent and adsorbate. However, the knowledge and information of adsorption selected natural dyes on BY are very limited and not been systematically studied. For this reason, present research has been investigated the application of selected natural dyes on BY with preliminary emphasis on adsorption and kinetic aspects in order to understand the dyeing mechanism of selected natural dyes on BY. Thus, this research was proposed models on describing the adsorption system of anthocyanin, betacyanin and curcumin pigments extracted from BBPD, RDFP and turmeric on BY based on fundamental knowledge.

### **1.3 Research Objectives**

The overall objective of this research is to optimize the extraction and the dyeing of natural dyes onto BY, and then followed by adsorption study. The specific objectives of this research are listed below:

- i. To optimize the extraction of selected natural from local resources conditions in order to maximize the colorant pigments recovery.

- ii. To optimize the dyeing conditions in order to maximize the percent of dye uptake during the process of dyeing natural dyes on BY.
- iii. To evaluate the dyeing adsorption by kinetically and adsorption isotherm between colorant pigments extracted from selected natural dyes onto BY.
- iv. To characterize the colorant pigments extracted from selected natural dyes, undyed and dyed BY.

#### 1.4 Research Roadmap

This study concentrates on the extraction of natural dyes extracted from BBPF, RDFP, and Turmeric, inclusive of dyeing them onto BY. Therefore, this research has focus on four major phases: extraction, dyeing, adsorption studies (kinetic, adsorption isotherm, and desorption) and characterization of the samples. A roadmap of this research is illustrated in Figure 1.1.

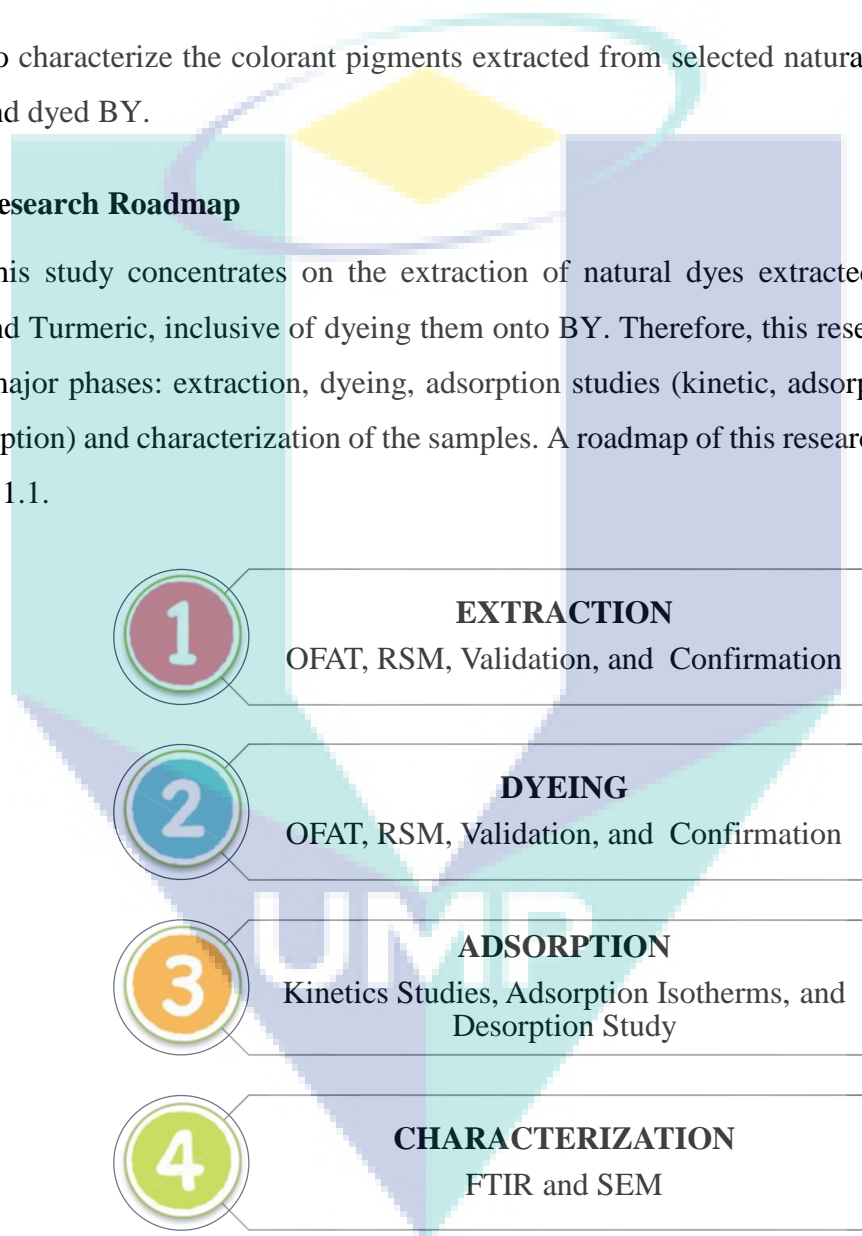


Figure 1.1 A roadmap of present research

## 1.5 Scope of the Study

In order to achieve the objectives outlined in this study, the following scope of the research has been identified and performed:

- i. To extract the anthocyanin, betacyanin and curcumin pigment from BBPF, RDFP, and Turmeric, respectively by water extraction.
- ii. The effective ranges of extraction condition factors of Temperature, Solid Liquid Ratio (SLR), pH and Time were determined using OFAT method for BBPF and Turmeric.
- iii. The optimization of extraction conditions were determined via Response Surface Method (RSM) using Design Expert V8.0.6 for BBPF and Turmeric.
- iv. The effective ranges of dyeing condition factors of Temperature, Dye bath Concentration, Dye bath pH and Time were determined using OFAT method.
- v. The optimization of dyeing conditions were determined via Response Surface Method (RSM) using Design Expert V8.0.6.
- vi. The adsorption behaviour during dyeing process was analyzed using Langmuir, Freundlich, Temkin and Dubinin-Radushkevich isotherm models.
- vii. The controlling mechanism of the adsorption process were examined using pseudo-first-order and pseudo-second order equations.
- viii. The characterizations of the extracted natural dyes, undyed and dyed of BY were performing a qualitative analysis using Scanning Electron Microscope (SEM) and Fourier Transform Infrared (FTIR).

## 1.6 Significance of the Study

At present, natural dyes play an important role in the textile industry specially to substitute synthetic dyes that have caused numerous environmental issues. This means; the development of natural dyes benefits all parties for its user-friendly attribute in the dyeing industry. As such, the study had successfully explored and captured some natural plants from

which dyes could be extracted and applied to selected textile fabrics. The study also plays a distinctive role in providing beneficial information to the textile and food industries, Art lecturers, students, and scholars. In addition, the study generates awareness towards unexplored plant dyes and finally, serves as a reference material to other research work. Moreover, the use of natural sources that derive from trees, leaves or fruit waste can be used as a good dye material. The use of these sources in obtaining natural dyes and natural fibres for the dyeing process is '2E' friendly, i.e. economic and environmental. Additionally, waste from the extraction of getting natural dyes can be transformed into organic fertilizer. Besides, the use of a wide range of pH and varied mordant generates the production of unlimited colour ranges for dyes. Therefore, the natural dye industry has begun gaining attention from worldwide due to the increasing demand for natural dye.

Traditionally, the extraction of natural dyes from plant materials is done by soaking or boiling method that requires longer extraction time, higher temperature, and higher water consumption. Extraction of colorant using the boiling method normally produces a small amount of yield. The low yield of natural dyes is a factor that limits the use of natural dyes, in comparison to synthetic dyes. Hence, a growing demand for developing suitable extraction technique has been noted for more efficient and effective extraction of natural textile dyes (Rahman et al., 2013). Hence, optimization of extraction and dyeing of natural dyes onto fibre are essential in order to maximize the quality and the quantity of natural dye extracted and dyed fibre, which is BY in this study, through the application of OFAT, and followed by optimization via RSM with Design Expert V8.0.6.

Adsorption is a process that has been widely used in the dyeing process. Recently, endless investigations have been undertaken on dyeing and functional finishing of textile materials, along with evaluation of thermodynamics and kinetic parameters (Rather et al., 2016; Tayebi et al., 2015; Sribenja and Saikrasun, 2015; Bhatti et al., 2013 and Lokhande and Dorugade, 1999). Besides, fundamental studies on adsorption kinetics and thermodynamics of dyeing processes are important to comprehend the dyeing mechanisms, as well as to improve the dyeing performance of natural dyes on various textile materials. Meanwhile, the adsorption isotherm curve describes the retention phenomenon of substances from aqueous media onto solid-phase at constant temperature and pH (Rather et al., 2016).

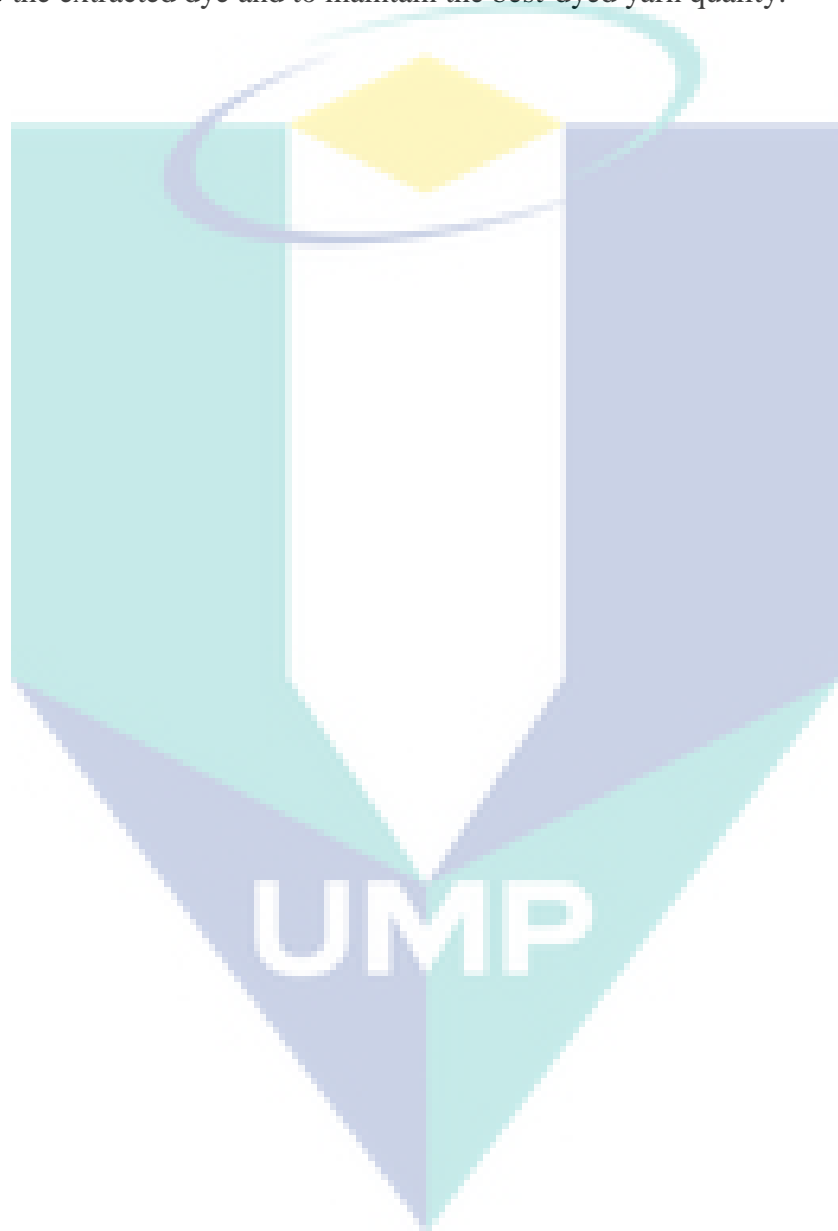
## 1.7 Thesis Outline

The thesis consists of eight chapters. It begins with the Chapter 1 (Introduction), where the background, the problem statement, and the research objectives are given focus. Besides, a research roadmap, as well as scope and significance of the study, is highlighted in this chapter. Next, Chapter 2 (Literature review) describes the literature on natural dye versus synthetic dye in relation to this work. Moreover, a brief description concerning the raw materials used in this research and the processes involved is also covered. Meanwhile, Chapter 3 (Material and methods) presents the details of the materials and chemicals utilized in this work, together with the overall experiment flowchart and the operational framework. In this chapter, the detailed experimental procedures and analytical methods are depicted for natural dyes extraction, dyeing of natural dyes on BY, adsorption studies (kinetic, isotherm, and desorption) and characterization of the samples. Furthermore, a description of the parameter design, the screening, and the optimization approaches are also outlined in this chapter. Moving on, the results and the discussions are composed into four chapters (Chapters 4-7). Chapter 4 (Results and discussion) elaborates the effects of extraction, the mathematical models, and the optimum conditions obtained by using RSM and OFAT for the extraction process. Later, in Chapter 5 (Results and discussion), design of parameter for dyeing of natural dyes on BY and optimization of process conditions are presented. On top of that, a detailed discussion of RSM models and optimum conditions achieved for dyeing BY with natural dyes is highlighted. Next, the kinetics studies and the adsorption isotherm for both dyeing process and desorption study are addressed in Chapter 6 (Results and discussion). The results of characterization of natural dyes extracted from BBPF, RDFP, and Turmeric, as well as DBY, are presented in Chapter 7. Lastly, the conclusions of the study, along with future recommendations are given in Chapter 8 (General conclusion and recommendations for future work). Finally, this thesis is completed with references and appendices.

## 1.8 Summary

This chapter introduces the natural and synthetic dyes for production of colorants in the textile industry. The process approach and the focus of this research work have been extensively elaborated, inclusive of the disadvantages of synthetic dye that have been

outlined as specific research problems in both textile industry and wastewater treatment. The synthetic dye is deleterious for it is harmful to the environmental and to the consumers. Thus, the use of natural dyes is a strategic measure in overcoming the arising issues. As such, the optimum conditions of extraction and dyeing processes have to be determined in order to maximize the extracted dye and to maintain the best-dyed yarn quality.





## CHAPTER 2

### LITERATURE REVIEW

#### 2.1 Introduction

In this chapter, the reviews of prior literature relevant to natural dyes and processes involving extraction, dyeing, adsorption, and characterization are discussed. It highlights the advantages and disadvantages associated with each process. The prime objective of this chapter is to review the prior literature on the processes involving extraction of selected natural dyes. Therefore, sources, properties, applications, composition, and colour pigment of natural dyes (BBPF, RDFP, and Turmeric). Moreover, the process of dyeing of natural dyes extracted from BBPF, RDFP, and Turmeric on Bamboo Yarn (BY), adsorption studies, mordanting, desorption and characterization of the samples are taken into account. The optimization strategies are also reviewed. In addition, this chapter attempts to identify ways to improve the extraction of natural dyes, dyeing properties of natural dyes extracted from BBPF, RDFP, and Turmeric on BY, as well as mordanting parts, in order to overcome the use of synthetic dyes.

#### 2.2 Extraction

Extraction refers to the separation method for a desired substance from a matrix. Scientists working in the field of natural colorant technology presently focus on improving extraction of colorant from plant material and its application onto surface modified fabric (Khan et al., 2014). Most pigments or colorant extracts that produce yellowish, brownish, and greenish colours have been successfully extracted with water and organic solvents, such as acetone, methanol, ethanol, or iso-propanol (Boonsong et al., 2012). Besides, standardization of extraction and dyeing profiles of some prominent dyes have been

developed under various conditions to achieve maximum yield and reproducible results (Sachan and Kapoor, 2007).

### 2.2.1 Types of Extraction

Table 2.1 portrays the literature for the types of extraction and solvents used by researchers in extracting various types of natural dyes. Solvent extraction is a commonly employed method for preparation of flower extracts. Natural colouring matters, depending upon their nature, can also be extracted by using organic solvents, such as acetone, petroleum ether, chloroform, ethanol, methanol, or a mixture of solvents, such as mixture of ethanol and methanol, mixture of water with alcohol, etc. The water/alcohol extraction method, on the other hand, is able to extract both water-soluble and water-insoluble substances from plant resources. The extraction yield is thus, higher as compared to the aqueous method because a larger number of chemicals and colouring materials can be extracted. Besides, if extraction is performed at a lower temperature, chances of degradation become lower (Radhakrishnan, 2014).

Solvent extraction (solid-liquid extraction) involves the process of leaching (simple physical solution or dissolution process). Leaching refers to the separation technique that involves removal of soluble solids from a solid mixture by employing a suitable solvent or solvent mixture. In fact, some of the influential factors in the solvent extraction procedure are the rate of transport of solvent into the material, the rate of solubilisation of soluble constituents in the solvent, and the rate of transport of solution (extract) out of the insoluble matter. Furthermore, solvent polarity, vapour pressure, and viscosity are also of importance to ensure effective extraction. Meanwhile, as for plant materials, adequate time is needed for diffusion of solvent via plant cell walls for dissolution of soluble constituents, as well as for diffusion of solution (extract) out to the surface of the cell wall. Additionally, flower extracts can be prepared either from fresh or dried samples. Prior to extraction, flower samples are subjected to air-drying or freeze-drying, followed by grinding, milling, or homogenization to obtain reduced sample particle size. These procedures are adhered to enhance the efficiency of extraction process and yield of the resulting extract. Moreover, various solvents, such as methanol, ethanol, hexane, acetone, ethyl acetate, and chloroform are having been commonly used for extraction (either in pure form or after dilution with distilled water).

Hence, selecting a solvent mainly relies on the solubility of the bioactive constituents, safety aspects, and several potentials (Voon et al., 2012).

Table 2.1 Literature for types of extraction and solvents used

<b>Types of Extraction</b>	<b>Solvent</b>	<b>Author</b>
Solvent extraction	Ethanol	Guesmi et al., 2012
Solvent extraction	Distilled water	Grover and Patni, 2011
Solvent extraction	n-hexane, ethanol, acetonitrile, chloroform, ethyl-ether, ethyl-acetate, petroleum ether, n-butyl alcohol, and methanol	Al-Alwani et al., 2015
Solid-liquid extraction and Soxhlet extraction	Methanol and distilled water	Celli and Brooks, 2016
Solvent extraction	Distilled water	Ali et al., 2009
Solvent extraction	Methanol	B and Ravi, 2013
Soxhlet extraction	n-hexane (99% assay) and methanol	Ahmad et al., 2009
Soxhlet extraction	Ethanol and distilled water	Kulkarni and Bodake, 2011
Solvent extraction	Ethanol and distilled water	Fathordoobady et al., 2016
Soxhlet extraction	Ethanol and isopropanol	Maniglia et al., 2014
Aqueous extraction and Microwave extraction	Distilled water	Sinha et al., 2012
Ultrasonic extraction	Distilled water	Sivakumar et al., 2009
Solvent extraction	Distilled water	Ali et al., 2009

### 2.2.2 Water Extraction

Most extraction involves water because its application in extraction is low in cost and eco-friendly. Besides, this is the most frequently and easily used technique to isolate plant pigments although some pigments (such as carotenoids and phenolic compounds) are hydrophobic in nature and have limited water solubility aspect. Water extraction, nonetheless, can be improved by using acidic, neutral, and basic extraction at varied temperatures to enhance the mechanism of natural dye extraction, such as the rupture of plant cell membranes, as well as the release and the transfer of natural dyes into water. However, the extraction yields and resulting physicochemical properties of plant pigment extracts strongly depend on the solvent, the temperature, and the pH, which can influence the solubility of the solute to be extracted. Thus, the use of water extraction under various conditions may provide varying yields and may have an impact on the resulting physicochemical properties of the pigment compounds.

However, due to its promising solvency behaviour towards the varying temperatures, water has recently received immense research attention. Hence, it is noteworthy that one could manipulate the physio-chemical properties of water in a sealed system by simultaneously adjusting the temperature and the pressure of the system, in retaining water in its liquid phase, while the temperature significantly rises above the boiling point of 100 °C. Water is also generally known as a highly polar solvent because it has a large number of hydrogen-bonded structures at ambient temperature and atmospheric pressure, as well as a high dielectric constant that makes it an unsuitable solvent to extract non-polar or organic compounds (Valizadeh et al., 2016). Besides, most plant pigment extraction methods are conventional in nature, such as solid-liquid extraction by water and organic solvents (acetone, ethanol, methanol, etc.), for which cost, toxicity, and flammability must be considered (Boonsong et al., 2012).

In addition, Wongcharee et al., (2007) asserted that the extracting solvent for BBPF was studied by a comparison of dyes extracted in water and ethanol. Extraction of blue dye from BBPF with water as the solvent has been studied by Suebkhampet and Sotthibandhu, (2012). Meanwhile, Fathordoobady et al., (2016) extracted RDFP using water and ethanol as their solvents, in which Ethanol/water 0/100 (v/v) resulted in improved amounts of the yield

and recovery of betacyanins. Due to the high polarity and hydrophilic structure of betacyanins, these components displayed relatively poor solubility in organic solvents. Thus, solvent extraction using water had been selected. Besides, standard profiles have been developed for the extraction of yellow dye from turmeric rhizomes via aqueous, solvent, and spray drying methods. The maximum yield was obtained with solvent extraction (Sachan and Kapoor, 2007). Other than that, Lokhande and Dorugade,(1999) extracted turmeric by using water as their solvent.

### **2.2.3 Natural Dye**

Dyes are one of the most important uses that derive from plants, as they are closely related to cultural practices, rituals, arts and crafts, fabrics, as well as to satisfy personal embodiment, however, dye yielding plants have yet to receive significant attention (Grover and Patni, 2011). The present dyes used for dyeing textile materials are classified as soluble, disperse, and pigments (Sengupta, 2003). In order for a substance to function as a dye, the dye must have suitable colour, capable of getting fixed to the fabric, and should not be fugitive after application upon fabric (Kulkarni and Bodake., 2011). Dyes are divided into two classes; natural dye and synthetic dye. Natural dyes are colorants extracted from natural things, such as animals, plants, and mineral, whereas synthetic dyes are fabricated dyes that derive from any synthetic resources, for example, petroleum by-products and earth minerals. Natural dyes are comprised of colorants obtained from animals or vegetable substances without any chemical process (Haddar and Baaka et al., 2014). Moreover, the colours obtained from natural colorants are generally soft, lustrous, and smooth to the human eye (Gedik et al., 2014). Natural dyes obtained from plants, insects/animals, and minerals are renewable and sustainable bio resource products that have minimum environmental impact and known since antiquity for their multiple uses, not only as food ingredients and for cosmetics, but also for textile colouration (Haddar et al., 2014). In fact, some plants yield various colours from different parts, such as flowers, leaves, stems, and even roots (Ratnapandian et al., 2012). Plants have the greatest biological diversity of all living organisms and produce a large variety of pigment compositions. Moreover, plant pigments have been once the main source of all traditional products before many methods were discovered to synthesize substances with similar properties from pest and diseases

(Boonsong et al., 2012). Natural dyes that are obtained mainly from plants generate a variety of colours like yellow, red, blue, brown, black, as well as a combination of these colours. For example, sources for yellow dyes are enormous and plants that yield yellow dyes actually outnumber those yielding other colours (Zhou et al., 2015). The utilization of natural dye pigments has many advantages because it is easy to extract, biodegradable, nontoxic, abundant, and environmental-friendly (Prima et al., 2017). Moreover, the growing interest in the potential use of natural dyes has offered them high compatibility with the environment, minimal toxicity, and low allergic reaction because they are all available in a range of natural shades, when compared to synthetic dyes. Natural dyes can be defined as colorants (dyes and pigments) that attach to a substrate via physical adsorption, mechanical retention, and formation of covalent chemical bonds or of complexes with salts or metals, or by solution. Dyes lose their crystal structures during application by dissolution or vaporisation and are often used for textile (dyeing) and food colorants (staining), whereas pigments retain their crystalline or particulate structure throughout their application (Zhang et al., 2014).

#### **2.2.3.1 Application of Natural Dye**

Natural dyes are important in the textile industry and the active compounds contained in them are valuable in many industries, such as pharmaceutical, food, etc. At present times, natural dyes are in demand not only in the textile industry, but also in cosmetics, leather, food, and pharmaceuticals (Grover and Patni, 2011). These natural dyes have been successfully applied to natural fibre fabrics, such as cotton, wool, silk, and flax (Zhang et al., 2014). In applying natural dyes, various dyeing and mordanting techniques, as well as post-treatment, have been used to improve colour fastness properties. As a result, optimization of the dyeing conditions with regard to the type of natural dye is rather common and a broad set of variations in the dyeing recipes can be found in the literature (Rather et al., 2016). Furthermore, it has been reported that many natural dyes do not only contribute to the natural shades, but also gave certain functions to fabrics, such as antibacterial activity, ultraviolet protection, and insect repellence (Zhang et al., 2014). On the other hand, pigments are used in inks, paints, and cosmetics (Visalakshi and Jawaharlal, 2013). In fact, some recently discovered properties of natural dyes, such as insect repellent, deodorizing, flame retardant, UV protection, fluorescence, and antimicrobial, besides being biocompatible, biodegradable,

renewable, and non-toxic, have revolutionized all industrial sectors, specifically the textile industry to produce more appealing and highly functional textiles with added value (Rather et al., 2016). Besides, natural dyes have been reported as potent antimicrobial agents, owing to the presence of the large amount of compounds like anthraquinones, flavonoids, tannins, naphthoquinones, etc., which exhibit strong antimicrobial properties (Baliarsingh et al., 2012).

However, natural dyes also have some drawbacks, for instance, colour yield, complexibility in the dyeing process, limited shades, reproducible results, blending issues, and inadequate fastness properties. Besides, lack of standardized profiles for extraction and textile dyeing are also major constraints. Furthermore, from the stance of synthetic dyes, natural dyeing is uncompetitive with regard to limited shades, less fastness properties, and higher cost (Sachan and Kapoor, 2007). Besides, when artisans are forced to switch over to other professions, a major setback affects the natural dyeing, while abandoning the traditional knowledge.

#### **2.2.3.2 Natural Dye versus Synthetic Dye**

The application of a number of synthetic dyes has detrimental effects on environment and associated allergic, toxic, carcinogenic, and harmful responses (Haddar et al., 2014). Many synthetic colorants have been classified as toxic when in contact with skin, thus requiring more safe clothing products, especially for babies and children (Mirjaliliet al., 2011). In fact, it is estimated that 10–35% of the dye is lost in the effluent during dyeing process, while in the case of reactive dyes, 50% of the initial dye load is present in the dye bath effluent (Velmurugan et al., 2010). Moreover, European Union (EU) and several world's renowned associations like Global Organic Textile Standards (GOTS), Food and Agriculture Organization (FAO), and Environmental Protection Agency's (EPA), have warned that many intermediates of synthetic dyes used for textile cause water pollution and interrupt the eco-balance of the globe (Adeel et al., 2017). Some have been reported to possess anti-UV, anti-microbial properties, and respiratory sensitivity to synthetic dyes (Mirjalili et al., 2011). Besides, studies have shown that synthetic dyes are suspected to release harmful chemicals that are allergic, carcinogenic, and detrimental to human health (Grover and Patni, 2011).

In addition, textile dyes are considered as the most polluting industrial process. Increase in the demand of dyed textile products with proportional increase in its manufacturing by utilizing synthetic dyes has contributed to severe water and soil pollution, and as a whole to our environment (Geelani et al., 2017). Dye has low degree of fixation on fibre, typically between 50 and 90%, resulting in the release of substantial amounts of the dye in the wastewater (Zuorro et al., 2013). However, natural dyes do not cause any pollution or waste water issues. In fact, natural dyes could greatly benefit the textile industry. Consumers, moreover, have become more aware of environmental issues; hence seeking products with green or organic label (Ratnapandian et al., 2012). Furthermore, interest in the use of natural dyes has been growing rapidly due to the result of stringent environmental standards imposed by many nations in response to toxic and allergic reactions associated with synthetic dyes. Due to the toxic and harmful effects derived from the utilization of synthetic dyes, the use of natural dyes for dyeing textile materials has been emphasised as natural dyes are eco-friendly, soft, beautiful, and possess attractive shades (Sribenja and Saikrasun, 2015).

Moreover, no plant pigments or colorants, including beta-carotene, xanthophyll, and quercetin, were revealed as non-toxic in both short-term and long-term toxicity profiles; displaying no adverse health effects and proving safe for human consumption even after taken for long durations (Boonsong et al., 2012 and Kulkarni and Bodake, 2011). Besides, natural dyes can exhibit better biodegradability (Shabbir et al., 2016) and generally have higher compatibility with the environment. Also, they can show lower toxicity and allergic reaction than synthetic dyes and from the economic point of view, production costs of natural dyes are influenced by production costs of raw materials, dyeing costs, and standardization costs (Haddar et al., 2014).

Thus, natural dyes and pigments emerged as important alternatives to potentially harmful synthetic dyes. When applied to fabrics, reactive groups in the dye molecule form stable covalent bonds with the fibres, imparting a bright and lasting colour to the final product. Moreover, there is a need of a more environmental-friendly dyeing substance like BBPF, RDFP, and Turmeric, which can be compared with synthetic dye.



### 2.2.3.3 Sources of Natural Dye

Natural dyes offer rich and varied source of dyestuff, as well as the possibility of an income through sustainable harvest and sales of these plants. The natural dyes present in plants and animals are pigmentary molecules, which impart colour to the materials, in which people have relied on insects, leaves, and roots of plants for thousands of years for dyeing in the textiles industry (Tayade and Adivarekar, 2013). Besides, a large number of plants and animal/insect sources have been identified for extraction of colour to be used in textile dyeing, for instance, the *Hibiscus mutabilis* (Gulzuba) on cotton (Haddar et al., 2014), hence suggesting the need to explore colorant potential of non-flowering parts of commonly grown, evergreen, and less expensive plants (Khan et al., 2014). In fact, several reports have described plant pigment extracts of *Indigoferatinctoria* L., *Baphicacanthuscusia* Brem, Butterfly Pea (*Clitoria ternatea* L.), and spinach (*Spinaciaoleracea*) in paper of Boonsong et al., (2012). Table 2.1 displays some sources of natural dyes extracted to produce various colours of dyes. Natural dyes contain many pigments, such as carotene (golden), pheophytin (olive-green), chlorophyll (blue green and yellow green), lutein (yellow), xanthophyll (yellow), and anthocyanins (red) (Boonsong et al., 2012). With that, this research had selected BBPF, RDFP, and turmeric as samples because they have not been widely used throughout the history, as well as due to the limited investigations made on their chemical properties, chemical compositions and dye ability on fibre or fabric.

A large, semi-transparent watermark logo for UMP (Universiti Malaysia Perlis) is centered on the page. It features a stylized 'U' and 'M' in light blue and green, with the letters 'UMP' in white below them.

Table 2.2 Natural sources for dye from various journals

Natural Sources	Natural Dye (Colour)	Reference
<i>Saracaasoca</i> and <i>Albizialebbeck</i>	Sa(Leaves):Yellow/Green Sa(Bark):Brown/Marron Al(Leaves):Yellow/Green Al(Bark) :Brown/Maroon	Baliarsingh et al., 2012
<i>OpuntiaLasiacantha</i> Pfeiffer	Red	Ali and El-Mohamedy, 2011
<i>OpuntiaFicus-indica</i>	Red	Guesmi et al., 2012
<i>Hibiscus mutabilis</i>	Green	Haddar et al., 2014
<i>Rhizophoraapiculata</i> Blume	Red	Punrattanasin et al., 2013
<i>Capsicum Annum</i>	Green	Kulkarni and Bodake, 2011
<i>Lawsoniainermis</i> L.	Yellow	Ali et al., 2009
<i>Woodfordiafruticosa</i> (Linn.) Kurzis	Yellow	Grover and Patni, 2011
Pomegranate	Brown	Sinha et al., 2012

#### 2.2.3.4 Blue Butterfly Pea Flower (BBPF)

The BBPF is the first source of natural dye used in this study that offers blue dye. The floral extracts and their isolated essential oils are traditionally believed to be rich in phytochemicals exhibiting rich bioactivity. These compounds are of interest to the local industry, as well as to the general population, and have been actively explored for various commercial applications, such as tea and bakery products (Voon et al., 2012). Moreover,

BBPF is also known as Asian pigeon wings, *Clitoria ternata* Linn or *Bunga Telang* in Malaysia. It belongs to the family Fabaceae (Vasisht et al., 2016). Besides, the BBPF is a wonderful twining plant that generously bears quite large flowers (about 2" across) with a beautiful shade of vivid cobalt blue with white and gold throat. The flowers appear throughout the warm weather. BBPF is a perennial twining herb; stem terete, more or less pubescent, leaves imparipinnate; petioles 2-2.5 cm long; including stipules 4mm long, linear, and acute. Other than that, the leaflets 5-7, subcoriaceous, 2.5-5 by 2-3.2 cm flowers axillary, solitary; pedicels 8-13mm long; bracts small, linear; bracteoles 6-13mm long, roundish, and obtuse. BBPF has a diploid chromosome with the number  $2n = 16$ . The plant is a tall, slender, and climbing herbaceous vine with five leaflets, white to purple flowers, and has deep roots. BBPF is self-pollinated and several segregating genotypes have been identified, suggesting partial out-crossing. BBPF grows well in a range of soil types (pH 5.5–8.9), including calcareous soils, besides tolerating excess rainfall and drought. The primary method of propagation is by seed, and the plant can be grown with or without support, such as trellises, for efficient pod harvesting. BBPF plants produce large quantities of seed and re-seed due to seed shattering at maturity (Morris, 2009).

In addition, its flowers bloom in a variety of colours, namely dark blue, light blue, mauve, and white (Mukherjee et al., 2008). The wild BBPF plants can be found in abundance in Malaysia. Thus, the BBPF is selected as a sample in this research. The plant bears solitary, axillary, and papilionaceous flowers with bright and blue petals, as well as white or light yellow centre. Many ornamental flowering plants have lines or cultivars with different flower colours. The variety of flower colours is mainly due to the chemical structures of the varied anthocyanins accumulated in the flower (Mukherjee et al., 2008). Figure 2.1 shows the image of BBPF.

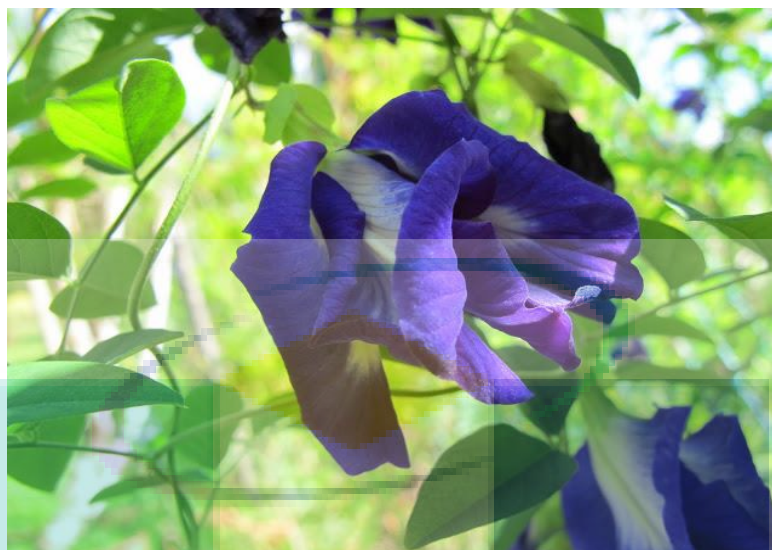


Figure 2.1 Blue Butterfly Pea Flower (BBPF)

#### *Application of BBPF*

The BBPF plant is extensively grown for ornamental and medicinal purposes in the Asian subcontinent (India, Bangladesh, Indonesia, and Malaysia). In Malaysia, aqueous extract of the flower is normally used as a natural colouring agent to prepare a special dish made from glutinous rice (Voon et al., 2012). Moreover, the BBPF has been commonly used as natural food colorant and healthy beverage worldwide (Pasukamonset et al., 2016).

The dried flowers have been reported for use in treating haemorrhoids, dysentery, diarrhoea, liver diseases, piles, disorders of mucous membranes, leucorrhoea, menorrhagia, ulcers, wounds, burning sensations, skin diseases, fever, headache, herpes, the list is endless (Grover and Patni, 2011). Additionally, several studies have recently demonstrated the health-promoting effects of the BBPF, including ant glycation, antidiabetic, and anti-inflammatory activities (Pasukamonset et al., 2016). Thus, it has been implicated to have several medicinal properties (Lee and Abdullah, 2011). Clotides (biologically active peptides) (present in flowers, seeds, and nodules) have been isolated from heat-stable fractions of BBPF extract. These clotides showed potential antimicrobial activity against *E. coli* and cytotoxicity against HeLa cells (Voon et al., 2012). In the Southeast Asia, the blue flower pigment is traditionally utilized as food colorant due to its high stability (Mukherjee

et al., 2008). The morphological features (or) phenotypic characters appear as slender downy stems with leaves having multiple leaflets of elliptical shape and flowers of blue or white in colour, which are a rich source of pharmacologically active secondary metabolites, such as polyphenolic flavonoid anthocyanin glycosides, pentacyclic triterpenoids, and phytosterols. Flavonols i.e., kaempferols, quercetin, and myricetin, as well as their glycosides, have been used to treat body aches, infections, urinogenital disorders, and asanthelmintic and antidote to animal stings. BBPF is also commonly used as brain tonic in the Ayurveda system of traditional Indian herbal medicine to ameliorate intelligence and to intensify memory function (John et al., 2015).

On top of that, the plant has often been used as a laxative, diuretic, brain tonic, and for antiulcer herbal formulation. Various pharmacological actions of BBPF, such as memory enhancement, enhancement of acetylcholine, anti-stress, antidepressant, tranquilizing effects, analgesic, antipyretic, anti-inflammatory, and anti-diabetic, have been widely reported (Raghu et al., 2016). BBPF possesses nootropic, anxiolytic, antidepressant, anticonvulsant, sedative, antipyretic, anti-inflammatory, and analgesic activities. In an isolated study, BBPF have been found to enhance memory and increase acetylcholine content in rats (Taur and Patil, 2011). The roots of the plant are used in the treatment of mental disorders and in various other ailments in the Indian Ayurveda (Vasisht et al., 2016). The root has sharp bitter taste; cooling, acrid; laxative, diuretic, alexiteric, anthelmintic; tonic to brain; good for diseases related to the eye, ulcers of the cornea, tuberculous glands, elephantiasis, and headache (Patil et al., 2009). Its extracts possess a wide range of pharmacological activities, including antimicrobial, antipyretic, anti-inflammatory, antiasthmatic, hepatoprotective analgesic, diuretic, local anaesthetic, antidiabetic, insecticidal, blood platelet aggregation-inhibiting, as well as for vascular smooth muscle due to its relaxing properties (Verma et al., 2013).

#### *Composition of BBPF*

The flower petal of BP has a bright blue colour containing a wide variety of polyphenols, mainly flavonoid anthocyanins. The main polyphenol constituents found in the flower petal of BBPF are ternatin anthocyanins (Pasukamonset et al., 2016). Structural studies of anthocyanins of BBPF have been reported. They were found to be mainly ternatins,

fifteen of them, which were mainly malonylated delphinidin 3,3,5-triglucosides having 3,5-side chains with alternative D-glucose and p-coumaric acid units and delphinidin 3-O-(2-O- $\alpha$ -rhamnosyl-6-O-malonyl- $\beta$ -glucoside (Lee and Abdullah, 2011). Moreover, the blue colour of BBPF, which represents the existence of anthocyanin, has been applied for endless applications. This is consistent with the property of anthocyanin that can easily dissolve in water due to its chemical properties. Besides, the variation in chemical structure that occurs in response to changes in pH is indeed the chief reason why anthocyanins are often used as a pH indicator, as they change from blue in alkaline solution to red in acidic solution (Suebkhampet and Sotthibandhu, 2012).

Furthermore, in the BBPF, three flower varieties are available: blue petal cultivar Double blue (BBPF), a mauve petal variety (WM), and a white petal variety (WW), which exhibit their distinctive constitution of anthocyanins and flavonol glycosides. BBPF accumulates a set of 15 polyacylated anthocyanins and ternatins. Ternatins refer to a group of 15 delphinidin 3-O-(6-O-malonyl)- $\beta$ -glucoside-3-O-5-O-glucosides that are p-coumaroylated or variously glucosyl-p-coumaroylated at 3-O and/or 5-O-glucosyl groups. Polyacylation of ternatins with p-coumaroyl groups is one of the primary reasons for its blue petal because polyacylation with aromatic acyl groups generally contribute to make anthocyanins bluish under a physiological pH via intramolecular co-pigmentation among the aromatic acyl groups and anthocyanidin chromophore (Kogawa et al., 2007).

In addition, the BBPF plant contains protein that range from 14% to 20%, while the seeds contain 38% protein, 5% total sugars, and 10% oil (Morris, 2009). The fatty acid content of BBP seeds includes palmitic, stearic, oleic, linoleic, and linolenic acids. The seeds also contain beta-sitosterol (Taur and Patil, 2011). BBPF is also well-known to accumulate ternatins, a group of (poly)acylated anthocyanins, in the petals. These are delphinidin 3-(6-O-malonyl) glucoside derivatives with acylated glucose chains of various lengths or simply glucosyl groups at both the 3-O and 5-O positions. Moreover, the detailed structures of 15 flavonol glycosides from the petals of the same cultivar have been identified recently (Kazuma et al., 2003). In addition, other phytochemical compounds, including triterpenoids, flavonol glycosides, and steroids, have been isolated from BPF for further investigations (Phruksanan et al., 2014).

## *Anthocyanin*

Anthocyanin plays a major role in the colorant pigment for BBPF that gives the blue colour to this flower. In fact, the BBPF has been adopted as a sample in the studies of floral anthocyanins (Lee and Abdullah, 2011). Water soluble anthocyanins have become increasingly important and have received great interests in numerous researches as they do not only impart beautiful coloration to food systems, but also possess antioxidant properties and health benefits, such as enhancement of sight acuteness and antioxidant (Lee and Abdullah, 2011). In addition, the stability of anthocyanins is correlated with structural features of anthocyanins and it is also affected by several factors, such as heat, pH, light, the presence of enzymes, phenolic acids, oxygen, sugars, sulphur dioxide, and metal ions (Lee and Abdullah, 2011).

Furthermore, anthocyanins are characterized by two absorption bands: Band I – 475-560 nm (visible region) and Band II – 275-280 nm (UV region). Besides, the actual colour of extract relies on the number and the position of hydroxyl and methoxy groups. When these are fixed, the colour then depends upon pH and solvent (Patil et al., 2009). The sensitization of wide band gap semiconductors using natural pigments has been commonly ascribed to anthocyanins. The anthocyanins belong to the group of natural dyes responsible for several colours in the red–blue range, found in fruits, flowers, and leaves of plants, thus functioning as a direct dye (Wongcharee et al., 2007).

Anthocyanins are responsible for most blue, red, and other related colours in flowers and fruits. Low temperature, dark, absence of oxygen, and low pH (2–4) lead to the stability of anthocyanins. In addition, the presence of non-anthocyanin polyphenolics significantly increases anthocyanin stability due to the occurrence of copigmentation reactions. In precise, copigmentation is a phenomenon, in which pigments and other colourless organic compounds, or metallic ions, form molecular or complex associations, resulting in an increase in the colour intensity.

In fact, some studies demonstrated that copigmentation as a primary colour-stabilizing mode in plants and food products rich in anthocyanins. Copigmentation generally occurs in the following four interactions: self-association, metal complexation, intramolecular

copigmentation, and intermolecular interactions. Among the four interactions, intermolecular and intramolecular copigmentation are the most important mechanisms for copigmentation. Intramolecular copigmentation, in which the central anthocyanin chromophore and aromatic acyl residues covalently linked to their glycosyl moieties, is predominant in flower vacuoles.

On the other hand, intermolecular copigmentation occurs when colourless compounds are attracted to anthocyanins via weak hydrogen bonds and hydrophobic forces. Many compounds may be copigments, such as flavonoids, alkaloids, amino acids, organic acids, nucleotides, polysaccharides, metals, and anthocyanins themselves (Pan et al., 2014). Furthermore, the absorption peak of BBPF extract had been found to be about 580 and 620 nm. The difference in the absorption characteristics is due to the various types of anthocyanins and colours of the extracts (Wongcharee et al., 2007). Figure 2.2 and Figure 2.3 illustrate the common chemical structure of anthocyanin and the chemical structures of cyanidin 3-glucoside in BBPF, respectively.

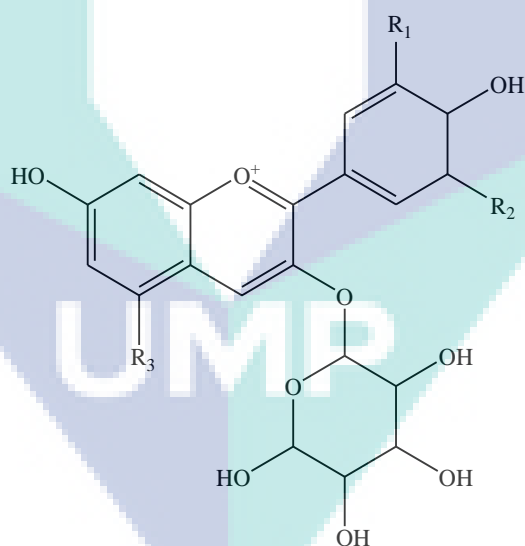


Figure 2.2 Common chemical structure of anthocyanin

Source: Wang et al.,(2014)



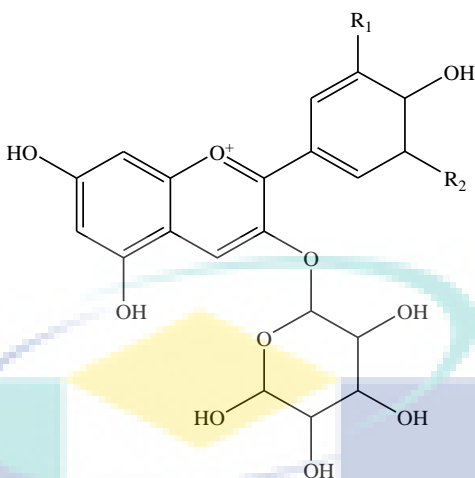


Figure 2.3 Chemical structures of cyanidin 3-glucoside in BBPF

Source: Wongcharee et al., (2007)

#### 2.2.3.5 Red Dragon Fruit Peel (RDFP)

The RDFP (Figure 2.4) is the second natural dye used in this research that provides red dye. The Red Dragon Fruit (RDF) species belong to the vine cacti from the subfamily of Cactoideae of the tribe Cacteeae. This tribe contains many species with edible fruits mostly known as pitaya, or pitahaya. The common name of these fruits is pitaya since they contain scales on the fruit skin and thus, known as ‘the scaly fruit’. In the last two decades, efforts have been made to develop the cultivation of dragon fruit (DF), a vine species of the genus *Hylocereus*. Some of them contain pulp of red and/or purple colours of various hues (Wybraniec et al., 2001). The red pitahaya or RDF (*Hylocereus polyrhizus*) is well known for its aesthetically pleasing deep purple colour pulp with numerous small soft seeds (Gengatharan et al., 2015).

Recently, fruits from the Cactaceae family have been considered as a rich source of betacyanins. Among them, the flesh of RDF (*Hylocereus polyrhizus*), which is native to Thailand, Vietnam, Taiwan, South of America and some other parts of the world, is becoming popular in Malaysia due to its unique appearance, appealing red and purple colours, great nutritive value, and bioactive specifics. Its polyphenolics is comprised of simple phenols, phenylpropanoids, flavonoids, and tannins; possessing aromatic ring, as well as one or more hydroxyl group alternatively, which offers rich antioxidants (Fathordoobady et al., 2016).

Furthermore, being an epiphyte, it clings to its support and can obtain nutrients from cracks where organic material concentrates. The fleshy succulent stems are three-sided (occasionally four or five) and lobed along the ridges, which have small swellings equipped with short spines. The RDF has already received worldwide recognition as an ornamental plant for its large, scented, and night-blooming flowers. Its fame has spread across the world for its fruit, especially in Asian countries like Vietnam, Taiwan, Malaysia, and the Philippines. Moreover, DF comes in a number of varieties; the three varieties that have been commercialised are *Hylocereus undatus* with red-skinned fruit and white flesh, *Hylocereus polyrhizus* (RDF) with red-skinned fruit and red flesh, and *Hylocereus megalanthus* (Yellow DF) with yellow-skinned fruit with white flesh. In Malaysia, about 927.4 hectares have been established for DF plantation for both local consumption and export markets; thus increasing the RDF farm size due to the escalating demand (Lim et al., 2010). The fruit has gained popularity at least in part as a result of the attractive appearance of the flesh and due to the potential health benefits that come from the high levels of betacyanins characterised by the red- or purple-coloured DF varieties (Obenland et al., 2016).



Figure 2.4 Red Dragon Fruit (RDF)

#### *Application for RDF*

The pulp of RDF is used in Israel to produce red-violet colour ice cream juices (Wybraniec et al., 2001). In fact, the public concern about possible or proven harmful effects of artificial food colorants has increased the search for natural colour sources. Betalains, as such, displays great potential in colouring a broad array of food products. In view of this,

betacyanin from RDF are the most promising, not only as colouring agents, but also for its antiradical potential (Stintzing et al. , 2002). RDF has widely brought about high interest due to its attractive colour, pleasant taste, high content of nutrients, senescence-retarding, and cancer-preventing effects (Tao et al., 2014). The RDF has recently drawn much attention from growers worldwide, not only because of its red–purple colour and economic value as a food product, but also for its ant oxidative activity from the betacyanin contents (Lim et al., 2010).

This fruit has high appeal in the European and United States market and is widely cultivated in Malaysia, China, Okinawa, Israel, and Vietnam. The fruit is rich in betacyanin, such as betanin, phylloactin, hylocerenin, and their isomers (Gengatharan et al., 2015). Betacyanin, as well as polyphenols in the RDF, exhibit strong antioxidant activities and could potentially help protect against disorders in the body mitigated by oxidative stress (Obenland et al., 2016).

#### *Composition of RDFP*

The most important fruit pigments in RDFP are betacyanin and betaxanthins (betalains) (Wybraniec et al., 2001). Betalains are composed of red–violet betacyanin and yellow betaxanthins, as well as water-soluble pigments that provide colours in its flowers and fruits. The percentages of oil extracted from red and white flesh seed oils were 18.33 % and 28.37 %, respectively, in which the oil content for the white fruits significantly ( $P < 0.05$ ) higher than that of the red one (Lim et al., 2010).

#### *Betacyanin*

Betacyanin are phytochemicals in the class of red and yellow indole-derived pigments, belonging to the group of betalains, inclusive of betaxanthins, found abundantly in the plant Caryophyllales, such as red beet and RDF. Both betalains and anthocyanin are water soluble pigments found in the vacuoles of plant cells and they are responsible for the bright colours of flowers and fruits. In fact, betalains are aromatic indole derivatives synthesised from tyrosine (Taira et al., 2015). Moreover, betalain derivatives can be classified as betacyanin (red-violet colour,  $\lambda_{\max}$  at 540 nm) and betaxanthins (yellow-orange colour,  $\lambda_{\max}$  at 480 nm), depending on the residues attached to its main structure. The former

exhibits a closed structure of cyclo-DOPA (cyclo-3,4-dihydroxy-phenylalanina) and can be substituted with sugar and acyl groups, while the latter is conjugated with amines and amino acids (Celli and Brooks, 2016).

Betacyanin, which is an essential betalain, are associated with the most abundant red colour exhibited by fruits, flowers, and other parts of plants, which are actually found in about 12 plant families. This pigment is a compelling candidate for colouring low acid foodstuff, such as dairy products and beverages. As anthocyanin lose their pictorial power and shade at pH from 3 to 7, betacyanin are more stable in this condition. In betacyanin, acylation generates more antioxidant capacity, while lower in glycosylation (Fathordoobady et al., 2016).

In the visible region, the absorbance spectrum of RDFP pigment extracted by water shows a broad peak at 530 nm, which is caused by red-violet betanin dye called betacyanin. From the absorbance results, the best solvent of RDFP are methanol, ethanol, and water (Al-Alwani et al., 2015). Figure 2.5 illustrates the chemical composition of betacyanin in the RDFP dye.

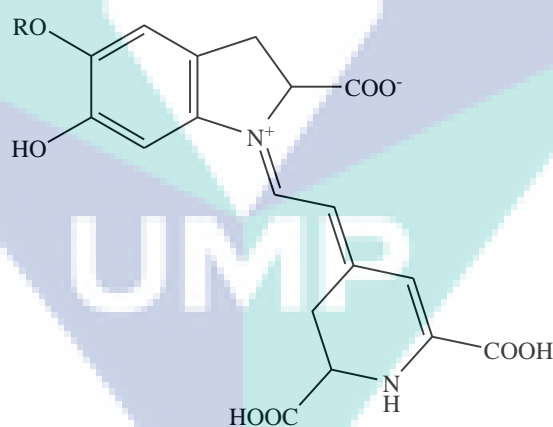


Figure 2.5 Chemical composition of betacyanin in RDFP

Source: Wybraniec et al., (2001)

### 2.2.3.6 Turmeric

The third natural dye used in this study is extracted from the rhizome of Turmeric. The global turmeric production is approximately 1100,000 t/year. At present, it is used primarily as a natural colouring agent to replace synthetic dyes in chutneys, pickles, mustard,

butter, and cheese, among other products (Osorio-Tobón et al., 2014). Turmeric is also known for its rhizomes products (Osorio-Tobón et al., 2016). Its scientific name, *Curcuma longa L.*, belongs to the family Zingiberaceae, commonly known as turmeric. Moreover, it is a rhizomatous perennial herb with primary and secondary rhizomes; and its shape varies from spherical to slightly conical, hemispherical, or cylindrical (Maniglia et al., 2014).

The Turmeric (*Curcuma longa L.*) plant that derives from the ginger family has been extensively cultivated in tropical parts of the South and Southeast Asia (Valizadeh et al., 2016). Turmeric is native to India, distributed throughout tropical and subtropical regions of the world, and widely cultivated in the Southeast Asia (Martins et al., 2013). Turmeric is an important common flavouring spice of daily use (Krishnakumar et al., 2015). A recent report indicated that the export and demand of Indian turmeric have increased due to the increase in food and non-food uses. The use of turmeric and its value-added products is recognized globally and hence, the production has been increased to meet the demands (Anusuya and Sathiyabama, 2016).

At present, it is cultivated in many regions of the world with India being the largest producer and exporter of turmeric, as well as numerous value-added products. The countries that import turmeric from India are United Arab Emirates, Sri Lanka, Japan, Bangladesh, United Kingdom, Malaysia, South Africa, Netherlands, and Saudi Arabia, which accounts for 75% of world imports. The USA alone imports 97% of the turmeric and its value-added products from India (Sathiyabama et al., 2016). Figure 2.6 shows the image of turmeric rhizome.



Figure 2.6 Rhizome of Turmeric

#### *Application of Turmeric*

To date, the application of turmeric as a dye has greatly increased especially to substitute synthetic additives (Osorio-Tobón et al., 2016). Turmeric is a well-known natural dye extracted from the fresh or dried rhizomes. The dye present is the chemical known as curcumin, belonging to the Diaroylmethane class. It is a substantive dye capable of directly dyeing silk, wool, and cotton. The shade produced is fast to washing, but its fastness to light is poor. Turmeric is mainly valued for its principal colouring constituent curcumin, which imparts the yellow colour on textile fibres and food items (Sachan and Kapoor, 2007). Turmeric dyeing can be overdyed with indigo for production of fast greens (Radhakrishnan, 2014). The rhizomes of the perennial turmeric are the source of the colour (Sachan and Kapoor, 2007).

Due to the properties possessed by turmeric and the general interest in substituting synthetic additives with natural compounds; turmeric and derivative products, such as turmeric powder, extracts, and oleoresins, have great potential in the food industry and in the markets of natural additive products (Osorio-Tobón et al., 2016). Moreover, turmeric has been used for food flavouring, colour, and as a component in traditional medicine (Nguyen et al., 2017). Turmeric is one of the oldest natural colouring agents used worldwide from ancient times (Sachan and Kapoor, 2007).

Additionally, being a colorant, curcuminoids have great potential in food and pharmaceutical industries. To date, turmeric and its derivatives have sparked great interest due to their pharmacological properties (Osorio-Tobón et al., 2016), as well as in dietary spice, foods and textile colouring, and curing broad ranges of diseases (Valizadeh et al., 2016). Turmeric is an edible and herbaceous plant, which has been used in Thai traditional medicines for a long time due to its endless pharmacological activities. Turmeric rhizome powder had many pharmacological effects, such as the treatment of irritable bowel syndrome, peptic ulcer, and inflammatory bowel disease (Monton et al., 2016). Turmeric dye is the brightest of naturally occurring yellow dyes with powerful antiseptic that revitalizes the skin, while indigo giving a cooling sensation (Grover and Patni, 2011). *Curcuma longa* L, an important spice used in cosmetics and colouring agent, has also been used in Indigenous System of Medicine (Sachan and Kapoor, 2007). Curcumin possesses various bioactive properties and is used in modern medicine (Sachan and Kapoor, 2007). The root of this plant consists of the rhizome, which is the most useful part for culinary and medicinal purposes.

Furthermore, it has a wide range of biological properties, including antioxidant, anti-inflammatory, anti-mutagenic, anti-carcinogenic, and anti-angiogenic properties (Anusuya and Sathiyabama, 2016 and Martins et al., 2013). Other than that, turmeric is a potential candidate to treat cystic fibrosis, Alzheimer's disease, malaria, and cancer (Maniglia et al., 2014). Moreover, turmeric has the main active constituent curcumin, which has been widely used among cancer patients, especially those that derive from plants (Yue et al., 2016). The rhizomes of *Curcuma longa* provide yellow and flavourful powder when dried and ground, which have long been used in Chinese and Ayurveda medicines.

#### *Composition of Turmeric*

The chromophores of natural yellow dyes consist of flavonoids, carotenoids, hydroxylanthraquinones, and bis- $\alpha,\beta$ -unsaturated diketone polyphenols (Zhou et al., 2015). Besides, *Curcuma longa* L. is a vital source of the natural yellow dye. Besides, turmeric rhizome contains curcuminoid compounds (2-6%), volatile oil (3-7%), fibre (2-7%), mineral matter (3-7%), protein (6-8%), fat (5-10%), moisture (6-13%), and carbohydrate (60-70%) (Sachan and Kapoor, 2007). In fact, the common volatile oils found in turmeric rhizome are r-turmerone (38%), a-turmerone (19%), and b-turmerone (15%). Besides, the major active

compounds of turmeric rhizome are curcuminoids, including bisdemethoxycurcumin (3–8%), demethoxycurcumin (12-18%), and curcumin (72-78%) with a purity of  $\geq 95\%$  for those available commercially (Monton et al., 2016).

Despite of the mentioned features, curcuminoids display poor stability and low aqueous solubility (Martins et al., 2013). Moreover, the yellow colour of the rhizomes is due to the presence of a group of phenolic compounds called curcuminoids (Osorio-Tobón et al., 2014). The main active constituent in turmeric is the secondary metabolite curcumin (1,7-bis-(4-hydroxy-3-methoxyphenyl)-1,6-heptadiene-2,5-dione) (Sathiyabama et al., 2016), and curcumin is the most abundant curcuminoid found in turmeric (Nguyen et al., 2017).

### *Curcumin*

Curcumin is the colorant pigments that contribute the yellow shade to the extracted dye from its rhizome. This herb is bright yellow in colour because it has Curcumin, which is a diphenolic compound (Maniglia et al., 2014). Besides, it is the component obtained via turmeric solvent extraction i.e., ground rhizomes of *Curcuma longa L.* (*Curcuma domestica* Valetton) and purification of the extract via crystallization. Curcumin (1,7-bis(4-hydroxy-3-methoxyphenyl)-1,6-heptadiene-3,5-dione) is extracted from the ground roots of *Curcuma longa L.*, a plant growing abundantly in the East Indies and China, and well known in both traditional and modern medicine due to its antioxidant, anti-inflammatory, antifungal, and anticancer properties (Zhou et al., 2015). Moreover, as mentioned earlier, curcumin is often used as spice, cosmetic ingredient, natural medicine, food preservative, food colorant, and textile colorant. Other than that, the active ingredient, curcumin, is frequently described as a chemopreventive agent for colorectal cancer (Yue et al., 2016). Curcumin is the principal constituent of the yellow dye, along with other constituents like monodesmethoxycurcumin and bisdesmethoxycurcumin, which also contribute some amounts of pigment and flavour. The colouring matter is bright yellow amorphous powder, easily dispersible in water, ethanol, and isopropyl alcohol. In fact, it has been classified as CI Natural Yellow 3 and also a direct dye.

The curcumin is the main colouring constituent of the turmeric and as depicted in some reports, its content varies from 2-8 %, depending on certain variety and habitat (Sachan



and Kapoor, 2007). Acid dyes, in general, are more resistant to ozone fading than disperse dyes and, hence, the latter almost entirely have been substituted by acid dyes in the nylon carpet dyeing industry. The poor resistance to ozone fading of disperse dyes is attributed to their relatively small molecular size and lack of ionic character. Ozone is a strong oxidizing agent that eliminates chromophores from some dyes. For instance, ozone can attack the anthraquinone ring of a dye molecule and convert it into colourless phthalic acid derivatives (Lokhande and Dorugade, 1999). The  $\lambda_{\max}$  values, as determined via spectroscopic estimation, had been 426 nm for extracted dye and 420 nm for curcumin (Sachan and Kapoor, 2007). Thus, the chemical structures of curcuminoids make them less soluble in water at acidic and neutral pH, but soluble in methanol, ethanol, dimethyl sulfoxide, and acetone. The curcuminoids also give yellow-orange coloration to turmeric powder due to the wide electronic delocalization within the molecules that display strong absorption between 420 and 430 nm in organic solvent (Amalraj et al., 2016).

The curcuminoid, specifically curcumin, is considered as a hydrophobic natural polyphenolic material, which is poorly soluble in hydrocarbon solvents. Curcumin, at acidic condition, is insoluble in water and neutral pH; but soluble in basic solvents. Thus, various surfactant micellar systems (acetone, methanol, and ethanol) have been added to curcumin in order to enhance its solubility in water. Besides, it is stable at high temperatures and in acids, but otherwise in alkaline conditions and in the presence of light. Furthermore, the value of turmeric products has been proven to be proportionally related to the curcuminoid content. On top of that, the quantitative estimation of curcuminoids could be determined photometrically, depending on its absorbance values at the wavelength of 420 nm (Valizadeh et al., 2016). Meanwhile, the UV/VIS detector was set to a wavelength of 425 nm (Martins et al., 2013). However, the poor bioavailability of curcumin emanates from its aqueous insolubility at physiological pH (11 ng/L), hydrolytic instability due to highly labile bis- $\alpha,\beta$ -unsaturated  $\beta$ -diketone structure, rapid metabolism, and fast elimination, thus limiting applications (Krishnakumar et al., 2015).

Furthermore, curcumin is chemically a diarylheptanoid, which involves several functional groups. The ring systems, which are phenols, are connected by two  $\alpha, \beta$  unsaturated carbonyl groups. Meanwhile, the diketones form stable enols and are readily

deprotonated to form enolates, hence, the  $\alpha$ ,  $\beta$  carbonyl groups experience nucleophilic addition. In a way, such compound could indicate a good radical scavenging capacity. Besides, the stability of the curcumin tincture solutions against radiation is very poor at high doses. Additionally, the principal colouring components of curcumin exhibit anti-oxidative, antimutagenic, and antibacterial attributes (Cosentino et al., 2016). Figure 2.7 shows the chemical structure for curcumin in turmeric.

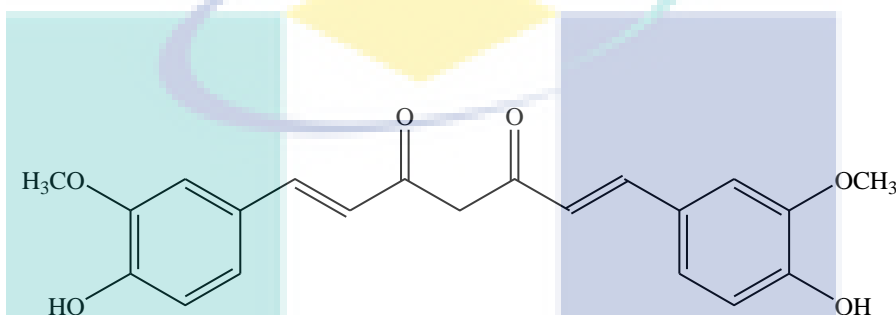


Figure 2.7 Chemical structure for curcumin in turmeric

Source: Cosentino et al.,(2016)

#### 2.2.4 Optimization Strategies

Optimization reflects the improvement of a performance for a process, a product or a system in order to achieve maximum benefits. Generally, the term ‘optimization’ is used in analytical chemistry as a means of discovering conditions applicable to a procedure that generates the best possible response. As such, screening is one way that determines the factors that return the best possible outcome (response). Generally, there are two different strategies for screening: one-factor-at-a-time (OFAT) and Response Surface Method (RSM). The process of extracting natural dyes from BBPF, RDRP, and turmeric had been optimized in order to determine the optimum conditions for every variable studied. The process of optimization for the study referred to the response surface plan.

##### 2.2.4.1 Parameters of the Extraction Conditions

The following subsections discuss various extraction of natural dyes parameters, including temperature, time and solid liquid ratio (SLR). These variables are varying widely in literature. A few of literature reviews on the extraction natural dyes from BBPF dye, RDRP dye and turmeric dye. Thus, the general natural dyes extraction studies were being reviewed.

### *Extraction temperature*

In the previous study, Sachan and Kapoor (2007) was subjected the extraction of turmeric dye to be warming at 90°C The experiments of extraction of natural dye from Henna, Neem and Turmeric in distilled water were conducted at temperature 60 °C (Tech, 2012). Pomegranate, BBPF and marigold flower were used for the extraction of dyes and the experiments conducted by Kanchana et al. (2013) in aqueous extraction at temperature (28 and 100 °C). However, Wongcharee et al.(2007) was studied the effect of extracting temperature of dyes from fresh rosella and BBPF at 25, 50, 70 and 100 °C by using water as an extracting solvent. The extraction of natural dyes above than 100 °C caused the dye lost their colours due to the degradation of colorant pigments content in the dyes.

### *Extraction time*

The experiments of extraction of natural dye from Henna, Neem and Turmeric in distilled water were conducted for 60 minutes (Tech, 2012). Wongcharee et al.(2007) were extracted fresh rosella and BBPF dyes for 30 minutes. The RDFP was extracted for 30 min previously reported in Taira et al. (2015). Based on these three studies, the extraction of natural dyes was performed at specific time by Tech (2012). Wongcharee et al.(2007) and Taira et al. (2015) did not detail on how the extraction time were affected the dye recovery.

### *Solid Liquid Ratio/ Concentration*

The literature reviewed, all of the studied reviewed were varied the concentrations widely depending on the ratio of material's weight and solvent used. In previous extraction of natural dyes studies, Guesmi et al. (2012) has been extracted the dye from cactus pears with ethanol at ratio 0.625:10. Turmeric's rhizome was used as a sources of natural dyes by Sachan and Kapoor (2007) and the extraction of turmeric dye was done at ratio 1.25:10. The experiments of extraction of natural dye from Henna, Neem and Turmeric in distilled water were conducted by Tech (2012) at ratio 5:10. The powder of BBPF was gradually dissolved in distilled water at a ratio 1:10 (Suebkhampet and Sotthibandhu, 2012). Pomegranate, BBPF and marigold used for the extraction of dyes experiments were conducted in aqueous extraction at ratio 1:10 (Kanchana et al., 2013). Fresh rosella and BBPF of was extracted at ratio 1:10 in paper of Wongcharee et al. (2007). Dry petals of BBP was extracted with

distilled water at ratio 1.7:10 (Lee and Abdullah, 2011). The RDFP was extracted with 80% aqueous Ethanol at ratio 5.2:10 (Taira et al., 2015).

#### **2.2.4.2 One-Factor-At-A-Time (OFAT) Approach**

Optimization of extraction of natural dyes are definitely important in gaining optimum consuming condition of dye with the highest colorant pigments concentration. In the OFAT method, one parameter is variant, while the rest are constant (Nasirizadeh et al., 2012). Engineers and scientists often perform OFAT experiments, which vary only one factor or variable at a time, while keeping others fixed (Czitrom, 1999). Running OFAT experiments is a sequential learning process. Besides, the use of OFAT designs allows investigators to determine more rapidly if a factor has any effect and the continually receive information from each run rather than having to wait until the entire experiment is completed (Qu and Wu, 2005). It is, therefore, necessary to employ a sequential study with OFAT methods and RSM on optimization of extraction of natural dyes from BBPF, RDRP, and turmeric. Unfortunately, the OFAT has some disadvantages as it requires runs, impossibility in estimation of interactions, and probability of missing optimum values. Despite of these drawbacks, some researchers have articulated the essentiality of OFAT under certain conditions (Nasirizadeh et al., 2012). On the other hand, terms consists of an empirical modelling technique, which has been used to evaluate the correlation between the experimental and the predicted results (Haddar et al., 2014). Thus, RSM is definitely needed for application.

#### **2.2.4.3 Response Surface Method (RSM)**

The Response Surface Method (RSM) is a useful statistical technique for designing experiments, building models, evaluating the effects of several factors, searching optimum conditions for desirable responses, and reducing the number of experiments (Nasirizadeh et al., 2012). In fact, the objective of the present study is to provide an overview of the existing research studies on extraction of natural dyes with the aid of RSM. The RSM was applied to determine the optimized conditions for extraction of natural dyes from BBPF, RDRP, and turmeric.

In this work, the factorial experimental design methodology was employed to estimate the influence of the various selected variables in the dyeing process. Factorial designs are widely used to investigate the effects of experimental factors and the interactions between those factors, that is, how the effect of one factor varies with the level of the other factors in a response. Besides, some of the advantages of factorial experiments are the relatively low cost, the reduced number of experiments, and the increasing possibilities to evaluate interactions between the variables. Therefore, in order to get the best conditions and to determine the level of parameters for extraction of natural dyes; the process should be optimized. In addition, the central composite design (CCD) technique is a very useful tool that provides statistical models, which can help in understanding the interactions between the parameters that have been optimized. In CCD, all effective factors are optimized simultaneously. Moreover, the CCD in RSM was used to develop a response surface quadratic model to describe the dye extraction process and dyeing the natural dyes process onto BY. However, to the best of the researcher's knowledge, no study has looked into the application of RSM on optimization of extraction of natural dyes from BBPF, RDRP, and turmeric, as well as optimization of dyeing of natural dyes on BY. Therefore, in order to evaluate the effects of parameters and to optimize these media components, RSM was employed in the present study. The RSM is definitely an effective statistical technique to optimize complex processes.

### **2.3 Dyeing**

Dyeing is a process of colouring material, whereby the colour becomes part of the substrate. The permanency of the colour is depending upon the dye and the process of application. Real dyeing is a permanent colour change and the dye is absorbed by being chemically combined with the substrate. Textile industry is a sector that generates most pollutants and harming the environment with poor working conditions, besides contributing to energy and water waste, as well as contamination. Hence, it is crucial to reduce the textile production environmental footprint and the consideration on how materials can allow for a more sustainable future, whilst simultaneously, promoting and enhancing one's wellbeing and lifestyle (Carvalho and Santos, 2015). The effectiveness of the dyeing process is crucial to the success of the textile industry, paying attention to how colours influence consumers.

Nevertheless, dyeing methods have often been associated with water waste, fossil fuel generated energy, toxicity, and contamination; posing a serious threat to the environment and human health (Carvalho and Santos, 2015). As part of the routes to solve the problems of the dyeing industry, both fundamental physical studies on the dyeing process and chemical modifications are significant. However, to the author's knowledge, very limited information is available with regard to the physical and chemical studies in enhancing the dye ability of dyeing on bamboo fibre (Sribenja and Saikrasun, 2015). Hence, it is possible to use pigment and colorant extracts as dyes (Boonsong et al., 2012).

### **2.3.1 Fibre**

Fibre has been widely used in the textile industry where the substances originate from either natural or synthetic sources. Natural fibres derive from plants, animals, and geological materials, while synthetic or chemical fibres are fibres whose chemical composition, structure, and properties are altered during the manufacturing process. Besides, natural fibres are usually used to manufacture other materials like cotton, silk, and wool, whereas those synthetic include nylon, acrylic, and polyester. Recently, several studies have reported the dyeing of natural fibres, such as cotton, silk, wool, linen, jute, and flax with natural dyes (Mirjalili et al., 2011). Natural fibres mainly derive from two distinct origins: animal or vegetable. Fibres from animal origin include wool, silk, mohair, and alpaca.

On the other hand, fibres of plant origin include cotton, flax or linen, ramie, jute, and hemp, to name a few. Moreover, it had been reported that natural dyeing of certain plant-based textiles can be less successful than their animal equivalent. So, extensive work had been conducted to improve the light fastness properties of various naturally-dyed textiles (Grover and Patni, 2011). Natural fibres are opted because those synthetic are hydrophobic, highly crystalline, non-polar polymers, and the absence of active chemical groups in their polymer structure (Haddar et al., 2014). Besides, with the growing demand for more comfortable, healthier, and environmental- friendly products, efforts in research and development activities in the textile industry have emphasised on using renewable and biodegradable resources and environmentally sound manufacturing processes in textiles. In this view, the new type of regenerated fibres, which are an alternative to those conventional

and cotton, have gained importance in apparel and home textile manufacturing (Erdumlu and Ozipek, 2008).

Vegetable, animal, and mineral fibres are part of the natural fibres. Several sources of fibres are seed, leaf, stem, etc. Plants produce two types of natural fibres: one is primary fibre, while the other is secondary fibre (Mittal et al., 2016). Fibre that is directly obtained from plant root is known as primary fibre, whereas those secondary are the by-products (Mittal et al., 2016). Natural fibres are available in abundance, biodegradable, and renewable resources; in opposition to synthetic fibres (Pinho et al., 2010).

### **2.3.1.1 Types of Fibres**

Numerous types of fibres are used in the textile industry and investigated in researches specially to overcome numerous issues pertaining to the disadvantages of using some fibres. Table 2.1 shows the types of fibres examined by various researchers. In fact, prior studies have investigated the dyeing effects on natural fibres that derive from animals and plants. Natural fibres, in addition, have been broadly used in the apparel industry due to their great properties (Peng et al., 2016). Thus, as limited studies had associated BY with dyeing properties, mordanting effect, and adsorption study; the BY had been selected in this research. As bamboo fibre requires less amount of dye for the same shade depth and appears better, softer similar to the texture of silk, and dries quickly; the use of bamboo fibre as cotton substitute is better for environment, along with less use of dye and consequently, less waste (Tausif et al., 2015).

Furthermore, studies that enhance the eco-friendliness of textile products have generally concentrated on wet processing of textile substrates to produce dyed and finished fabrics with minimal use of chemicals, water, and energy (Tausif et al., 2015). As the dyeing characteristics of bamboo fabrics are better than other cellulose fabrics, it is expected to have more promising results by US dyeing of bamboo fabric (Larik et al., 2015). Cotton is made of cellulose molecules with organized fibres with certain physical and chemical properties, as well as low cost, generating high quality textiles. Nevertheless, bamboo has properties that are more interesting. In fact, BY are made of cellulose in a ligneous matrix with a unique structure, unidirectional fibre- reinforced composite with many nodes along its length.

Besides, BY has antibacterial and antifungal effects with ecologic and low cost production (Pinho et al., 2010).

Table 2.3 Types of fibres used in the dyeing process by various researchers

<b>Type of Fibres</b>	<b>Reference</b>
Bamboo Cellulose Fabric	Larik et al., 2015
Wool	Guesmi et al., 2012
Cotton	Ali et al., 2009
Cotton	Ratnapandian et al., 2012
Cotton	Ali et al., 2009
Woollen Yarn	Rather et al., 2016
Woollen Yarn	Shabbir et al., 2016
Wool Fabric	Zhang et al., 2014
Wool Fabric	Ren et al., 2016
Ramie Fabric	Zheng et al., 2011
Silk	Tayade and Adivarekar, 2013
Silk Fabric	Punrattanasin et al., 2013
Cotton Fabric	Haddar et al., 2014
Acrylic Fibres	Haddar et al., 2014

### 2.3.1.2 Bamboo Yarn (BY)

Bamboo Yarn (BY) is made by 100% Bamboo fibre (BF) and it undergoes several processes in producing the yarn as the final product. BF is obtained from bamboo pulp, which is extracted from the bamboo stem and leaves by wet spinning, as well as the process of hydrolysis-alkalisation and multi-phase bleaching, which is rather similar to that of viscose rayon fibre (Erdumlu and Ozipek, 2008). In fact, recent environmental conservation regulations have given considerable importance to renewable and natural materials. BY is a renewable natural resource of cellulose nature and it originates from the grass family (Larik et al., 2015). BF is abundantly available in most tropical countries and it has been considered as the world's best-known natural engineering materials. For instance, this material has been neglected in India like a golden hen, as it is the most underutilized natural resource with a



contributing share of 45 % of the worldwide bamboo forests (Kumar et al., 2016). Bamboo is the fastest growing grass that does not require replanting after harvesting. Besides, bamboo plant does not require pesticides or fertilizers for cultivation; thus dismisses pollution (Majumdar and Pol, 2014).

Furthermore, bamboo has emerged as the ultimate green material that meets the definition of renewable and sustainable raw material without harming the environment. Moreover, bamboo is one of the fastest growing plants with a rapid renewal rate of 34 years, besides being used as feedstock. Bamboo viscose fibre is produced by adhering to the method similar to that of viscose process. Bamboo, in comparison to the usual source of wood pulp, has been found to have lower environmental impact with significant reduction in carbon footprint and land use (Tausif et al., 2015). Bamboo viscose fibre is regenerated from the bamboo plant that requires no irrigation and can be grown in a natural environment without pesticides. The bamboo viscose fibre production process from bamboo pulp could be eco-friendly if the production involves closed-loop system without any harmful substance going into the eco-system (Tausif et al., 2015). Figure 2.8 shows an example of the BY.

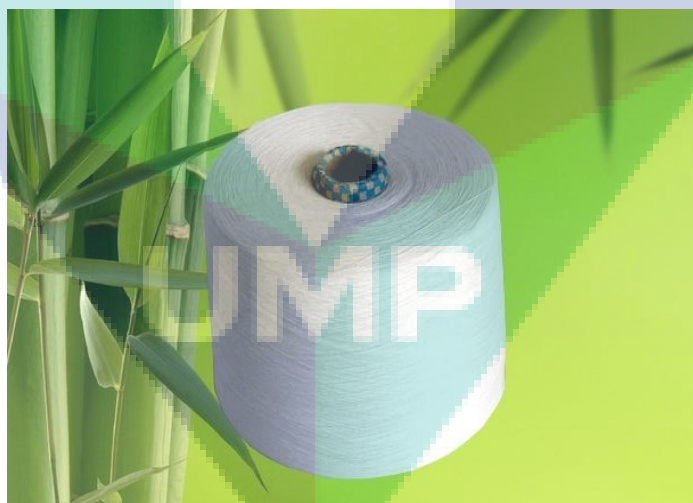


Figure 2.8 Bamboo yarn (BY) produced from 100% of bamboo fibre

### 2.3.1.3 Properties of BY

The BY is regenerated from the bamboo grass. It is lighter in weight, soft and smooth to handle, and has excellent wicking properties. This is mainly due to its high porosity, which

also contributes to its cooler feel. Besides, it has been claimed to be more sustainable than most of the textile fibres. Due to its many unique properties, BY has gained attention towards its use for textiles, specially apparels (Larik et al., 2015). In recent years, BY has attracted great attention as the most abundant renewable biomass materials that can be used in textiles and composite reinforcement. It possesses many excellent properties when used as textile materials, such as high tenacity, excellent thermal conductivity, resistant to bacteria, as well as high water and perspiration adsorption (Nayak and Mishra, 2016). Moreover, the cross-section of BY contains micro gaps and micro holes that enhance moisture absorption and ventilation (Tausif et al., 2015).

BY is breathable, cool, extremely soft, has high moisture absorption capacity, and pleasant lustre. In addition, it possesses inherent anti-bacterial and anti-UV properties (Tausif et al., 2015). In most cases, BY surfaces have negative charges (Liu et al., 2015). Therefore, the adsorption of positively-charged dyes onto BY is becoming a promising technique to manufacture functional textiles, besides enhancing the dye strength. BY is finer in diameter, less hairy, more flexible, and stretchable than cotton yarns (Majumdar and Pol, 2014). Bamboo is also a fast growing natural fibre with cellulosic fibres aligned along the length of the bamboo that provides maximum tensile strength, flexural strength, and rigidity (Kumar et al., 2016).

Moreover, BY has better antimicrobial and UV protection. Thus, it is interesting to study the handle behaviour, which is governed by the low stress mechanical properties of bamboo and bamboo blended with woven fabrics (Majumdar and Pol, 2014). Besides, the chemical and physical properties of cellulose do not only give strength and elasticity to the fibre, but also water affinity (due to its many hydroxyl groups) and permeability (Pinho et al., 2010).

#### **2.3.1.4 Application of BY**

Natural BY has many excellent properties and thus, explains its potential in textiles (Nayak and Mishra, 2016). BY constitutes a recent kind of natural material that has a huge application probability in the textile field due to some of its unique properties. For instance, it has a unique structure that makes it superior to other natural lignocellulose fibres (Nayak

and Mishra, 2016). Furthermore, due to the distinctive characteristics of regenerated BY, such as its natural antibacterial and biodegradable properties, high moisture absorption capacity, softness, brightness, as well as UV protective features; bamboo textile products have started to edge into the textile market. With its high moisture absorption capacity, breathability, and fast drying attributes due to its unique micro-structure; BY ensures comfort in various applications (Erdumlu and Ozipek, 2008). Bamboo is also an attractive plant fibres with a high potential to be used in polymer composite industry due to its light weight, high strength, biodegradability, and low cost (Sribenja and Saikrasun, 2015). Also, there has been a recent increase in the use of BY reinforced polymeric composite materials mainly due to the use of advanced processing technologies (Kumar et al., 2016). Among the natural fibres, bamboo pulp fibres made from cellulose of dissolved bamboo pulp have been applied in apparels, such as undergarments, sports textiles, T-shirts, and socks. The bamboo pulp fibres are also naturally smooth and very soft, therefore, they can be worn next to the skin (Peng et al., 2016). BY also has desirable comfortable properties, including good moisture absorption and permeability, as well as excellent dyeing and finishing abilities (Peng et al., 2016). For instance, knitted fabrics made from bamboo viscose yarns exhibited higher moisture vapour transmission and lower thermal resistance than cotton fabrics (Majumdar and Pol, 2014). Besides, bamboo fabrics have a very soft feel. Therefore, bamboo fabrics are popularly used for undergarments, socks, and sports clothing (Majumdar and Pol, 2014).

In recent times, these cellulosic fibres and waste cellulosic products, such as shell flour, wood flour, and pulp, have been extensively used for reinforcement of various thermosetting and thermoplastic resins. Moreover, natural fibre-based composites, especially those BY-based, have drawn huge interest due to their environmental-friendly and sustainable nature (Kumar et al., 2016). Since prehistoric times, natural dyes have been used for many purposes, such as colouring of natural fibres wool, cotton, and silk, including fur and leather (Mirjalili et al., 2011). Due to high fibre porosity, the bamboo textiles produce higher colour yields when dyed. Furthermore, issues revolving around the environment in conjunction to dyeing textiles have gained prime attention by the dyeing industry for quite some time (Larik et al., 2015).

### 2.3.1.5 Composition of BY

Natural cellulosic fibres consist of four main parts: cellulose, hemicelluloses, lignin, and pectin. The crystalline cellulosic part is distributed in the amorphous lignin matrix and provides reinforcement to the so-formed natural composite (Kumar et al., 2016). In addition, bamboo contains cellulosic fibres, which are a biological and functional material made of glucose with  $\beta$ -1,4-glucoside bonds and more than ten thousand of these D-glucopyranose sections without branching (Pinho et al., 2010). The major chemical constituents of bamboo are cellulose, hemicellulose, and lignin; accounting for over 90 % of the total mass, while the minor constituents are soluble polysaccharides, waxes, resins, tannins, proteins, and ashes. Other than that, bamboo culms consist of 60–70 % holocellulose (cellulose and hemicellulose = holocellulose), pentosans (20–25 %), hemicelluloses, and lignin (each amounts to about 20–30 %).

Overall, bamboo contains 40–50 % of  $\alpha$ -cellulose, which is comparable with the reported  $\alpha$ -cellulose contents of softwoods (40–52 %) and hardwoods (38–56 %). The content of cellulose in this range makes bamboo a suitable raw material for the pulp and paper industry. BY contains more than 70 % cellulose (Bamboo species: *Neosinocalamus affinis*, abundantly found in China). In general, the cellulose amounts as ‘holocellulose’ to more than 50 % of the chemical constituents. However, the attributes of hemicelluloses and particularly lignin are greater than that of flax and little less than that of jute fibre. Non-cellulose substances like pectin and hemicelluloses influence the fibre properties in terms of strength, flexibility, moisture, and density in a significant manner. Cellulose and hemicelluloses are carbohydrate polymer constituents of simple sugar monomers. Cellulose, like other plant cellulose, consists of linear chains of  $\beta$ -1-4-linked glucose anhydride units. Above 90 % of hemicelluloses in bamboo are comprised of xylan (4-O-acetyl-4-O-methyl-d-glucuronoxylan, a relatively short polymer with the degree of polymerization at 200). On the other hand, lignin (a typical grass lignin) is a polymer of phenyl-propane units (p-hydroxyphenyl) (H), guaiacyl (G), and syringyl (S) in a molar ratio of 10:68:22 (Nayak and Mishra, 2016). Figure 2.9 shows the chemical structure of cellulose in BY.

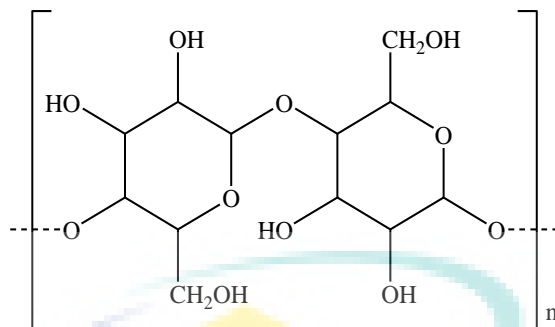


Figure 2.9 Chemical structure for cellulose BY

### 2.3.2 Mordanting

Most of the colouring dyes which extracted from natural resources were not capable of producing permanent colours on textiles by themselves. Textile fibres, especially cellulosic, do not have much affinity for most natural dyes; hence these are subjected to an additional step known as mordanting (Radhakrishnan, 2014). The fibres had to be prepared for the reception of the dye by impregnation with metallic oxides such as those of aluminium, iron, or tin. These substances were known as mordant. Essentially, they open the pores and combine with the fibre and this enables the dye to be chemically bonded. The mordant used in the past have been evaluated for their pre-mordanting and post-mordanting effects (Sachan and Kapoor, 2007). In fact, mordanting highlights two important aspects; the mordant and the method of mordanting.

#### 2.3.2.1 Types of Mordant

Mordant refers to a substance that is used to set dyes on fabrics or tissue sections by forming a coordination complex with the dye, which then gets attached to the fabric or tissue. It can be used for dyeing fabrics, or for intensifying stains in cell or tissue preparations. Moreover, the term 'mordant' derives from the Latin word, "mordere", which means 'to bite'. In the past, it was thought that a mordant helped the dye bite into fibres so that it would hold fast during washing. As such, a mordant is often a polyvalent metal ion. The resulting coordination complex of dye and ion is colloidal, which can be either acidic or alkaline (Tech, 2012). Therefore, mordant play a very important role in imparting colour onto fabrics.

Since mordant have affinity for both textile fibres and dyes, they act as a link between the fibre and the dyestuff. Thus, dyes without affinity for fibre can be applied by using mordant. In the case of dyes having affinity for fibre, the use of mordant increases the fastness properties through the formation of an insoluble complex of the dye and the mordant within the fibres, which also improves the colour. Metal mordant are often used for dyeing of textiles with natural dyes. Metal salts of aluminium, chromium, tin, copper, and iron have been used as mordant by traditional dyers. To date, chromium has been red-listed under eco-regulations and therefore, should not be used to maintain the eco-friendly nature of dyed textile material.

Copper is also in the restricted category, but its permissible levels are higher and can therefore, be used in small amounts so as not to cross the permissible limit on dyed textile. Meanwhile, tin is not restricted by many eco-labels, but its presence in effluent is not desirable from the environmental stance. Next, alum and iron can be considered as ecologically safe mordant as they are naturally present in the environment in large amounts. Different colours from the same dyestuff can be obtained by using various metallic mordant because colours obtained from natural dyes derive from the formation of coloured insoluble dye complexes with metal salts or mordant. Besides, dye complexes with varied metals have varying colours and may also differ in fastness properties. For instance, alizarin forms a red lake or complex with aluminium and a violet lake with iron. Similarly, onion natural dye, which is yellow in colour, changes to orange with stannous chloride mordant, whereas grey with ferrous sulphate (Radhakrishnan, 2014).

The mordant used in combination with varied ratios gave varying shades (Kulkarni and Bodake, 2011). In fact, most natural dyes need a mordanting chemical (preferably metal salt or suitably coordinating complex forming agents) to establish an affinity between the fibre and the dye or the pigment molecules. After mordanting, the metal salts anchoring to the fibres, attracts the dye/organic pigment molecules to be anchored to the fibres and to develop the bridging link between the dye molecules and the fibre by forming coordinating complexes (Visalakshi and Jawaharlal, 2013). Besides, the chemical nature of mordant and the fibre-mordant-dye interactions greatly modify the colour attributes in the dyed fabric.

Besides, the most commonly used mordant in natural dyeing to alter the colorimetric parameters and the fastness properties of dyed textile materials are aluminium, potassium dichromate, copper sulphate, ferrous sulphate, and stannous chloride (Rather et al., 2016). Although some papers have suggested tea pigments as textile dyes, most dyeing procedures demand mordant to improve colour fastness and to change the apparent colour (Ren et al., 2016). Furthermore, most natural dyes need a chemical in the form of metal salts to develop an affinity to the fibres and pigment. These chemicals are known as mordants (Kulkarni and Bodake, 2011).

Furthermore, in order to retain the colour of natural dyes selected in this research, Alum had been opted as the mordant. Alum or lime is added to this solution as a mordant, though in several parts of India, dyeing is done without mordant (Grover and Patni, 2011). Potash alum, which is a double sulphate of potassium and aluminium, is the most widely used aluminium mordant for natural dyeing that can be used alone or with cream of tartar or as a basic alum for mordanting. When used alone, the material, before dyeing, is boiled in a solution of alum. In addition, the amount of mordant required depends on the shade to be dyed. If deeper shades are sought, more mordant is needed. Generally, 10–20 % of alum can be used on the weight of the material (owm). Meanwhile, if used along with cream of tartar, alum powder (20 % owm) is mixed with cream of tartar (40 % owm) in some warm water and diluted to the required volume. Alum in the form of basic aluminium sulphate (neutral alum) has been used as a mordant for cotton. This is prepared by adding sodium hydroxide or carbonate solution to the aqueous solution of alum until the precipitate is formed to dissolve upon stirring. On top of that, the material to be treated is dipped in the alum solution and the latter is then fixed by other chemicals or ageing. Furthermore, it is preferable to fix the alumina on the fibre by precipitating it with salts, such as sodium carbonate or sodium phosphate, to obtain good dyeing results. Besides, neutral soap solution can also be used for this purpose (Radhakrishnan, 2014).

In this research project, the mordant Aluminium Sulphate (Alum) was used as the mordant to absorb the dyes from BBPF, RDFP, and Turmeric on BY. This is because; Alum is easily available and it has no toxic properties, which makes it safe for customer use. It is also the most common type of mordant used for dyeing process for natural dye. However, it

should be handled with care and not ingested. Moreover, the use of mordant promotes the binding of dye to fibre by forming a chemical bridge that enhances the dye uptake of the fibre (Sribenja and Saikrasun, 2015). So far, most of the dyeing processes use metallic mordant and many metallic mordant are, unfortunately, toxic and have serious effect upon the environment (Sribenja and Saikrasun, 2015). Mordants are also an essential component for natural dyeing processes to achieve a broad spectrum of colours with varied patterns and special performance features on numerous natural and synthetic textile materials (Rather et al., 2016).

Mordanting with alum can generate bright strawberry shade, which is slightly lighter, stronger, and redder. Moreover, alum has shown the highest colour value (WS=6.46), and followed by iron, while tin gave marginal increase in the colour value compared to the control, which happened to be 4.85 (Lokhande and Dorugade, 1999). Moreover, many scopes are available to use the turmeric dye in order to obtain numerous colour shades using safe mordant under eco-friendly textile dyeing. A variety of shades, for instance, bright yellow, golden glow, ivory, sunset yellow, buff, light khaki, golden yellow, cream, smoke brown, pineapple, olive green, lemon, etc., could be retrieved (Sachan and Kapoor, 2007).

### **2.3.2.2 Types of Mordanting Methods**

Several types of mordanting processes are available, whereby first, the mordant is applied and followed by dyeing (pre-mordanting process) or by simultaneous application of the dye and the mordant (meta-mordanting process) or with after treatment of the dyed material with the mordant (post-mordanting process). As this study attempted to analyse the effect of mordant on DBY, post-mordanting was selected as the method of mordanting in order to justify the effect of mordant itself on DBY. This is because; pre-mordanting involves padding with the mordant first, and followed by padding with the dye. Padding with a dye-mordant mixture is known as meta-mordanting or simultaneous mordanting, while initial padding of dye, and followed by mordant is known as post-mordanting (Ratnapandian et al., 2012). As such, three processes of mordanting were employed: pre-mordanting, simultaneous mordanting, and post-mordanting. After dyeing, the dyed material was washed with cold water and dried at room temperature (Kulkarni and Bodake, 2011).



In the post-mordanting method, the fabric, after dyeing, is treated with mordant in a separate bath. The final colour is developed at the last phase. Iron salts are applied in this stage to produce grey and black shades. In the meta-mordanting or simultaneous mordanting method, both dyeing and mordanting processes are carried out in the same bath (Radhakrishnan, 2014). Table 2.4 presents the literature of mordanting methods and the types of mordant commonly used in studies that looked into dyeing.

Table 2.4 Literature of mordanting methods and the types of mordants used for dyeing

Method of Mordanting	Type of Mordant	Author
Pre-Mordanting, Meta-Mordanting and Post-Mordanting	Copper sulphate and ferrous sulphate	Kulkarni and Bodake, 2011
Pre-Mordanting, Meta-Mordanting and Post-Mordanting	Copper sulphate and ferrous sulphate	Ratnapandian, et al., 2012
Post-Mordanting	Aluminium sulphate, ferrous sulphate, and ferric sulphate	Zhou et al., 2015
Post-Mordanting	Alum, ferrous sulphate, and stannous chloride	Shabbir et al., 2016
Pre-Mordanting, Meta-Mordanting and Post-Mordanting	Alum, potassium dichromate, ferrous sulphate hydrate, copper sulphate hydrate, stannous chloride and sodium chloride	Meksi et al., 2012
Pre-Mordanting and Post-Mordanting	Alum and ferrous sulphate	Ali et al., 2009
Pre-Mordanting, Meta-Mordanting and Post-Mordanting	Aluminium potassium sulphate, ferrous sulphate, copper sulphate, and stannous chloride	Punrattanasin et al., 2013

### 2.3.3 Optimization Strategies

Optimization reflects the improvement of a performance for a process, a product or a system in order to achieve maximum benefits. Generally, the term ‘optimization’ is used in analytical chemistry as a means of discovering conditions applicable to a procedure that

generates the best possible response. As such, screening is one way that determines the factors that return the best possible outcome (response). Generally, there are two different strategies for screening: one-factor-at-a-time (OFAT) and Response Surface Method (RSM). The process of extracting natural dyes from BBPF, RDRP, and turmeric, as well as the dyeing of natural dyes selected onto BY had been optimized in order to determine the optimum conditions for every variable studied. The process of optimization for the study referred to the response surface plan.

### 2.3.3.1 Parameters of the Dyeing Conditions

The following chapter discusses various natural dyeing parameters, including dye concentration, mordant, treatment time, and pH. Surprisingly, these variables vary widely in literature. General natural dyeing studies were reviewed instead of only studies using selected natural dyes because very few studies investigated selected dyes on BY.

#### *Dye bath concentration*

Overall, concentration of dye bath for extraction of natural dyes varied widely depending on dye and fabric or yarn used. Adeel et al. (2017), Tech (2012) and Koyuncu (2014) added dye to the dye bath based on their weight of fabric or yarn used in the experiment. Adeel et al. (2017) was carried out the dyeing of cotton with marigold flower using material to liquid ratios of 0.100, 0.500, 0.033, 0.025, 0.020 and 0.017 g/mL in a series of experiments. Tech (2012) were tested 3 natural dyes, including Henna, Neem and Turmeric dye and their dyeing concentration were carried out at concentration of 0.100 g/mL. The woollen yarns were dyed in a bath containing extracted *Rubia tinctorum* L. dye at 0.001 g/mL (Koyuncu, 2014). Based on these three studies, the dye bath concentration studied by Tech (2012) and Koyuncu(2014) were exceptionally effective because it only needed 0.100 and 0.001 g/mL concentration respectively to produce colour strength comparable to other natural dyes. Adeel et al. (2017)'s wide range of dye bath concentrations suggests natural dye concentration varies substantially between dyes. When testing marigold flower dye, Adeel et al. (2017) did not use a dye bath with a specific dye bath concentration but reinforcing the idea of optimal dyeing techniques for natural dyes.

### *Dye bath pH*

From the literature review, three studies investigated the effect of pH on the dyeing process. All the studies used similar procedures to modify the dye bath pH by some variation in acids or alkaline. Dye bath pH can have significant effects on colour strength (Adeel et al., 2017). Variation of dye bath pH (4, 5, 6, 7, 8 and 9) were tested in the paper of Adeel et al. (2017). Dyeing of cotton with Henna, Neem and Turmeric dye were carried out at range of pH 4.5 to 10 by Tech (2012). However, Koyuncu (2014) was carried out the experiment at fixed pH. The woollen yarns were dyed at pH 5 in a bath containing extracted *Rubia tinctorum* L. dye (Koyuncu, 2014). The studies were discovered that pH was playing important role in the dyeing process.

### *Dyeing time*

In previous natural dye studies, dyeing time stayed consistent for dyeing of natural dyes by Tech (2012), Kanchana et al. (2013) and Koyuncu (2014) except Adeel et al., (2017). Tech (2012) was left the cotton in Henna, Neem and Turmeric dye for 60 minutes. The dyeing process of woollen yarns with *Rubia tinctorum* L. dye was performed for 45 minutes by Koyuncu (2014). While Kanchana et al. (2013) was performed the dyeing of cotton with pomegranate, BBPF and marigold flowers dyes for 30 minutes. Adeel et al. (2017) left the test sample of cotton in marigold flower extract for 25, 30, 40, 55, 70 and 85 minutes. Adeel et al., (2017) did not use a specific time in the dyeing process and promotes the optimization in gaining the best conditions for dyeing their samples.

### *Dyeing temperature*

In previous studies, dyeing temperature varied within a small range. In Adeel et al., (2017)'s study, the effect of dyeing temperature on colour strength of marigold flower colorant has been observed and the dyeing was carried out at 30, 40, 50, 60, 70 and 80 °C. the dyeing of cotton with Henna, Neem and Turmeric dye were done by Tech (2012) at temperature 60°C. Koyuncu, (2014) was performed the experiment of dyeing the woollen yarns with *Rubia tinctorum* L. dye initially at 25°C and the temperature was gradually raised till boiling point (94°C-98°C). The dyes of pomegranate, BBPF and marigold flowers were

extracted and the dyeing process was done at 28 and 100°C (Kanchana et al., 2013). Above that temperature range, the dye bath lost up to 100 % of its colours.

### **2.3.3.2 One-Factor-At-A-Time (OFAT) Approach**

Optimization of dyeing process are important in gaining optimum conditions for dyeing of selected natural dyes on BY with the highest percent dye uptake. It is necessary to employ a sequential study with OFAT methods and RSM on optimization of dyeing of natural dyes from BBPF, RDRP, and turmeric on BY. The application of RSM was essential in order to overcome the limitation of using OFAT.

### **2.3.3.3 Response Surface Method (RSM)**

In the present of study, an overview of the existing research studies on dyeing of natural dyes on BY with the aid of RSM are being provided. The RSM was applied to determine the optimized conditions for dyeing process. Therefore, in order to get the best conditions and to determine the level of parameters for dyeing of natural dyes on BY; the process should be optimized. However, to the best of the researcher's knowledge, no study has looked into the application of RSM on optimization of dyeing of natural dyes on BY. Therefore, in order to evaluate the effects of parameters and to optimize these media components, RSM was employed in the present study. The RSM is definitely an effective statistical technique to optimize complex processes.

## **2.4 Adsorption**

Adsorption is an effective and relatively inexpensive method used in the treatment processes. Highly porous adsorbents with good selectivity, such as activated carbon, have shown excellent ability as an effective adsorbent in removing many aqueous contaminants; both organic and inorganic, such as dyestuffs and certain metal ions. Besides, the high adsorption capacity of activated carbon is a result of its high surface area, extensive porosity in the interior of the particles, and the presence of various types of surface functional groups (Chan et al., 2012). An adsorption isotherm represents how adsorption molecules reach the equilibrium state during the adsorbing process in both liquid and solid phases. Besides, the time required to reach the equilibrium state is known as adsorption equilibrium time. Furthermore, the balance between adsorbing time and dye adsorption capacity reflects the

saturated adsorption capacity of the bio sorbent under the various operating conditions. Additionally, data analysis is required to fit different isothermal adsorption models to determine the model that best fits for the adsorbing process (Zhang et al., 2015). In the case of bamboo fibre, there is poor adhesion between the fibre and the natural acid dyes. Besides, the adsorption study on bamboo dyeing system has yet to be studied systematically. In this study, the adsorption behaviour and the kinetics of dyeing of natural dyes selected in this study on BY had been investigated. As such, Langmuir, Freundlich, Temkin and Dubinin-Radushkevich isotherms were employed to determine the fit of the equilibrium adsorption data of natural dye onto BY. Table 2.5 presents the literature on several adsorption studies using various isotherms, adsorbents, and adsorbates.

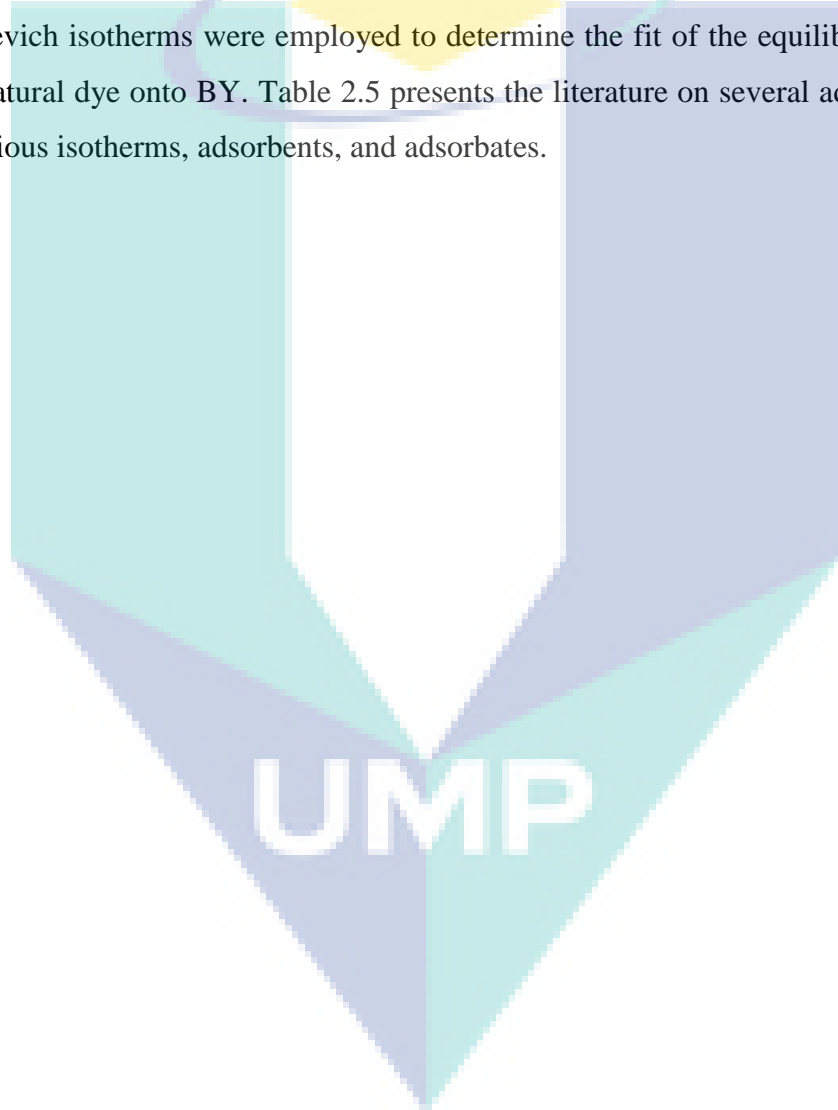


Table 2.5 Literature on adsorption studies using various isotherms, adsorbents, and adsorbates

<b>Isotherm</b>	<b>Adsorbent</b>	<b>Adsorbate</b>	<b>Author</b>
Langmuir and Freundlich	Silica aerogel	Rhodamine B and Methylene blue	Han et al., 2016
Langmuir	Pine Cone Powder Modified with $\beta$ -Cyclodextrin	safranine O, brilliant green and methylene blue	Debnath et al., 2016
Langmuir and Freundlich	Wool	Gardenia yellow natural dye	Shen et al., 2014
Langmuir	Clay/polyaniline/ $Fe_3O_4$ nanocomposite	Brilliant green, Methylene blue, and Congo red	Mu et al., 2016
Langmuir, Freundlich, Redlich-Peterson, and Hill	Woollen yarn	<i>Adhatoda vasica</i> natural dye	Rather et al., 2016
Langmuir	Bamboo fibre	cationic copolymer nanoparticles	Liu et al., 2015
Langmuir	ZnO nanoparticles	cationic dye (malachite green) and anionic dyes (acid fuchsin and Congo red)	Zhang et al., 2016
Langmuir, Freundlich, Tempkin, Toth, Redlich-Peterson and Sips	Bamboo Derived Activated Carbon	Acid Yellow 117 (AY117) and Acid Blue 25 (AB25)	Chan et al., 2012
Langmuir and Freundlich	woollen yarn	<i>Terminalia chebula</i> natural dye	Shabbir et al., 2016
Langmuir, Freundlich, Redlich-Peterson, Tempkin, and Toth	Activated carbon, Bagasse pith, Fullers earth, Kudzu, Peat, Lignite, Silica and Peanut hulls	Basic blue 3, Basic yellow 21, and Basic red 22	Allen et al., 2004)

### 2.4.1 Principal of adsorption

Adsorption is a surface-based process that is basic for the equilibrium process named physisorption. In physisorption, adsorbate adheres to the surface of the adsorbent through weak intermolecular interactions, for example, van der Waals forces and covalent bonding. Then again, chemisorption is likewise a kind of adsorption, in which a molecule adheres to a surface by forming chemical bonds via interaction of ionic bonding and hydrogen bonding.

With a specific end goal to get an unmistakable perspective of the method of fascination of the colour to the fibre, information of the strengths which tie the colours to the strands is of evident significance in the present audit. In most dyeing processes, the material to be coloured is carried into contact with a transfer medium containing the colour. The most widely recognized transfer medium is water, in which the colour might be dissolved or dispersed. During dyeing the dye passes through this solution or dispersion into the fibre. The transport of the dye from the solution into the fibre might be viewed as involving three stages. Transfer of dye from the bulk of the solution to the fibre surface, sorption of dye at the fibre surface, and penetration of the dye into the interior of the fibre substance.

The main activity in any dyeing processes is consequently the concentration of the dye molecules at the internal surface of the fibre as the dye can reach. The concentration so produced is however, not usually sufficient to give a usefully deep coloration and fastness properties required of a dyed material. It is required that the dye be associated strongly with the fibre to make it resistant to such agents as water, detergents, perspiration, weather, solvent etc. For this to be achieved, other factors must be brought into play. These are the chemical forces which can operate between a dye molecule and a fibre molecule, and also those between the dye molecules themselves which can cause their association into larger units. These forces have been classified as ionic forces, hydrogen bonding, covalent bonding and van der Waals forces

### **2.4.1.1 Ionic Interaction**

This is the mutual attractions between positive centres in a fibre and negative centres in a dye molecule and between negative fibre sites and positive centre in a dye molecule. This is the case when an atom transfers its electron to another atom, the one that lost the electron becoming positively charged while the atom that received the electron will become negatively charged. These types of forces play a large part in the dyeing of protein fibres with acid and direct dyes, nylon with acid dyes and polyacrylics with basic dyes.

### **2.4.1.2 Hydrogen Bonding**

These result from the acceptance by a covalently bound hydrogen atom of a lone pair of electrons from an electron donor atom. Hydrogen bonding can act in five different ways which are intermolecularly extending over many molecules, intermolecularly joining two molecules together, intermolecularly where the electron donating is by double bond linkage, intramolecularly forming a chelate ring and intramolecularly as in hydrogen fluoride (HF<sub>2</sub>). Hydrogen bonding has some properties of normal valency bonding. They interact when the atoms approach within very close distance to each other. They are relatively of the order of 8.4-49.4 kJ/Mol. They are relatively easy to form and break. Hydrogen bonding is applied almost in all dyes in all systems.

### **2.4.1.3 Covalent Bonding**

These are chemical bonds between dyes and substrate molecules. They are brought about by chemical reaction between a reactive dye molecule and the substrate molecule, example hydroxyl group of a cotton fibre. In fact, covalent bonding has to do with primary valency bonding where each of the participating atoms has to donate one electron to the common linkage. This is the strongest of all dye and fibre bonds. They have the highest energy of about 84 kJ/Mol. Covalent bonding is the bond responsible in reactive dye bond on leather, wool and nylon.



#### 2.4.1.4 Van Der Waals Forces

These are forces existing between atoms and molecules of all substances and are small compared with the other inter-atomic forces present in the dyeing process. They are the result of second order wave mechanical interaction of the  $\pi$  orbital of dye and fibre molecules. These forces are especially effective when the dye molecules are linear, i.e. long and flat and can approach close enough to the fibre molecules or molecular unit.

#### 2.4.2 Desorption

Desorption is a process, in which a substance is released from or through a surface. This process is the opposite of sorption, which refers to either adsorption or absorption. This occurs in a system being in the state of sorption equilibrium between bulk phase (fluid, i.e. gas or liquid solution) and an adsorbing surface, which in most cases, is in the form of solid. When the concentration of substance in the bulk phase is lowered, some of the sorbed substance changes to the bulk state. After adsorption, the adsorbed chemical would remain on the substrate, provided the temperature remains low. However, if the temperature rises, so does the likelihood of desorption to occur (Adeel et al., 2017). In this research, after performing all the experiments of adsorption process, a simple procedure was carried out to determine if desorption of the dye did take place after the drying process. Based on the above details, most findings have been only related to the adsorption process of synthetic dyes as adsorbate onto many varied adsorbents, such as hen feathers, moss peat, and dried kudzu, to name a few. The adsorption process of natural dyes onto adsorbents, however, is to no avail, probably because none had been conducted. Therefore, this research had looked into the efficiency of adsorption of natural dyes onto adsorbents. This research, hence, may become the source for many more upcoming researches concerning the adsorption of different natural dyes on adsorbents.

## 2.5 Characterization

Characterization, or examining the structure or properties of a material, is commonly included in textile dyeing studies to examine dyes and yarns. Common characterization tests include Fourier-Transform Infrared (FTIR) spectroscopy, Scanning Electron Microscope (SEM), and ultraviolet-visible (UV-VIS) spectrophotometer. Of these tests, FTIR was the most commonly used test in the literature reviewed (Bukhari et al., 2017, Bhuiyan et al., 2017, Zhang et al., 2016 and Shahid et al., 2017)

The FTIR spectra were used to identify the presence of functional groups within the natural dyes and BY (Haddar et al., 2014). The FTIR, in fact, is the most preferred method of infrared spectroscopy. This can help determine compatibility and dye ability of selected natural dyes on BY. Analysing the chemical structures present on the dye could give insight into which colorant pigments are present in BBPF dye, RDFP dye and turmeric dye. Knowledge of these chemical groups could further strengthen the ability to determine the dye ability of dyes on BY. The scanning electron microscope (SEM) is usually used to intuitively investigate the surface structure of a solid (Haddar et al., 2014). In this study, SEM was employed to examine the surface structure of both undyed and dyed bamboo yarns, which to identify phases based on qualitative chemical analysis of dyes on BY. Meanwhile, as for this research, UV-VIS spectrophotometer had been employed to determine the amount of colour pigment contents in natural dyes and the amount of colour pigments adsorbed onto BY. Furthermore, the wavelength applied to investigate the adsorptions of blue, red, and yellow dyes extracted from BBPF, RDFP, and Turmeric were 525nm, 538nm, and 419nm, respectively.

## 2.6 Summary

The research emphasises on the utilization of vast diversity of natural resources of dyes and fibre for use in the textile industry in place of their synthetic counterparts. This is aimed to safeguard human health, offer convenience to consumers, as well as to protect and to prolong life on Earth. Natural dyes play an important role in the textile industry in order to produce safe fabric for consumers, to be environmental-friendly, and to reduce costs. Thus, the enhancement of all the aspects, beginning from extraction parts until the dyeing of the

fabrics itself had been looked into. In fact, the natural fibre should produce highly comfortable fabrics for users, besides keeping away one from deleterious aspects, both to human and to our environment. Most research conducted on natural dyeing has used cotton as its test fabric. Few studies were found that applied natural dye to non-cotton natural fabrics or synthetic fabrics. This narrows the research's applicability. Most dyeing variables investigated regarding natural dyeing in the literature were fairly similar, but there was little to no explanation for extraction of the natural dyes extracted from BBPF, RDFP, and turmeric. These natural dyes are not yet to be commercially used in the textile industry. Therefore, the natural dyes need to be commercialized in order to replace and to provide an alternative way of applying the synthetic dye in the textile industry. Moreover, the application of selected natural dyes on the BY was not being reviewed by other researcher. As such, there is a need to focus far on the area of research and developmental effort on natural dyes and natural fibres.

The optimizing of extraction of natural dyes and dyeing them onto natural fibre have to be applied in this area in order to reduce the cost of productions, besides avoiding any waste in the textile industry. Hence, as experimental design was devised in order to study the effects of process variables on dyeing quality, as well as to determine their optimum conditions. The colour pigments from BBPF, RDFP, and turmeric were extracted by using water as their solvent. Water is the safest, cheapest, and the most ideal solvent used in industrial applications. However, the Alum mordant was also applied on the dyeing of natural dyes due to the limited ideal accelerating effect and resulting dyed fibres, while the post-mordanting method had been adopted. The adsorption study, in addition, is important to comprehend the mechanisms of dyeing natural dyes on BY. Hence, four adsorption isotherms; Langmuir, Freundlich, Temkin, and Dubinin-Radukevich model isotherms, and the kinetic studies of dyeing natural dyes onto BY were investigated by using Pseudo-first order model and Pseudo-second order model were applied in order to determine the fit of the experiment data and mechanism of the adsorption of each colorant pigments onto BY.

## CHAPTER 3

### MATERIALS AND METHODOLOGY

#### 3.1 Introduction

This research was undertaken to characterize Blue Butterfly Pea Flower (BBPF), Red Dragon Fruit Peel (RDFP), and Turmeric as raw materials for natural extraction of dyes, while Bamboo Yarn (BY) was employed as the fibre for dyeing process. The optimization of extraction natural dye and dyeing the BY are also explained in this chapter. In this chapter, the conceptual framework for the study concerning natural dyes and process of dyeing it onto BY is presented. Furthermore, this study is comprised of four phases: i) characterization of fibre and colour of dyes, ii) extraction of natural dyes and dyeing of natural dyes onto BY, iii) adsorption study of dyeing natural dyes onto BY, as well as iv) mordanting and desorption studies. This chapter also provides information pertaining to the experimental procedures for extraction of dyes from BBPF, RDFP, and Turmeric; the process of BY mordanting; and the process of dye adsorption onto BY. For ease of comprehension, a flow diagram summarizing the overall experimental approach for the dyeing process of natural dyes onto BY is illustrated in Figure 3.1.

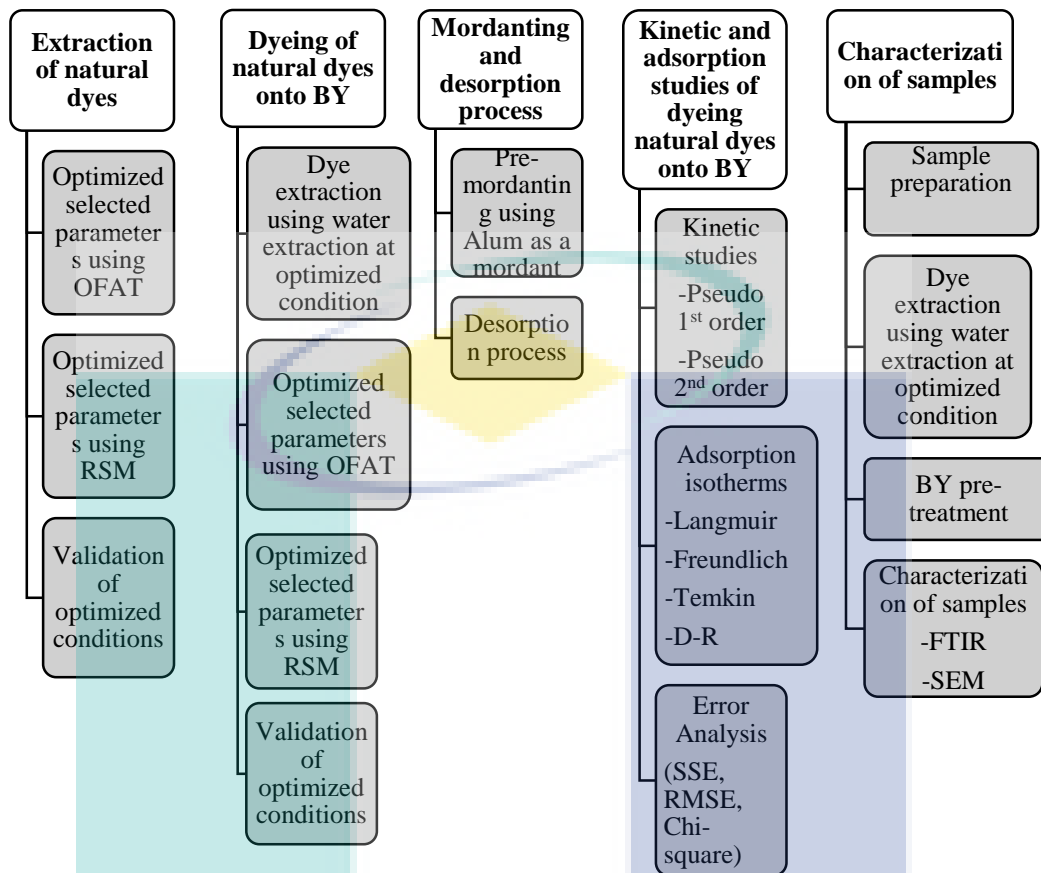


Figure 3.1 Experimental flowchart for dyeing of natural dyes from BBPF, RDFP and Turmeric on BY.

## 3.2 Materials

### 3.2.1 Chemicals and Reagents

All the chemicals used in the current study were of analytical grade and purchased from various suppliers. The list of chemicals used in this study is given in Appendix A. Furthermore, dissolved water was used to prepare various solutions and reagents.

### 3.2.2 Blue Butterfly Pea Flower (BBPF)

The BBPF were obtained from the backyard at the researcher's home and neighbours at Taman Mahkota Aman, Kuantan, Pahang. The raw material was kept dried in the oven at the laboratory and then, was ground.

### **3.2.3 Red Dragon Fruit Peel (RDFP)**

The RDF were collected from a commercial orchard located at Gambang, Pahang, Malaysia. The raw material was peeled to get its waste, which was then blended and stored at -20°C for not more than 2 days (48 hours), so that the blended material was kept fresh and to avoid the colour from fading due to oxidation process.

### **3.2.4 Turmeric**

The fresh turmeric was obtained from a mall in Taman Tas, Kuantan, Pahang. The raw material was peeled and then blended into small pieces. The blended turmeric was stored at -20°C for not more than 2 days (48 hours) in order to preserve it fresh and to avoid the colour from fading due to oxidation.

### **3.2.5 Bamboo Yarn (BY)**

Bamboo yarns (BY) were provided by Pusat Tenun Pekan, Pahang, which was made with 100% of bamboo fibres.

## **3.3 Operational Framework**

This research was conducted to determine the optimum parameters for extraction of natural dyes and optimum parameters for dyeing of natural dyes on BY. The schematic diagram that summarizes the main experimental procedure of this study is presented in Figure 3.2.

### **3.3.1 Phase 1: Extraction of natural dyes**

This phase describes the extraction of natural dyes from BBPF, RDFP, and Turmeric. The objective of this phase was to determine the optimum conditions of parameters for the extraction of colours from natural dyes deriving from BBPF, RDFP, and Turmeric. In fact, this phase is comprised of two steps: i) the study on the effects of extraction Time, Temperature, and Solid Liquid Ratio (SLR) upon extraction of natural dyes via OFAT method, and ii) the optimization of extraction of natural dyes via CCD in RSM, as well as the determination of optimum conditions that looked into the influences of extraction Time, Temperature, and SLR, as determined by OFAT as well. Phase 2: Dyeing of natural dyes onto BY.

### **3.3.2 Phase 2: Dyeing of natural dyes on BY**

In this phase, the results of the optimum conditions of influential parameters for extraction of natural dyes from BBPF and Turmeric were employed to prepare the extracted dyes, while that for RDFP was referred to literature review. Moreover, the BY was dyed by using the prepared extracted dyes. Thus, the effects of dyeing time, temperature, SLR, and pH were studied. The significant factors that affected the dyeing of extracted dyes on BY were identified by using the OFAT method. Moreover, the optimization of dyeing natural dyes on BY process was carried out and the interactions among the significant variables (dyeing time, temperature, dye bath concentration, and dye bath pH) that governed the DB were determined with RSM.

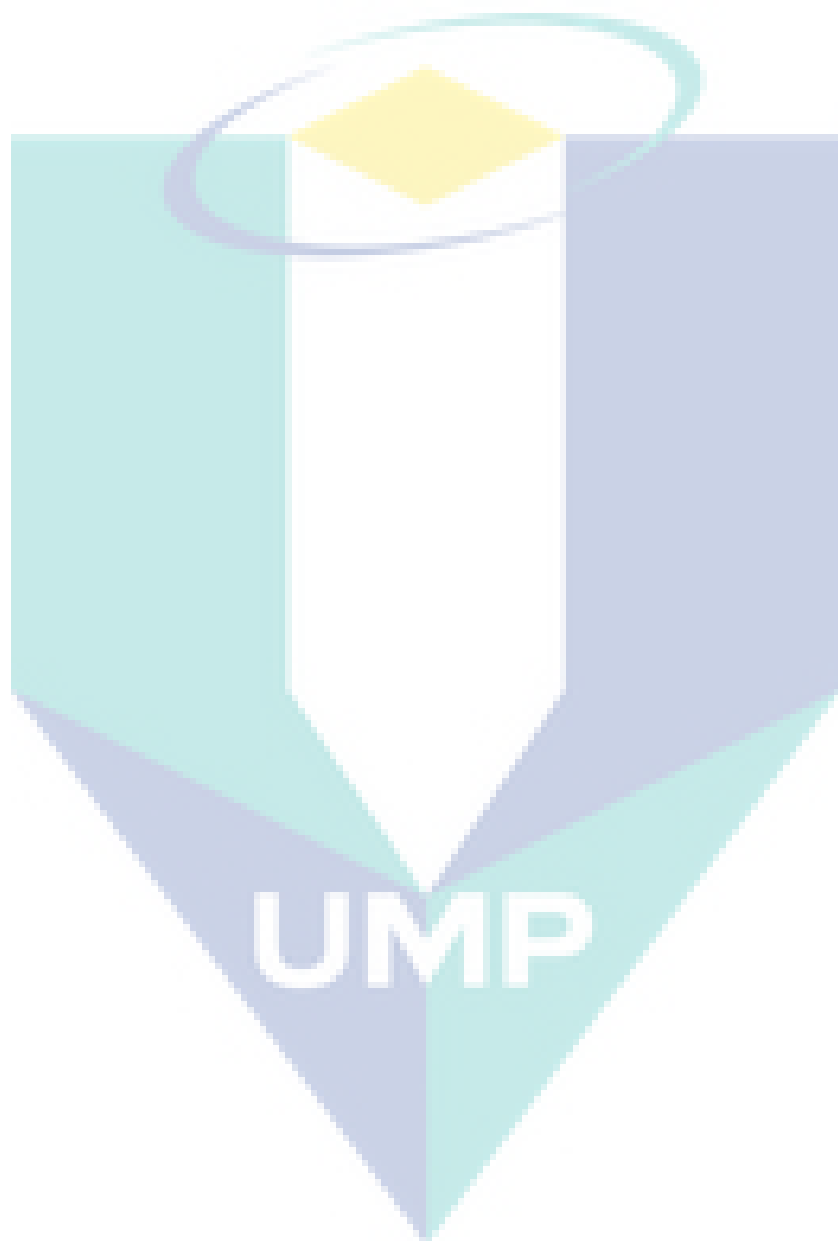
### **3.3.3 Phase 3: Adsorption study of dyeing natural dyes onto BY**

The fundamental studies on adsorption isotherm, kinetics of dyeing natural dyes via BY process, and the desorption process are important to comprehend the dyeing mechanisms, besides improving the dyeing performance of natural dyes on BY. Hence, in order to understand meticulously the attributes of natural dyes on BY, the parameters of equation adsorption isotherms by Langmuir, Freundlich, Temkin, and Dubinin-Radushkevish isotherm models equation, as well as evaluation of model equations and the error analysis, had been conducted. The desorption process was performed to analyse the effects of Alum mordant on DBY by adopting the post-mordanting method, as well as to investigate the desorption process of natural dyes from DBY.

### **3.3.4 Phase 4: Characterization of samples**

The characterization of samples was carried out by using UV-VIS spectroscopy, FTIR spectroscopy, and SEM. The samples included were extracted dyes; blue, red, and yellow dyes extracted from BBPF, RDFP, and Turmeric respectively, PBY, DBY and MBY. The UV-VIS spectroscopy was conducted to identify the absorbance reading from these samples. Thus, calculation was done to determine the colour pigment contents and concentration. Meanwhile, the FTIR spectroscopy was performed to confirm the structure of the samples by indicating the functional group of colour pigments and BY. Other than that, since this study had employed the reaction process, better understanding of characteristics of

the raw materials and products is very important in order to elucidate the correlations between raw materials for the extraction process and the dyeing process. Additionally, the structural, the optical, and the surface morphology of the samples were observed using SEM.





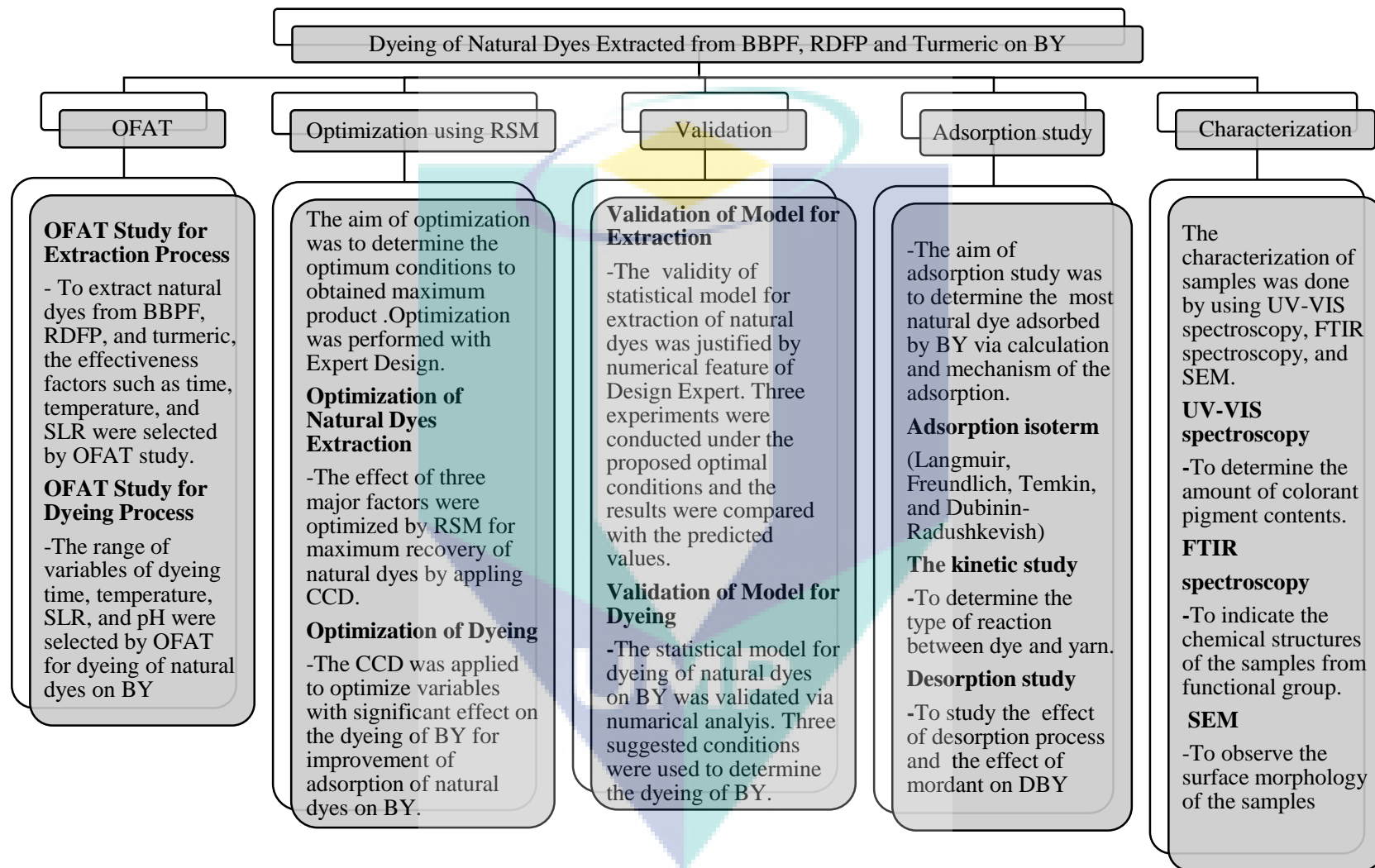


Figure 3.2 Schematic diagram of operational framework of this study

### **3.4 Extraction of Natural Dyes**

#### **3.4.1 Preparation of Anthocyanin Extract from BBPF**

The extraction of blue natural dye was prepared by using water extraction. BBPF was first cleaned and dried in oven at temperature 35 °C in order to remove all the moisture content from the flower for 24 hours. Then, the flower was ground into small pieces, about 1mm, to increase its surface area. Then, the blue natural dye was extracted by applying a ratio of 0.12 g/mL corresponding to the ratio of 1.2 g of raw material to 10 mL of water (Suebkhampet and Sotthibandhu, 2012 and Kanchana et al., 2013). The mixture was then centrifuged at 4 °C and 10000 rpm for 15 minutes (Makasana et al., 2016). The mixture was filtered to collect the supernatant dye. Finally, filtration of the supernatant was done by using whatman filter paper, while the pH was adjusted with HCl and NaOH, if needed (Suebkhampet and Sotthibandhu, 2012). The preparation of extraction BBPF dye was given in Appendix C 1.

#### **3.4.2 Preparation of Betacyanin Extract from RDFP**

The natural dye was prepared by using water extraction. The purpose of using water extraction is to ascertain that the colour is safe from any chemical or harmful substance. RDFP was first cleaned and the unnecessary part of the dragon fruit peel was discarded. The dragon fruit peel was then blended into small pieces, about 1 mm, to increase its surface area. Then, the red natural dye was extracted by applying a ratio of 0.12 g/mL corresponding to the ratio of 1.2 g of raw material to 10 mL of water. The mixture was then centrifuged at 4 °C and 10000 rpm for 15 minutes (Fathordoobady et al., 2016). The mixture was filtered to collect the supernatant dye. The mixture was again centrifuged at 4 °C and 12000 rpm for 10 minutes to completely eliminate the presence of sediment or precipitate in the dye solution. Finally, filtration of the supernatant was done by using filter paper (Al-Alwani et al., 2015), while the pH was adjusted with HCl and NaOH, if needed. The resulting extract was used for further analysis. The preparation of extraction RDFP dye was given in Appendix C 2.

### **3.4.3 Preparation of Curcumin Extract from Turmeric**

The turmeric was first cleaned and the peels were removed. The turmeric was then blended into small pieces, about 1mm, to increase its surface area. Then, the yellow natural dye was extracted by applying a ratio of 0.12 g/mL corresponding to the ratio of 1.2 g of raw material to 10 mL of distilled water. The mixture was then centrifuged at 4 °C and 10000 rpm for 15 minutes (Anusuya and Sathiyabama, 2016). The mixture was filtered to collect the supernatant dye. The mixture was again centrifuged at 4 °C and 12000 rpm for 10 minutes (Sachan and Kapoor, 2007) to ascertain the elimination of any sediment or precipitate in the dye solution. Finally, filtration of the supernatant was done by using a stainless filter paper, while the pH was adjusted with HCl and NaOH, if needed. The resulting extract was used for further analysis. The preparation of extraction turmeric dye was given in Appendix C 3.

### **3.4.4 OFAT of Extraction Process**

The effects of extraction time, temperature, and solid to liquid ratio (SLR) on the natural dyes extraction had been determined with the OFAT method in order to derive at the optimum range of parameters. The variation of the process parameters employed for each study is portrayed in Table 3.1 which had been selected based on previous reports concerning extraction of natural dyes (Ali et al., 2009 and Sinha et al., 2012). The readings of absorbance for all samples were measured by using UV-VIS Spectrophotometer and the results were recorded. The first parameter was then varied until an optimum reading of absorbance was attained. This optimum value for the first factor was then used, while the second parameter was varied, and so on. For the initial OFAT experiment, the level of two factors out of three had been held constant. The concentration of colorant pigments of each natural dyes being calculated using calibration curve of the standards.

Table 3.1 OFAT for Extraction of BBPF and Turmeric

Study	Time (minutes)	Temperature °C	SLR (g/mL)
<b>BBPF</b>			
Time	5,10,15,20,25,30,40	60	1:20
Temperature	10	30,40,50,60,70,80	1:20
SLR	10	60	1:5,1:10,1:20,1:30,1:40,1:50
<b>Turmeric</b>			
Time	5,10,15,20,25,30,40	60	1:20
Temperature	10	30,40,50,60,70,80	1:20
SLR	10	60	1:5,1:10,1:20,1:30,1:40,1:50

### 3.4.5 RSM of Extraction Process

The optimization study on natural dyes extraction was further continued with the central composite design (CCD) of RSM for blue, red, and yellow dye yields, while selectivity as the dependant variables or responses of the design experiment (Sachan and Kapoor, 2007). The optimum levels of the three major independent variables, namely time, temperature, and SLR had been selected from the results derived from the OFAT study. The range of optimum conditions for all parameters had been analysed in the software Design Expert V 8.0.6. This method is suitable to fit a quadratic surface, and it helps to optimize the effective parameters with a minimum number of experiments, besides looking into the interaction between the parameters. In addition, the experimental design was conducted by using the Design Expert software (version 8.0) developed based on the CCD. The CCD was performed with a  $2^3$  full factorial CCD of a combination of factors at two levels (high, +1 and low, 1 levels), including six star points (axial) corresponding to any value of 2 and six replicates at the centre points (coded level 0, midpoint of high, and low levels); thus resulting in 15 sets of experimental runs. Furthermore, the ranges and the levels of independent variables are listed in Table 3.2. In this design, the extraction of the natural dyes from BBPF, RDFP, and Turmeric were examined to determine the effects of independent variables upon each dye i.e., temperature of extraction, time of the extraction, and SLR. The ranges of each parameter were evaluated in OFAT and inserted in the RSM. Generally, the primary objective of RSM is to optimize the response based on the factor investigated. As such, the Design Expert software (version 8.0) was used to develop the experimental plan and to optimize the independent variable for temperature, time, and SLR for the extraction of the

selected natural dyes in this research. The statistical significance of the second-order model equation was also determined by carrying out the Fisher's statistical test for analysis of variance (ANOVA). In precise, a good model must be significant based on *F*-value and *P*-value, while being insignificant for Lack of Fit. Other than that, the proportion of variance exhibited by the multiple coefficient of determination  $R^2$  should be close to 1. This is because; when it is closer to 1, a better correlation between the experimental and predicted values can be achieved. Additionally, the optimum values of the input variables were acquired via numerical analysis through the use of Design Expert program based on the criterion of desirability. As such, three sets of experiments were carried out under the proposed optimal conditions to validate the CCD developed model. On top of that, a confirmation experiment was also carried out to prove the model.

Table 3.2 Ranges and levels of independent variables involved in CCD for extraction of natural dyes

Variables	Symbol	Range and levels				
		- $\alpha$	-1	0	1	+ $\alpha$
<b>BBPF</b>						
Temperature, ° C	A	5	25	45	65	85
Time, min	B	10	15	20	25	30
SLR, g/mL	C	0.062	0.083	0.104	0.125	0.246
<b>Turmeric</b>						
Temperature, ° C	A	12.5	30	47.5	65	82.5
Time, min	B	15	20	25	30	35
SLR, g/mL	C	0.062	0.083	0.104	0.125	0.246

### 3.5 Dyeing of Natural Dyes on Bamboo Yarn (BY)

By using the values of optimum conditions for dye bath concentration, temperature, and time in extracting BBPF and turmeric, while for RDFP based on literature review, the dyeing of BY samples had been conducted.

#### 3.5.1 Sample Preparation

The preparation of the blue natural dye was prepared similar to the previous procedure, but this time, employing the optimum conditions for SLR, temperature, and time in the extraction process. The absorbance of natural dye solution prepared was measured by

using UV-Vis Spectrophotometer and the results were recorded. The experiment then was continued to the dyeing of BY with 1:100 ratio weight of BY in blue dye solution. The BY in blue dye solution was agitated in the incubator shaker KS4000i at about 100 rpm at room temperature. The samples of BBPF, RDFP and turmeric dye was left 30 minutes at pH 4.2, 4.5 and 8.5 respectively. The reading of dye solution after the dyeing process was recorded. The pH was later adjusted with HCl and NaOH, if needed. The preparation of dyeing of BBPF, RDFP and turmeric dye were given in Appendix C 4, Appendix C 5 and Appendix C 6 respectively.

### **3.5.2 Mordanting Process**

The BY, which represented the fibres in this experiment, was first subjected to thorough washing with distilled water. By using the optimum conditions of extraction in preparing the natural dyes and the optimum conditions of dyeing natural dyes on BY, the dried DBY was then soaked in a 25 % aluminium sulphate (Alum) solution, which functioned as a mordant. The mordant solution was heated up to 70°C and then left to cool for 45 minutes. The fibres were then removed from the mordant solution and rinsed well with water. The preparation of mordanting process for dyed BY with BBPF, RDFP and turmeric dye were given in Appendix C 7.

### **3.5.3 OFAT of Dyeing Process**

The effects of dyeing time, temperature, SLR of the dyes solution, and pH of the dyes solution on the dyeing of natural dyes on BY had been examined with the OFAT method to derive at the optimum range of parameters. The variation of the process parameters employed for each study is presented in Table 3.3, which had been selected based on prior reports concerning the dyeing of natural dyes onto fibre (Ali et al., 2009 and Punrattanasin et al., 2013). Optimization of dyeing is really important in gaining optimum consuming condition of dye and reagents with the highest exhaustion (Nasirizadeh et al., 2012). In the OFAT method, one parameter is variant, while the others are held constant. For the initial OFAT experiment, the level of three factors out of four were held constant. The preparation for dyeing of natural dyes on BY sample adhered to the similar procedure by changing one parameter. The dyeing of BY with natural dyes solution samples underwent OFAT in order to determine the optimum conditions of dyeing natural dyes on BY for

dyeing time, temperature, SLR of the dyes solution, and pH of the dyes solution. Furthermore, the absorbance of dyes solution before and after dyeing for all samples were measured using UV-VIS Spectrophotometer and the results were recorded.

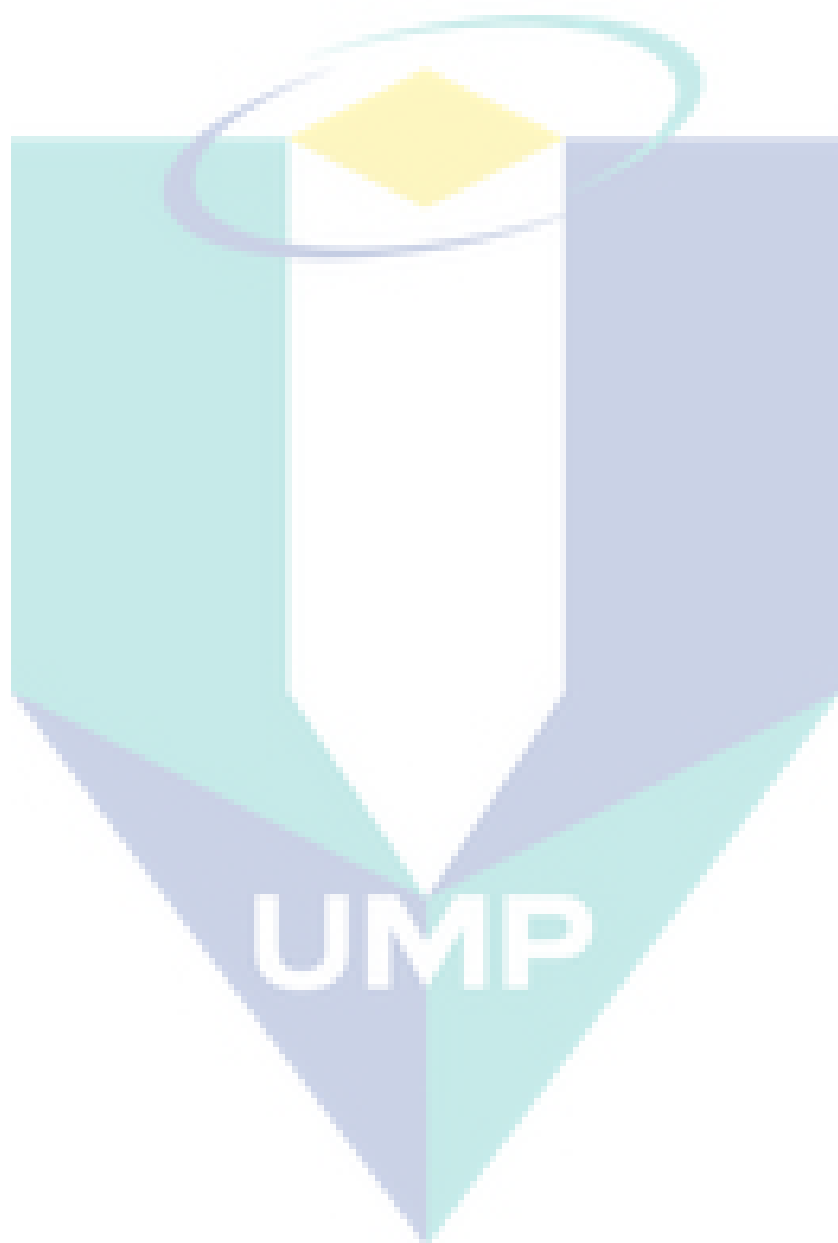


Table 3.3 OFAT for Dyeing of BBPF, RDFP, and Turmeric on BY

<b>Study</b>	<b>Time (min)</b>	<b>Temperature °C</b>	<b>SLR (g/mL)</b>	<b>pH</b>
<b>BBPF</b>				
Time	5,10,15,20,25,30,40	60	1:10	5.2
Temperature	30	30,40,50,60,70,80,90	1:10	5.2
SLR	30	60	1:5,1:10,1:20,1:30,1:40,1:50	5.2
pH	30	60	1:10	2,3,5,7,0,11
<b>RDFP</b>				
Time	5,10,15,20,25,30,40	50	1:10	4.5
Temperature	30	30,40,50,60,70,80,90	1:10	4.5
SLR	30	50	1:5,1:10,1:20,1:30,1:40,1:50	4.5
pH	30	50	1:10	2,3,5,7,0,11
<b>Turmeric</b>				
Time	5,10,15,20,25,30,40	60	1:10	8.5
Temperature	30	30,40,50,60,70,80,90	1:10	8.5
SLR	30	60	1:5,1:10,1:20,1:30,1:40,1:50	8.5
pH	30	60	1:10	2,3,5,7,0,11



### 3.5.4 RSM of Dyeing Process

After the range of optimum conditions and absorbance for all parameters had been determined from the OFAT approach, CCD in RSM was carried out in order to obtain the optimum values for dyeing time, temperature, SLR of the dyes solution, and pH of the dyes solution. The range of optimum conditions for all parameters were further analysed with the software Design Expert V 8.0.6. The CCD was used to investigate the significance of the effects of dyeing time, temperature, SLR of the dyes solution, and pH of the dyes solution on dyeing natural dyes on BY. As such, the ranges and the levels of the variables are listed in Table 3.4. As a result, a four-factor and four-level CCD led to 21 runs for both RDFP and Turmeric, while a three-factor and four-level led to 15 runs for BBPF in order to carry out the optimization of the dyeing of BY parameters. The experimental sequence was randomized in order to minimize the effects of the uncontrolled factors. In fact, the CCD consists of  $2n$  factorial points with  $2n$  axial points and central points. The centre points are used to determine the experimental error and the reproducibility of the data. Besides, the independent variables are coded to the  $(-1, +1)$  interval, where the low and high levels are coded as  $-1$  and  $+1$ , respectively. Additionally, the statistical significance of the model equation and the regression coefficient had been determined by performing the analysis of variance (ANOVA). This analysis included Fischer's test ( $F$ -test), its associated probability, inclusive of the determination of coefficient ( $R^2$ ) and correlation coefficient ( $R$ ). The optimum values of the input variables were acquired via numerical analysis by utilizing the Design Expert program based on criterion of desirability. Hence, three sets of experiments were carried out under the proposed optimal conditions to validate the CCD developed model. On top of that, a confirmation experiment was also carried out to prove the model.

Table 3.4 Ranges and levels of independent variables involved in CCD for dyeing of natural dyes on BY

Variables	Symbol	Range and levels				
		$-\alpha$	-1	0	1	$+\alpha$
<b>BBPF</b>						
SLR, g/mL	A	0.02	0.062	0.104	0.146	0.188
Time, min	B	5	35	65	95	125
pH	C	0	1	5	9	13
<b>RDFP</b>						
SLR, g/mL	A	0.977	0.1	0.123	0.146	0.169
Time, min	B	50	70	90	110	130
pH	C	0	1	3	5	7
Temperature, ° C	D	30	50	70	90	110
<b>Turmeric</b>						
SLR, g/mL	A	0.02	0.062	0.104	0.146	0.188
Time, min	B	20	40	60	80	100
pH	C	0	1	3	5	7
Temperature, ° C	D	30	50	70	90	110

### 3.6 Adsorption Study of Dyeing Natural Dyes on Bamboo Yarn (BY)

#### 3.6.1 Equilibrium time

The experiment to determine the time required for the adsorption to reach equilibrium was performed by applying the batch technique at room temperature (25 °C). The test tubes were filled with 20 mL of stock dye solution and 0.2 g of the BY was placed into the test tube, which was later agitated in incubator shaker KS4000i at 100 rpm at room temperature. Next, the liquid samples were taken after 10-minute interval for 100 minutes and the concentration of dye adsorbed had been analysed by using the UV-Vis Spectrophotometer.

#### 3.6.2 Adsorption isotherm

Varied dye concentration solutions were prepared by using different dilution factors of the dye. The dilution factors were 1.07, 1.15, 1.25, 1.36 and 1.50 respectively (Table 3.5). Besides, distilled water was used as blank in this analysis. The optical density of the solution was then measured by adding the dye solution into the cuvette using a micropipette and then,

placing the cuvette into the spectrophotometer. In addition, the wavelength was set to 525, 538, and 419 nm for blue, red, and yellow dyes, respectively which has been referred previous research work in the literature review. The optical density for each dye concentration was then recorded. The 0.3 g of BY was soaked in a 30 mL test tube containing the dye solution at varied concentrations. Then, they were left until reach equilibrium time for dye solution and another 24 hours for drying process. After equilibrium time reached, the fabric was removed from the test tubes and then, the dye solution remaining in the test tubes underwent the similar process to determine the optical density of the solution using a spectrophotometer. After obtaining the optical density readings before and after the adsorption process, the values were introduced to the equation mentioned below to calculate the total anthocyanin content in BBPF, betacyanin content in RDFP, and curcumin content in turmeric, which had been adsorbed by the BY.

Table 3.5 Water and Dye ratio for Dilution Factor

Dilution Factor	Water (mL)	Dye (mL)
1.07	2	28
1.15	4	26
1.25	6	24
1.36	8	22
1.5	10	20

### 3.6.3 Adsorption isotherm models

Adsorption isotherms were used to describe the correlations between the adsorbent concentrations and the adsorbate amount on the unit mass of adsorbent at equilibrium. Furthermore, adsorption isotherms revealed information related to the physicochemical attribute concerning the adsorption proceeds and the interaction of dyes with the surface of the adsorbent. Besides, an accurate mathematical description of equilibrium adsorption capacities, even if empirical, is indispensable for reliable predictive modelling of adsorption systems and quantitative comparisons of adsorption behaviour for the varied adsorbent systems or for varied conditions within any given system (Allen et al., 2004). As such, three adsorption isotherms, namely Langmuir, Freundlich, Temkin and Dubinin-Radushevich isotherm models were used to determine the fit of experimental data. Additionally, the non-

linear least-squares fitting procedure was applied to identify the most appropriate model for adsorption behaviour of natural dyes onto BY. The amount of dye adsorbed per unit weight of BY at equilibrium  $q_e$  (mg/g BY) was calculated by using eq.(3.1). Besides, the adsorption capacity  $q_e$  (mg of dye per g of adsorbent) was calculated by using the following equation. Where  $C_0$  is the initial dye concentration (mg/L) in the solution,  $C_e$  is the Unbound dye concentration (mg/L) at equilibrium,  $V$  is the initial volume (L) of the dye solution,  $m$  is the dry adsorbent dosage (g), and  $W$  is the weight of BY (g) (Bu et al., 2016).

$$q_e = \frac{(C_0 - C_e)V}{W} \quad 3.1$$

### 3.6.3.1 Langmuir Isotherm

Langmuir isotherm, as described by the adsorbate-adsorbent systems, looks into the extent of adsorbate coverage dependent on one molecular layer at or before a relative pressure of unity is attained. Although the isotherm is usually used to describe chemisorption, the equation also obeys moderately low coverages by a number of systems, which can be used to describe the behaviour of binary adsorbate systems. In fact, the most widely used two-variable equation to determine the adsorption characteristics is the Langmuir isotherm. The Langmuir adsorption isotherm model has been successfully applied to many other real sorption processes. Graphically, it is characterized by a plateau and an equilibrium saturation point, where no further adsorption can take place once a molecule occupies a particular site. On top of that, the Langmuir theory has related a rapid decrease of intermolecular forces of attraction with increased distance (Shabbir et al., 2016). Theoretically, a saturation value is reached beyond, in which no further sorption can take place. The saturated monolayer curve, moreover, can be represented by the expression presented in eq. (3.2). Where  $q_e$  and  $C_e$  are the amount of dye adsorbed per gram of BY (mg/g) and dye concentration (mg/mL) in dye bath at equilibrium, respectively. Meanwhile,  $q_{max}$  (mg/g BY) is the maximum dye adsorbed per unit weight of BY for complete monolayer adsorption, and  $K_L$  is the Langmuir constant related to affinity of the binding sites (mL/mg).

$$\frac{1}{q_e} = \frac{1}{q_{max}} + \frac{1}{q_{max}K_L C_e} \quad 3.2$$

### 3.6.3.2 Freundlich isotherm

Freundlich isotherm is also an adsorption isotherm, in which a curve is related to the concentration of a solute on the surface of adsorbent to the concentration of solute that is present in liquid, in which it is in contact. Freundlich isotherm is usually used to describe interactions between adsorbate and adsorbent, where multilayer adsorption takes place with non-uniform distribution of adsorption heat and affinities over the heterogeneous surface (Shabbir et al., 2016). Moreover, the linear form of Freundlich equation can be represented as follows.

$$q_e = a^f C_e^{b_f} \quad 3.3$$

$$\log q_e = \log K_f + \frac{1}{n} \log C_e \quad 3.4$$

Where  $q_e$  and  $C_e$  are the amount of dye adsorbed per gram of BY (mg/g) and dye concentration (mg/mL) in dye bath at equilibrium respectively. Meanwhile,  $K_f$  is the Freundlich adsorption constant, and  $n$  is the adsorption intensity. Moreover,  $K_f$  and  $n$  can be determined from slope and intercept of linear plot  $\log q_e$  versus  $\log C_e$ . In fact, the value of  $n > 1$  represents favorable adsorption

### 3.6.3.3 Temkin isotherm

This isotherm contains a factor that explicitly weighs in adsorbent–adsorbate interactions. By ignoring the extremely low and large value of concentrations, the model assumes that heat of adsorption (function of temperature) of all molecules in the layer would decrease linearly rather than logarithmic with coverage (Dada et al., 2012). As depicted in the equation below, its derivation is characterized by a uniform distribution of binding energies (up to some maximum binding energy), which is carried out by plotting the quantity sorbed  $q_e$  against  $\ln C_e$  and the constants are determined from the slope and the intercept.

$$q_e = \frac{RT}{b_T} \ln A_T C_e \quad 3.5$$

$$q_e = B_1 \ln K_T + B_1 \ln C_e \quad 3.6$$

$$q_e = \frac{RT}{b_T} \ln A_T + \frac{RT}{b_T} \ln C_e \quad 3.7$$

Where  $C_e$  (mg/L) is the equilibrium concentration of dye solution,  $q_e$  (mg/g) and  $K_L$  (L/mg) are the maximum adsorption capacity and equilibrium adsorption constant for Langmuir isotherm model, respectively. Meanwhile,  $K_F$  (L/mg) of Freundlich isotherm model is related to the magnitude of adsorption driving force, and  $1/n$  implies the degree of non-linearity between solution concentration and adsorption (Zhang et al., 2016). On top of that,  $K_T$  (L/mg) is the equilibrium binding constant of Temkin isotherm model corresponding to the maximum binding energy, Constant  $B_1$  is related to the heat of adsorption,  $RT$  is associated to the adsorption heat, and  $A_T$  refers to the equilibrium constant corresponding to the maximum bind energy. The isotherm parameters of  $b_T$  were calculated from the intercept and the slope of the plot  $q_e$  versus  $\ln C_e$ .

#### 3.6.3.4 Dubinin-Radushkevish isotherm

Dubinin–Radushkevich isotherm is generally applied to express the adsorption mechanism with the Gaussian energy distribution onto a heterogeneous surface (Dada et al., 2012). The model has often been successfully fitted with high solute activities and intermediate range of concentrations data. This isotherm is normally used to determine if the adsorption is chemical or physical in nature (Wei and Brien, 2014). The D-R isotherm equation and its linearized form are given in Eq. (3.9)

$$q_e = q_D \exp(-\beta_D \varepsilon^2) \quad 3.8$$

$$\ln q_e = \ln q_D - \beta_D \varepsilon^2 \quad 3.9$$

Where  $q_e$  is the adsorption capacity at equilibrium (mol/g),  $q_D$  is Dubinin–Radushkevich monolayer saturation capacity (mol/g),  $\beta_D$  is constant related to the mean free energy of adsorption per mole of the adsorbate ( $\text{mol}^2/\text{J}^2$ ), and  $\varepsilon^2$  is polyani potential related to equilibrium concentration ( $\text{J}^2/\text{mol}^2$ ).

$$\varepsilon = RT \ln(1 + 1/C_e) \quad 3.10$$

Where R is the gas constant (8.314 J/mol. K), T is absolute temperature (K), and  $C_e$  is the equilibrium dye concentration. By plotting  $\ln q_e$  versus  $\varepsilon^2$ ,  $q_D$  and  $\beta_D$  can be obtained. Furthermore, constant  $\beta_D$  gives an idea about the mean free energy,  $E_{DR}$  (kJ/mol) of adsorption per mole of the dye when it transfers to the surface of the solid from infinity in the solution. However, if the adsorbent surface is heterogeneous and homogeneous, sub regions are considered and mean free energy value could be calculated by using Eq. (3.11).

$$E_{DR} = \frac{1}{\sqrt{2\beta_D}} \quad 3.11$$

This parameter is useful to estimate the type of adsorption interaction. If the adsorption process is primarily physical in nature, such as van der waals forces, the average free energy typically falls in the range of 1–8 kJ/mol. Nonetheless, if  $E_{DR}$  is between 8 and 16 kJ/mol, the adsorption process is chemisorption via ion exchange.

Table 3.6 The linearized equation transformed and intercept for isotherms model

Isotherm	Linearized Equation	Y-axis	Slope, m	X-axis	Intercept, C
Langmuir	$\frac{1}{q_e} = \frac{1}{q_{max}} + \frac{1}{q_{max}K_L C_e}$	$\frac{1}{q_e}$	$\frac{1}{q_{max}K_L}$	$\frac{1}{C_e}$	$\frac{1}{q_{max}}$
Freundlich	$\log q_e = \log K_F + \frac{1}{n} \log C_e$	$\log q_e$	$\frac{1}{n}$	$\log C_e$	$\log K_F$
Temkin	$q_e = \frac{RT}{b_T} \ln A_T + \frac{RT}{b_T} \ln C_e$	$q_e$	$\frac{RT}{b_T}$	$\ln C_e$	$\frac{RT}{b_T} \ln A_T$
Dubinin-Radushkevish	$\ln q_e = \ln q_D - \beta_D \varepsilon^2$	$\ln q_e$	$\beta_D$	$\varepsilon^2$	$\ln q_D$

### 3.6.4 Kinetic study

In order to elucidate the adsorption kinetic process, pseudo-first- and pseudo-second-order kinetic equations were adopted to describe the adsorption process. The pseudo-first-order and pseudo-second-order kinetic models are expressed in Eq. (3.12) and Eq. (3.13).

$$\log(q_e - q_t) = \log q_e - \frac{K_1}{2.303} t \quad 3.12$$

$$\frac{t}{q_t} = \frac{1}{K_2 q_e^2} + \frac{1}{q_e} t \quad 3.13$$

Where  $q_e$  and  $q_t$  are the amounts of dyes adsorbed on BY (mg/g) at equilibrium and time  $t$ , respectively. Besides,  $K_1$  (1/min) refers to the equilibrium rate constant of pseudo-first-order, while  $K_2$  (g /mg.min) is the rate constant of pseudo-second-order. Hence, the kinetic parameters were calculated for dye adsorption on BY (Bu et al., 2016).

### 3.6.5 Desorption Process

In order to ascertain the feasibility of the dye adsorption experiment, it is necessary to determine if the dye solution on the fibre did undergo desorption when it was soaked in water. Therefore, this feasibility test was carried out upon the fibre with the best concentration of dye adsorbed. Thus, the MBY with the best dye concentrations had been soaked in 20 mL of water in test tubes and after 10 minutes, the optical density of the water solution was taken and the reading was recorded.

### 3.6.6 Calculations of anthocyanin pigments

The total anthocyanin content was determined spectrophotometrically at 525 nm based on the standard calibration curve as in Eq. (3.14). Moreover, the total anthocyanin were quantified using equivalents cyanidin-3-glucoside (mg/L) (Pan et al., 2014). MW is the molecular weight of cyanidin (449.2 g/mol), V is the volume of extract, DF is the dilution factor,  $\epsilon$  is the mean molar absorptivity (29600 mol.cm/L) and L is the path length (1 cm).

$$\text{Total anthocyanin content} \left( \frac{\text{mg}}{\text{L}} \right) = \frac{A \times \text{MW} \times \text{DF}}{\epsilon \times L} \times 1000 \quad 3.14$$

The difference in anthocyanin content (AC) can be determined by using the following formula:

$$\text{AC}(\text{before adsorption}) - \text{AC}(\text{after adsorption}) = \text{AC on BY} \quad 3.15$$



### 3.6.7 Calculations of betacyanin pigments

The total betacyanin content was determined based on the method reported by Fathordoobady et al. (2016), in which the maximum absorbance of betacyanin was 538 nm. The experiment was conducted by using a spectrophotometer with diluted aqueous extracts of RDFP using UV-Vis spectrophotometer. The total betacyanin content is calculated by using Eq. (3.16).

$$\text{Total Betacyanin Content} \left( \frac{\text{mg}}{\text{L}} \right) = \frac{A(MW)V(DF)}{\epsilon L} \times 1000 \quad 3.16$$

Where A is the value of absorption at the maximum absorbance ( $\lambda = 538\text{nm}$ ), MW is the molecular weight of betacyanin (550 g/mol), V is the volume of extract, DF is the dilution factor,  $\epsilon$  is the mean molar absorptivity (60000 mol.cm/L), and L is the path length (1 cm) (Fathordoobady et al., 2016). Besides, the difference in betacyanin content(BC) can be determined using the following formula:

$$\text{BC}(\text{before adsorption}) - \text{BC}(\text{after adsorption}) = \text{BC on BY} \quad 3.17$$

### 3.6.8 Calculations of curcumin pigments

The curcumin content was estimated as per the method using standard calibration curve. Fresh turmeric was extracted with water. The level of intensity of yellow colouring both extract and standard had been measured at 425 nm using a spectrophotometer (Hmar et al., 2016) and the curcumin content was calculated from the following Eq.(3.18):

$$\text{Total Curcumin Content} \left( \frac{\text{mg}}{\text{L}} \right) = \frac{A(MW)V(DF)}{\epsilon L} \times 1000 \quad 3.18$$

Where, A is the value of absorption at the maximum absorbance ( $\lambda = 425\text{nm}$ ), W is the molecular weight of curcumin (368.38 g/mol), L is cell length in cm, C is the concentration in mg/mL, V is the volume of extract, DF is the dilution factor, and  $\epsilon$  is the mean molar absorptivity (23800 mol.cm/L). The difference in curcumin content (CC) can be determined by using the following formula:

$$\text{CC}(\text{before adsorption}) - \text{CC}(\text{after adsorption}) = \text{CC on BY} \quad 3.19$$

### 3.6.9 Adsorptive capacity

The amount of dye adsorbed onto a fabric in equilibrium can be calculated by using the following formula (Aboul-Fetouh et al., 2010):

$$q_e = \frac{(C_o - C_e)V}{W} \quad 3.20$$

Where,  $C_o$  is the initial concentration of solution (mg/L),  $C_e$  is the equilibrium concentration of solution (mg/L),  $V$  is the volume of solution (L), and  $W$  is the weight of adsorbent BY (g).

## 3.7 Characterization of the Samples

### 3.7.1 Fourier Transform Infra-Red (FTIR) Spectroscopy Analysis

A small quantity of the dye extract was digested with paraffin oil. The dissolved sample was then spread on a transparent sodium chloride cell and placed back in the mountable holder and then scanned. The spectrograph of the percentage transmittance was obtained and the number of the various functioning groups present in the sample assessed.

### 3.7.2 Scanning Electron Microscope (SEM) Analysis

Before SEM characterization, the surface dusts are removed by blowing a compressed gas. Gloves must be worn all the time during sample preparation and transfer. The samples are mounted on a stub of metal with adhesive, coated with 40-60 nm of metal such as Gold/Palladium and then observed in the microscope.

## 3.8 Summary

This chapter were discussed the methodology used in the extraction of the selected natural dyes from local resources. The extraction of natural dyes was optimized using OFAT method. The ranges of parameters selected in this study was then used for further optimized via RSM. The dyeing process and adsorption methodology has been extensively elaborated. Furthermore, the characterization of samples also has been discussed in this chapter.

## CHAPTER 4

### EXTRACTION OF NATURAL DYES

#### 4.1 Introduction

The present study was carried out to extract the selected natural dyes and then, dyed upon BY, which is inclusive of the process of extraction of natural dyes from BBPF, RDFP, and Turmeric, dyeing of the three natural dyes (BBPF, RDFP, and Turmeric) onto BY, adsorption of the dyeing, and characterization of the samples. As such, the results and discussion of this work are composed of four chapters, namely Chapter 4: extraction of the natural dyes, Chapter 5: dyeing of the natural dyes on bamboo yarn (BY), Chapter 6: adsorption study on the dyeing of natural dyes, and Chapter 7: the characterization of the samples. In this chapter, the experimental results of extraction of natural dyes are presented. The extraction of these natural dyes had been optimized by using OFAT and RSM procedures, which are discussed in detail in the following subsections.

#### 4.2 Design of Parameters for Natural Dye Extraction

Basically, the research was carried out for parameter design or optimization of the chemical process in order to determine the impact of one variable at a time for an experimental response. The extraction of two natural dyes from BBPF and Turmeric were optimized by the OFAT approach for maximum extraction of natural dyes. The objective of the OFAT approach is to study the effect reaction of extraction on the solid liquid ratio (SLR) of BBPF and Turmeric, time, and temperature. In the first step of optimization process, the effective range of factors listed for extraction of natural dyes had been observed. The influences of three operational parameters upon extraction of natural dyes had been evaluated by applying the OFAT method. The colorant pigment that gives blue colour to the dye is known as anthocyanin (Kazuma et al., 2003). Curcumin is responsible for the yellow colour

(Amalraj et al., 2016). The results on the effect of the three parameters of BBPF extracts were obtained from OFAT, whereby the optimum conditions range was further optimized in RSM and the related effects of extraction parameters are discussed in detail in the following subsection.

#### 4.2.1 Effect of solid liquid ratio (SLR)

Various levels of the SLR were investigated to determine the optimum SLR for the extraction of maximum recovery of BBPF dye. Figure 4.1 shows the effect of SLR on extraction of BBPF and turmeric dye at constant values of temperature (60 °C), time (10 minutes), and pH (4.2 and 8.5 respectively). The highest concentration of anthocyanin content in blue dye achieved was 34.945 µg/mL with an SLR of 0.100 g/mL. The absorbance at SLR 0.10 mg/L was higher due to the maximum amount of anthocyanin dissolved in distilled water and it reached the equilibrium point. The concentration of anthocyanin content of blue dye, nevertheless, dropped significantly with further increase in SLR, indicating the reduced concentration of colorant pigment and that the anthocyanin had attained its saturation point in distilled water at SLR 0.200 g/mL. Moreover, the effect of SLR for extraction of natural dye was observed. It clearly shows that the increase in weight of solid turmeric added into the 50 mL of distilled water further increased the concentration of curcumin content in dye solution. This resulted in increment of curcumin content in the yellow dye until SLR was at 0.100 g/mL which is highest point at 14.425 µg/mL, until it attained equilibrium. The concentration of curcumin was found to increase with the increasing SLR up to 0.100 g/mL. Furthermore, due to the increase in SLR, the concentration and the viscosity of the solvent decreased, whereas the dissolving capacity of the pigment was found to increase. Maran et al., (2015) research on extracting the natural pigments from *Bougainvillea glabra* flower. Their research was observed that as SLR increased, viscosity of the solvent increased as well, which led to the decrease in concentration of curcumin in the dye (Maran et al., 2015). Sinha et al., (2012) has been reported that the extraction of dye increased with increasing the weight of dried pomegranate rind.

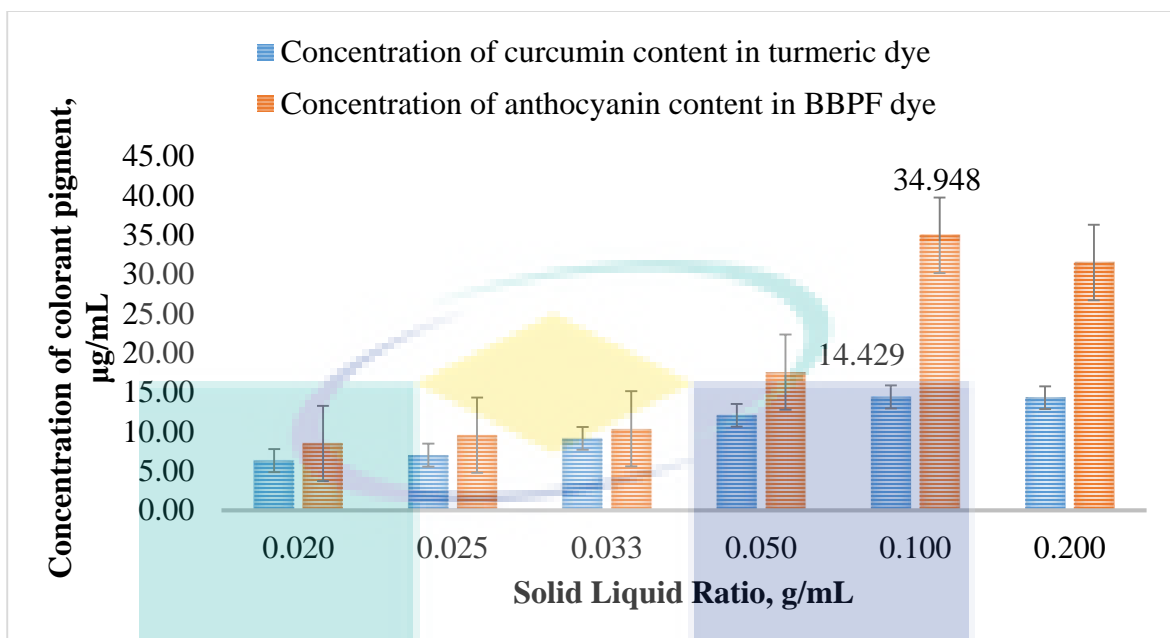


Figure 4.1 Effect of SLR on the extraction of the BBPF dye and turmeric dye at temperature ( $60\text{ }^{\circ}\text{C}$ ), time (10 minutes), and pH (4.2 and 8.5 respectively)

#### 4.2.2 Effect of extraction temperature

In order to evaluate the effect of temperature on the extraction of colorant pigments in the BBPF and turmeric dye, six temperature levels varying from  $30\text{--}80\text{ }^{\circ}\text{C}$  were employed, while keeping the other parameters constant. Besides, the related data are presented in Figure 4.2. The concentration of anthocyanin, nonetheless, increased with the hike in temperature until it reached a maximum value of  $19.787\text{ }\mu\text{g/mL}$  at  $60\text{ }^{\circ}\text{C}$  when other factors were fixed; SLR at  $0.05\text{ g/mL}$ , time at 10 minutes, and pH 4.2. Moreover, as noted, the concentration of anthocyanin increased with the increase in extraction temperature until it reached a maximum value at  $60\text{ }^{\circ}\text{C}$ , and then, it decreased. The increment in the extracted anthocyanin amount with the increasing extraction temperature is also reported in Arici et al., (2016). Moreover, the raising temperature up to the critical level, at which the extraction of anthocyanin increased due to the increasing diffusion coefficient and solubility of anthocyanin; indicated that the anthocyanin extraction increases with the increase in extraction temperature. Increasing the temperature leads to a steady decrease in water permittivity, viscosity and surface tension, but rise in its diffusivity properties which assisted the extraction process (Valizadeh et al., 2016). Permittivity, also called electric

permittivity, is a constant of proportionality that exists between electric displacement and electric field intensity. The historical term for the relative permittivity is dielectric constant. Increases in the temperature of the extraction cause the decreases in the permittivity of the water or dielectric constant and decreases the electric flux density. This caused reduces the inability of the surface of yarn to hold their electric charge for long period of times or to hold large quantities of charge. Thus, the concentration of the colorant pigment extracted being increases until the equilibrium achieved. Figure 4.3 shows the degradation of anthocyanin mechanism when the extraction temperature reached higher than 70 °C. However, temperature higher than 60 °C resulted in decreased absorbance due to decomposition of anthocyanin. This result is in agreement with the findings obtained by Arici et al., (2016), who reported that anthocyanin extracted form tulip petal was degraded at higher temperature levels. Similar findings were reported by Dranca and Oroian, (2016) for anthocyanin and phenolic compounds extraction from eggplant (*Solanum melongena* L.) peel and it indicates the high temperatures than 70 °C could also cause higher degradation rates of anthocyanin and phenolic compounds.

The temperature of extraction of turmeric dye was varied from 30-80 °C at constant for SLR at 0.050 g/mL, 10 minutes, and pH 8.5. As observed, the concentration of curcumin increased with the increase of extraction temperature until it reached a maximum value at 60 °C, and then, it decreased. This is most probably due to the decrease in dielectric constant of water and decreases in the electric flux density, which dissolved more curcumin. This caused the surface of yarn unable to hold their electric charge for long period of times or to hold large quantities of charge and caused the increment in the concentration of curcumin extracted until the temperature achieved 60 °C. In addition, the decrease in surface tension and viscosity of water might assist in dissolving the curcumin. However, temperature higher than 60 °C resulted in the decrease in colorant pigment content in dye solution due to the decomposition of curcumin at a higher temperature. The decrease in extraction at higher temperature could be due to degradation and hydrolysis of polyphenolic compounds that exist in curcumin which has been reported by Valizadeh et al., (2016) where they studied on high performance curcumin subcritical water extraction from turmeric (*Curcuma longa* L.).

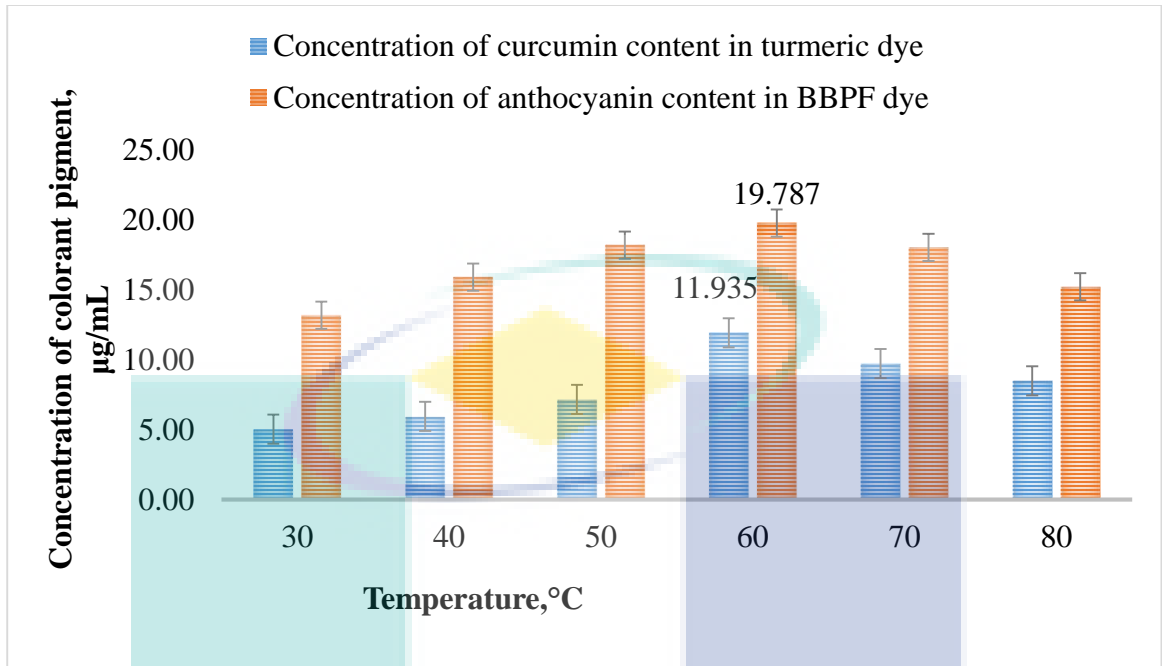


Figure 4.2 Effect of temperature on the extraction of the BBPF dye and turmeric dye at SLR at 0.050 g/mL, 10 minutes, and pH (4.2 and 8.5 respectively)

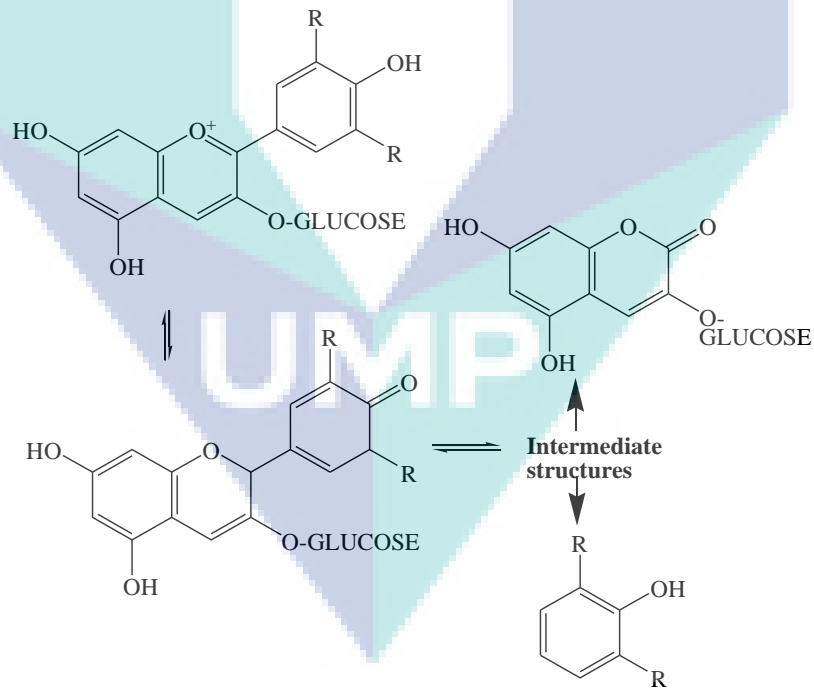


Figure 4.3 Degradation of anthocyanin mechanism at temperature higher than 70 °C  
Source: Teknologi et al., (2012)

### 4.2.3 Effect of extraction time

Different levels of extraction time ranging from 5-40 minutes were tested to determine the possible optimum value for maximum extraction of BBPF and turmeric dye. Besides, the effect of time on extraction of anthocyanin pigment in BBPF dye and curcumin pigment in turmeric dye is illustrated in Figure 4.4. The longer the extraction time, the higher the concentration of anthocyanin until dye exhaustion attained equilibrium and later, a decrease in colorant pigment content was noted after further increase in time over 20 minutes. The decline in concentration of anthocyanin is attributed to the decomposition of anthocyanin at a longer time at 60 °C. As mentioned above, the increasing extraction time resulted in an increase in the anthocyanin amount. In normal conditions, where degradation of anthocyanin is neglected, one could expect that maximum anthocyanin were extracted at upper endpoints of the established design due to the direct proportion observed between anthocyanin amount and extraction time (Arici et al., 2016).

The extraction time had been varied to range from 5 to 30 minutes in order to determine the possible optimum value for maximum extraction of curcumin where the extraction factors of SLR, temperature, and pH were 0.05 g/mL, 60 °C, and 8.5, respectively, had been kept constant. Besides, the longer the extraction time, the higher the concentration of curcumin until dye exhaustion attained equilibrium. Moreover, a decrease in concentration of curcumin was noted after further increase in time over 25 minutes. As such, the decline in concentration of curcumin is attributed to the decomposition of curcumin at a longer time at 60 °C. The exposure of pigments for a longer period resulted in the structural destruction of pigments, thus reducing colorant pigment concentration (Maran et al., 2015). This may be attributed to the decomposition of colouring component at longer times (Ali et al., 2009). Sinha et al., (2012) studied the effect of extraction time on the extraction of dye from rind of pomegranate and they also reported that extraction of dye increased with increasing the amount of pomegranate rind as well as extraction time.



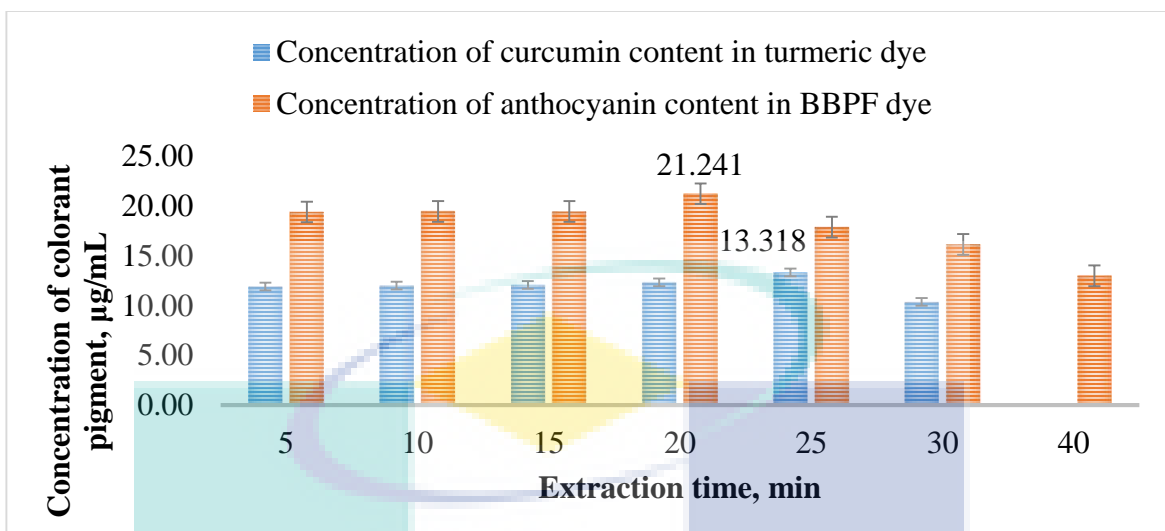


Figure 4.4 Effect of time on the extraction of BBPF dye and turmeric dye

### 4.3 Optimization of Natural Dyes Extraction by RSM

In the final step of the optimization process, the central composite design (CCD) under Response Surface Method (RSM) was used to develop quadratic model in order to obtain the true optimum conditions for maximum natural dyes recovery, as well as to validate the CCD developed model. A careful optimization of process variables used for extraction of natural dyes from BBPF and Turmeric is definitely significant to ascertain the optimum conditions achieved; hence, the next step is dyeing of extracted dyes on BY. The response data obtained from the OFAT of extraction of natural dyes were loaded into the Design Expert (2008) statistical tool and run to generate regression parameters, which was further continued with RSM. The RSM is a useful statistical technique used to design experiments, build models, evaluate the effects of several factors, search the optimum conditions for desirable responses, and reduce the number of experiments (Nasirizadeh et al., 2012). RSM uses experimental designs, such as the CCD, to fit a model by employing the least squares technique. The CCD matrix with coded and actual variables, including experimental responses absorbance, is discussed in the preceding subsection. In this design, absorbance had been defined as the absorbance for colorant pigment obtained in the extracted dyes, whereby curcumin in turmeric dye and anthocyanin in BBPF dye, which had been measured via UV-VIS spectrophotometer.

### 4.3.1 Extraction of BBPF dye

The independent variables for temperature, time, and SLR are represented by variables A that ranges from 55 to 65 °C, B ranges from 15 to 25 minutes, and C ranges from 0.083 to 0.125 g/mL, respectively, as shown in Table 4.1. The effects of temperature of extraction, time of the extraction, and SLR on the extractability of dye from BBPF based on various combinations are depicted in Table 4.2 The Actual Level of Independent Variables for BBPF.

Table 4.1 Constraint for Extraction Conditions for BBPF

Factor	Name	Units	Lower Limit	Upper Limit
A	Temperature	°C	55	65
B	Time	min	15	25
C	Solid liquid ratio	g/mL	0.083	0.125

Table 4.2 The Actual Level of Independent Variables for BBPF

RUN	Coded variables			Actual variables			Responses
	A	B	C	Extraction Temperature (°C)	Extraction Time (minutes)	SLR (g/ mL)	Concentration of Anthocyanin, (µg/mL)
1	0	0	1	60	20	0.125	44.621
2	0	0	0	60	20	0.104	44.362
3	1	0	0	65	20	0.104	42.879
4	0	1	0	60	25	0.104	41.483
5	0	0	0	60	20	0.104	44.310
6	0	-1	0	60	15	0.104	43.155
7	0	0	0	60	20	0.104	44.310
8	1	-1	1	65	15	0.125	38.672
9	-1	0	0	55	20	0.104	44.621
10	0	0	0	60	20	0.104	44.397
11	-1	1	1	55	25	0.125	45.310
12	-1	-1	-1	55	15	0.083	44.621
13	0	0	-1	60	20	0.083	44.621
14	0	0	0	60	20	0.104	44.345
15	1	1	-1	65	25	0.083	40.483

### 4.3.2 Extraction of turmeric dye

The independent variables for extraction of turmeric dye for temperature, time, and SLR are represented by variables A (55 to 65 °C), B (20 to 30 minutes), and C (0.083 to 0.125 g/mL), respectively, as exhibited in Table 4.3. The effects of temperature of extraction, time of extraction, and SLR on the extractability of dye from turmeric had been determined by dispersing 10.0g of sample in 100 mL of distilled water based on various combinations, as displayed in Table 4.4.

Table 4.3 Constraint for Extraction Conditions for Turmeric

Factor	Name	Units	Lower Limit	Upper Limit
A	Temperature	°C	55	65
B	Time	min	20	30
C	Solid Liquid Ratio	g/mL	0.08	0.13

Table 4.4 The Actual Level of Independent Variables for Turmeric

RUN	Coded variables			Actual variables			Responses
	A	B	C	Extraction Temperature (°C)	Extraction Time (minutes)	SLR (g/ mL)	Concentration of Curcumin, (µg/mL)
1	0	0	-1	60	25	0.083	11.857
2	0	0	0	60	25	0.104	11.877
3	-1	1	1	55	30	0.125	12.279
4	1	-1	1	65	20	0.125	9.630
5	0	1	0	60	30	0.104	10.727
6	0	0	1	60	25	0.125	11.857
7	0	0	0	60	25	0.104	11.844
8	-1	-1	-1	55	20	0.083	12.091
9	0	0	0	60	25	0.104	11.864
10	-1	0	0	55	25	0.104	12.091
11	0	-1	0	60	20	0.104	11.351
12	0	0	0	60	25	0.104	11.864
13	0	0	0	60	25	0.104	11.812
14	1	0	0	65	25	0.104	11.240
15	1	1	-1	65	30	0.083	10.344

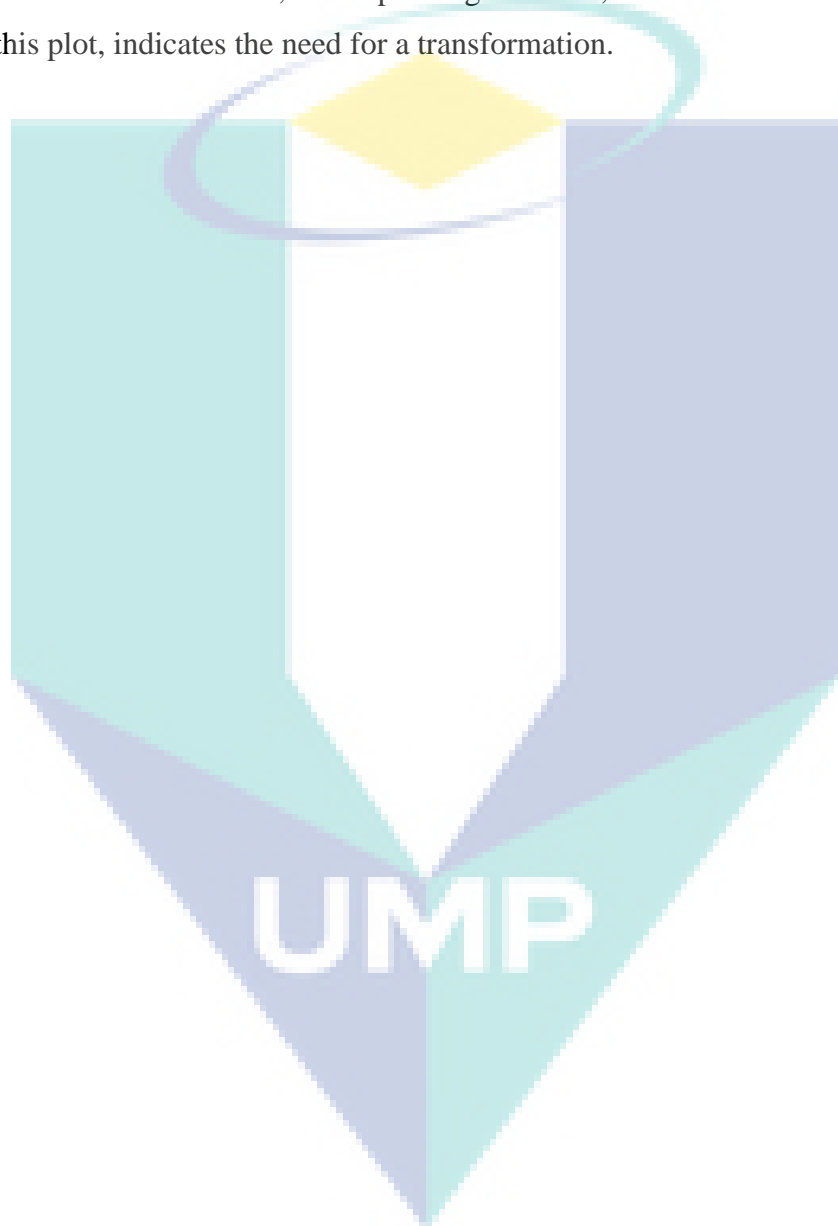
### 4.3.3 Diagnosis of model properties

The statistical properties of model can best be diagnosed by inspecting various diagnostic plots, such as plot of normal probability, studentized residuals, and outlier T. Nevertheless, the most essential diagnostic plot is the normal probability plot of the studentized residuals. The studentized residuals are defined as the residuals divided by the calculated standard deviation of residual that measures the number of standard deviations distinguishing the actual values from those predicted. Besides, the normal probability plot for BBPF dye (Figure 4.5) indicated if the residuals adhered to normal distribution, in which the points were in a straight line, except for some moderate scatter even with normal data. Moreover, the definite patterns like an "S-shaped" curve indicate that a transformation of the response may provide a better analysis.

The residuals versus predicted is a plot of the residuals versus the ascending predicted response values. This refers to a visual check for the assumption of constant variance. The plot, hence, should be a random scatter with consistent top to bottom range of residuals across the predictions. In Figure 4.6, the plot is ideally and randomly scattered; suggesting that the variance of the actual observations is constant for all values of both the external and internal studentized residuals, for the studentized residuals lie in the range between 3 and -3 for extraction of BBPF dye. Thus, it had been revealed that the proposed models were indeed distinctly adequate and reasonable, but demand a violation of the independence or constant variance assumption because outliers run with residuals outside the red lines on the plot. An outlier is an observation that does not fit well by the model. This hints that the observation has a problem, the use of wrong model, or a combination of the both. Thus, the expanding variance, as well as smiles and frowns found in this plot, indicates the need for a transformation.

The normal probability plot of extraction for yellow dye from turmeric, as shown in Figure 4.7, indicates that the residuals reflected a normal distribution. Moreover, the plot of residuals versus predicted displayed in Figure 4.8 shows that the plot was randomly scattered with a consistent top to bottom range of residuals across the predictions. The variance of the actual observations for all values for both external and internal studentized residuals was constant. This has been proven by its lie that ranges between 3 and -3. Thus, it has been

revealed that the proposed models were distinctly adequate and reasonable, but required a violation of the independence or constant variance assumption because the outliers run with the residuals outside the red lines on the plot. An outlier is the observation that refers to unfit model. This can mean that the observation has a problem, a wrong model has been used, or the combination of both. Thus, the expanding variance, as well as the smiles and frowns found in this plot, indicates the need for a transformation.



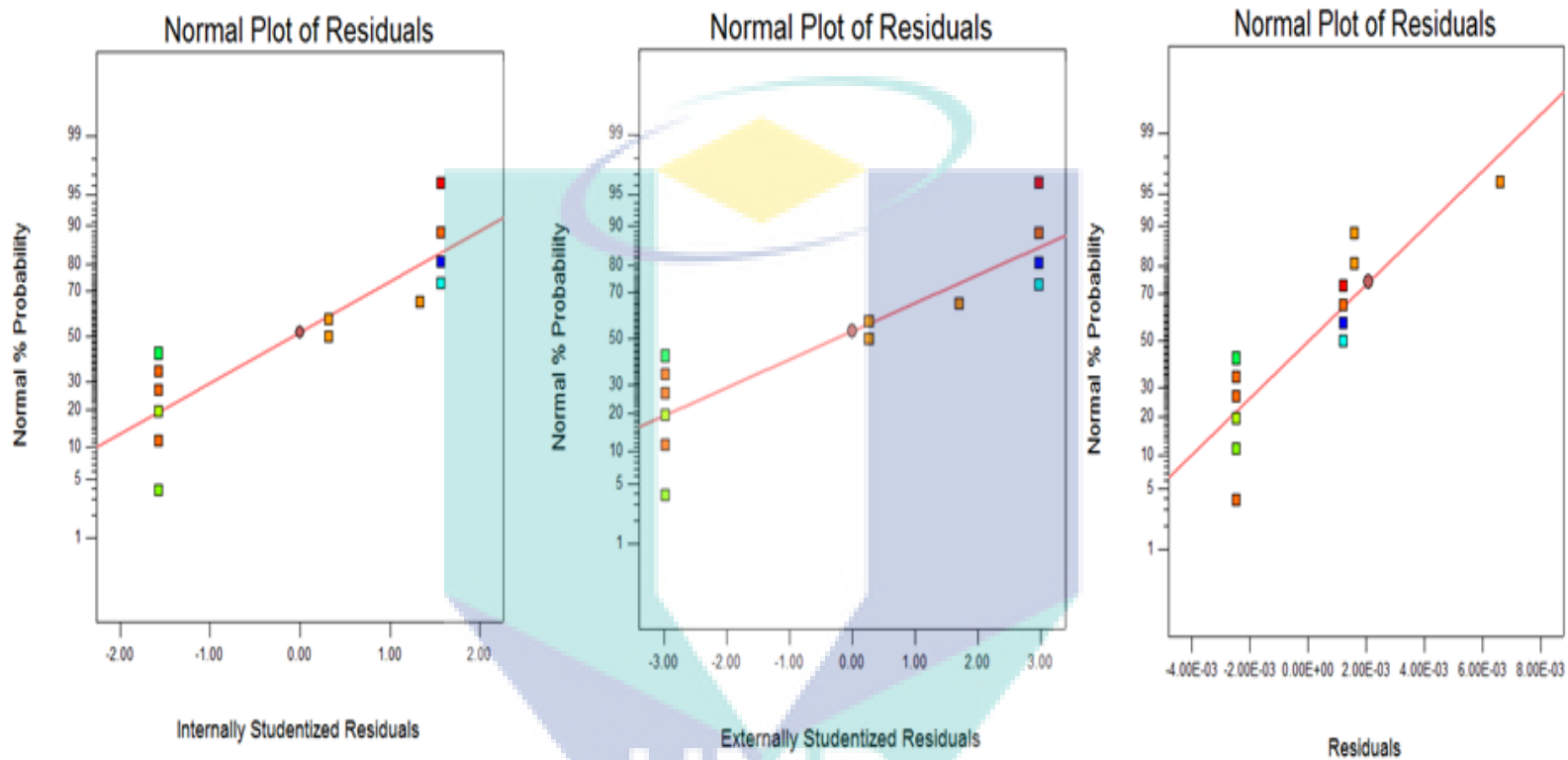


Figure 4.5 Normal probability plot of for BBPF extraction

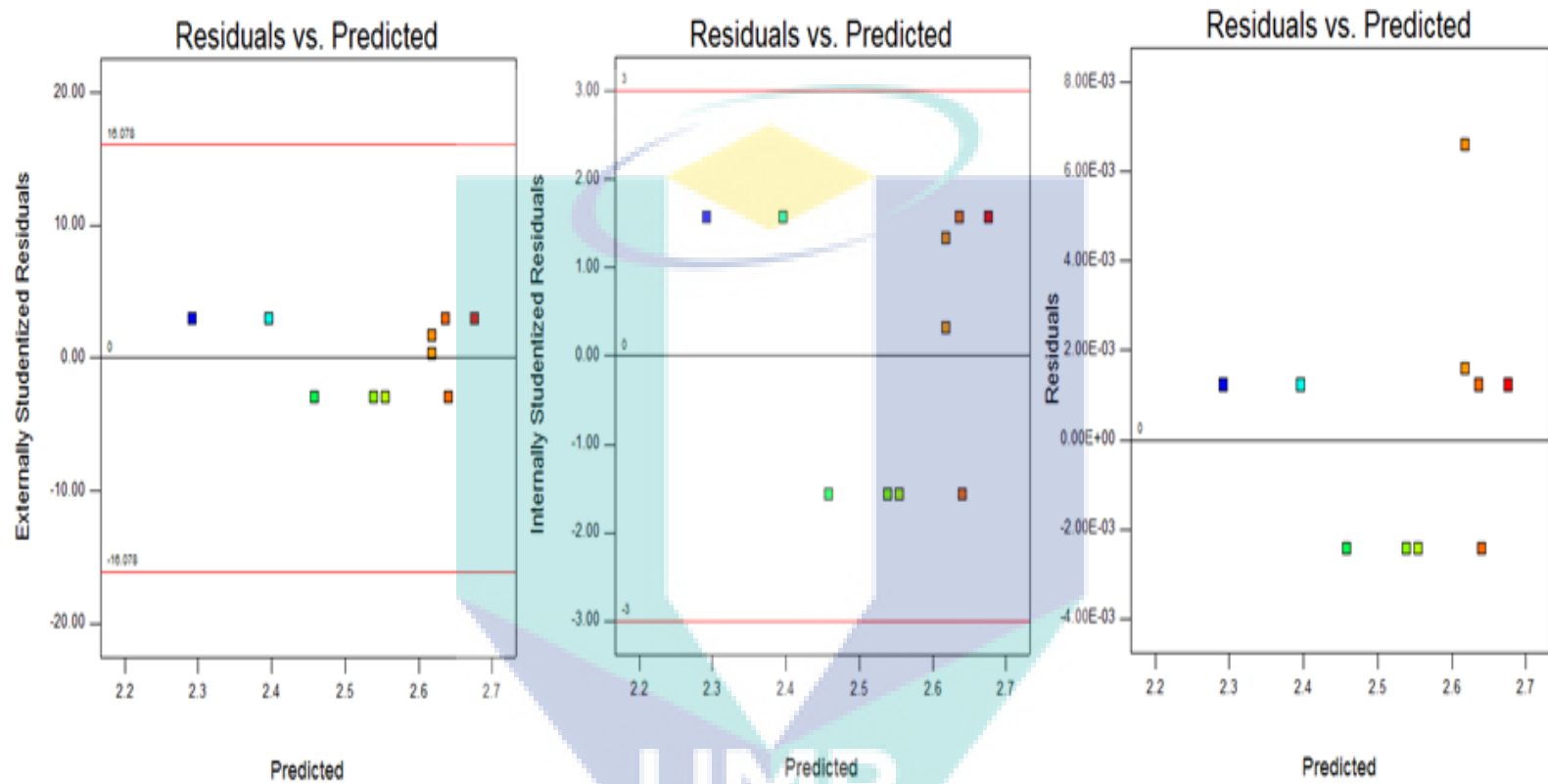


Figure 4.6 Plot of residuals versus predicted responses of BBPF extraction

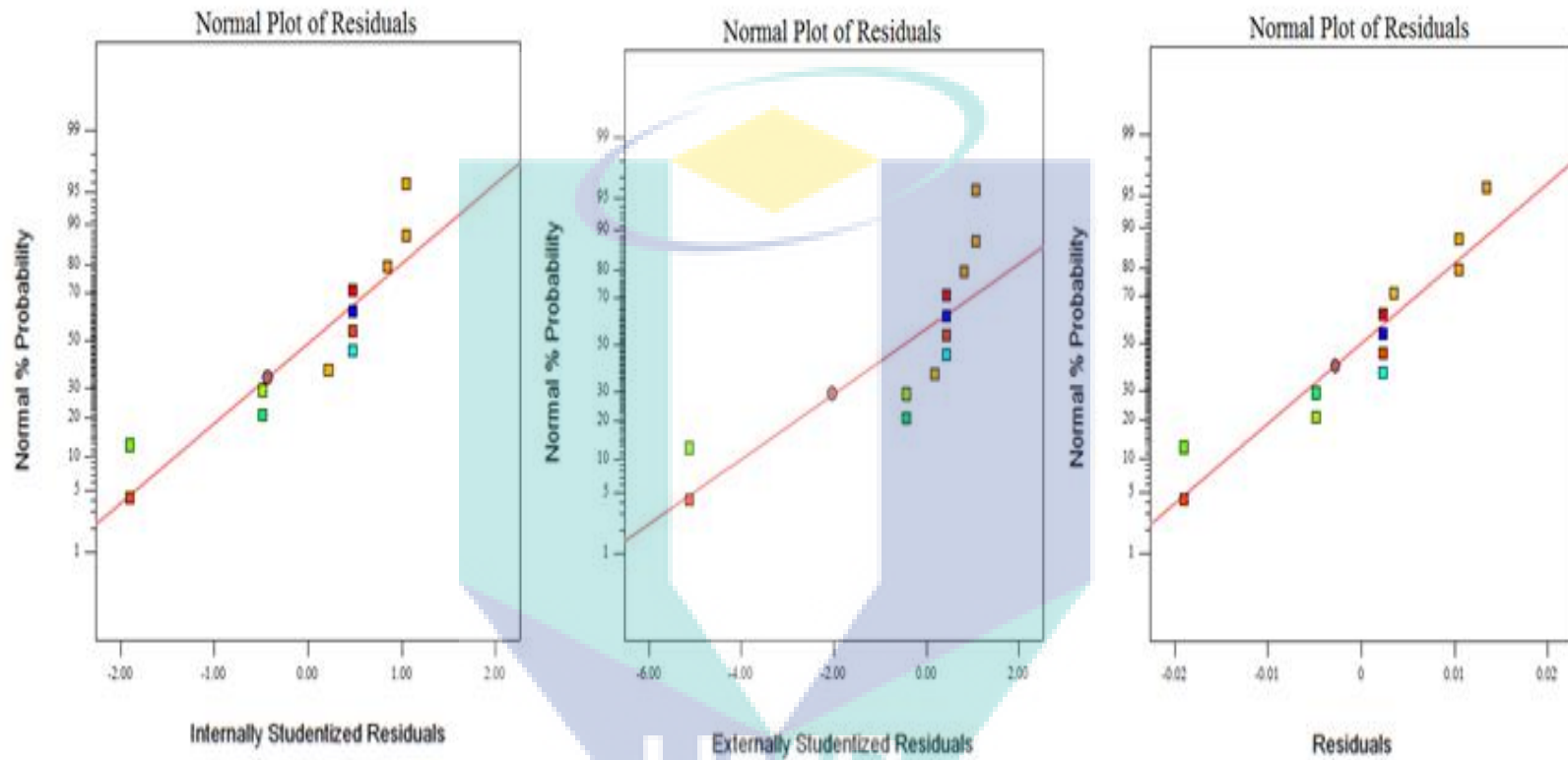


Figure 4.7 Normal probability plot for turmeric extraction



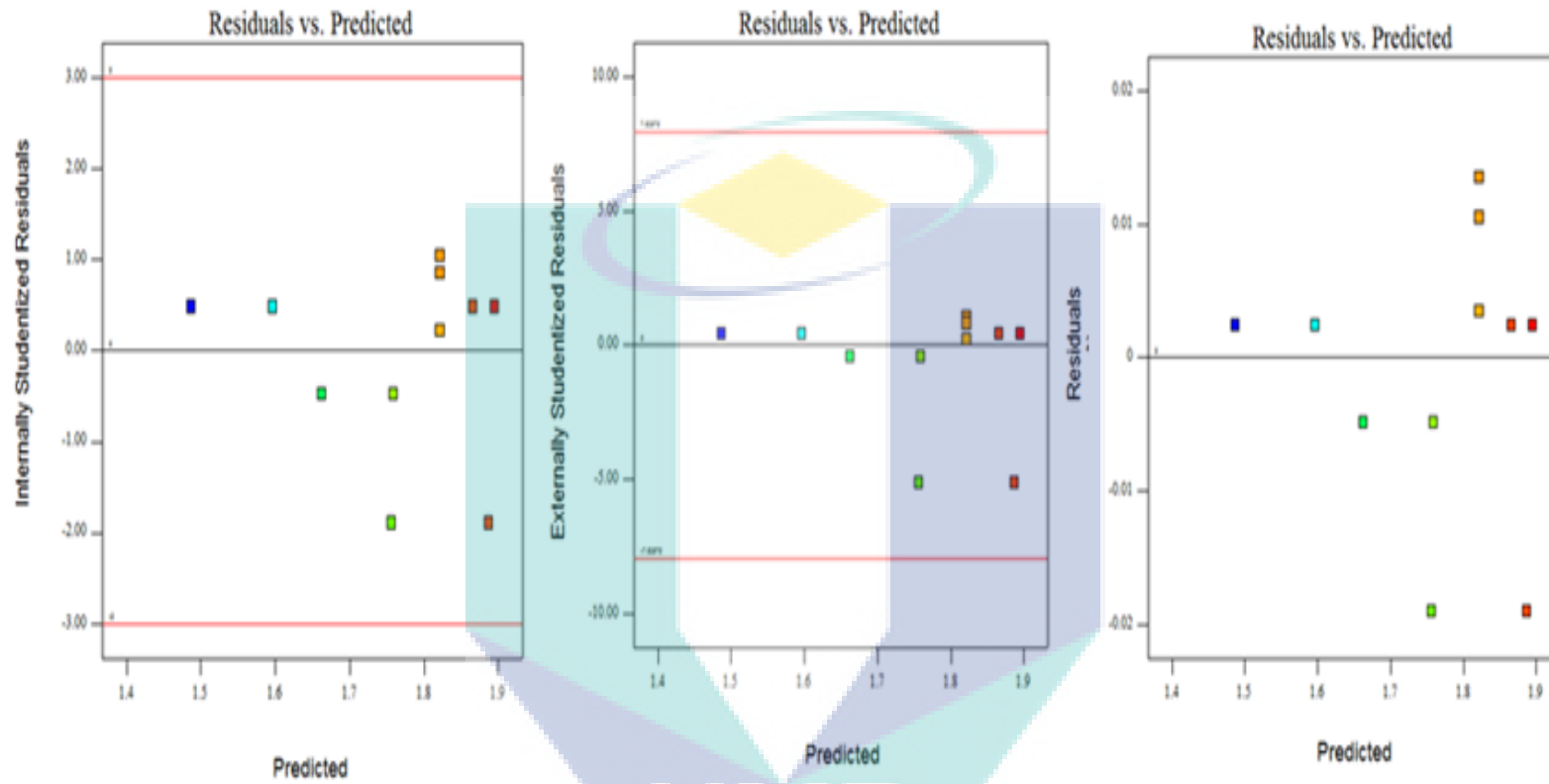


Figure 4.8 Plot of residuals versus predicted responses of turmeric extraction

#### 4.3.4 Optimization of process condition

The effects of temperature (A), time (B), and SLR (C) process variables on the extraction of blue dye from BBPF and yellow dye from turmeric were further analysed by using a stimulated three-dimensional response surface and contour plots based on the quadratic model. The influence of these input variables had been determined by using CCD to specifically identify the optimum conditions that could increase the colorant pigment (anthocyanin and curcumin) yields in BBPF and turmeric dye solutions, respectively. Furthermore, the results of ANOVA for the quadratic model represent the extraction of blue dye from BBPF, as presented in Table 4.5. Furthermore, as shown in Table 4.5, the ANOVA of factorial design for extraction of BBPF dye, the Model F-value of 394.27 implies that the model is indeed significant. Thus, there is only a 0.25% chance that an F-value this large could occur due to noise. Other than that, the values of "Prob > F" less than 0.0500 indicate that the model terms are significant. In this case, temperature (A), time (B), two-level interactions between temperature and SLR (AC), two-level interactions between time and SLR (BC), second-order effect of temperature ( $A^2$ ), second-order effect of time ( $B^2$ ), and second-order effect of SLR ( $C^2$ ) prove to be significant model terms, and they had been found to be responsible for the extraction of blue dyes from BBPF. Moreover, values greater than 0.1000 indicates that the model terms are insignificant. If there are many insignificant model terms (excluding those required to support hierarchy), model reduction may improve the model.

Meanwhile, the multiple correlation coefficient  $R^2$  was 0.9994, which indicated a good agreement between the experimental and the predicted values, as well as 99.94% of the variability in the response that could be explained by the model, while only 0.06% of the total variation that is poorly described by the model. Moreover, the "Lack of Fit F-value" of 5.99 implies the Lack of Fit is insignificant relative to pure error. Besides, there is a 24.70% chance that a "Lack of Fit F-value" this large could occur due to noise, which further proved that the obtained model was desirably fit. Furthermore, the "Pred  $R^2$ " of 0.8401 is in reasonable agreement with the "Adj  $R^2$ " of 0.9969; i.e. the difference is less than 0.2, while the "Adeq Precision" measures the signal to noise ratio. A ratio greater than 4 is desirable in

this case. The ratio of 63.829, nevertheless, indicates an adequate signal. As such, this model can be used to navigate the design space.

In addition, quadratic effect of time ( $B^2$ ), two-level interactions between time and SLR (BC), and two-level interactions between temperature and SLR (AC) were found to be the most significant terms to exhibit the principal effect towards the extraction of BBPF dye, and followed by the main effects of temperature (A) and time (B). Moreover, the secondary effect on anthocyanin yield in the BBPF dye was found to be quadratic effect of temperature ( $A^2$ ) and quadratic effect of SLR ( $C^2$ ). However, the main effects of SLR (C) and two-level interactions between temperature and time (AB) had been insignificant. Hence, the ranking of the model terms based on the statistical significant (F-value) in the study of BBPF dye extraction is as follows:  $B^2 > BC > AC > A > B > A^2 > C^2 > AB > C$ .

Other than that, the equation in terms of coded variable can be used to make predictions about the response for given levels of each factor. By default, the high levels of the factors are coded as +1, while the low levels of the factors are coded as -1. The coded equation is useful for identifying the relative impact of the factors by comparing the related factor coefficients. The empirical models in terms of coded variable obtained as function of temperature (A), time (B), and SLR (C) are depicted in Eq. (4.1) and Y represents concentration of anthocyanin. The insignificant terms, however, were excluded from the model equations.

$$Y = +2.6184 - 0.0505A - 0.0485B + 0.0163AB - 0.0848AC + 0.1058BC - 0.0285A^2 - 0.1115B^2 + 0.0220C^2 \quad 4.1$$

Hence, these models can be used to predict and to optimize the extraction of BBPF dye within the experimental constraints.

Table 4.5 Analysis of variance (ANOVA)for extraction of BBPF dye

Source	Sum of squares	Degree of freedom	Mean square	F-value	Prob > F
<b>Model</b>	0.1549	9	0.0172	394.2721	0.0025(significant)
<b>A-TEMPERATURE</b>	5.1005E-03	1	0.0051	116.8276	0.0085
<b>B-TIME</b>	4.7045E-03	1	0.0047	107.7572	0.0092
<b>C-SLR</b>	0.0000	1	0.0000	0.0000	1.0000
<b>AB</b>	3.5208E-04	1	0.0004	8.0645	0.1049
<b>AC</b>	9.5768E-03	1	0.0096	219.3567	0.0045
<b>BC</b>	1.4911E-02	1	0.0149	341.5327	0.0029
<b>A<sup>2</sup></b>	2.0022E-03	1	0.0020	45.8612	0.0211
<b>B<sup>2</sup></b>	3.0969E-02	1	0.0310	709.3543	0.0014
<b>C<sup>2</sup></b>	1.2321E-03	1	0.0012	28.2214	0.0337
<b>Residual</b>	8.7317E-05	2	4.3658E-05		
<b>Lack of Fit</b>	7.4817E-05	1	7.4817E-05	5.9853	0.2470(insignificant)
<b>Pure Error</b>	1.2500E-05	1	1.2500E-05		
<b>Cor Total</b>	0.1550	11			
<b>Std. Dev.</b>	0.0066				
<b>Mean</b>	2.5593				
<b>C.V. %</b>	0.2582				
<b>R<sup>2</sup></b>	0.9994				
<b>Adj R<sup>2</sup></b>	0.9969				
<b>Pred R<sup>2</sup></b>	0.8401				
<b>Adeq Precision</b>	63.8290				

As inferred in Table 4.6, the ANOVA of factorial design for extraction of yellow dye from turmeric showed that the computed  $F$  and  $\text{Prob} > F$  were 80.94 and 0.0004, respectively. Hence, this implies that the model was highly significant with low probability. The results obtained adequately suggest that the present mathematical model was good in predicting the experimental results with the model having a significant effect on response. In this case, the main effects of temperature (A), time (B), two-level interactions between temperature and SLR (AC), two-level interactions between time and SLR (BC), and second-order effect of time ( $B^2$ ) had been significant model terms. Besides, values greater than 0.1000 indicated that the model terms were insignificant. Meanwhile, the multiple correlation coefficient  $R^2$  was 0.9930, which indicated a good agreement between the experimental and the predicted values, as well as depicting 99.30% of the variability in the response that could be explained by the model, while only 0.70% of the total variation that was poorly described by the model. Moreover, the "Lack of Fit F-value" of 7.71 implied that the Lack of Fit is insignificant in relation to pure error. Moreover, there is a 25.73% chance that a "Lack of Fit F-value" this large could occur due to noise. Furthermore, insignificant lack of fit is good as it demonstrates desirably fit model. Other than that, the "Pred R-Squared" of 0.9271 is in reasonable agreement with the "Adj R-Squared" of 0.9807, whereas the "Adeq Precision" measures the signal to noise ratio, in which a ratio greater than 4 is desirable. The ratio of 28.765, however, indicates an adequate signal. Hence, this model could be used to navigate the design space.

In addition, quadratic effect of time ( $B^2$ ), two-level interactions between time and SLR (BC), and two-level interactions between temperature and SLR (AC) were found to be the most significant terms to display principal effects towards the extraction of turmeric dye, and followed by the main effects of temperature (A) and time (B). Moreover, the quadratic effect of SLR ( $C^2$ ), the two-level interactions between temperature and time (AB), the quadratic effect of temperature ( $A^2$ ), and the main effect of SLR (C) had been insignificant. Hence, the ranking of the model terms based on the statistical significant (F-value) in the study of curcumin yield in the turmeric dye is  $B^2 > BC > AC > A > B > C^2 > AB > A^2 > C$ . The equation in terms of coded variable, therefore, can be used to make predictions about the response for the given levels of each factor.

The empirical models for extraction of turmeric dye in terms of coded variable obtained as functions of temperature (A), time (B), and SLR (C) are expressed in Eq. (4.2), where Y represents concentration of curcumin. Furthermore, the insignificant terms were included in the model equations. However, if there are many insignificant model terms (excluding those required to support hierarchy), model reduction may improve the model.

$$Y = +1.8215 - 0.0655A - 0.0480B + 0.000C + 0.0203AB - 0.0828AC + 0.1038BC - 0.1107B^2 \quad 4.2$$

Hence, these models can be used to predict and to optimize the extraction of BBPF dye within the experimental constraints.

The logo for UMP (Universitas Muhammadiyah Purwokerto) is a large, downward-pointing arrow shape. It is composed of several overlapping geometric shapes in shades of teal and light blue. The letters 'UMP' are written in a bold, white, sans-serif font across the center of the arrow's shaft.

UMP

Table 4.6 Analysis of variance (ANOVA) for extraction of turmeric dye

Source	Sum of Squares	Degree of freedom	Mean square	F-value	Prob > F
<b>Model</b>		6		80.94	0.0004(significant)
<b>A-TEMPERATURE</b>	8.5805E-03	1	8.5805E-03	28.4338	5.9559E-03
<b>B-TIME</b>	4.6080E-03	1	4.6080E-03	15.2699	1.7428E-02
<b>AB</b>	5.4675E-04	1	5.4675E-04	1.8118	0.2495175
<b>AC</b>	9.1301E-03	1	9.1301E-03	30.2550	5.3265E-03
<b>BC</b>	1.4352E-02	1	1.4352E-02	47.5595	2.3181E-03
<b>B<sup>2</sup></b>	3.6741E-02	1	3.6741E-02	121.7524	3.8351E-04
<b>Residual</b>	1.2071E-03	4	3.0177E-04		
<b>Lack of Fit</b>	1.1571E-03	3	3.8569E-04	7.7139	0.2573(insignificant)
<b>Pure Error</b>	5.0000E-05	1	5.0000E-05		
<b>Cor Total</b>	0.1722	11			
<b>Std. Dev.</b>	0.0174				
<b>Mean</b>	1.7662				
<b>C.V. %</b>	0.9836				
<b>R<sup>2</sup></b>	0.9930				
<b>Adj R<sup>2</sup></b>	0.9807				
<b>Pred R<sup>2</sup></b>	0.9271				
<b>Adeq Precision</b>	28.7652				

#### 4.3.5 Interaction effect of variables

An interaction occurs when the response differs depending on the setting of two factors. In fact, they appear with two non-parallel lines, indicating that the effect of one factor depends on the level of the other. As such, the 3D Surface plot is a projection of the contour plot that gives shape, in addition to colour and contour. Moreover, it can demonstrate the correlations between responses, mixture components, and/or numeric factors. Hence, the interaction and response surface graphs had been generated to estimate the optimum conditions of BBPF dye extraction as a function of independent variables A, B, and C, as displayed from Figure 4.9 until Figure 4.11. The effects of temperature and time on extraction of BBPF dye when the SLR was set at 0.08 g/mL as the centre point is shown in Figure 4.9. Meanwhile, the effects of temperature and time on extraction of BBPF dye, keeping the SLR at 0.08 g/mL as the centre point, are presented in Figure 4.10. The predicted concentration of anthocyanin reading of the extracted dye increased at lower values of both temperature and time, but decreased at higher values. Besides, the maximum concentration of anthocyanin of 44.50  $\mu\text{g/mL}$  was predicted at 55  $^{\circ}\text{C}$  and 15 minutes (Figure 4.9). These results demonstrated that low temperature resulted in higher concentration of anthocyanin (44.64  $\mu\text{g/mL}$ ), as stipulated in run 12 (Table 4.2). However, at higher temperature and time; 65  $^{\circ}\text{C}$  and 25 minutes, (in run 15), the concentration of anthocyanin dramatically decreased to 40.48  $\mu\text{g/mL}$ .

Therefore, it is evident that the predicted concentration of anthocyanin continuously decreased with the increase in temperature showed in Figure 4.10 (from 46.50  $\mu\text{g/mL}$  at 55  $^{\circ}\text{C}$  to 44.80  $\mu\text{g/mL}$  at 65  $^{\circ}\text{C}$ ), when the SLR was maintained at 0.13 g/mL. Conversely, an opposite result was found with a low level of SLR (0.08 g/mL), in which the concentration of anthocyanin decreased from 43.50  $\mu\text{g/mL}$  at 55  $^{\circ}\text{C}$  to 41.80  $\mu\text{g/mL}$  at 65  $^{\circ}\text{C}$ ). These results demonstrated a negative correlation with temperature, but positive correlation with SLR. Based on these results, the higher SLR (0.13g/mL) and lower temperature (55  $^{\circ}\text{C}$ ) could generate higher concentration of anthocyanin (45.31  $\mu\text{g/mL}$ ), as portrayed in run 11 (Table 4.2). However, extremely low SLR (0.0083 g/mL in run 15) and higher temperature (65  $^{\circ}\text{C}$ ) decreased the concentration of anthocyanin value to 40.48  $\mu\text{g/mL}$ .



Figure 4.11 shows the effects of time and SLR on extraction of BBPF dye. It is clear that the predicted concentration of anthocyanin at a medium level of temperature; 60 °C, reduced with the increase in time (from 45.5 µg/mL at 15 minutes to 40.20 µg/mL at 25 minutes), especially when the SLR was held at 0.08 g/mL. Furthermore, a reciprocal result was discovered with high SLR (0.13 g/mL), in which the concentration of anthocyanin increased from 41.50 µg/mL at 15 minutes to 43.1µg/mL at 25 minutes (Figure 4.11). Thus, a short time could give lower concentration of anthocyanin (38.67 µg/mL) with higher SLR 0.125 g/mL, as demonstrated in run 8 (Table 4.2). Meanwhile, at longer time (25minutes) and higher SLR (0.13 g/mL) and in run 11, the concentration of anthocyanin increased to 45.31 µg/mL.

Other than that, Figure 4.12 presents the interactive effects of temperature and time on the extraction of yellow dye from turmeric while keeping the extraction SLR at 0.10 g/mL as the centre point. This figure shows that the predicted concentration of curcumin in the turmeric dye decreased with the increase of temperature from 11.80 µg/mL at 55 °C to 10.80 µg/mL at 65 °C when the time was maintained at 20 minutes. At longer time (30 minutes), a reciprocal phenomenon was noted, where the concentration of curcumin decreased (from 11.00µg/mL at 55 °C to 9.80 µg/mL at 65 °C). These outcomes indicated that high temperature resulted in decrement of concentration of curcumin (9.63 µg/mL), as interpreted in run 4 (Table 4.4). However, the concentration of curcumin in turmeric dye increased to 12.23 µg/mL at low temperature (55 °C in run 3).

Meanwhile, Figure 4.13 depicts the influences of extraction temperature and SLR on the concentration of curcumin from turmeric dye when the time was held constant at 25 minutes. At high SLR (0.13 g/mL), increment in temperature led to a rapid decrease in concentration of curcumin reading from 12.90 µg/mL at 55 °C to 10.80 µg/mL at 65 °C. However, at low SLR (0.08 g/mL) condition, concentration of curcumin of the colorant pigment increased up to 12.00µg/mL at 65 °C. These results demonstrated high SLR and low temperature condition, which facilitated higher concentration of curcumin in turmeric dye (12.23 µg/mL), as attained in run 3 (Table 4.4). Furthermore, lower SLR (at 0.08 g/mL in run 8) reduced it to 12.09 µg/mL.

In addition, the interaction relationship between extraction time and SLR for extraction of turmeric dye at 60 °C is presented in Figure 4.14. A notable and constant increment in concentration of curcumin was observed for increased extraction time (from 10.80 µg/mL at 20 minutes to 11.50 µg/mL at 30 minutes) when SLR was retained at high level (0.13 g/mL). At low SLR condition (0.08 g/mL), a complementary result was noted, in which the concentration of curcumin decreased slightly from 11.50 µg/mL at 20 minutes to 10.20 µg/mL at 30 minutes for extraction. Meanwhile, at high SLR (0.13 g/mL) condition, the concentration of curcumin increased with the increase in time up to its middle point (25 minutes) and then, returned to its initial value (11.80 µg/mL) at 30 minutes. Furthermore, Table 4.4 depicts that low SLR (0.08 g/mL in run 15) condition caused the value of concentration of curcumin to reduce to 10.34 µg/mL, while high SLR (0.13 g/mL in run 3) led to maximum concentration of curcumin (12.23 µg/mL).



UMP

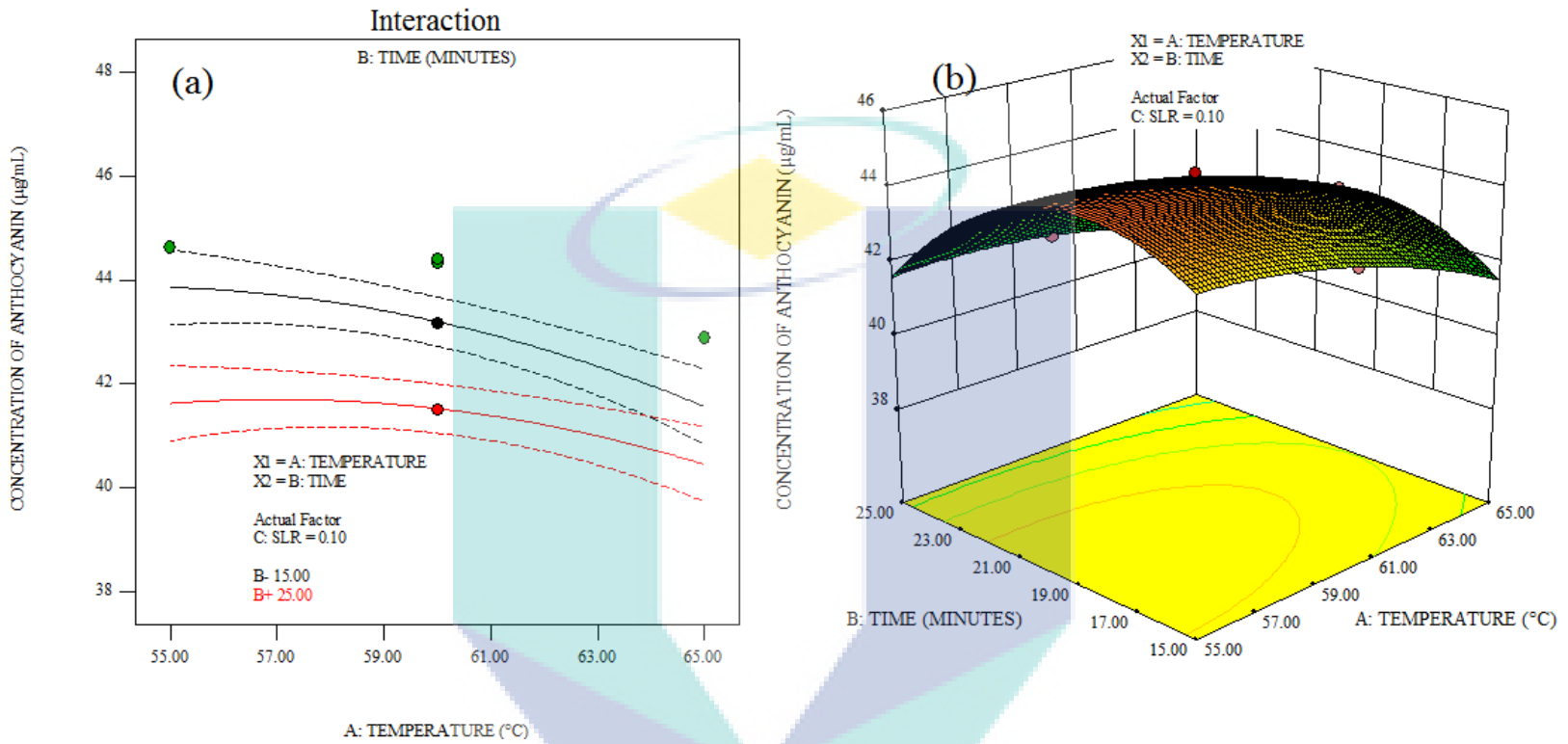


Figure 4.9 Effects of temperature and time on extraction of BBPF dye: (a) interaction and (b) response surface graph

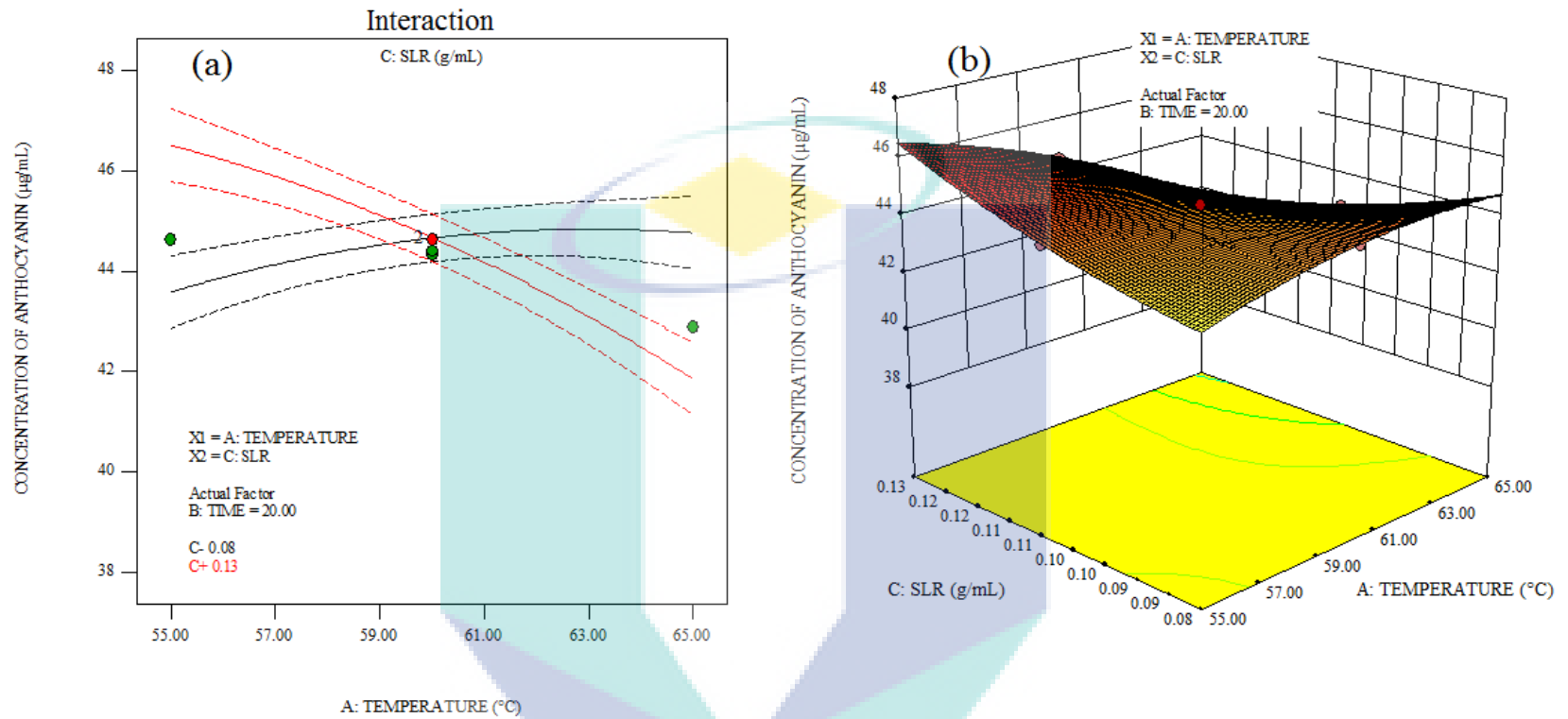


Figure 4.10 Effects of temperature and SLR on extraction of BBPF dye: (a) interaction and (b) response surface graph

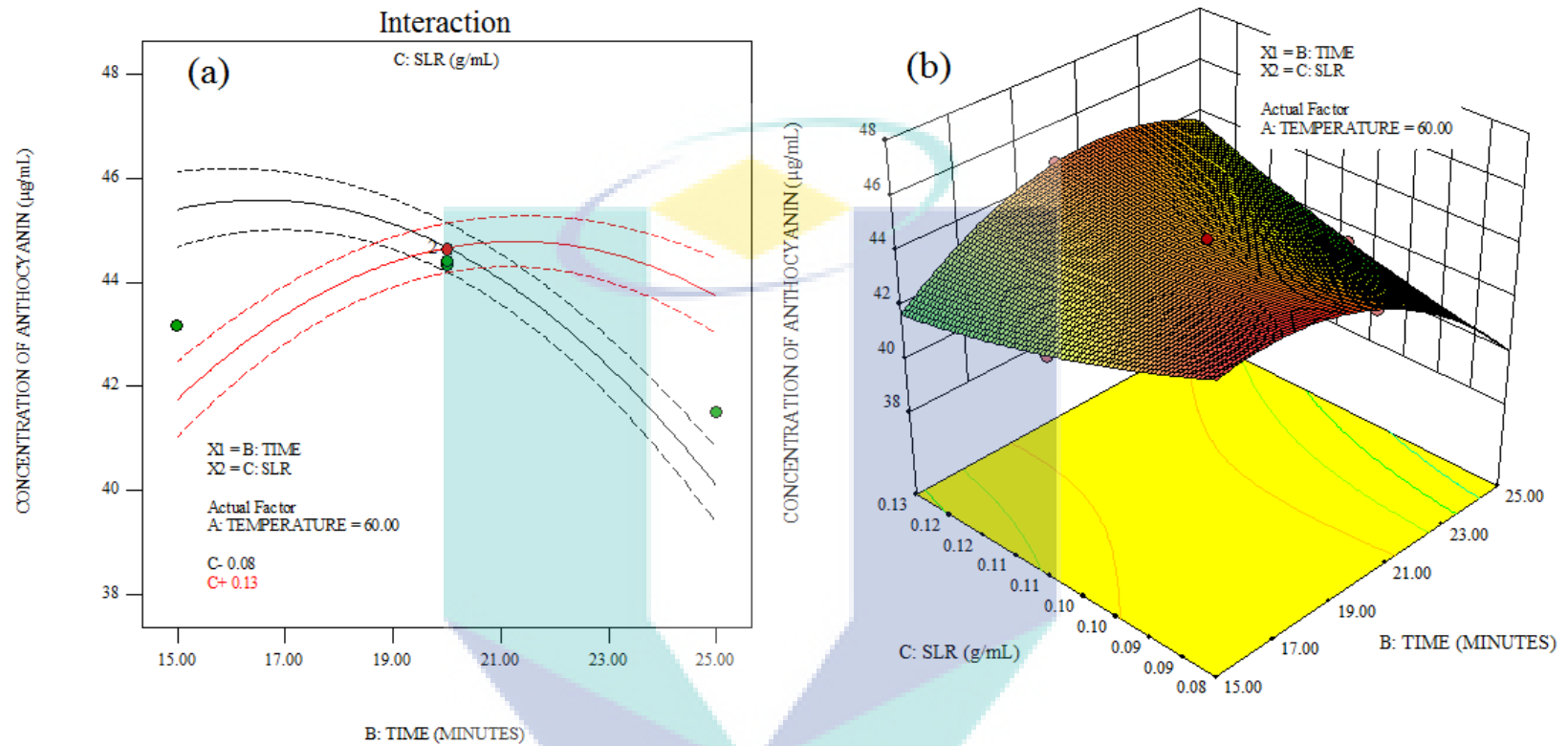


Figure 4.11 Effects of time and SLR on extraction of BBPF dye: (a) interaction and (b) response surface graph

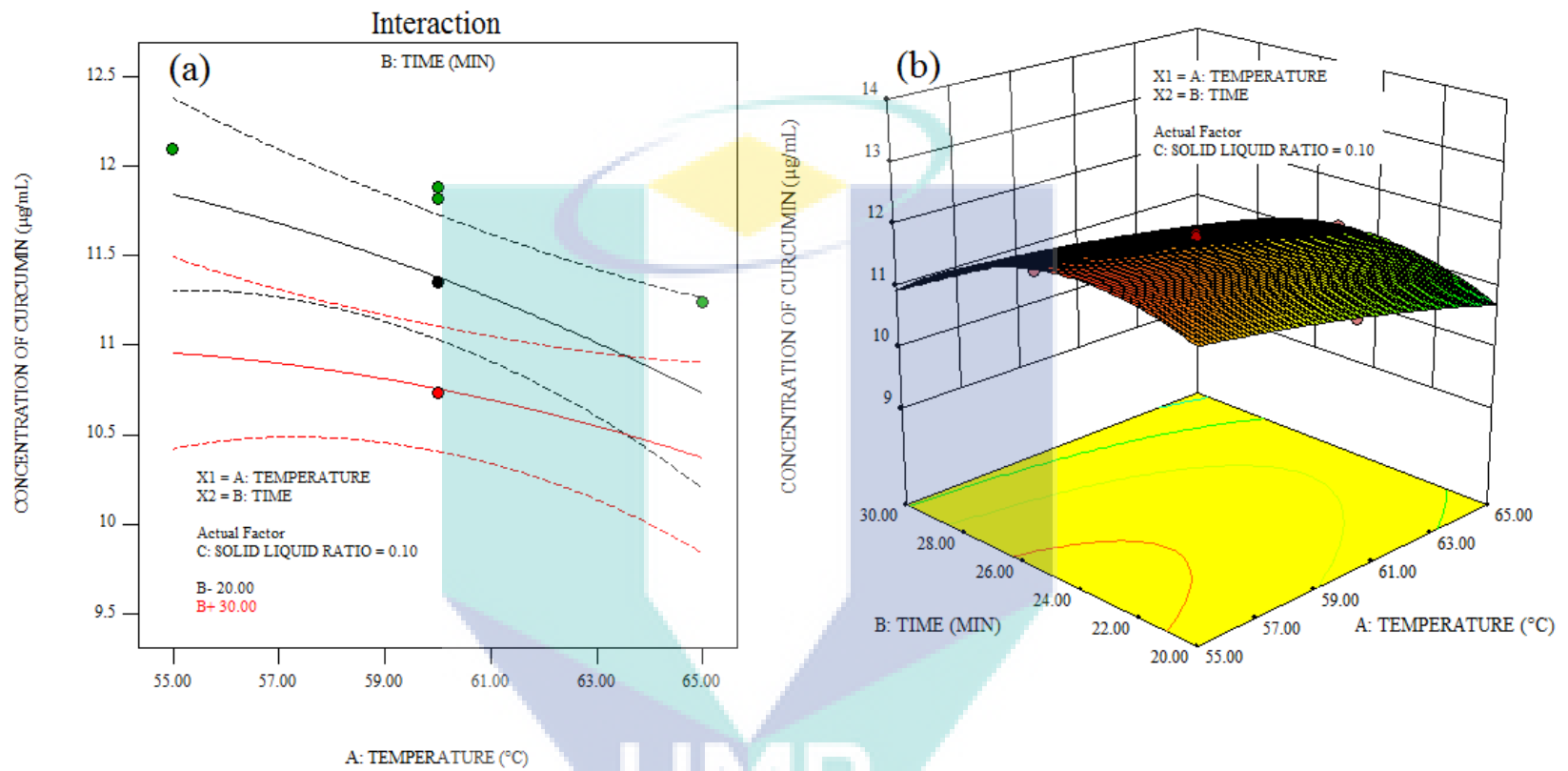


Figure 4.12 Effects of temperature and time on extraction of turmeric dye: (a) interaction and (b) response surface graph

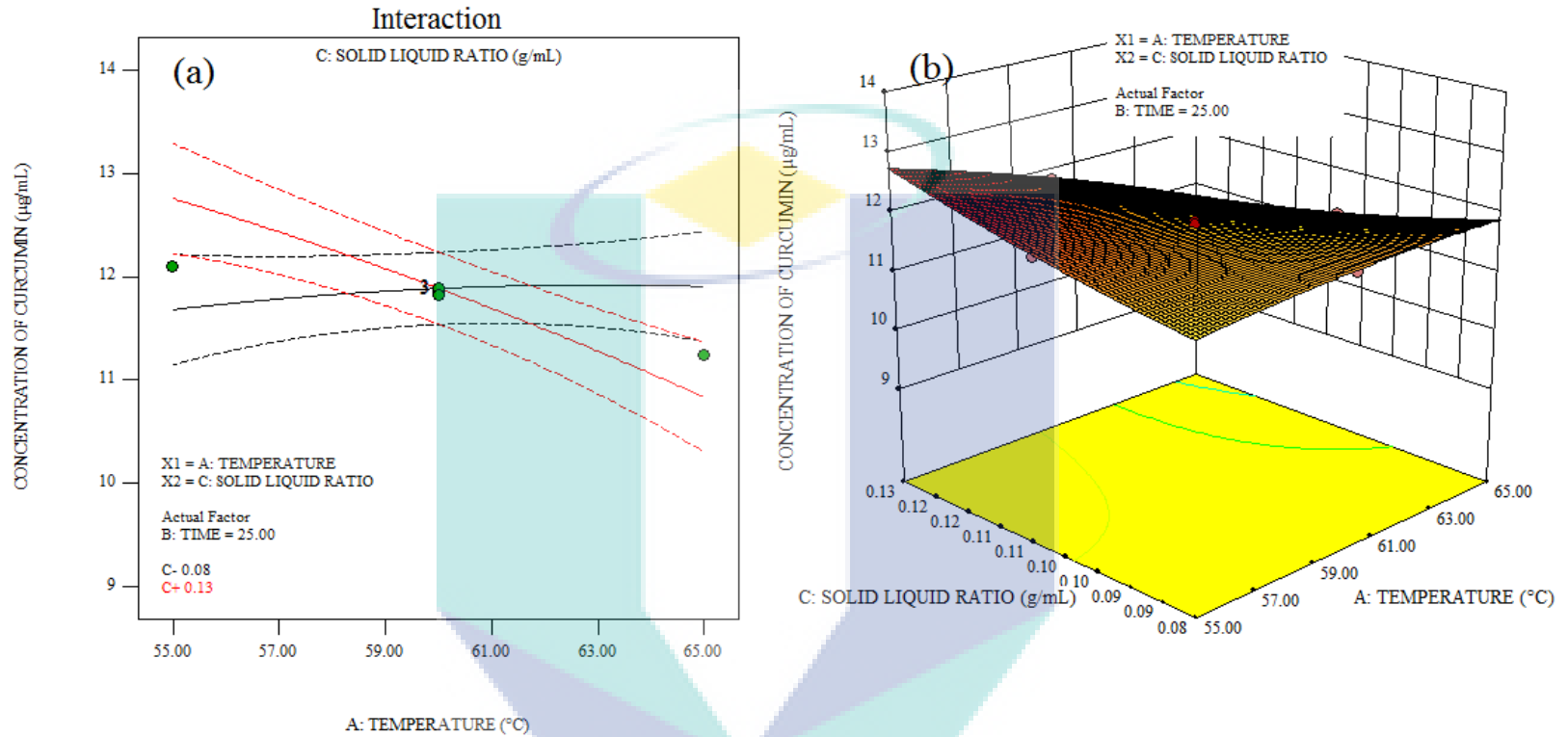


Figure 4.13 Effects of temperature and SLR on extraction of turmeric dye: (a) interaction and (b) response surface graph

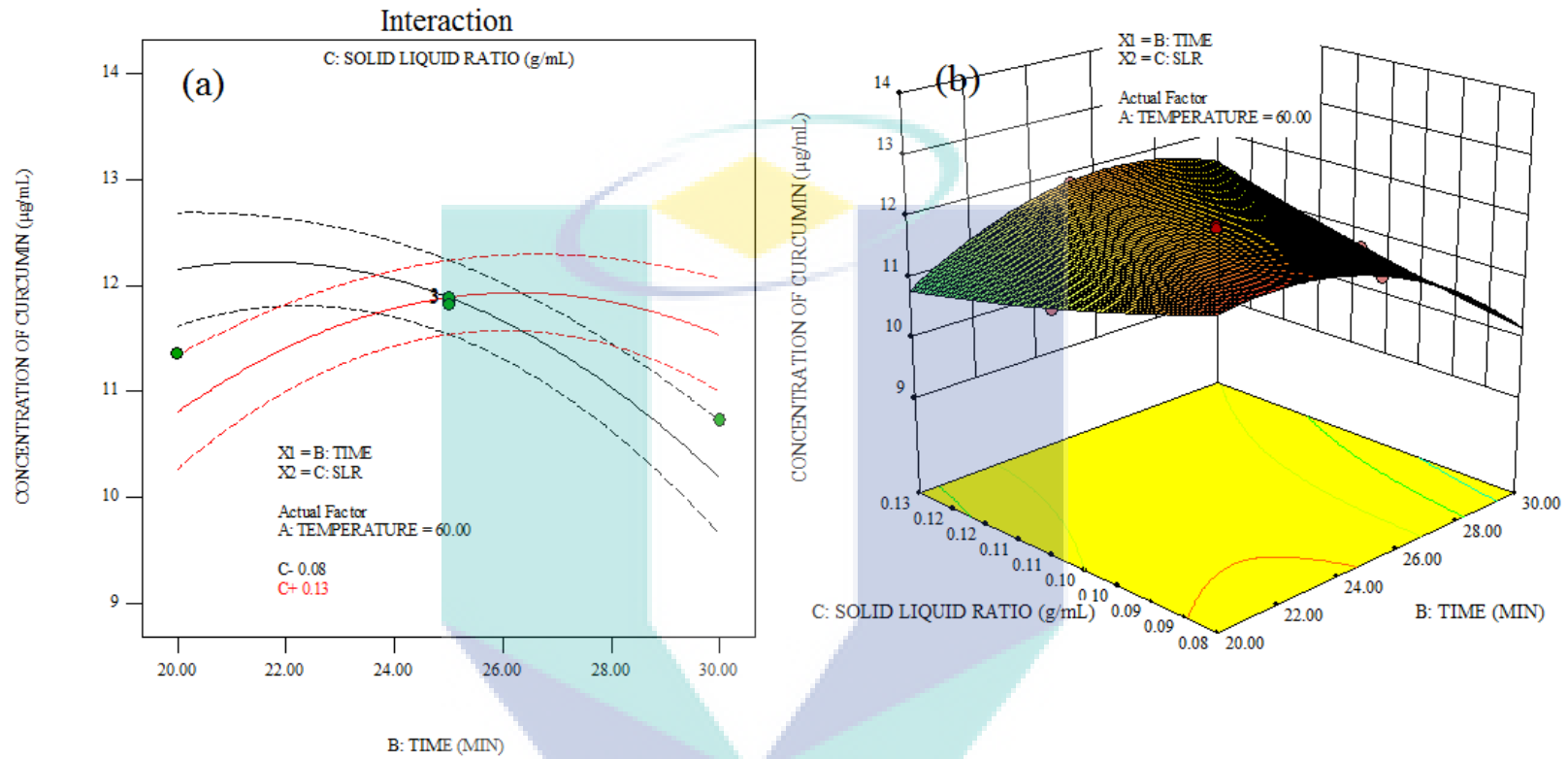


Figure 4.14 Effects of time and SLR on extraction of turmeric dye: (a) interaction and (b) response surface graph



### 4.3.6 Model validation

Adequacy of the developed empirical method has to be verified or validated in order to confirm the accuracy of the prediction made. The regression equation is generated in predicting the extraction of natural dyes at any particular temperature, time, and solid liquid ratio within a range of levels defined earlier. The predicted values of dyes yields were calculated by using the regression model and the findings were compared with experimental values. The most compatible estimation model among mean, linear, quadratic, and cubic expressions of each response variable had been identified based on all the statistical analyses, inclusive of sequential model, sum of squares, lack of fit tests, and model summary statistics. When a model is selected, an analysis of variance is calculated to assess how well the model represents the data. After optimization, the dyes were extracted with the optimum conditions that had been determined.

$$Residual = (Actual\ value - Predicted\ value) \quad 4.3$$

$$\% Error = \frac{Residual}{Actual\ value} \times 100 \quad 4.4$$

On top of that, the results depicted in Table 4.7 show that the percentage errors ranged from 1.665 % for extraction of BBPF dye to 1.848 %. Meanwhile, Table 4.8 portrays that the percentage errors for extraction of yellow dye from turmeric ranged from 0.4738 % to 1.5070 %. Thus, both extractions imply that the empirical model developed had been considerably accurate for responding terms as the percentage error between the experimental and the predicted values were well within the acceptable value of 5 %, suggesting that the model adequacy is reasonably within the 95 % of confidence interval. As such, further analysis with regard to ideal operational process for optimum extraction of natural dyes would be based on this developed model.

Table 4.7 The results of verification process of BBPF dye extraction

No	Temperature	Time	SLR	Predicted Concentration of Anthocyanin	Desirability	Actual Concentration of Anthocyanin	Percentage error,%
1	55.00	15.00	0.10	43.948	0.944	44.707	1.665
2	55.00	15.12	0.10	44.000	0.943	44.845	1.848
3	55.00	15.39	0.10	44.121	0.942	44.966	1.843

Table 4.8 The results of verification process of turmeric dye extraction

No	Temperature	Time	SLR	Predicted Concentration of Curcumin	Desirability	Actual Concentration of Curcumin	Percentage error,%
1	55.00	25.00	0.12	12.649	1.000	12.708	0.4584
2	55.00	27.00	0.12	12.299	1.000	12.500	1.6054
3	55.00	22.00	0.10	12.208	0.987	12.026	1.5070

UMP

#### 4.3.7 Confirmation

Test for confirmation is definitely a significant and necessary step in the RSM because it is a direct evidence of the empirical model obtained. The results of confirmation of run at the predicted optimum conditions for BBPF and turmeric dyes extraction are presented in Table 4.9 and Table 4.10 respectively. The optimum extraction of BBPF dye for temperature, time, and SLR were determined as 55 °C, 15 minutes, and 0.10 g/mL respectively, while for turmeric dye extraction; 55 °C, 25 minutes, and 0.12 g/mL respectively. In these optimized conditions, the model predicted a maximum concentration of colorant pigments of 44.95 µg/mL (BBPF dye in Table 4.9) and 12.66 µg/mL (Turmeric dye in Table 4.10) with a probable difference of 2.643 and 1.963 respectively at 95 % confidence interval. Furthermore, in order to confirm these results, confirmation experiments were performed by employing the model that suggested the optimum conditions and the concentration of colorant pigment, which resulted in 44.62 µg/mL (BBPF dye) and 12.71 µg/mL (turmeric dye). The optimum expected concentration of colorant pigment displayed were rather close to the confirmation results, thus indicating that these models are indeed reasonable and reliable. The concentration of the colorant pigments extracted from OFAT were shown lower than the concentration of the colorant pigments extracted resulted in the RSM. Thus, proving the optimization of the extraction natural dyes by using RSM was the best tool.

Table 4.9 The results of confirmation process of BBPF dye extraction

Temperature	Time	SLR	Predicted Concentration of Anthocyanin	Desirability	Actual Concentration of Anthocyanin	Percentage error,%
55.00	15.00	0.10	43.948	0.944	44.621	1.478

Table 4.10 The results of confirmation process of turmeric dye extraction

Temperature	Time	SLR	Predicted Concentration of Curcumin	Desirability	Actual Concentration of Curcumin	Percentage error,%
55.00	25.00	0.12	12.656	1.000	12.708	0.4075

UMP

## CHAPTER 5

### DYEING OF NATURAL DYES ON BAMBOO YARN (BY)

#### 5.1 Introduction

The objectives of this chapter are to optimize the dyeing conditions of BY in order to produce DBY at the best dyeing conditions, as well as to study the effects of dyeing temperature, dyeing time, concentration of dye bath, and dye bath pH of natural dyes extracted from BBPF, RDFP, and turmeric on dyeing BY. The effects of dyeing time, temperature, SLR of the dye bath, and dye bath pH on the dyeing of natural dyes on BY had been examined by using the OFAT method to design the optimum range of parameters. Then, the results were analysed by using CCD in RSM via Design Expert V 8.0.6. As such, a detailed discussion on the optimization of dyeing of natural dyes on BY is depicted in this chapter.

#### 5.2 Design of Parameter for Dyeing of Natural Dye on Bamboo Yarn(BY)

The research of natural dyes was then continued to optimize the chemical processes of dyeing of natural dyes on BY in order to determine the influence of one variable at a time for an experimental response. Three natural dyes (BBPF, RDFP, and turmeric) in dyeing were used and all of them were optimized via OFAT approach for maximum natural dyes extraction. Hence, the objective of the current OFAT is to study the effect reaction of dyeing on the effects of dyeing time, temperature, SLR of the dye bath, and dye bath on BY. As for the initial OFAT experiment, the level of three factors out of four was held constant. The preparation of dyeing of natural dyes on BY sample had been done by adhering to the similar procedure by changing a parameter. The impacts of operational parameters on dyeing of

natural dyes onto BY had been examined by applying the OFAT method, as further explained in the following subsections.

The objective of OFAT is to study the effect reaction of dyeing of BY on dyeing time, temperature, SLR of dye bath, and dye bath pH. In the first step of the optimization process, the effective range of factors listed for dyeing of blue natural dye from BBPF, RDFP and turmeric on BY had been observed. The influences of four operational parameters (dyeing time, temperature, SLR of dye bath, and dye bath pH) on dyeing of natural dyes on BY were evaluated via OFAT method, as depicted in the following subsections.

### **5.2.1 Effect of dyeing time**

The levels of dyeing time had been varied; the absorbance of dyeing time were taken from 20 to 90 minutes and 1:100 of ratio weight of BY in blue dye solution used, which had been obtained to determine the optimum value for maximum adsorption of anthocyanin, betacyanin and curcumin on BY. The dyeing time of blue dye from BBPF were analysed at pH 4.2, 0.10 g/mL, 70 °C, and 525 nm for dye bath pH, blue dye bath concentration, temperature, and wavelength, respectively. The effect of dyeing time on the percentage of dye uptake that represents the percentage of anthocyanin, betacyanin and curcumin adsorbed the BY is shown in Figure 5.1. It was observed that the percentage of dye uptake obtained increased as the time was increased until dye exhaustion was attained at 60 minutes (interior of fibre was in amorphous form, hence offering maximum fixation). Other than that, a decrease was noted in the percentage of dye for anthocyanin uptake after further increase in time over this value. Therefore, longer dyeing time means higher adsorption of anthocyanin on BY until dye exhaustion attains equilibrium, while the decline in dye ability may be attributed to the desorption of the dye molecules as a consequence of long dyeing time. However, the optimum time for dyeing of blue dye on BY was obtained at a range of 50 to 70 minutes.

The effect of dyeing time on the dye ability of BY with RDFP extract was conducted at different duration of time where the absorbance of dyeing time was taken from 20 to 100 minutes with 1:100 of ratio weight of BY in red dye solution in order to determine the optimum value for maximum adsorption of betacyanin onto BY. Moreover, as shown in

Figure 5.1, the percentage of dye uptake (the adsorption of betacyanin adsorbed on BY) obtained increased as the time increased up to 90 minutes. Then, it began to decline with prolonged time. The decline in the dye ability (percentage of dye uptake) might be attributed to desorption of the dye molecules as a consequence of long dyeing time. Moreover, insignificant increase was observed after the dyeing time was hiked. Therefore, the optimum time for dyeing of red dye on BY was 90 minutes. This studies was similar with the research done by Khan et al.,(2014). Natural dye was extracted by Khan et al.,(2014) from red calico leaves powder (RP) for dyeing irradiated fabric . The results revealed that less percent dye uptake was produced when cotton fabrics were dyed for shorter time and the maximum percent dye uptake was obtained when dyed for 50 minutes. Initially in the start, dye rate was low, while after increasing dyeing time, surface modified fabric showed better uptake of dye. Dyeing for longer time might have shifted more colorant from irradiated cotton fabric to dye bath. So the rate of desorption became high and low strength was observed.

Besides, the dyeing time of dyeing turmeric dye on BY increased at the initial stages of dyeing until the equilibrium time was attained at 60 minutes. This had been due to the rapid attachment of the dye to the surface of BY. At 60 minutes, the maximum adsorption of curcumin on the BY was confirmed by the highest value of the percentage of dye uptake. However, insignificant increase was noted after the dyeing time was hiked due to exhaustion in dye. Moreover, the optimum time range for dyeing yellow dye on BY was obtained within 40 to 80 minutes. Guesmi et al., (2012) isolated indicaxanthin from fresh orange-yellow fruits and applied on wool fabric. The studied indicates that the percent dye uptake obtained depend on the dyeing time. The percent dye uptake was increased as the time increases up to 90 min and then it decreases. From 90 min, the effect of dyeing time can be attributed to the thermal stability of indicaxanthin and its escape from the fibre. The result indicates that 90 min is a suitable time for dyeing with indicaxanthin dyes.

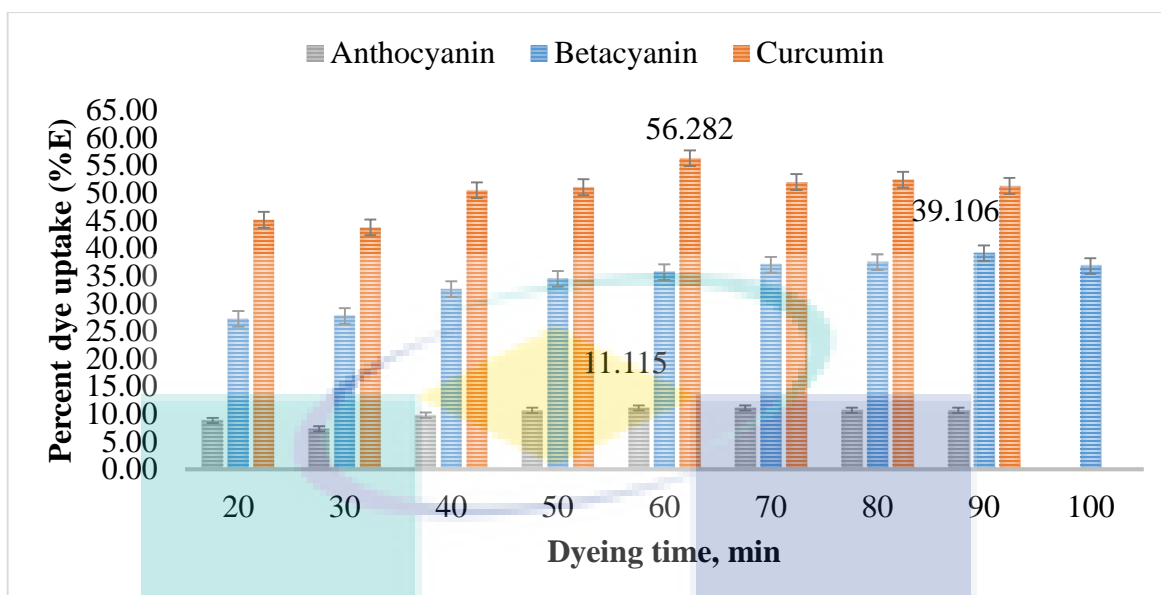


Figure 5.1 Effect of time on dyeing of BBPF, RDFP and turmeric dye on BY

### 5.2.2 Effect of dyeing temperature

About 0.5 g of BY was soaked in 50 mL of extracted blue dye solution, which had been set at pH 4.2, 30 minutes, 0.10 g/mL, and 525 nm for dye bath pH, time, dye bath concentration, and wavelength, respectively. In fact, the effect of dye bath temperature on the dyeing quality of BY with BBPF extract was studied within the range of 30–90 °C. The results of this study are further demonstrated in Figure 5.2. This figure clearly indicates that the percentage of dye uptake values failed to affect the percentage of dye uptake for anthocyanin because only slight changes had been noted for the percentage of dye uptake, which could be neglected.

The dyeing of red dye which was extracted from RDFP has been set at pH 4.5, 30 minutes, 0.10 g/mL, and 538 nm for dye bath pH, time, dye bath concentration for extracted red dye solution, and wavelength, respectively. Hence, the effect of dyeing temperature upon natural dye from RDFP on BY is demonstrated in Figure 5.2. Dyeing BY in the RDFP extracted dye solution showed that increasing temperature increased the adsorption of the betacyanin as the percentage of dye uptake further increased. As observed, the adsorption of betacyanin increased with the increase of dyeing temperature and thus, reached a maximum value at 70 °C, and later, it decreased. The temperature caused an increase in the reaction rate in the range of 60 to 80 °C, which was reflected in the dye-extracted productivity.



The dyeing uptake ability of curcumin on BY evaluation is presented in Figure 5.2. The dye molecules rapidly rushed onto BY until the temperature reached 70 °C. Same results was shared by Guesmi et al., (2012) in which the percent dye uptake for indicaxanthin extracted from fresh orange-yellow fruits increases with the dyeing temperature with a pronounced manner up 70 °C then decreased. However, at low temperature, the dye molecules adsorbed slowly as the reading of the percentage of dye uptake had been lower. Furthermore, the mobility of the dye ions increased at higher temperature and the adsorption of curcumin on BY enhanced until the equilibrium temperature was attained. Furthermore, when the temperature exceeded 70 °C, the colorant pigment began to face hydrolytic degradation, thus giving the opportunity for other impurities to sorb on BY. Hence, the range of dyeing temperature from 50 to 90 °C was further optimized. The results was indicated that the maximum adsorption of colorant pigment of betacyanin and curcumin on BY at dyeing temperature of 70 °C. Khan et al.,(2014) has been stated that dyeing process was done above that temperature of 70 °C caused the colorant faced hydrolytic degradation and other impurities got a chance to sorb at surface of fabric causing unevenness and dull shades.

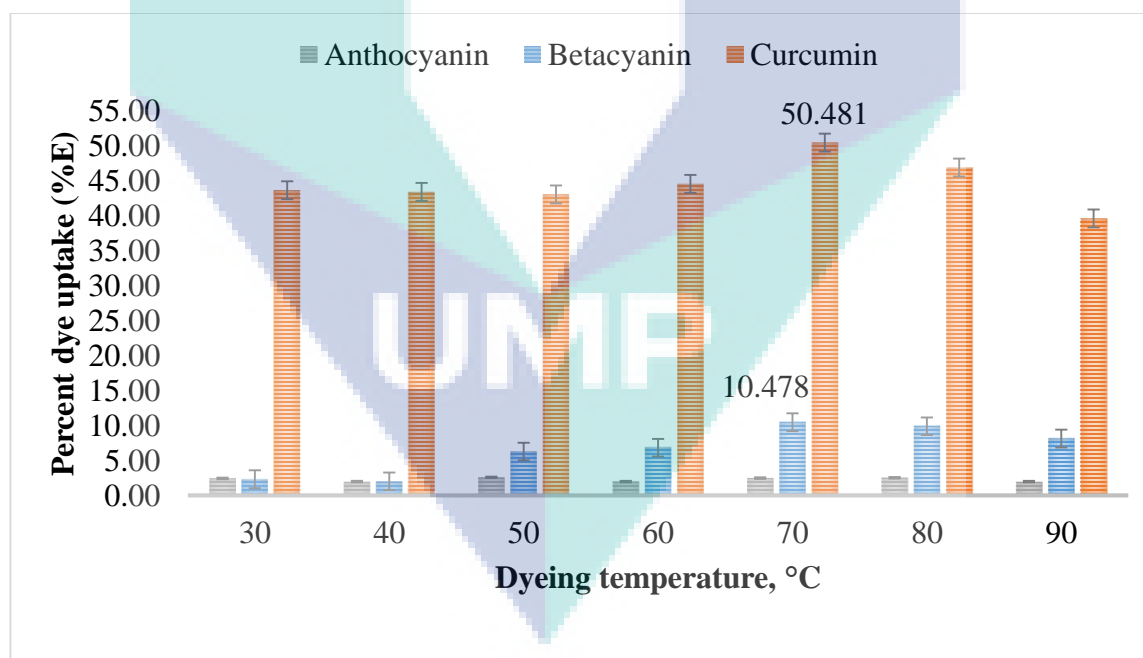


Figure 5.2 Effect of temperature on dyeing of BBPF, RDFP and turmeric dye on BY

### 5.2.3 Effect of dye bath concentration

The dyeing of natural dye from BBPF on BY was observed in the presence of varying the dye bath concentrations of extracted blue dye, where 1:100 of ratio weight of BY in blue dye solution had been used. The 0.5 g of BY was soaked in 50 mL of varying dye bath concentrations of extracted blue dye solutions, which had been set at pH 4.2, 30 minutes, 70 °C, and 525 nm for dye bath pH, time, temperature, and wavelength, respectively. Besides, Figure 5.3 shows the percentage of dye uptake for adsorption of anthocyanin on BY with the BBPF extracted dye solution. The percentage of dye uptake increased with the increase of dye bath concentration, a decreased was noted when it reached 0.10 g/mL of dye bath concentration. This effect had generally been considered as an important dyeing variable in the natural dyeing process. The dyeing of natural dye from RDFP was observed in the presence of varying the dye bath concentrations of extracted red dye with 1:100 of ratio weight of BY in red dye solution. The 0.5 g of BY was soaked in 50 mL of varying dye bath concentrations of extracted red dye solution, which had been set at pH 4.5, 30 minutes, 70 °C, and 538 nm for dyeing pH, time, temperature, and wavelength, respectively. In fact, Figure 5.3 shows the percentage of dye uptake for betacyanin on BY. Besides, the percentage of dye uptake increased with the increase in dye bath concentration, but the adsorption began to decrease when it reached a dye bath concentration at 0.10 g/mL.

Figure 5.3 shows that the percentage of dye uptake for curcumin on the BY increased with the increasing dye bath concentration until the dye bath concentration reached 0.10 g/mL. The adsorption of curcumin, which is known as colorant pigment in turmeric dye on BY, increased with the increment of dye bath concentration. However, at 0.10 g/mL of dye bath concentration, the interaction between the dye and the BY had been the strongest. Thus, the optimum range of dye bath concentration between 0.05 g/mL and 0.2 g/mL was further optimized in the RSM experiment. Furthermore, the low concentration of dye bath gave less colour depth for BBPF, RDFP and turmeric dye. The higher dye bath concentration, however, resulted in accumulation of dye molecules as they aggregated onto BY, which led to unevenness. Guesmi et al., (2012) has been studied the dyeing of wool fabrics with indicaxanthin from fresh orange-yellow fruits and the resulted on percent dye uptake increases as the concentration of the dye increased up to certain level (20 mg/L), after which the fibres started to become saturated.

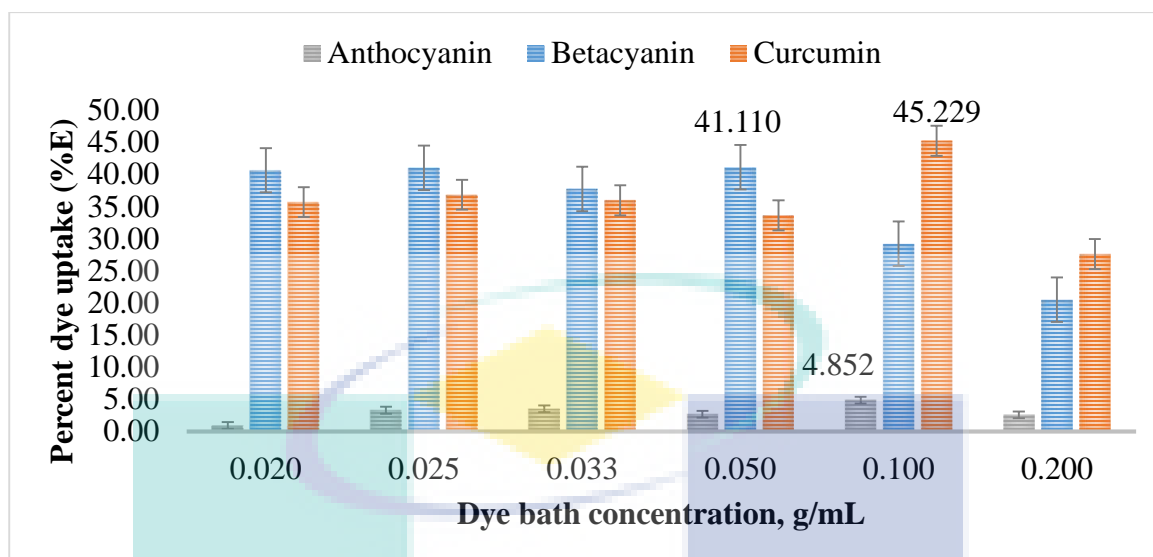


Figure 5.3 Effect of dye bath concentration on dyeing of BBPF, RDFP and turmeric dye on BY

#### 5.2.4 Effect of dye bath pH

The levels of dye bath pH had been varied, where 1:100 of ratio weight of BY in blue dye solution had been used in order to determine the optimum value for maximum adsorption of anthocyanin on BY. The dyeing time of blue dye was analysed at 30 minutes, 0.10 g/mL, 70 °C, and 525 nm for dyeing time, dye bath concentration, temperature, and wavelength, respectively. Besides, the pH of the dyeing bath was varied from 3 to 11. The effect of this variation on the percentage of dye uptake for anthocyanin on BY is reported in Figure 5.4, where the adsorption of anthocyanin on BY increased as the pH decreased for dyeing bath. The effect of dye bath pH can be attributed to the correlation between dye structure, the fibres used and dye stability. (Guesmi et al. 2012)

Moreover, the adsorption of anthocyanin on BY increased from the initial pH 2 until pH 5, and then decreased at higher pH values. The effect of dye bath pH, thus, can be attributed to the correlation between dye structure and BY. The anthocyanin compounds are the main colorant species present in BBPF. They are soluble in water containing hydroxyl groups. Moreover, their molecular structures present an important electronic density due to its highly conjugated system. Moreover, at pH 5, the anthocyanin compounds possessed high affinity for BY through the obtained maximum percentage of dye uptake. Meanwhile, the

BY, which is a natural cellulosic fibre, has high affinity towards water (due to its many hydroxyl groups) and permeability. The results of pH optimization experiments further indicated that the surface of BY might have greater negative potential, partly due to the increasing dissociation of OH group present in the cellulosic fibre. This may be explained by the important attraction that take place between both the protonated terminal OH groups of BY and the anthocyanin molecular structure that displayed high electronic density. However, when the pH of the dyeing bath raised, the dye ability decreased due to the decreasing number of protonated terminal OH groups of BY, and therefore, the attraction decreased as well. This dissociation caused less interaction between the dye molecules (Adeel et al., 2017). The carboxyl groups of fabric (formed at the surface after irradiation) were suppressed in dye bath with acidic pH and the fabric might allow great sorption of dye, thus resulting in higher depth. In fact, similar observation was found in the study conducted by Adeel et al., (2017), where the maximum dye uptake was noted at the dyeing bath pH of 5. Maintaining the dye bath pH higher than the optimal value (5) could cause lower colour strength. Besides, the anthocyanin existed primarily in the form of red flavylium cation. Increasing the pH value caused fast loss of the proton and produced quinoidal base forms; blue or violet. At the same time, hydration of flavylium cation occurred and the carbinol or pseudo base was generated, which slowly reached equilibrium and produced chalcone in faint yellow. The relative amounts of above four forms of anthocyanin at the equilibrium condition, nevertheless, varied based on the pH values because the colour of the solution was red under strong acidic condition ( $\text{pH} < 3.0$ ), but stayed yellow under alkaline condition with pH value above 7 (H. Wang et al., 2014).

The effect of the dye bath pH can be attributed to the correlation between dye structure and BY. In the study by Ren et al., (2016), the effect of dye bath pH value on the application of tea natural pigment in wool played a key role and its chemical structures were directly related to the performance of dyed fabric. The levels of dye bath pH had been varied with 1:100 of ratio weight of BY in red dye solution in order to determine the optimum value for maximum adsorption of betacyanin on BY. The dyeing time of red dye was analysed at 30 minutes, 0.10 g/mL, 70 °C, and 538 nm for dyeing time, dye bath concentration, temperature, and wavelength, respectively. The effect of pH value on the percentage of dye uptake for betacyanin on BY is illustrated in Figure 5.4, where the maximum adsorption of

betacyanin on BY was observed at pH 3. However, when the dye bath pH exceeded this value, the colour yield decreased considerably. At low level of pH, low interaction occurred, which is susceptible to occur between betacyanin structure and BY. At pH >3, the hydroxyl groups of the betacyanin began to convert to alkoxide ion that would interact ionically with the protonated terminal groups of BY via ion exchange reaction. This ionic attraction would decrease the percentage of dye uptake of the BY. After pH of 3, all the protonated terminal groups fixed on BY do not interacted with the betacyanin, with no additional dye adsorption, and the maximum percentage of dye uptake was obtained at this value. Furthermore, the electrostatic repulsion between the anionic colorants and the protein fibres led to the decrease in the adsorption of betacyanin on BY.

In particular, the pH value for all OFAT experiments was keep constant at 8.5, but for the analysis of the effect of dye bath pH on dyeing of turmeric dye on BY, as shown in Figure 5.4. The range of pH varies from 2 until 11 had been set for dyeing of turmeric dye on BY. The pH of the dye bath plays an important role in the whole dyeing process because it influences not only the dye bath chemistry, but also the surface charge on the BY itself. BY contains both hydroxide ion ( $\text{OH}^-$ ) and carboxylate ion ( $\text{COO}^-$ ), which indicated that the carboxylate ion site had been responsible for dye binding through electrostatic interactions. Furthermore, the bamboo structure consists of cellulose, a polymer built on monomeric glucose units. Subsequently, cellulose is susceptible to hydrolysis when heated in acidic medium. Thus, the dyeing of BY must be realized at pH values above 4. At higher pH values (>8), the side chain hydroxyl groups can be ionized, thus increasing the negative surface charge considerably. Furthermore, the percentage of dye uptake of curcumin increased at acidic medium from pH 2 until pH 5, but began to decrease at higher pH values. This is because; at the alkaline medium, the reaction of hydroxide ions ( $\text{OH}^-$ ) would convert the ammonium ions ( $\text{NH}_3^+$ ) to amino ( $\text{NH}_2$ ), thus contributing to the production of more carboxylate ions ( $\text{COO}^-$ ) on BY. Therefore, electrostatic repulsion between the anionic colorant and the BY took place, and further decreased the percentage of dye uptake of curcumin pigment on BY. Moreover, the range of pH from 1 to 5 had been opted to further optimize the dyeing conditions in RSM. From this result, the dyeing BY with BBPF, RDFP and turmeric dyes were observed that the colorant pigments were adsorbed onto BY in acidic media. Similar studies reported by Uddin, (2015) where the higher the alkalinity of the

extraction mango leaves dye bath, the greater was the pH drop rate. The drop rate became gradually slower while gradually approaching to more acidic bath from neutral bath. The different results was revealed by Khan et al., (2014) where the colorant being sorbed more onto irradiated cotton in alkaline media. Form

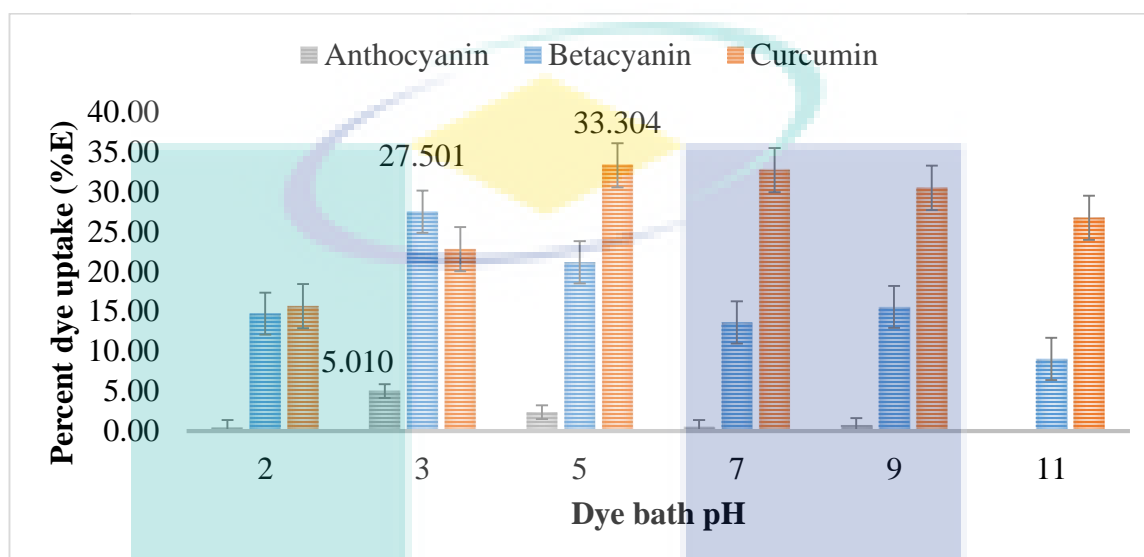


Figure 5.4 Effect of BBPF, RDFP and turmeric dye bath pH on BY

### 5.3 Optimization of Natural Dyes Dyeing on Bamboo Yarn (BY) via RSM

The optimum conditions range data obtained from the OFAT of dyeing of natural dyes on BY had been transferred into the Design Expert (2008) statistical tool. The regression parameters were run to generate it and then were further continued with Response Surface Method (RSM). The experimental design was devised using the Design Expert software (version 8.0.6) developed based on Central Composite Design (CCD). The CCD was conducted with a  $2^3$  full factorial CCD of combinations factors at two levels (high, +1 and low, -1 level), including six star points (axial) corresponding to any value of 2 and six replicates at the centre points (coded level 0, midpoint of high, and low levels). Moreover, four effects of independent variables were investigated for each dye in dyeing of natural dyes on BY from BBPF, RDFP, and Turmeric i.e., dyeing temperature, dyeing time, dye bath pH, and dye bath concentration of the extracted dyes. In this study, the primary objective of RSM is to optimize the response based on the factor investigated. The Design Expert software (version 8.0.6) was further used to develop the experimental plan, besides optimizing the

independent variables of dyeing temperature, dyeing time, dye bath pH, and dye bath concentration of extracted dyes for dyeing of natural dyes on BY in this research. The RSM is generally used to examine the correlations between one or more response variables and a set of quantitative experimental variables or factors (Haddar et al., 2014). Furthermore, RSM uses experimental design of the CCD to fit a model by employing the least squares technique. The statistical significance of the second-order model equation was determined by performing the Fisher's statistical test for ANOVA. In fact, ANOVA is used to investigate and model the correlations between a response variable and one or more independent variables. The significance of each coefficient, furthermore, is determined by applying the t-test. Besides, the p-values denote the significance of the coefficients. They are important to comprehend the pattern of mutual interactions between the variables. The larger the magnitude of t-test and smaller the p-value, the more significant is the corresponding coefficient (Jabasingh et al., 2016). The lower and the upper limit of the selected parameters were set based on optimum range resulted in the OFAT.

### 5.3.1 Dyeing of BBPF dye on BY

The independent variable for dye bath concentration of extracted blue dye solution, time, and dye bath pH were represented by variables A ranging from 0.062 to 0.146 g/mL, B ranging from 35 to 95 minutes, and C ranging from pH 1 to 9, respectively, as listed in Table 5.1. The effects of dye bath concentration, time, and dye bath pH on the percentage of dye uptake for anthocyanin from BBPF dye had been determined by dispersing 0.2 g of BY in 20mL of extracted blue dye solution based on various combinations with 1:100 of ratio BY dispersed in extracted dye, as portrayed in Table 5.2.

Table 5.1 Constraint for the dyeing of blue dye from BBPF on BY conditions

<b>Factor</b>	<b>Name</b>	<b>Units</b>	<b>Lower Limit</b>	<b>Upper Limit</b>
<b>A</b>	Dye bath concentration	g/mL	0.062	0.146
<b>B</b>	Time	Minutes	35	95
<b>C</b>	Dye bath pH	-	1	9

Table 5.2 The actual level of independent variables for the dyeing of blue dye from BBPF on BY

Run	Coded variables			Actual variables			Response		
	A	B	C	Dye bath concentration, g/mL	Time, minutes	Dye bath pH	Absorbance before	Absorbance after	Percent dye uptake, %E
1	-1	1	1	0.083	80	7	2.654	2.444	7.913
2	0	0	0	0.104	65	5	2.854	2.456	13.945
3	0	0	0	0.104	65	5	2.886	2.456	14.900
4	0	2	0	0.104	95	5	2.658	2.409	9.368
5	0	0	0	0.104	65	5	2.638	2.468	6.444
6	0	0	2	0.104	65	9	2.125	2.114	0.518
7	0	-2	0	0.104	35	5	2.854	2.444	14.366
8	-2	0	0	0.062	65	5	2.824	2.456	13.031
9	0	0	0	0.104	65	5	2.800	2.468	11.857
10	0	0	-2	0.104	65	1	2.537	2.523	0.552
11	-1	-1	-1	0.083	50	3	2.366	2.293	3.085
12	0	0	0	0.104	65	5	2.685	2.456	8.529
13	1	1	-1	0.125	80	3	2.553	2.523	1.175
14	2	0	0	0.146	65	5	2.589	2.444	5.601
15	1	-1	1	0.125	50	7	2.545	2.505	1.572



### 5.3.2 Dyeing of RDFP dye on BY

The independent variables for dye bath concentration of extracted red dye solution, time, and dye bath pH by variables A ranging from 0.062 to 0.146 g/mL, B ranging from 70 to 110 minutes, C ranging from pH 1 to 5, and D ranging from 50 to 90 °C respectively, are shown in Table 5.3. The effects of dye bath concentration, time, dye bath pH, and temperature on the percentage of dye uptake for betacyanin from RDFP dye had been determined by dispersing 0.2g of BY in 20mL of extracted red dye solution based on varied combinations with 1:100 of ratio BY dispersed in extracted dye, as presented in Table 5.4.

Table 5.3 Constraint for dyeing of red dye from RDFP on BY conditions

Factor	Name	Units	Lower Limit	Upper Limit
A	Dye bath concentration	g/mL	0.062	0.146
B	Time	Minutes	70	110
C	Dye bath pH	-	1	5
D	Temperature	°C	50	90

Table 5.4 The actual level of independent variables for dyeing of red dye from RDFP on BY

Run	Coded variables				Actual variables				Response		
	A	B	C	D	Dye bath concentration, g/mL	Time, minutes	Dye bath pH	Temperature, °C	Absorbance before	Absorbance after	Percent dye uptake, %E
1	-1	1	1	1	0.083	100	4	80	1.279	1.085	15.168
2	0	0	0	0	0.104	90	3	70	1.291	1.117	13.478
3	0	0	2	0	0.104	90	5	70	1.229	1.168	4.963
4	-2	0	0	0	0.062	90	3	70	1.233	1.108	10.138
5	0	0	0	2	0.104	90	3	90	1.249	1.106	11.449
6	1	-1	1	1	0.125	80	4	80	1.327	1.098	17.257
7	2	0	0	0	0.146	90	3	70	1.502	1.203	19.907
8	-1	-1	1	-1	0.083	80	4	60	1.317	1.200	8.884
9	0	0	0	-2	0.104	90	3	50	1.254	1.195	4.705
10	0	2	0	0	0.104	110	3	70	1.271	1.124	11.566
11	1	1	-1	-1	0.125	100	2	60	1.301	1.197	7.994
12	0	0	0	0	0.104	90	3	70	1.640	1.091	33.476
13	0	0	0	0	0.104	90	3	70	1.649	1.098	33.414
14	0	0	0	0	0.104	90	3	70	1.652	1.106	33.051
15	-1	1	-1	1	0.083	100	2	80	1.285	1.129	12.140
16	1	-1	-1	1	0.125	80	2	80	1.442	1.225	15.049
17	0	0	-2	0	0.104	90	1	70	1.165	1.093	6.180
18	0	0	0	0	0.104	90	3	70	1.280	1.142	10.781
19	-1	-1	-1	-1	0.083	80	2	60	1.249	1.152	7.766
20	1	1	1	-1	0.125	100	4	60	1.317	1.173	10.934
21	0	-2	0	0	0.104	70	3	70	1.399	1.209	13.581

### 5.3.3 Dyeing of turmeric dye on BY

The independent variables for dye bath concentration of extracted yellow dye solution, time, and dye bath pH are represented by variables A ranging from 0.062 to 0.146 g/mL, B ranging from 40 to 80 minutes, C ranging from pH 1 to 5, and D ranging from 50 to 90 °C, respectively, as shown in Table 5.5. Meanwhile, the effects of dye bath concentration, time, dye bath pH, and temperature on the percentage of dye uptake for curcumin from turmeric dye had been determined by dispersing 0.2 g of BY in 20mL of extracted yellow dye solution based on various combinations with 1:100 of ratio BY dispersed in extracted dye, as portrayed in Table 5.6.

Table 5.5 Constraint for dyeing of yellow dye from turmeric on BY conditions

<b>Factor</b>	<b>Name</b>	<b>Units</b>	<b>Lower Limit</b>	<b>Upper Limit</b>
<b>A</b>	Dye bath concentration	g/mL	0.062	0.146
<b>B</b>	Time	Minutes	40	80
<b>C</b>	Dye bath pH	-	1	5
<b>D</b>	Temperature	°C	50	90

Table 5.6 The actual level of independent variables for dyeing of yellow dye from turmeric on BY

Run	Coded variables				Actual variables				Response		
	A	B	C	D	Dye bath concentration, g/mL	Time, minutes	Dye bath pH	Temperature, °C	Absorbance before	Absorbance after	Percent dye uptake, %E
1	0	0	0	0	0.104	60	3	70	2.284	2.046	10.420
2	1	-1	1	1	0.125	50	4	80	2.721	2.602	4.373
3	-1	1	1	1	0.083	70	4	80	2.143	2.140	0.140
4	0	0	0	0	0.104	60	3	70	2.602	2.495	4.112
5	0	2	0	0	0.104	80	3	70	2.537	2.459	3.074
6	-1	-1	1	-1	0.083	50	4	60	2.032	1.359	33.120
7	-2	0	0	0	0.062	60	3	70	2.482	2.398	3.384
8	1	1	-1	-1	0.125	70	2	60	2.509	2.495	0.558
9	0	0	0	0	0.104	60	3	70	1.900	0.759	60.053
10	-1	1	-1	1	0.083	70	2	80	2.398	2.237	6.714
11	0	0	2	0	0.104	60	5	70	2.086	1.509	27.661
12	1	1	1	-1	0.125	70	4	60	2.495	1.879	24.689
13	0	0	-2	0	0.104	60	1	70	1.087	0.855	21.343
14	1	-1	-1	1	0.125	50	2	80	2.602	2.585	0.653
15	0	0	0	0	0.104	60	3	70	1.920	0.764	60.208
16	-1	-1	-1	-1	0.083	50	2	60	1.910	1.900	0.524
17	0	-2	0	0	0.104	40	3	70	2.537	2.520	0.670
18	0	0	0	-2	0.104	60	3	50	2.456	2.310	5.945
19	0	0	0	2	0.104	60	3	90	2.357	2.289	2.885
20	2	0	0	0	0.146	60	3	70	2.553	2.509	1.723
21	0	0	0	0	0.104	60	3	70	1.910	0.760	60.209

### 5.3.4 Diagnosis of model properties

The statistical properties of model developed in this research were diagnosed by inspecting various diagnostic plots (plot of normal probability, studentized residuals, and outlier T). The normal probability plots for dyeing of BBPF, RDFP, and Turmeric dyes on BY are displayed from Figure 5.5 until 5.7. The plots indicated that the residuals adhered to normal distribution, in which the points were in a straight line. Besides, the plots of normal probability of dyeing BBPF dye on BY resulted in definite patterns like the "S-shaped" curve, which indicated a transformation of the response might provide better analysis.

Meanwhile, the residuals versus predicted refers to a plot of the residuals versus the ascending predicted response values. The residuals versus predicted plot for dyeing of BBPF, RDFP, and Turmeric dyes on BY are shown in Figure 5.8, Figure 5.9, and Figure 5.10 respectively. These plots were in a random scatter with consistent top to bottom range of residuals across the predictions. All these plots suggested that the variance of the actual observations is constant for all values for both external and internal studentized residuals, as studentized residuals are found in the range between 3 and -3. Moreover, it has been revealed that the proposed models were distinctly adequate and reasonable. Thus, violation is not needed for the independence or constant variance assumption because the outliers run with residuals inside the red lines on the plot. This means the observation has no problem and the model is indeed fit for use; thus dismissing the need for a transformation.

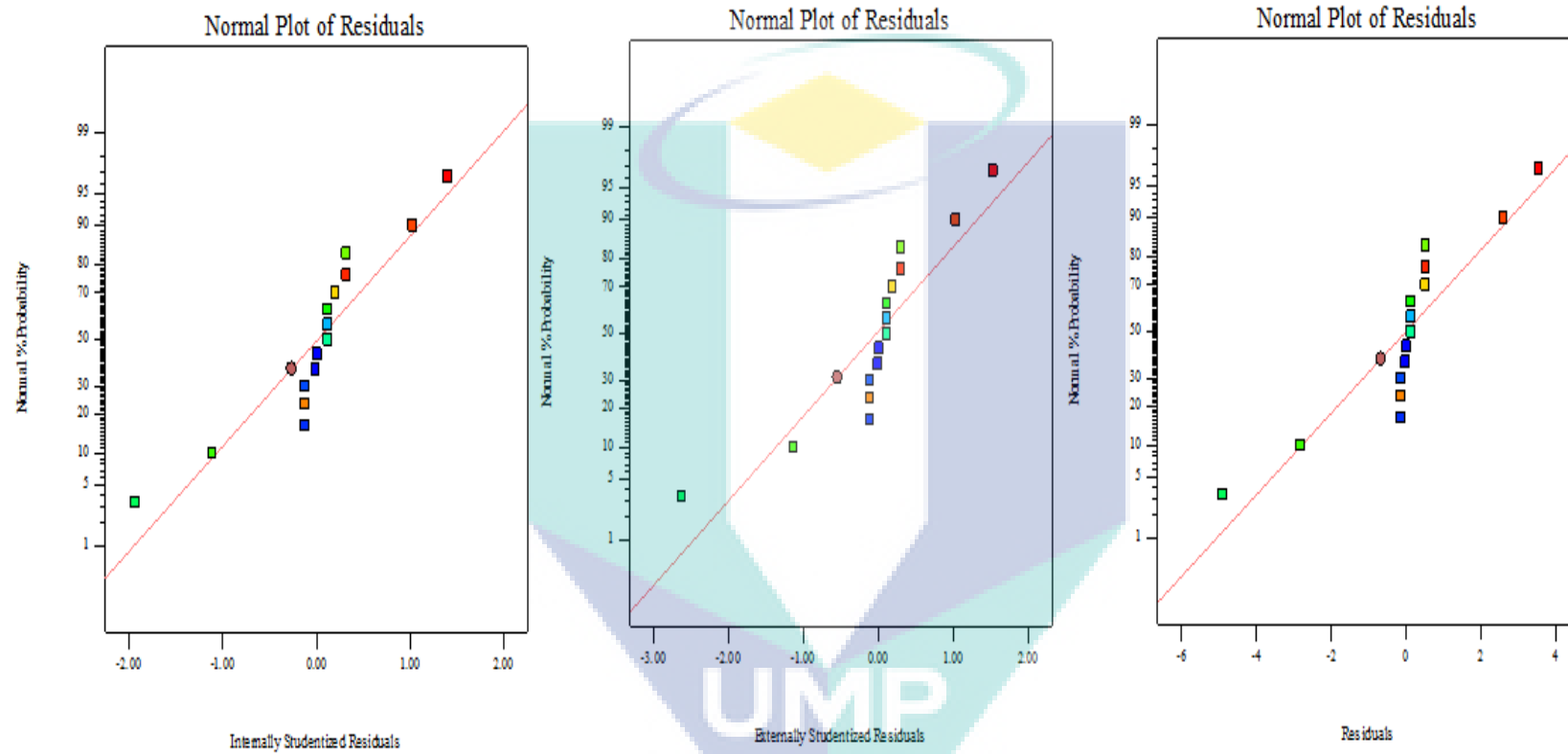


Figure 5.5 Normal probability plots for dyeing of BBPF dye on BY

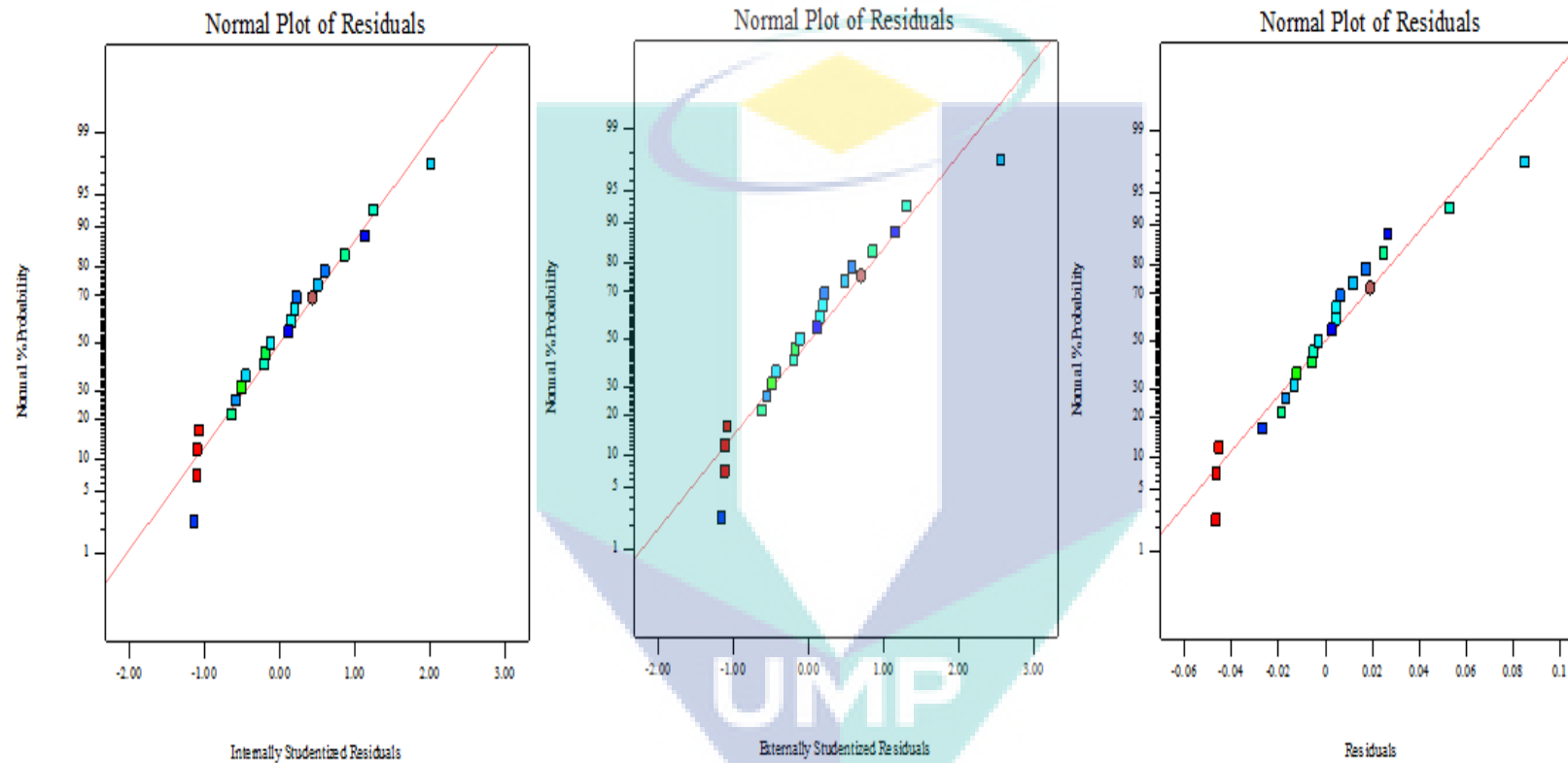


Figure 5.6 Normal probability plots for dyeing of RDFP dye on BY

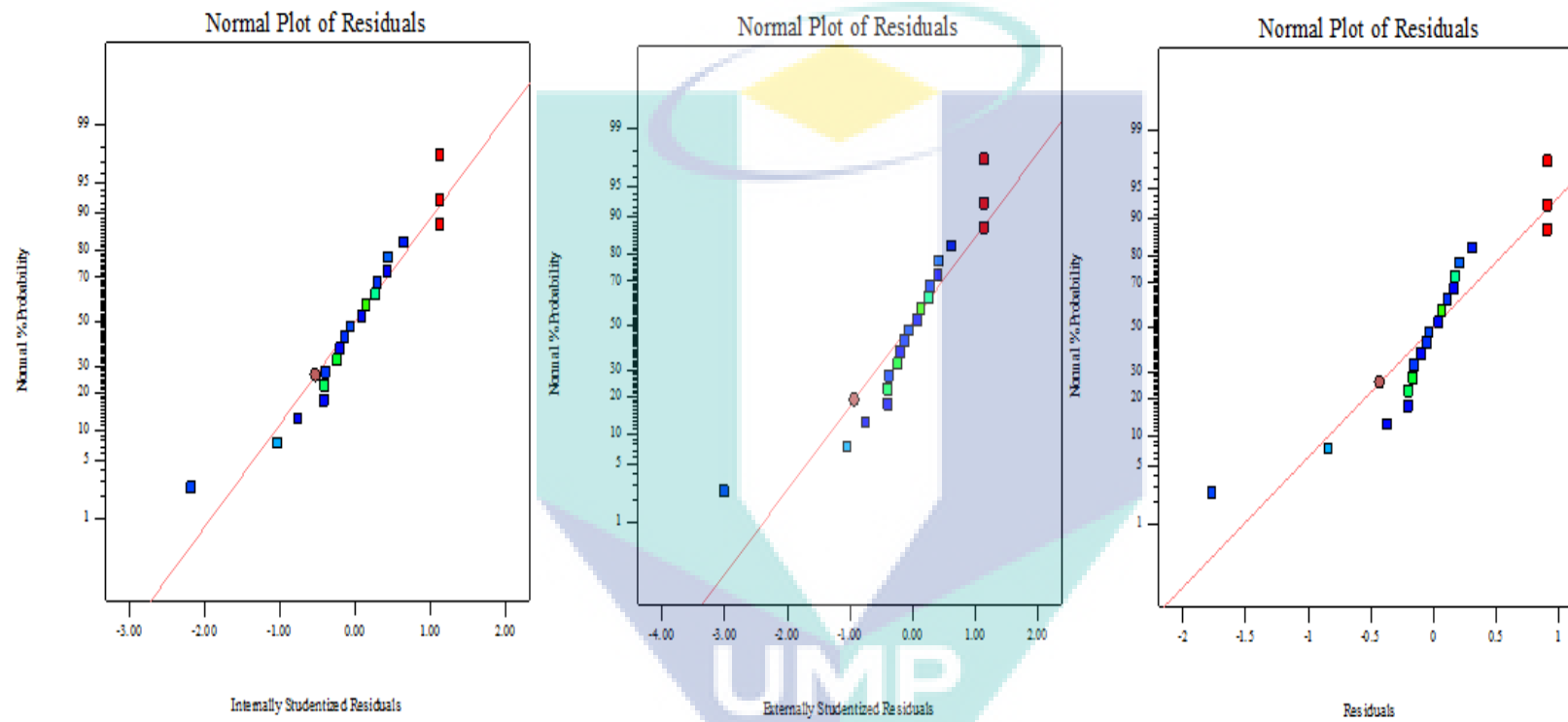


Figure 5.7 Normal probability plots for dyeing of turmeric dye on BY



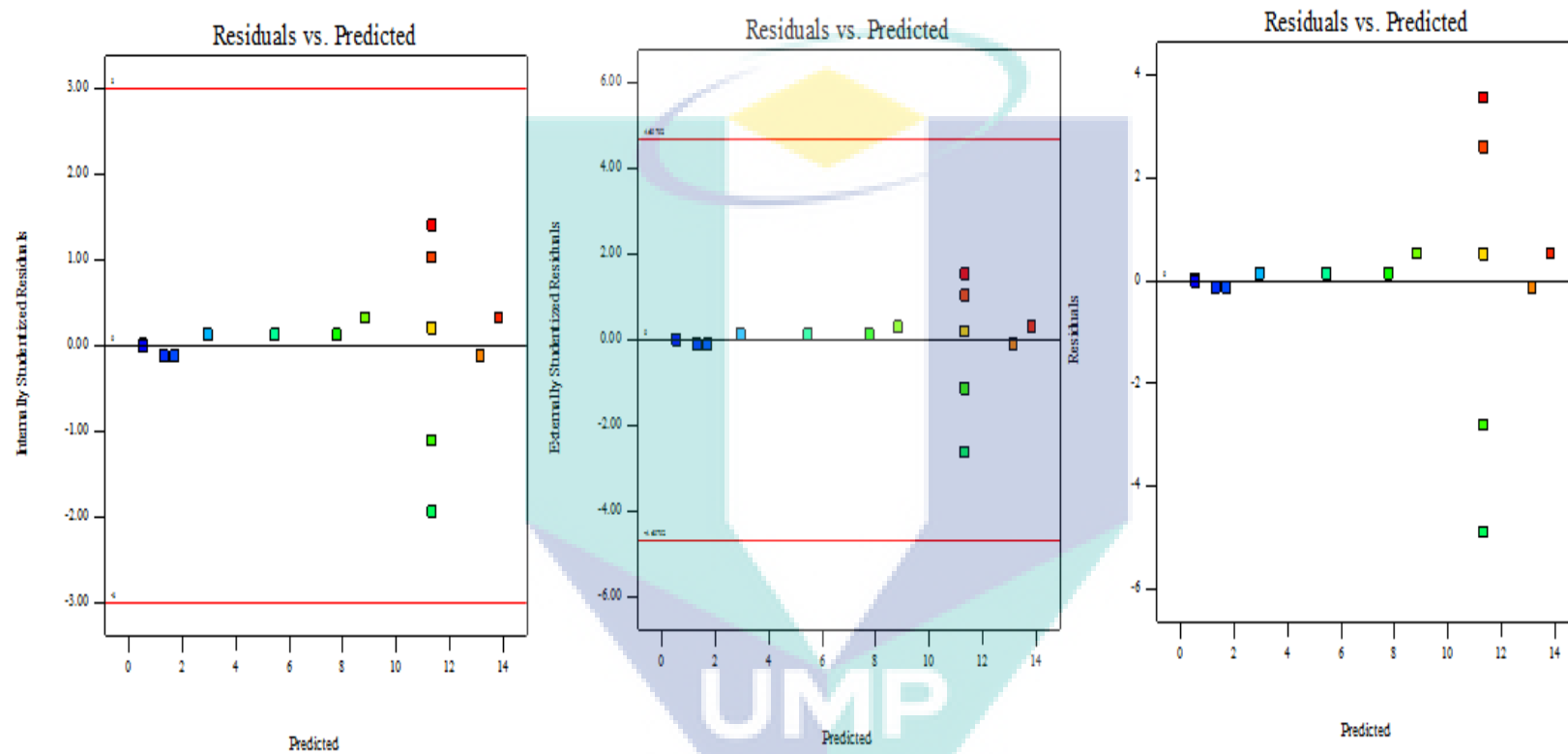


Figure 5.8 Residuals versus predicted plot for dyeing of BBPF dye on BY

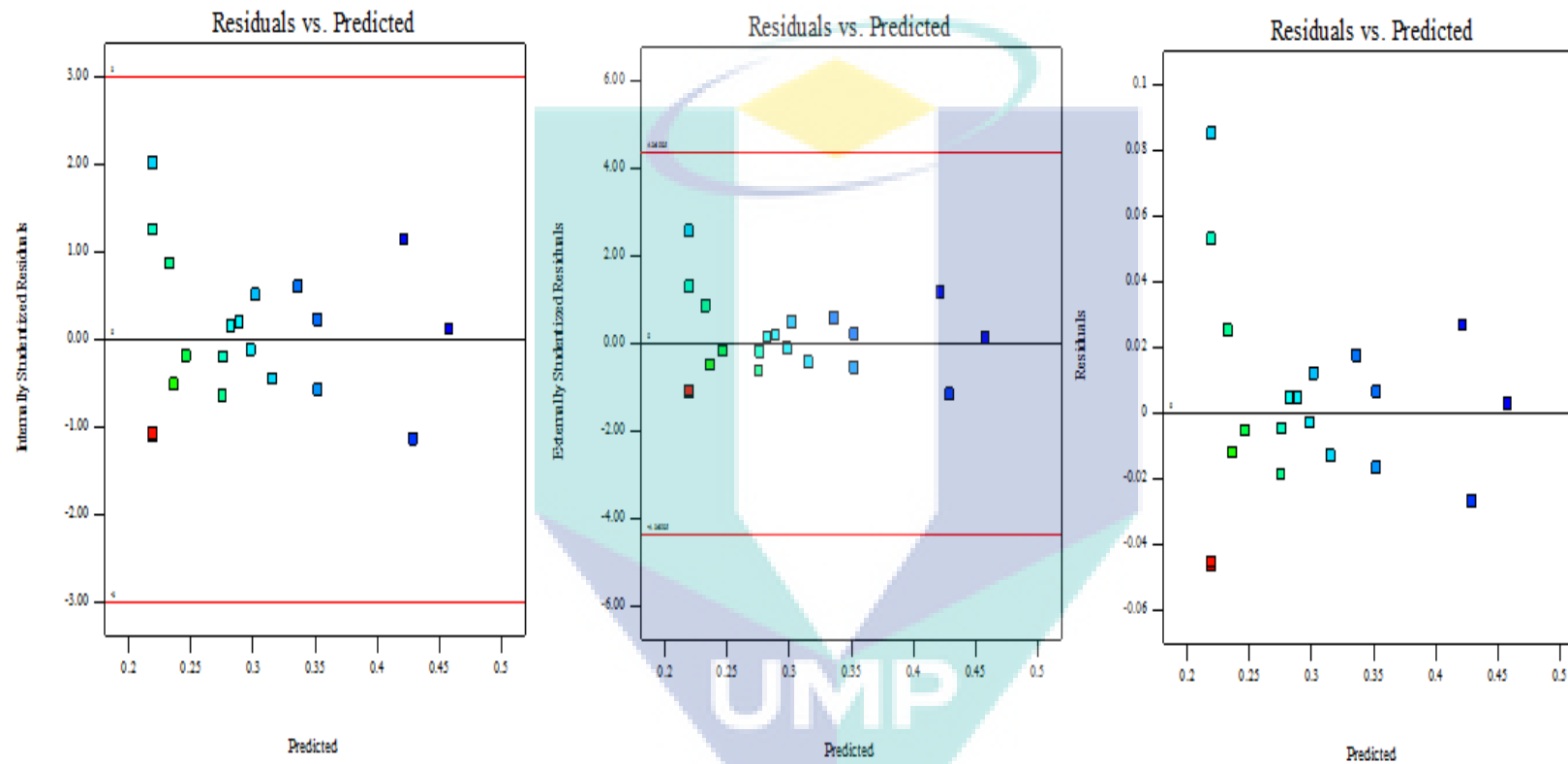


Figure 5.9 Residuals versus predicted plots for dyeing of RDFP dye on BY

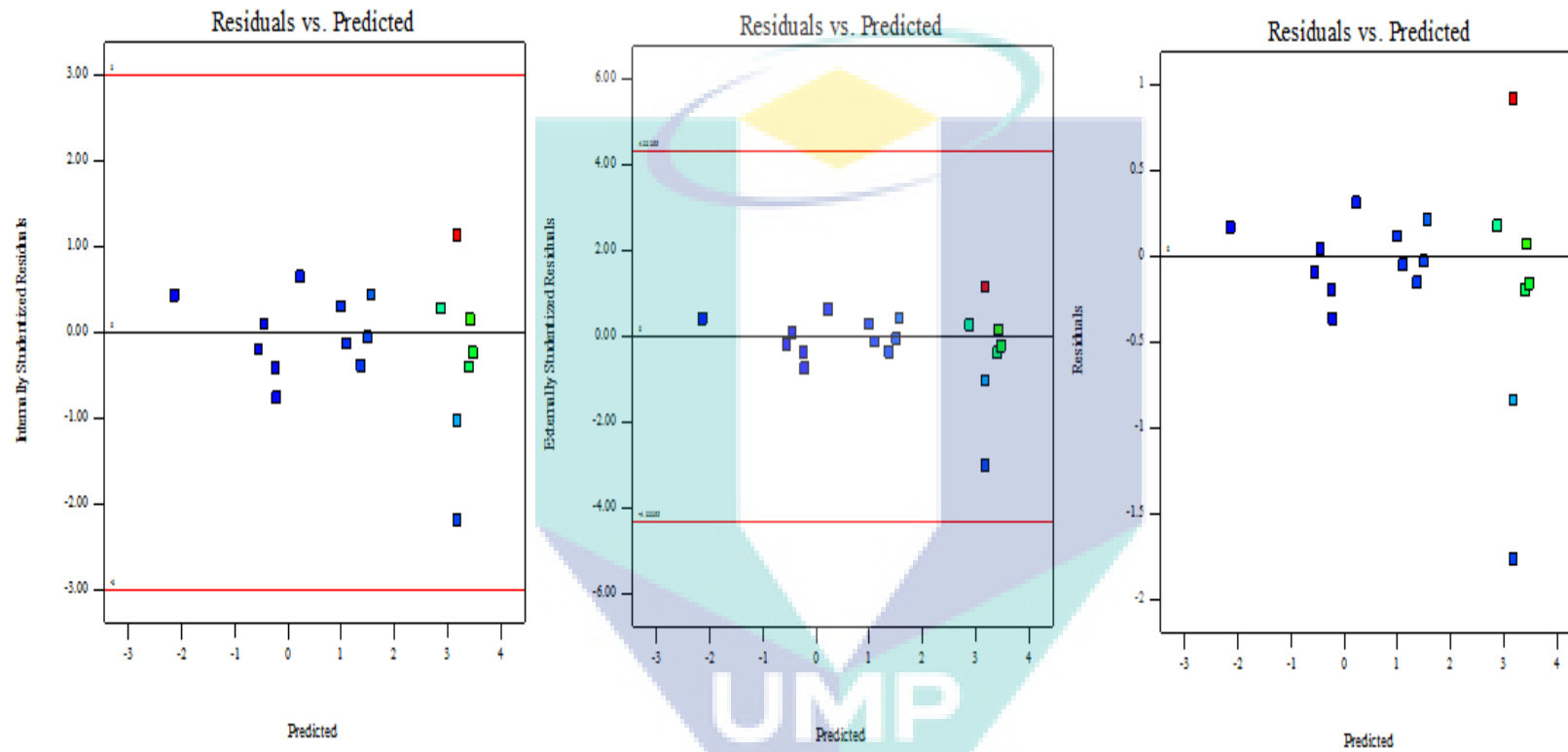


Figure 5.10 Residuals versus predicted plots for dyeing of turmeric dye on BY

### 5.3.5 Optimization of process condition

In order to investigate and to determine the optimum process condition of the effects of dye bath concentration (A), dyeing time (B), and dye bath pH (C) process variables on the dyeing of extracted dyes from BBPF, RDFP, and turmeric on BY, the influence of these input variables were established by the Design Expert software (Version 8.0.6) by employing CCD. The results of CCD experiments with varied combinations for dye bath concentration (A), dyeing time (B), dye bath pH (C), and dyeing temperature (D) process variables on the dyeing of extracted dyes from BBPF on BY are presented, along with mean values predicted and experimental responses for the percentage of dye uptake as the response.

Moreover, ANOVA, regression coefficient estimate, and test of significance for percentage of dye uptake, and %E of anthocyanin (colorant pigment in BBPF dye) are shown in Table 5.7. The model F-value of 6.5402 further implies its significance. Moreover, there is a 1.21% chance that an F-value this large could occur due to noise. The values of Prob > F less than <0.0050 indicate the significance of the model terms. The determination of coefficient ( $R^2$ ) was 0.8674 for percentage of dye uptake for anthocyanin on BY. Besides,  $R^2$  implied a sample variation of 86.74%, as attributed to the variable and only 13.26% of the total variance could not be explained by the model. In fact, the  $R^2$  values were in reasonable agreement with the adjusted determination of coefficient (Adj  $R^2$ ) value of 0.7348. The predicted determination of coefficient (Pred  $R^2$ ) at 0.8006 is in reasonable agreement with the Adj  $R^2$  of 0.7348. Furthermore, "Adeq Precision" measures the signal to noise ratio. A ratio greater than 4 is desirable and the ratio of 6.6688 indicates an adequate signal. This model, therefore, can be used to navigate the design space. The coefficient of variation (CV) indicates the degree of precision with which the experiments were compared. Moreover, a lower value of coefficient of variation (CV) at 36.32 % indicated the precision with which the experiments had been conducted. The "Lack of Fit F-value" of 0.02 further implies the Lack of Fit that is insignificant in relation to pure error. In addition, there is a 99.46% chance that a "Lack of Fit F-value" this large could occur due to noise. On top of that, the insignificant lack of fit is good.

On the other hand, the quadratic effect of dye bath pH ( $C^2$ ), the main effect of dye bath concentration (A), as well as the three-level interactions between concentration,

dyeing time, and dye bath pH (ABC), were found to be the most significant terms to display the principal effects towards dyeing of BBPF dye on BY. Hence, the ranking of the model terms, based on the statistical significant (F-value) in the study of dyeing of BBPF dye on BY is as follows:  $C^2 > A > ABC$ . The data obtained was scrutinized by applying the multiple regression analysis based on the predicted response Y obtained as a function of dye bath concentration (A), dyeing time (B), and dye bath pH (C) process variables on the dyeing of extracted dye from BBPF, which is expressed as follows:

$$Y = +11.3441 - 1.2495A - 1.2495B - 1.3063AB - 2.3573AC - 0.5070A^2 - 2.7023C^2 + 4.6986ABC \quad 5.1$$

Furthermore, Y is the predicted response variable for the percentage of dye uptake, % E. These equations, in terms of coded factors, can be used to make predictions about the response for given levels of each factor. Moreover, the coded equation is useful to identify the relative impact of the factors by comparing the factor coefficients.

The logo for UIMP (Universitas Islam Mataram) is a large, downward-pointing arrow. The arrow is divided into four quadrants by a vertical and a horizontal line. The top-left and bottom-right quadrants are light blue, while the top-right and bottom-left quadrants are light purple. The letters "UIMP" are written in white, bold, sans-serif font across the center of the arrow.

Table 5.7 Analysis of variance (ANOVA) for dyeing of BBPF dye on BY

Source	Sum of squares	Degree of freedom	Mean square	F-value	Prob > F
<b>Model</b>	341.8415	7	48.8345	6.5402	0.0121(significant)
<b>A-Dye bath concentration</b>	44.5099	1	44.5099	5.9610	0.0447
<b>B-Time</b>	12.4900	1	12.4900	1.6727	0.2369
<b>AB</b>	6.8252	1	6.8252	0.9141	0.3709
<b>AC</b>	14.8177	1	14.8177	1.9845	0.2018
<b>A<sup>2</sup></b>	6.3986	1	6.3986	0.8569	0.3854
<b>C<sup>2</sup></b>	181.7473	1	181.7473	24.3407	0.0017
<b>ABC</b>	63.3994	1	63.3994	8.4908	0.0225
<b>Residual</b>	52.2677	7	7.4668		
<b>Lack of Fit</b>	0.8784	3	0.2928	0.0228	0.9946(insignificant)
<b>Pure Error</b>	51.3893	4	12.8473		
<b>Cor Total</b>	394.1092	14			
<b>Std. Dev.</b>	2.7325				
<b>Mean</b>	7.5237				
<b>C.V. %</b>	36.3190				
<b>R<sup>2</sup></b>	0.8674				
<b>Adj R<sup>2</sup></b>	0.7348				
<b>Pred R<sup>2</sup></b>	0.8006				
<b>Adeq Precision</b>	6.6688				

The results obtained with central composite experimental design identified the best levels of the process variables of dye bath concentration (A), dyeing time (B), dye bath pH (C), and dyeing temperature (D) on the dyeing of extracted dye from RDFP on BY. As observed, a considerable variation was noted in the percentage of dye uptake for betacyanin from RDFP dye at varied values of the selected variables. Other than that, the ANOVA for the percentage of dye uptake meant for betacyanin on dyeing of RDFP dye on BY was used in order to validate the model, as depicted in Table 5.8. The quadratic model was employed to determine the relationship between the variables and the responses. As such, the F-value of the dyeing of RDFP dye on BY was 4.43, which is significant, similar to the P-values of the model, which are also significant. In fact, there is 1.68% chance that an F-value this large could occur due to noise. The insignificant "Lack of Fit F-value", F-value of 0.1763 is insignificant and indicated that the quadratic model was indeed valid for the present study. The minimum value of standard error design (0.0472), on the other hand, around the centroid indicated that the present model could be used to conduct the design space. The regression equation obtained after the ANOVA showed that the correlation coefficient ( $R^2$ ) was 0.8442 for dyeing of RDFP dye on BY. However, in this case, the  $R^2$  values of 0.8442 implied a sample variation of 84.42%, which was attributed to the variable and only 15.58% of the total variance could not be explained by the model. Besides, a measure of the amount of variation in the predicted data was also examined by the model as that predicted by  $R^2$ . Moreover, it was observed that the predicted  $R^2$  was 0.4763 for dyeing of RDFP dye on BY. Thus, the predicted  $R^2$  is in agreement with the adjusted  $R^2$ (0.6538). These results indicated a high correlation between the observed and the predicted values. Other than that, adequate precision refers to the measure of the range in predicted response relative to its associated error. In fact, a ratio greater than four is desired (Kousha et al., 2015). Therefore, as the ratio of 6.6900 is greater than 4, the reliability of the experiment data is confirmed. Hence, the quadratic model can be used to navigate the design space. Thus, the high  $R^2$  value, significant F-value, insignificant lack-of-fit P-value, and high adequate precision indicated high adequacy and validity of the models in predicting the optimum conditions for dyeing of RDFP dye on BY. Therefore, these models were used for further analysis.

The quadratic effect of dye bath pH ( $C^2$ ), the quadratic effect of temperature ( $D^2$ ), and main effect of the temperature (D) had been discovered to be the most significant terms to have the principal effect towards dyeing of RDFP dye on BY. Hence, the ranking of the model terms, based on the statistical significant (F-value) in the study of dyeing of RDFP dye on BY is given as follows:  $C^2 > D^2 > D$ . The data obtained were further scrutinized by applying the multiple regression analysis based on the predicted response Y, which was obtained as a function of dye bath concentration (A), dyeing time (B), dye bath pH (C), and dyeing temperature (D) process variables on the dyeing of extracted dye from RDFP. Y is the predicted response variable for the percentage of dye uptake, %E.

$$\frac{1}{\text{Sqrt}}(Y) = +0.2193 - 0.0165A + 0.0033B - 0.0018C - 0.0399D - 0.0051BC + 0.0034CD + 0.0124A^2 + 0.0158B^2 + 0.0516C^2 + 0.0397D^2 + 0.0398ABD \quad 5.2$$

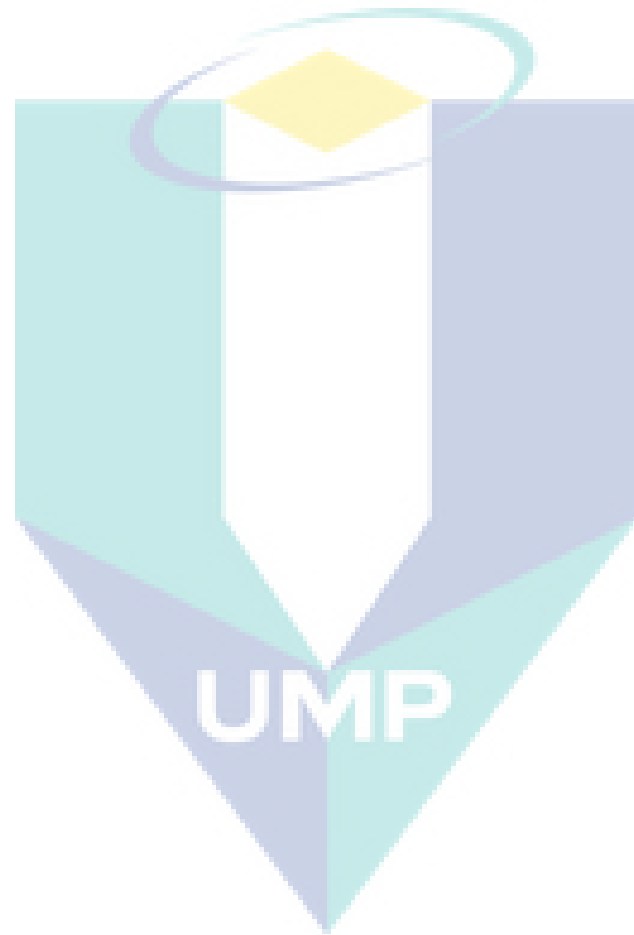
These equations, in terms of coded factors, can be applied to make predictions about the response for given levels of each factor. Furthermore, the coded equation is useful in identifying the relative impact of the factors by comparing the values of factor coefficient.

UMP



Table 5.8 Analysis of variance (ANOVA) for dyeing of BBPF dye on BY

Source	Sum of squares	Degree of freedom	Mean square	F-value	Prob > F
Model	1.0876E-01	11	9.8870E-03	4.4332	0.0168(significant)
A-Dye bath concentration	4.3358E-03	1	4.3358E-03	1.9441	0.1967
B-Time	1.7168E-04	1	1.7168E-04	0.0770	0.7877
C-Dye bath pH	5.1348E-05	1	5.1348E-05	0.0230	0.8827
D-Temperature	2.5531E-02	1	2.5531E-02	11.4476	0.0081
BC	2.1129E-04	1	2.1129E-04	0.0947	0.7652
CD	9.3215E-05	1	9.3215E-05	0.0418	0.8426
A <sup>2</sup>	3.5364E-03	1	3.5364E-03	1.5857	0.2396
B <sup>2</sup>	5.7337E-03	1	5.7337E-03	2.5709	0.1433
C <sup>2</sup>	6.0755E-02	1	6.0755E-02	27.2413	0.0005
D <sup>2</sup>	3.6087E-02	1	3.6087E-02	16.1806	0.0030
ABD	6.3428E-03	1	6.3428E-03	2.8440	0.1260
Residual	2.0072E-02	9	2.2302E-03		
Lack of Fit	3.6247E-03	5	7.2495E-04	0.1763	0.9578(insignificant)
Pure Error	1.6448E-02	4	4.1119E-03		
Cor Total	1.2883E-01	20			
Std. Dev.	4.7226E-02				
Mean	2.9527E-01				
C.V. %	15.9939				
R <sup>2</sup>	0.8442				
Adj R <sup>2</sup>	0.6538				
Pred R <sup>2</sup>	0.4763				
Adeq Precision	6.6900				



The ANOVA for the percentage of dye uptake for curcumin on dyeing of turmeric dye on BY had been employed in order to validate the model, as shown in Table 5.9. The “Model F value” of <0.0001 implies that the model is significant. The fitness of the model was further examined by determining the coefficient ( $R^2 = 0.8915$ ), which indicated that the sample variation exceeding 89.15% is attributed to the variables and only 10.85% of the total variance could not be explained by the model. From the ANOVA, the model F-value of <0.0001 hinted that the model was significant. Besides, values of probability >F less than 0.050 indicated that the model terms were significant. The predicted determination coefficient (Pred  $R^2 = 0.7718$ ) is in reasonable agreement with the adjusted determination coefficient (Adj  $R^2 = 0.7710$ ), which is also satisfactory to confirm the fitness of the model. In addition, the “Adeq Precision” measures the signal-to-noise ratio, whereby a ratio greater than 4 is desired. Hence, the ratio of 8.6847 indicated an adequate signal, which implied that this model could be used to navigate the design space.

In this case, AC, BC, CD,  $A^2$ ,  $B^2$ , and  $D^2$  were all significant model terms, whereas A, B, C, D, AB, AD, BD, and  $C^2$  were insignificant to the response. Hence, the ranking of the model terms, based on the statistical significant (F-value) in the study of dyeing of turmeric dye on BY is given as follows:  $CD > B^2 > BC > A^2 > AC > D^2$ . Furthermore, lack of fit (LOF) is a special diagnostic test that determines the adequacy of a model by comparing with pure error, based on the replicate measurements, and other than LOF, based on the model performance. LOF is significant at a significance level. Additionally, Table shows that the Prob >F-values had been 0.9952. Its revealing a desirable and significant LOF. The regression model for Ln of percentage of dye uptake, %E in terms of coded factors, is expressed in Eq. (5.3).

$$\begin{aligned} \text{LN}(Y) = & +3.1812 - 0.2856A + 0.3628B + 0.1491C - 0.1147D + 1.1894AC - \\ & 1.2785BC - 1.7506CD - 0.5950A^2 - 0.7251B^2 - 0.4601D^2 \end{aligned} \quad 5.3$$

Where A, B, C, and D refer to the coded values of the process variables of dye bath concentration (A), dyeing time (B), dye bath pH (C), and dyeing temperature (D) on the dyeing of extracted dye from turmeric on BY, respectively. In addition, the negative sign in front of the terms indicated the antagonistic effect, while the positive sign portrayed synergistic effect.

Table 5.9 Analysis of variance (ANOVA) for dyeing of turmeric dye on BY

Source	Sum of squares	Degree of freedom	Mean square	F-value	Prob > F
Model	56.1977	10	5.6198	7.3962	0.0030(significant)
A-Dye bath concentration	1.0910	1	1.0910	1.4358	0.2614
B-Time	1.7604	1	1.7604	2.3169	0.1623
C-Dye bath pH	0.2976	1	0.2976	0.3916	0.5470
D-Temperature	0.1761	1	0.1761	0.2318	0.6417
AC	8.1281	1	8.1281	10.6974	0.0097
BC	9.3924	1	9.3924	12.3613	0.0066
CD	17.6080	1	17.6080	23.1739	0.0010
A <sup>2</sup>	9.2052	1	9.2052	12.1150	0.0069
B <sup>2</sup>	13.6699	1	13.6699	17.9909	0.0022
D <sup>2</sup>	5.5052	1	5.5052	7.2454	0.0247
Residual	6.8384	9	0.7598		
Lack of Fit	0.5020	5	0.1004	0.0634	0.9952(insignificant)
Pure Error	6.3364	4	1.5841		
Cor Total	63.0361	19			
Std. Dev.	0.8717				
Mean	1.6158				
C.V. %	53.9456				
R <sup>2</sup>	0.8915				
Adj R <sup>2</sup>	0.7710				
Pred R <sup>2</sup>	0.7718				
Adeq Precision	8.6847				

### 5.3.6 Interaction effect of variable

The 3D surface plots show the type of interaction that takes place between the tested variables; thus determining the optimum conditions (Kousha et al., 2015). The graphical representations of the regression equation, including the response surface graphs, contour plots, and interaction graphs, are presented for response of percentage of dye uptake for anthocyanin from BBPF dye on BY. Moreover, Figure 5.11 and Figure 5.12 illustrate the plots of the first-order polynomial equation, whereby only one variable was kept constant, while the other two are varied within the determined experimental ranges.

Furthermore, Figure 5.11 (a and b) illustrates the interactive effects of dye bath concentration (A) with dyeing time (B) on the percentage of dye uptake for dyed BY with BBPF dye by maintaining the dye bath pH at 5. The increasing dye bath concentration up to 0.105 g/mL brought about an increase in the percentage of dye uptake, but further increase in dye bath concentration led to a decrease in the percentage of dye uptake. In fact, the percentage of dye uptake was enhanced with the increasing dye concentration, which was relatively lesser at a higher dye bath concentration range chiefly due to the decreasing dyeing sites in BY. This is a common phenomenon observed in the textile dyeing practices. The percentage of dye uptake values for the dyed BY increased as the dye bath concentration was increased regardless of the high or low value of pH. At similar dye bath concentrations, the dyed BY, at a shorter time like 50 minutes, exhibited higher percentage of dye uptake, when compared to dyeing time of 80 minutes. In addition, Figure 5.12 indicates the simultaneous effects of dye bath concentration and dye bath pH on the percentage of dye uptake for dyeing of BBPF dye on BY. Moreover, the percentage of dye uptake increased with the increase in dye bath concentration and dye bath pH from 0.08 to 0.13 g/mL and pH 3 to 7, respectively.

These plots show the type of interaction between the tested variables, and hence, determining the optimum conditions (Jabasingh et al., 2016). Besides, in the second-order polynomial equation, two variables were kept constant while the other two were varied within the determined experimental ranges. Additionally, Figure 5.13 (a and b) illustrates the interactive effect of dyeing time (B) with dye bath pH (C) on the percentage of dye uptake values for dyed BY by keeping the dye bath concentration (A) and the temperature constant at 0.10 g/mL and 70 °C, respectively. These results revealed that the percentage

of dye uptake for dyed BY with RDFP dye had been dye bath pH dependent. The adsorption of betacyanin pigment on the surface of BY was strongly affected by the changes in the chemical structure of dye molecules and BY at varied pH values. As a result, the percentage of dye uptake first increased and then displayed decreasing trends, displaying the highest percentage of dye uptake value in the mid-range of dyeing time. Furthermore, a large possible quantity of anthocyanin might have been adsorbed onto the surface of BY within the initial 2.5-3.5 dye bath pH. This is due to the fact that at the beginning, the dye molecules were adsorbed rapidly because of the large availability of the dyeing sites; but after the amount of the dye attached to the BY reached its saturation point, the desorption rate increased; resulting in lower percentage of dye uptake values. Besides, Figure 5.14 (a and b) shows the 3D response surface plots that reflect the combined effects of dye bath pH (C) and temperature (D) on the percentage of dye uptake of dyeing of RDFP dye on BY at constant dye bath concentration (0.10 g/mL) and time (90 minutes). In the natural dyeing processes, both temperature and dye bath pH play very significant roles and are considered to be the most effective parameters in affecting the dye binding on the surface of the fibre. This surface plot suggests a positive relationship between the dye bath pH and the temperature of the dyeing solution to achieve the maximum percentage of dye uptake for betacyanin from RDFP dye. Moreover, in most cases, the percentage of dye uptake progressively increased as the temperature hiked up to 70 °C. However, further increase in temperature led to a decrease in the percentage of dye uptake. Initially, the increasing dyeing temperature enhanced the mobilization of the reacting species, hence the reaction rate as well. Nevertheless, at higher temperatures, an increase in the desorption rate of dye molecules might become higher than adsorption; resulting in the decreased amount of dyes being attached to the BY and consequently, a decrease in the percentage of dye uptake values.

Furthermore, the surface plots displayed in Figure 5.15 (a and b) show the interactive influence of dye bath concentration with dye bath pH when the temperature and the time were kept constant at 70 °C and 60 minutes respectively in relation to the percentage of dye uptake values for dyed BY with turmeric dye. Based on this figure, the increase in pH value up to 4.0 further increased the percentage of dye uptake for turmeric dye on BY. Moreover, this figure also exhibited an increase in the dye bath concentration up to 0.13 g/mL, which decreased the adsorption of curcumin pigment on BY at pH 2. Additionally, Figure 5.16 depicts the impacts of dyeing time and dye bath pH on the

percentage of dye uptake for curcumin from turmeric dye when the dye bath concentration and the temperature were held constant at 0.10 g/mL and 70 °C. At high dye bath pH of 4, the increase in the dyeing time led to a rapid decrease in the percentage of dye uptake. However, at a low pH of 2 condition, the percentage of dye uptake for the colorant pigment increases up to 70.0 % at 70 minutes. Furthermore, in dyeing of natural dye on BY, an increase in temperature usually leads to higher percentage of dye uptake on BY. Other than that, high temperatures could also cause higher degradation rates of curcumin uptake on BY. For instance, Figure 5.17 demonstrates the interaction effects of dyeing temperature and dye bath pH by retaining the dye bath concentration (0.10 g/mL) and the dyeing time (60 minutes). Nonetheless, at lower dyeing temperature of 60 °C and pH 4, the percentage of dye uptake was maximized, while higher temperature of 80 °C decreased the percentage of dye uptake for curcumin from turmeric dye on BY.



UMP

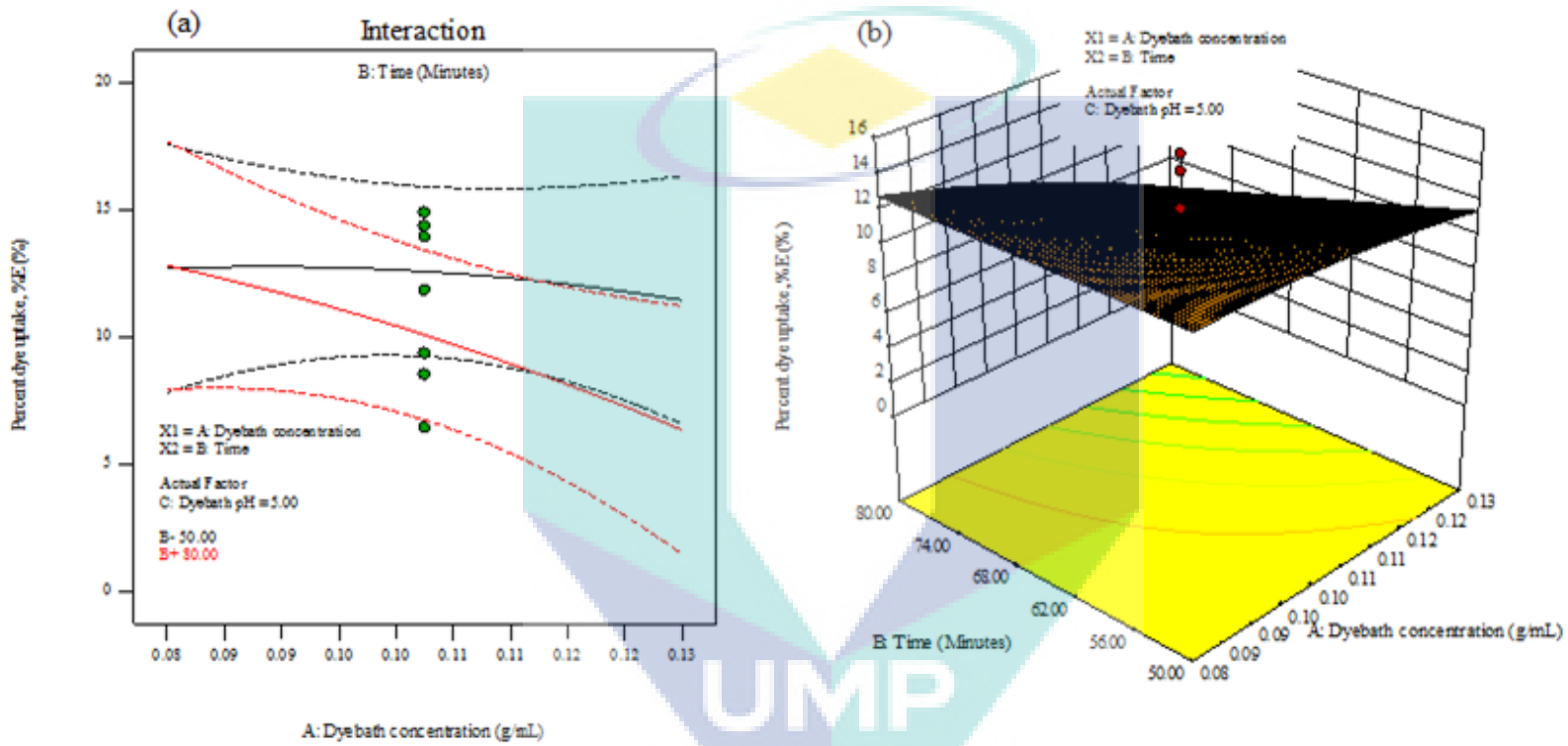


Figure 5.11 Effects of dye bath concentration and time on dyeing of BBPF dye on BY: (a) interaction and (b) response surface graph



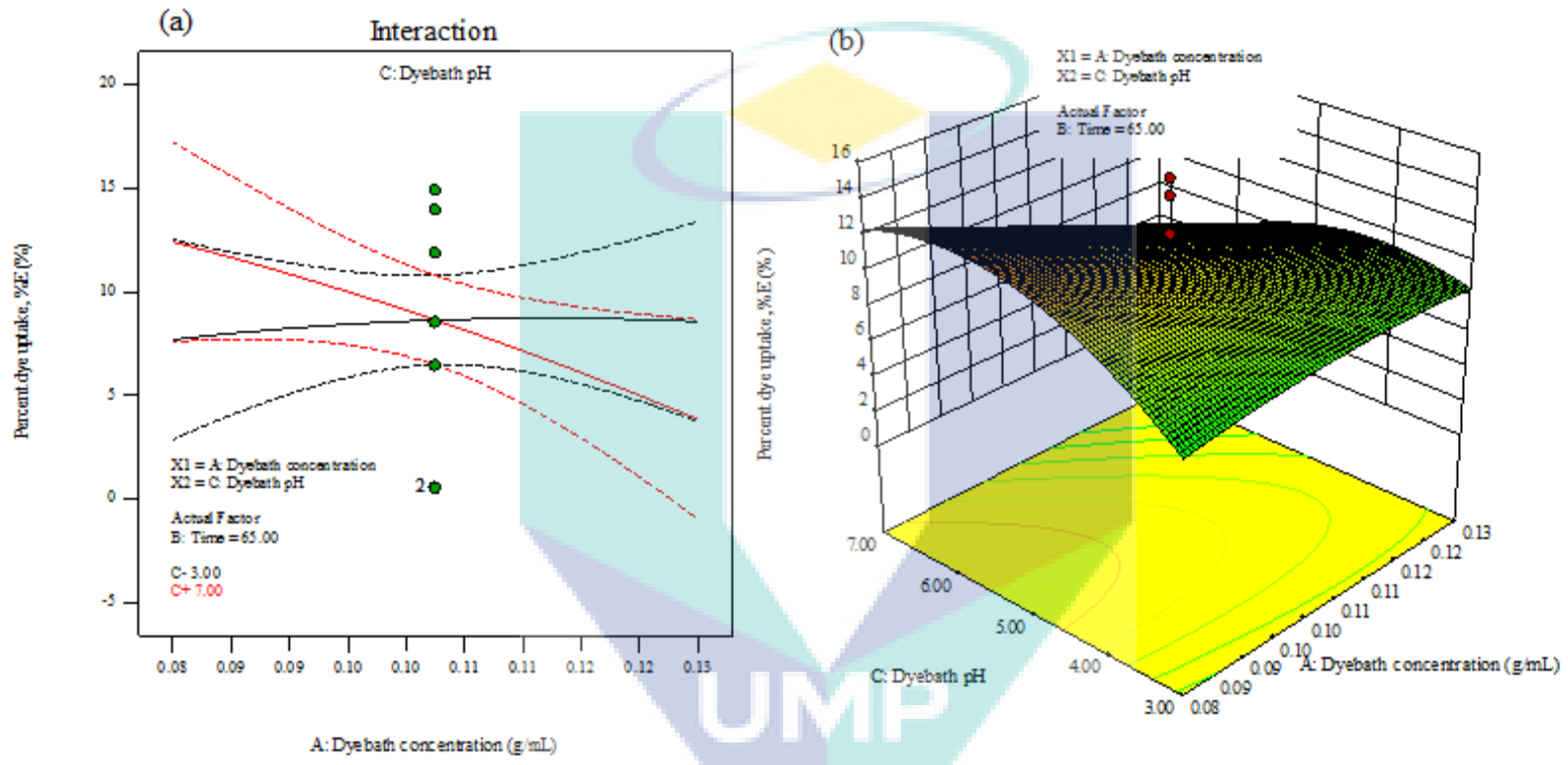


Figure 5.12 Effects of dye bath concentration and dye bath pH on dyeing of BBPF dye on BY: (a) interaction and (b) response surface graph

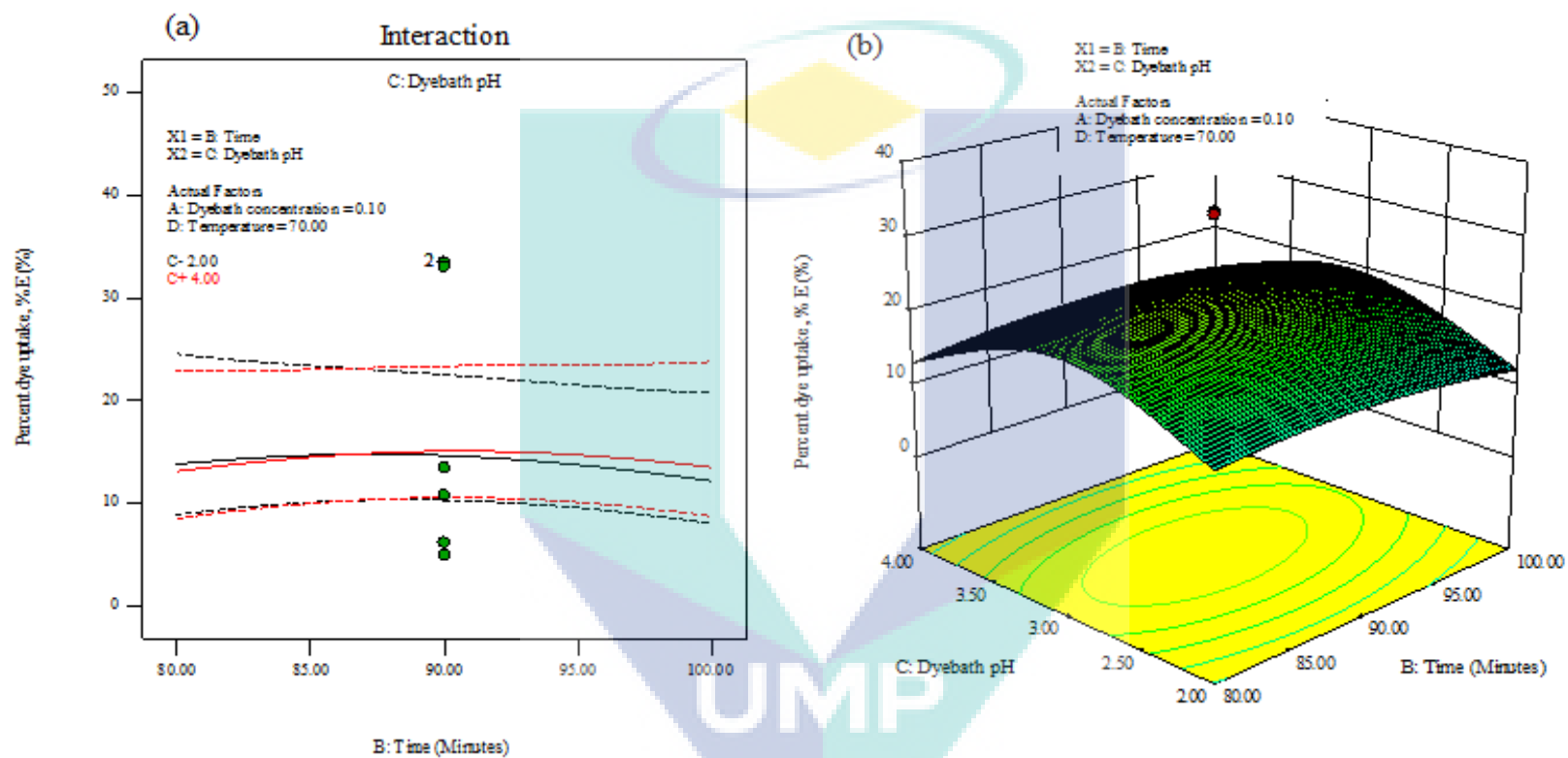


Figure 5.13 Effects of time and dye bath pH on dyeing of RDFP dye on BY: (a) interaction and (b) response surface graph

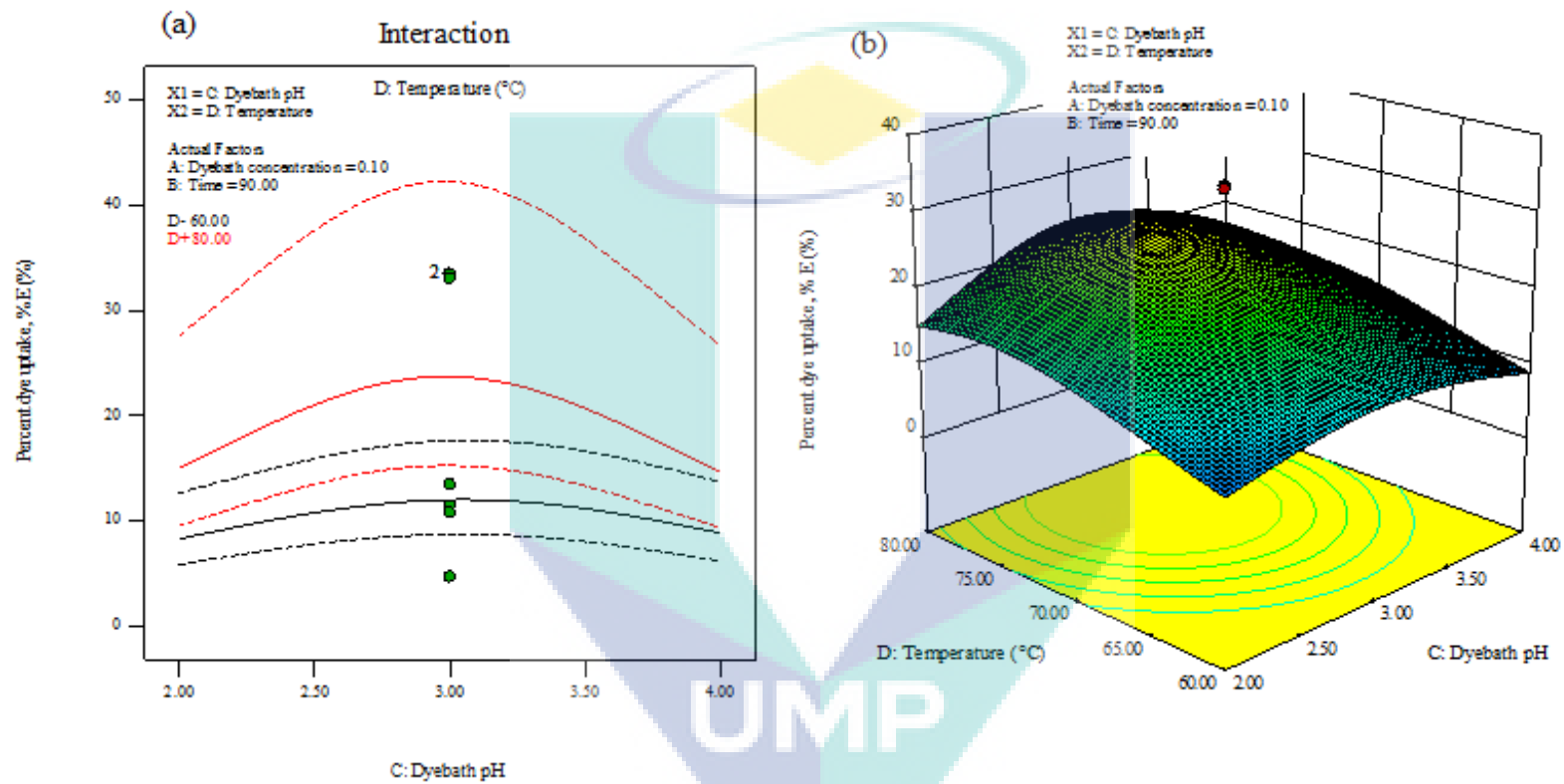


Figure 5.14 Effects of temperature and dye bath pH on dyeing of RDFP dye on BY: (a) interaction and (b) response surface graph

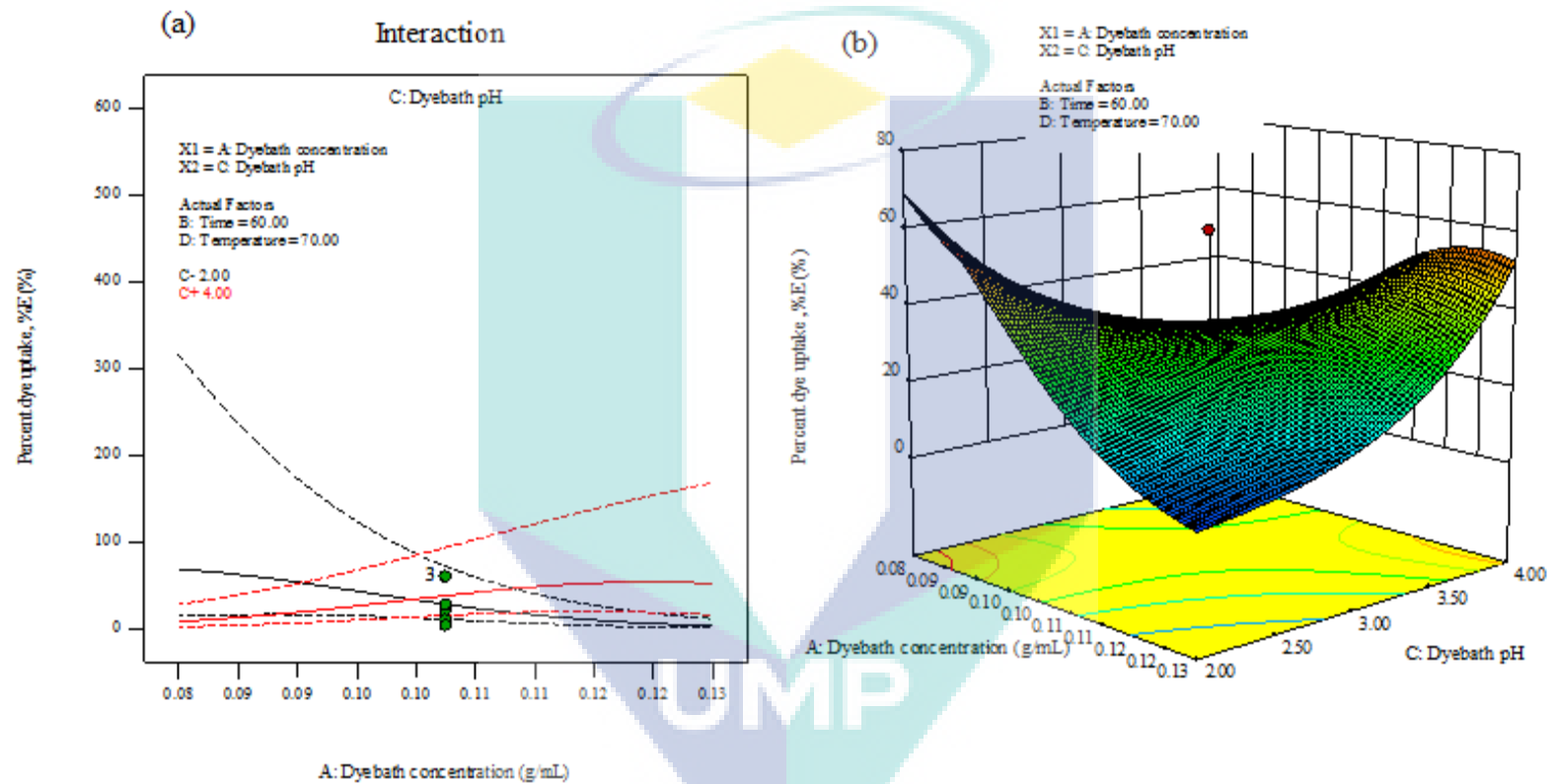


Figure 5.15 Effects of dye bath concentration and dye bath pH on dyeing of turmeric dye on BY: (a) interaction and (b) response surface graph

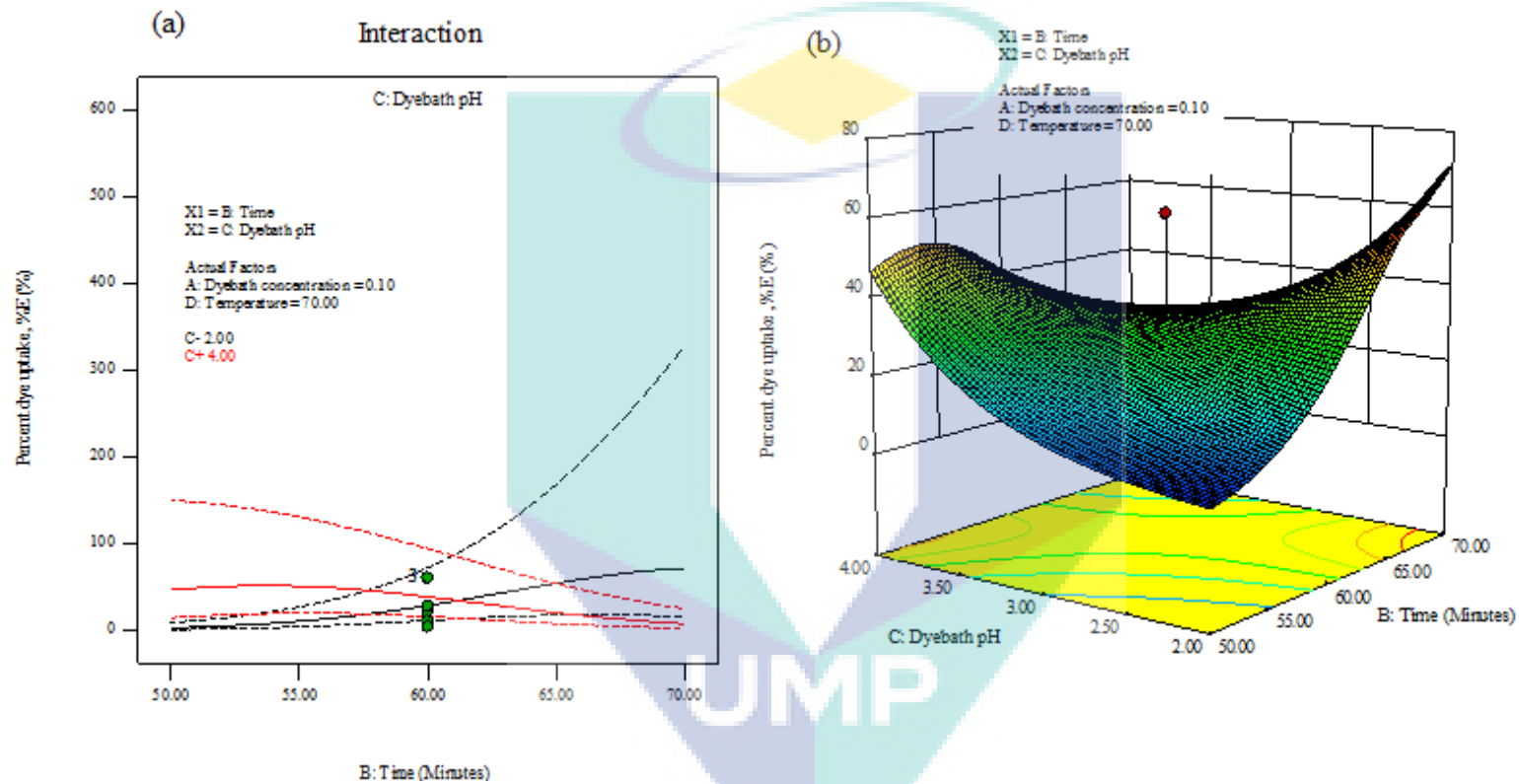


Figure 5.16 Effects of time and dye bath pH on dyeing of turmeric dye on BY: (a) interaction and (b) response surface graph

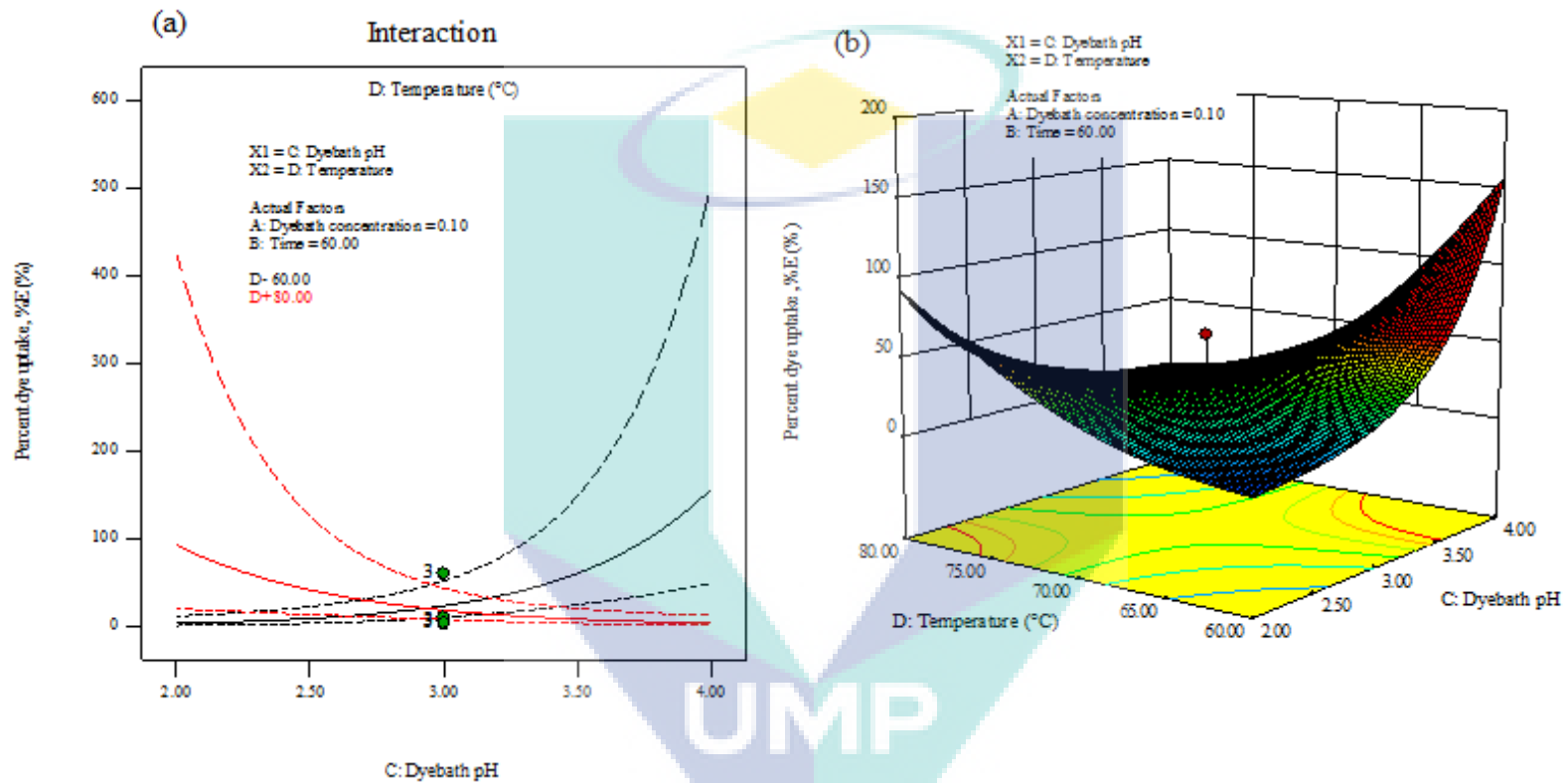


Figure 5.17 Effects of temperature and dye bath pH on dyeing of turmeric dye on BY: (a) interaction and (b) response surface graph

### 5.3.7 Model validation

In addition, a validation experiment was performed to verify the accuracy of the model. In order to validate the theoretical model, three samples of each natural dye had been performed from dyeing of BY with BBPF, RDFP, and turmeric dyes in optimum conditions, as dictated by the curves of response optimization. As such, Table 5.10 until Table 5.12 exhibit the maximum predicted percentage of dye uptake for BBPF, RDFP, and turmeric dyes respectively. A, B, C and D were denoted as dye bath concentration, time, dye bath pH and temperature.

Furthermore, Table 5.10 portrays the maximum predicted percentage of dye uptake for BBPF dye obtained at dye bath concentration of 0.083 g/mL, 60 minutes of dyeing time, and dye bath pH at 6.5. At these optimum conditions, the predicted percentage of dye uptake was 14.168 % with the desirability value of 0.949 for BBPF dye. Desirability value reflects the estimated functions that may represent the experimental model under the desired conditions. The percentage error for the selected optimum condition was 0.034 %.

Hence, the optimum conditions were modified by considering the operability of dyeing of BY with RDFP dye in the actual production conditions. Furthermore, the results depicted in Table 5.11 show that the percentage errors ranged from -0.106 % for dyeing of RDFP dye on BY to 0.139 %. Therefore, three optimum conditions were selected and tested experimentally to test the suitability of those optimum conditions in predicting the optimum response. The selected optimal conditions were dye bath concentration at 0.10 g/mL, dyeing time at 90 minutes, dye bath pH 3, and dyeing temperature at 70 °C. Thus, the predicted percentage of dye uptake was 22.830 % with 0.912 and 0.073 % of desirability and percentage error, respectively.

Meanwhile, Table 5.12 portrays that the percentage of errors for dyeing of yellow dye from turmeric on BY ranged from -0.022 % to 0.185 %. The maximum predicted percentage of dye uptake for turmeric dye had been at a dye bath concentration of 0.101 g/mL, dyeing time at 60 minutes, dye bath at pH 4.1, and dyeing temperature of 67 °C. Thus, it can be inferred that with the suggested optimal conditions, the predicted percentage of dye uptake was 60.209 % with the desirability value of 0.983 and the

percentage error of 0.042 %. Thus, these three dyeing of BY with BBPF, RDFP, and turmeric dyes implied that the empirical model developed had been considerably accurate for responding terms as the percentage error between the experimental and the predicted values were well within the acceptable value of 5 %, suggesting that the model adequacy is reasonably within the 95 % of confidence interval. Hence, the developed model of optimal conditions on dyeing BY with natural dyes had been validated.

Table 5.10 The results of verification process of dyeing of BBPF dye on BY

No.	A	B	C	Predicted %E	Desirability	Actual %E	Percentage error,%
1	0.083	60.00	6.5	14.168	0.949	14.173	0.034
2	0.083	60.00	6.2	14.110	0.945	14.118	0.054
3	0.083	60.01	7.0	13.885	0.929	13.901	0.113

Table 5.11 The results of verification process of dyeing of RDFP dye on BY

No.	A	B	C	D	Predicted %E	Desirability	Actual %E	Percentage error,%
1	0.100	90.00	3.0	70.00	22.830	0.912	22.847	0.073
2	0.100	90.00	3.0	70.01	22.820	0.908	22.852	0.139
3	0.100	88.96	3.0	70.00	22.869	0.907	22.845	-0.106

Table 5.12 The results of verification process of dyeing of turmeric dye on BY

No.	A	B	C	D	Predicted %E	Desirability	Actual %E	Percentage error,%
1	0.101	60.00	4.1	67.00	60.209	0.983	60.234	0.042
2	0.101	60.00	4.1	66.00	60.208	0.982	60.195	-0.022
3	0.101	59.00	4.1	67.00	60.210	0.981	60.321	0.185

### 5.3.8 Confirmation

The results that confirm the run at the predicted optimum conditions for dyeing of BBPF, RDFP, and turmeric dyes on BY are presented in Table 5.13, Table 5.14, and Table 5.15, respectively. The optimum conditions of dyeing BY with BBPF dye for dye bath concentration, dyeing time, and dye bath pH had been determined to be 0.083 g/mL, 60 minutes, and 6.5, respectively. Meanwhile, the optimized conditions of dyeing of RDFP dye and turmeric dye on BY for dye bath concentration, dyeing time, dye bath pH,



and dyeing temperature were 0.10 g/mL and 0.101 g/mL, 90 minutes and 60 minutes, pH 3 and pH 4.1, 70 °C and 67 °C, respectively.

Within these optimized conditions, the model predicted a percentage error of 0.062% (BBPF dye in Table 5.10), 0.086% (RDFP dye in Table 5.11), and 0.045% (Turmeric dye in Table 5.12) at 95% confidence interval. Therefore, the optimum conditions selected were resulted closely to the confirmation result, thus indicating that these models are indeed reasonable and reliable. The percent dye uptake of the colorant pigments from OFAT were shown lower than the percent dye uptake of the colorant pigments resulted in the RSM. Thus, proving the optimization of the dyeing bamboo yarn with the selected natural dyes by using RSM was the best tool.

Table 5.13 The results of confirmation process of dyeing of BBPF dye on BY

<b>A</b>	<b>B</b>	<b>C</b>	<b>Predicted %E</b>	<b>Desirability</b>	<b>Actual %E</b>	<b>Percentage error,%</b>
0.083	60.00	6.5	14.168	0.949	14.177	0.062

Table 5.14 The results of confirmation process of dyeing of RDFP dye on BY

<b>A</b>	<b>B</b>	<b>C</b>	<b>D</b>	<b>Predicted %E</b>	<b>Desirability</b>	<b>Actual %E</b>	<b>Percentage error,%</b>
0.100	90.00	3.0	70.00	22.830	0.912	22.850	0.086

Table 5.15 The results of confirmation process of dyeing of turmeric dye on BY

<b>A</b>	<b>B</b>	<b>C</b>	<b>D</b>	<b>Predicted %E</b>	<b>Desirability</b>	<b>Actual %E</b>	<b>Percentage error,%</b>
0.101	60.00	4.1	67.00	60.209	0.983	60.236	0.045

## CHAPTER 6

### ADSORPTION STUDY ON DYEING OF NATURAL DYES ONTO BAMBOO YARN

#### 6.1 Introduction

This chapter explains the significant effects of adsorption mechanism upon the dyeing of natural dyes on BY in order to observe the best colorant pigments adsorbed onto BY in the dyeing process carried out. Adsorption is widely used in dyeing processes, where the design and the efficient operation of adsorption processes require equilibrium adsorption data to be used in kinetics and mass transfer models. As such, three natural dyes were used in this research; BBPF, RDFP, and Turmeric. The colorant pigments of these three natural dyes, which are responsible for the colours of the dyes, are anthocyanin, betacyanin, and curcumin for BBPF, RDFP, and Turmeric, respectively. Moreover, the three major adsorption studies elaborated in this subchapter are isotherm studies with four linear equations, kinetic study, and desorption study. The isotherm and kinetics equations are the common mathematical studies that determine the reactions of adsorbents and sorbents in the mixtures. Isotherm equations mainly describe the interactions between adsorbents and sorbents via Langmuir, Freundlich, Temkin and Dubinin Radushkevich equations. Each of these equations determined the fitness of equilibrium data and explains the varied behaviour of the adsorption mechanism in dyeing the natural dyes on BY. In addition, the kinetic equations reveal the rate of adsorption (which is one of the criteria for efficiency of adsorbent) and also the mechanism of the adsorption for dyeing process on BY can be concluded from the kinetic studies.

## 6.2 Effect of Different Parameters of Adsorption Processes of Natural Dyes on BY

In optimising the equilibrium time of adsorption of dyes onto BY for each natural dye, varying time with 10 minutes' interval had been set. The effect of time on adsorption equilibrium and the effect of concentration of dyes by varies in dilution factor at equilibrium time were studied by analysing the amount of colorant pigments (anthocyanin, betacyanin, and curcumin) adsorbed onto BY (mg/g), as discussed in detailing the subsection below.

### 6.2.1 Effect of Time

The graph portraying anthocyanin, betacyanin, and curcumin contents on BY is plotted in Figure 6.1 to analyse the trend of the adsorption on BY at different time intervals. Based on the graph of colorant pigment contents on BY, the amount of colorant pigments adsorbed increased drastically until about 60 minutes for both anthocyanin and curcumin. After 60 minutes, the amount of anthocyanin and curcumin contents on BY decreased. This shows that the equilibrium time for adsorption of these two colorant pigments onto BY had been achieved at 60 minutes. As for betacyanin, the content of pigment increased gradually until it reached about 90 minutes; thus, indicating its equilibrium time at 90 minutes.

Since the adsorption time to reach equilibrium had been 60th minute for both anthocyanin and curcumin, while 90th minute for betacyanin, the concentration of dyes in the solution at equilibrium time had been used as  $C_e$  for these three types of dyes. The volume of solution ( $V$ ) was 0.03 L as the experiment was performed using test tubes containing 30mL of dye solution. The weight of BY used in 30 mL of the dye solution had been 0.300 g. Moreover, Figure 6.2 shows the exact amount of colorant pigments adsorbed onto BY, as determined. The trend of the data below is rather similar to those of anthocyanin, betacyanin, and curcumin contents on the BY data earlier. This means, the equilibrium time had been achieved at minutes 60, 60, and 90 for adsorption of anthocyanin, betacyanin, and curcumin extracted from dyes of BBPF, RDFP, and turmeric, respectively. This further confirmed that the strong electrostatic attractive force between the positively-charged colorant pigments and the negatively-charged BY surfaces had been the main driving force for adsorption. Later, the amount of colorant pigments adsorbed onto the BY increased gradually with the increasing contact time until the maximum amount was attained, which means that the adsorption equilibrium had

been successfully achieved. At this point, the amount of colorant pigments adsorbed onto BY is in the state of dynamic equilibrium. In precise, fast diffusion into the external surface of the adsorbent occurred due to rapid pore diffusion into the intra particle matrix to attain quick equilibrium. Since equilibrium had been attained at 60, 60, and 90 minutes for BBPF, RDFP, and turmeric dyes respectively, the experiment on the adsorption of colorant pigments onto BY at varied concentration dilution factors for BBPF, RDFP, and turmeric dyes had been performed for 60, 60 and 90 minutes respectively. The amount of curcumin from turmeric dye adsorbed onto BY,  $q_t$  in unit's mg/g had been higher than anthocyanin, which was extracted from BBPF dye, and followed by betacyanin from RDFP dye.

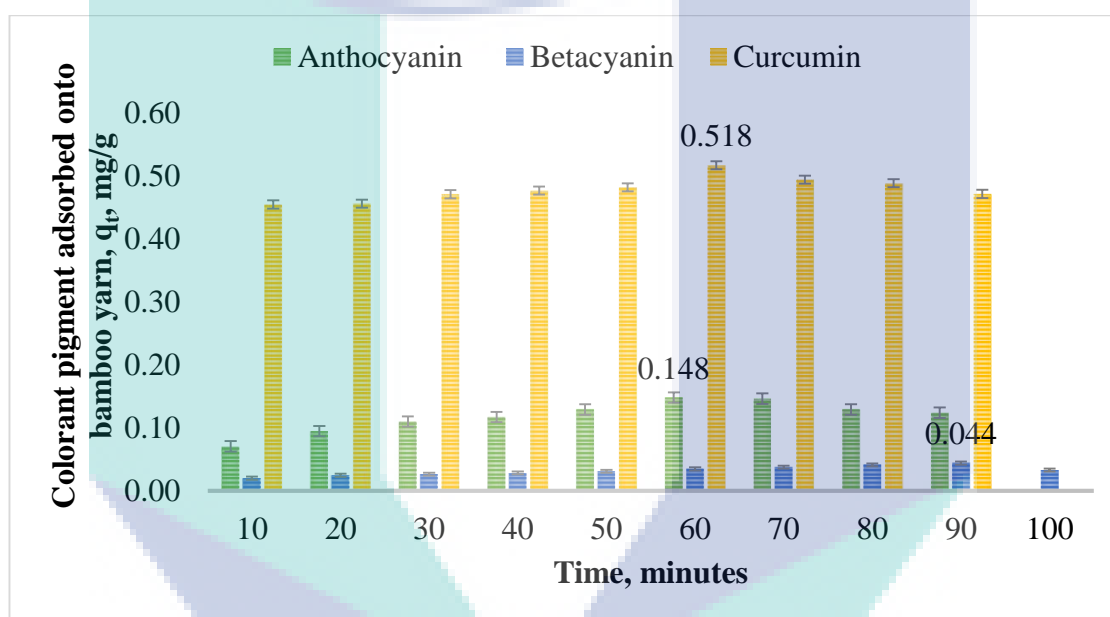


Figure 6.1 Amount of colorant pigments adsorbed onto BY at different time intervals

### 6.2.2 Effect of Dye Bath Concentrations

The contents of anthocyanin, betacyanin, and curcumin on BY could be determined by subtracting the anthocyanin or betacyanin or curcumin content on BY in the dye solution before the adsorption process was performed in the dye solution after the adsorption process was carried out at various dilution factors. The graph that exhibit the contents of anthocyanin, betacyanin, and curcumin upon BY has been plotted to analyse the trend of the amount of colorant pigment contents on various types of dyes at varied dilution factors. Moreover, Figure 6.2 illustrates the contents of anthocyanin, betacyanin, and curcumin upon BY at varied dilution factors. Based on the results, the dye bath concentration of the three dyes played an important role for colorant pigment

contents on BY. Furthermore, the graph displayed an increasing trend for the contents of anthocyanin, betacyanin, and curcumin, which could be noted with the increment in dilution factor. As the dilution factor increases, the dye baths would become more concentrated with anthocyanin, betacyanin, and curcumin contents. The number of available adsorption sites increases by increasing the dilution factor or concentration of dye. Therefore, results in an increase of the amount of adsorbed dye.

The graph that depicted the amount of dye adsorbed versus dilution factor was then plotted. Based on the results shown in Figure 6.2, the dye baths of BBPF, RDFP, and turmeric dye concentrations did play an important role in the adsorption of colorant pigments onto BY. The amount of colorant pigments adsorbed onto BY increased with the increase in dye bath concentration at a constant amount of BY. In precise, at lower dye bath concentrations, the ratio of number colorant pigments molecules to the available adsorption site is low. While at higher dye bath concentration, the ratio became higher and subsequently, the adsorption of colorant pigments depended on the dye bath concentration. Overall, the amount of anthocyanin extracted from BBPF dye adsorbed onto BY,  $q_t$  in unit's mg/g, had been higher than that of betacyanin from RDFP dye and followed by curcumin from turmeric dye.

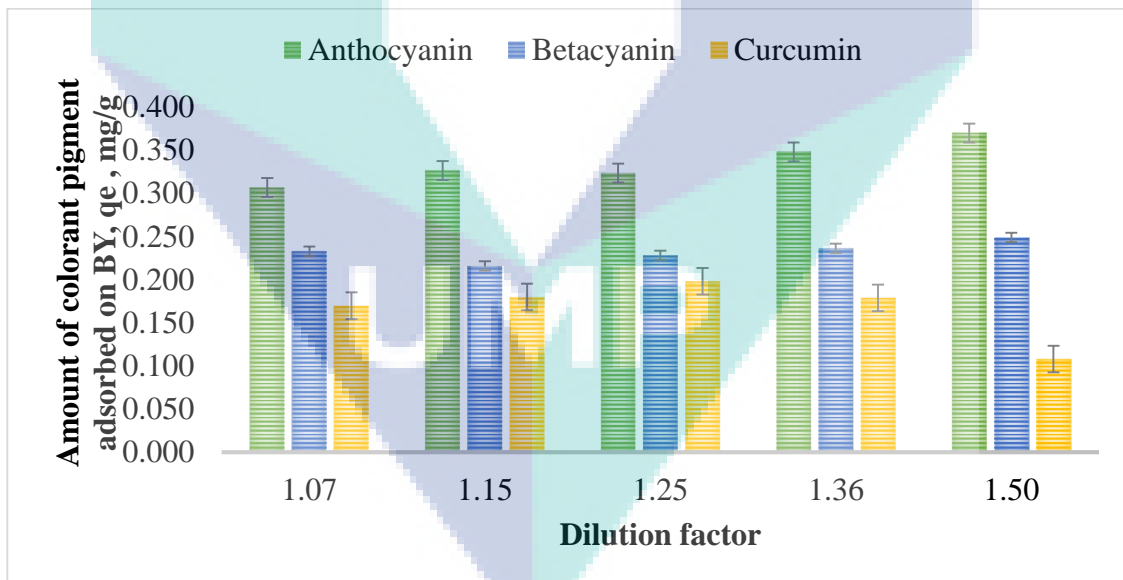


Figure 6.2 Amount of colorant pigments adsorbed onto BY at equilibrium time and various dilution factors

### 6.3 Adsorption Kinetics Modelling

The adsorption kinetics and mechanisms had been tested by using simplified kinetic models. These models include the pseudo-first order, the pseudo-second order, and the intra particle diffusion equation. The best fit was estimated in terms of coefficient determination,  $R^2$ . It had been necessary to determine the kinetics characteristics of the dyeing of natural dyes on BY. The findings of kinetic studies on dyeing of natural dyes on BY are addressed in Table 6.1.

Pseudo-first order model assumes that the adsorption of colorant pigments onto BY occurs due to a concentration difference of the adsorbate between adsorbent surface and the solution. Therefore, this process occurs only at the external mass transfer coefficient (Pathiraja, 2014). The Lagergen rate equation is the first rate equation for adsorption in a liquid or solid system based on solid capacity, as given in Eq. (6.1)

$$\frac{dq_t}{dt} = k_1 (q_e - q_t) \quad 6.1$$

After integration on the both sides of the equation and applying conditions for  $q_t=0$  at  $t=0$  and  $q_t=q_t$  at  $t=t$ , Eq. (6.2) can be used for kinetic analysis of the experimental results.

$$\log (q_e - q_t) = \log q_e - \frac{k_1}{2.303} t \quad 6.2$$

Where  $q_e$  is the amount of colorant pigments adsorbed onto BY at equilibrium (mg/g),  $q_t$  is the amount of colorant pigments adsorbed onto BY at time  $t$  (mg/g), and  $k_1$  is the equilibrium rate constant of pseudo-first order kinetic (1/min). From the equation, a linear curve of the  $\log (q_e - q_t)$  versus  $t$  was plotted. The slopes then corresponded to the value of  $k_1$ .

Then, the pseudo-second order equation was attempted to fit the adsorption of colorant pigments onto BY data. The pseudo-second order kinetic equation is given below.

$$\frac{dq_t}{dt} = k_2 [(q_e - q_t)]^2 \quad 6.3$$

Where  $k_2$  is the equilibrium rate constant of pseudo-second order kinetic model ( $\text{g mg}^{-1}\text{min}^{-1}$ ). After integrating Eq. (6.3), the following equation was obtained.

$$\frac{1}{q_t} = \frac{1}{(k_2 q_e^2) + (\frac{1}{q_e})t} \quad 6.4$$

In order to investigate the internal diffusion mechanism during the adsorption of the colorant pigments onto BY, the intra particle diffusion equation had been employed. The adsorption was investigated by using the Weber and Morris model, also known as the intraparticle diffusion model, which assumes the adsorption mechanism described elsewhere (Benjwal et al., 2016). Besides, it considers that the adsorption is usually controlled by an external film resistance, while mass transfer is controlled by internal or intra particle diffusion (Wei and Brien, 2014). The possibility of intra particle diffusion resistance affecting adsorption had been explored by using Eq. (6.5).

$$q_t = k_p t^{(1/2)} + C \quad 6.5$$

Where  $k_p$  is the intra particle diffusion rate constant ( $\text{mg.g}^{-1}.\text{min}^{-1}$ ) and  $C$  is the internal diffusion coefficient, as determined from the linear graph of  $q_t$  versus  $(\text{time})^{1/2}$ . However, in some cases, three linear sections on the plot of  $q_t$  versus  $t^{1/2}$  for anthocyanin, betacyanin, and curcumin can be noted.

The data are shown in Figure 6.3 and apparently, the adsorption of the colorant pigments of anthocyanin onto BY adhered to only the pseudo-first order model. However, other two colorant pigments of betacyanin and curcumin did not fit to this order model, in which similar observations were found in the adsorption of *Adhatoda vasica* natural dye onto woollen yarn by Rather et al.,(2016). The  $k_1$ , the calculated  $q_e$  ( $q_{e, \text{cal}}$ ), and the coefficient of determination ( $R^2$ ) were calculated and are tabulated in Table 6.1.

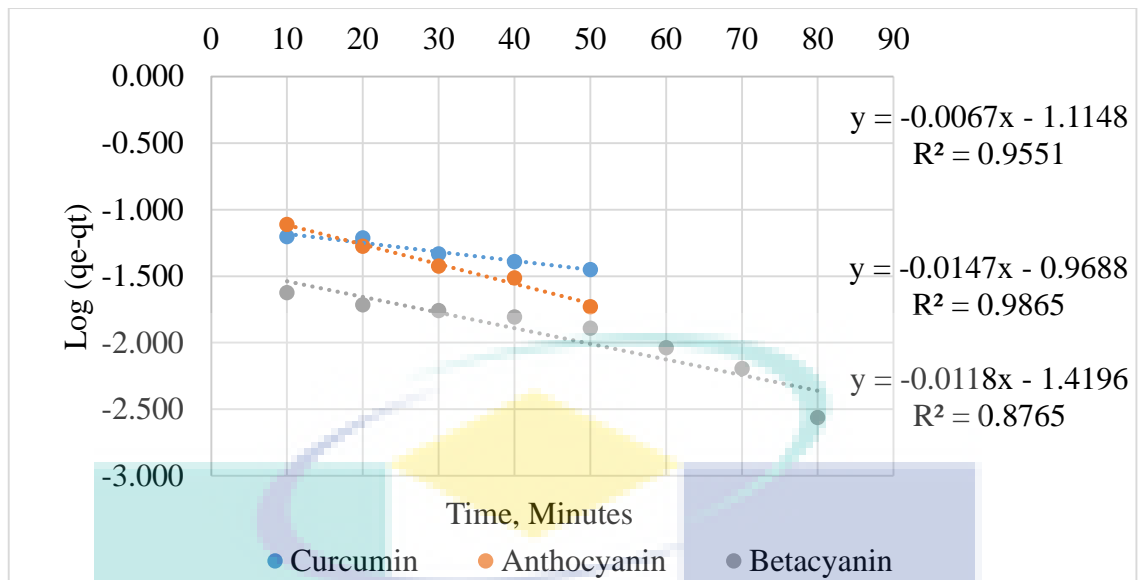


Figure 6.3 Pseudo-first order kinetic model for colorant pigments adsorption onto BY at 60 °C for both anthocyanin and curcumin, while 90 °C for betacyanin

In order to determine the applicability of the model, linear plots of  $t/q_t$  versus  $t$  for the adsorption of the colorant pigments of anthocyanin, betacyanin, and curcumin onto BY were plotted to obtain the rate parameters, as presented in Figure 6.4. The figure implies that the adsorption of the colorant pigments of anthocyanin onto BY failed to adhere to the pseudo-second order model. but the other two colorant pigments of betacyanin and curcumin fit to this order model rather well. The  $k_2$ , the calculated  $q_e$  ( $q_{e,cal}$ ), and the coefficient of determination ( $R^2$ ) were calculated and are depicted in Table 6.1.





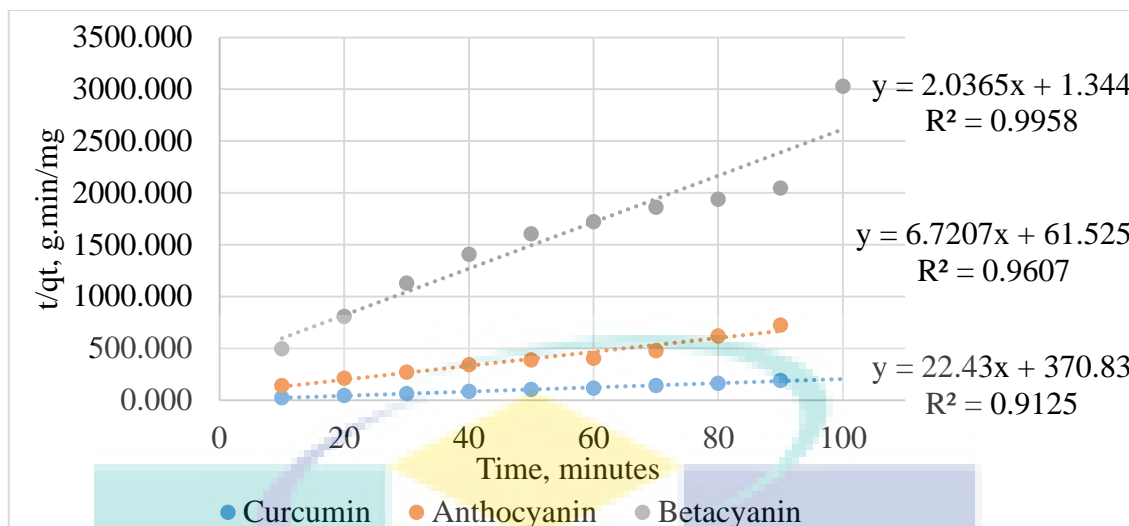


Figure 6.4 Pseudo-second order kinetic model for colorant pigments adsorption onto BY at 60 °C for both anthocyanin and curcumin, while 90 °C for betacyanin.

The experimental data, unfortunately, did not show a good linear fit with the pseudo-first order kinetic model for betacyanin and curcumin. From the experimental, the  $q_e$  ( $q_{e, \text{exp}}$ ) value did not agree with those calculated ( $q_{e, \text{cal}}$ ) for both betacyanin and curcumin. However, for adsorption of anthocyanin pigment showed a good linear fit using the pseudo-first order kinetic model, as reflected by the experimental  $q_e$  ( $q_{e, \text{exp}}$ ) value that was in line with those calculated ( $q_{e, \text{cal}}$ ) with relevant value of coefficient of determination ( $R^2$ ). On the other hand, a linear fit for  $t/q_t$  versus  $t$  was observed by using the pseudo-second order kinetic model, which displayed a fit for the adsorption of the colorant pigments of betacyanin and curcumin onto BY, in which similar results were observed for adsorption of curcumin dye on silk by Tayade and Adivarekar, (2013). These results that show good fit are shown in Table 6.1. The results revealed that the adsorption of the colorant pigments onto BY kinetics can be approximated as the pseudo-second order kinetic model for betacyanin and curcumin, while the pseudo-first order kinetic model for anthocyanin. Therefore, the rate-limiting step of dyeing of RDFP and turmeric dye on BY were chemical adsorption, whereas the dyeing mechanism is controlled via sharing or exchanging electrons between the adsorbent and the adsorbate as covalent bonding and ion exchange. This suggests that betacyanin and curcumin adsorption onto BY occurred due to both internal and external mass transfer mechanisms, whereas for anthocyanin, the internal mass transfer mechanism had taken place, which points to the reaction that is more inclined towards physisorption and the adsorption mechanism was controlled by van der Waals forces and hydrogen bonding between BY surface. The similar results in adsorption of dyeing of woollen yarn by *Terminalia chebula* extract,

as reported by Shabbir et al.,(2016). The equilibrium rate constant of pseudo-first order kinetic,  $k_1$ , of anthocyanin was found higher than that for betacyanin and curcumin, while the equilibrium rate constant of pseudo-second order kinetic,  $k_2$ , of curcumin had been higher than betacyanin, and followed by anthocyanin pigments.

Table 6.1 Kinetic parameters for colorant pigments adsorption onto BY

Colorant pigment	$q_{e,exp}$	Pseudo first order			Pseudo second order		
		$q_{e,cal}$	$k_1$	$R^2$	$q_{e,cal}$	$k_2$	$R^2$
<b>Anthocyanin</b>	0.148	0.033	0.032	0.986	0.368	0.036	0.960
<b>Betacyanin</b>	0.044	0.350	0.025	0.876	0.045	1.357	0.912
<b>Curcumin</b>	0.518	0.108	0.014	0.955	0.491	3.084	0.995

Figure 6.5 shows the plots intraparticle diffusion model for colorant pigments adsorption onto BY. The first portion represents external surface adsorption or instantaneous adsorption stage, while the second portion is a gradual adsorption stage where the intra particle diffusion is the controlling factor, and the last portion is the final equilibrium stage where the intra particle diffusion starts to decelerate due to the extremely low solute concentration in the solution. Furthermore, the plots of  $q_t$  versus  $(time)^{1/2}$  shows multi-linearity. Based on the plots, each portion represents a distinct mass transfer mechanism. In the colorant pigments for adsorption on BY, an initial portion relative to the boundary layer diffusion (film diffusion) was observed from 10-60 minutes for adsorption of anthocyanin and curcumin, while 10-90 minutes for adsorption of betacyanin onto BY. Then, the mass transfer step in colorant pigments adsorption onto BY was the film diffusion. This could have occurred due to the presence of a rigid and non-porous surface, as well as low value BY surface area. In addition, the molecular size of the colorant pigments might be higher than the average pore radius of BY, inhibiting internal diffusion. As a result, the values of C in Eq. 6.5 which is the point of intercept are 0.439, 0.052, and 0.011 for curcumin, anthocyanin, and betacyanin, respectively. This shows that the curcumin pigment displayed greater boundary layer effect than anthocyanin, and followed by betacyanin. This model portrays a plot of uptake that is linear and the adsorption process did involve intra particle diffusion. The plots, nonetheless, did not pass through the origin where it indicated some degree of boundary layer control.

The results showed that the intra particle diffusion is not the rate-limiting step that control the rate of adsorption because the experimental data showed better compliance with pseudo-second order kinetic model for betacyanin and curcumin, while the pseudo-first order kinetic model for anthocyanin in term of higher correlation coefficient value  $R^2$  compared intra particle diffusion. The adsorption of betacyanin and curcumin pigments on BY was shared similar result with Mu et al.,(2016), Rather et al., (2016), Tayade and Adivarekar, (2013) and Gamal et al., (2010). Mu et al.,(2016) has been prepared, characterized and applied the dye on well-defined two-dimensional superparamagnetic clay or polyaniline or  $Fe_3O_4$  nanocomposite. The study was revealed that the adsorption kinetics well fitted pseudo second-order kinetic model. Rather et al., (2016) studied the adsorption and kinetic studies of *Adhatoda vasica* natural dye onto woollen yarn. The kinetic data was best fitted to Pseudo-second order kinetic model with least standard deviation and highest regression coefficient, implying that the nature of adsorption process was chemisorption suggesting that the main operating forces and dyeing mechanism are controlled by electrostatic interaction and hydrogen bonding between woollen yarn and dye components. Tayade and Adivarekar, (2013) has been investigated the adsorption kinetics of cumin dye on silk fabric. The adsorption kinetics of cumin dye on silk fabric was found to follow the pseudo second order kinetic model. Gamal et al., (2010), kinetic studies showed that adsorption profiles of all reactive dyes adsorption onto cotton fibre followed pseudo-second order model with multi-step diffusion process.

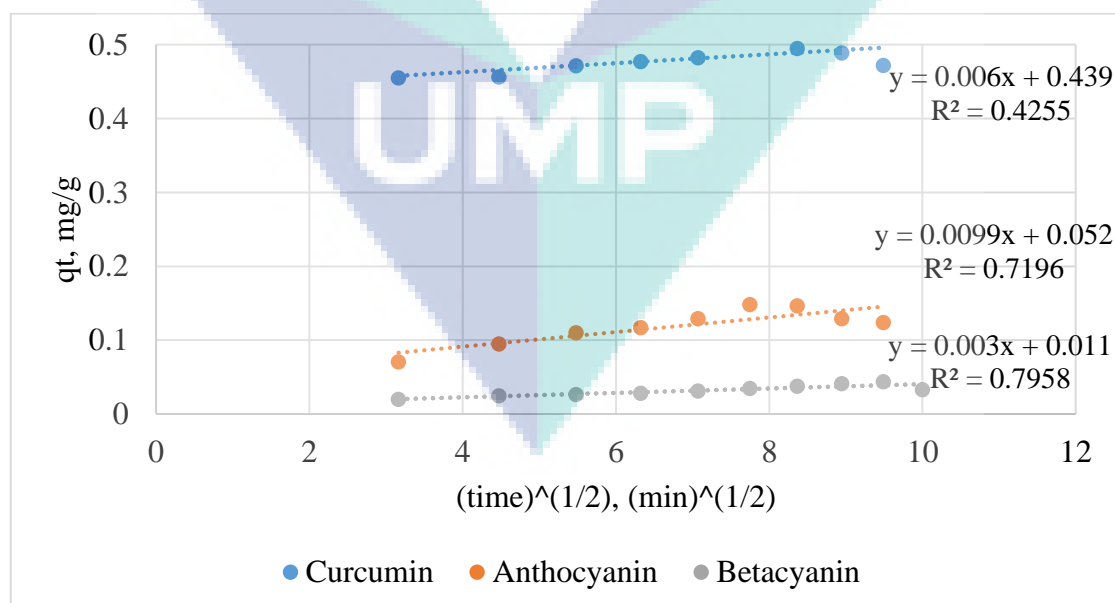


Figure 6.5 Intraparticle diffusion model for colorant pigments adsorption onto BY

## 6.4 Adsorption Isotherm

The equilibrium isotherm is essential in predictive modelling for analysis and designing of adsorption systems. Moreover, the theoretical evaluation and interpretation of thermodynamic parameters, such as heats of adsorption, are deemed as invaluable tools in the adsorption equilibrium. Successful representation of the dynamic adsorptive separation of solute from solution onto an adsorbent is dependent upon a good description of the equilibrium separation between the two phases. An equilibrium is established when the amount of solute adsorbed onto the adsorbent is equal to the amount being desorbed. The equilibrium solution concentration, therefore, is retained at constant. Plotting solid-phase concentration against liquid-phase concentration graphically depicts the equilibrium adsorption isotherm. In this research, the isotherm tested aided in the process of selecting the best colorant pigments of the adsorption of natural dyes onto BY. Hence, in order to maximize the design of adsorption system of the interaction between colorant pigments and BY, it had been important to establish the most appropriate correlation for the equilibrium curve. Thus, four adsorption isotherm models; Langmuir, Freundlich, Temkin, and Dubinin-Radushkevich equations, were used to further describe the adsorption equilibrium. The Langmuir isotherm is mainly applied to describe the monolayer adsorption that happens on the homogeneous surface of the adsorbent (Zhang et al., 2016). The Freundlich model, on the other hand, describes heterogeneous surface adsorption and multilayer adsorption under various non-ideal conditions (Zhang et al., 2016). Meanwhile, Temkin isotherm assumes that the heat of adsorption of all molecules in the layer decreases linearly with coverage (Zhang et al., 2016). Lastly, the Dubinin-Radushkevich isotherm is generally applied to express the adsorption mechanism with a Gaussian energy distribution onto a heterogeneous surface and it is usually applied to distinguish between physical and chemical adsorption (Dada et al., 2012). Hence, the varied isotherm equations of Langmuir, Freundlich, Temkin, and Dubinin-Radushkevich isotherm models tested in this study are discussed in the following subsections.

### 6.4.1 Langmuir isotherm

A linear plot of  $1/q_e$  against  $1/C_e$  had been plotted. Figure 6.6 shows the Langmuir isotherm on the adsorption of colorant pigments (a) anthocyanin, (b) betacyanin, and (c) curcumin onto BY. The Langmuir constant  $K_L$  and  $q_{max}$  were calculated using the slope and the intercept of the line, obtained from the plot of  $1/q_e$  against  $1/C_e$ . A linear plot with high regression coefficient ( $R^2=0.989$ ,  $0.979$ , and  $0.671$  for anthocyanin,

betacyanin, and curcumin respectively) suggests that adsorption mechanism could be described by Langmuir isotherm only for anthocyanin and betacyanin adsorption onto BY, indicating that anthocyanin and betacyanin molecules did interact with the ionic sites of BY via ionic interactions. In addition, the description of Langmuir isotherm can be also be expressed in terms of the dimensionless constant separation factor for equilibrium parameter,  $R_L$  (Shabbir et al., 2016), as defined in the following:

$$R_L = \frac{1}{1 + K_L C_0} \quad 6.6$$

Where  $C_0$  is the initial dye concentration (mg/L) and  $K_L$  is Langmuir constant.  $R_L$  value indicates the type of isotherm to be irreversible ( $R_L=0$ ), favourable ( $1 > R_L > 0$ ), linear ( $R_L=1$ ) or unfavourable ( $R_L > 1$ ) (Shabbir et al., 2016). In the present study that looked into the dyeing properties of BBPF, RDFP and turmeric dyes onto BY, the value of  $R_L$  was observed to be very close to 1 (0.974 and 0.997), indicating that the adsorption of betacyanin and curcumin pigments on BY respectively had been favourable and linear, while the  $R_L$  for anthocyanin was observed to appear between 1 and 0 (0.698), indicating a favourable adsorption as shown in Table 6.2.

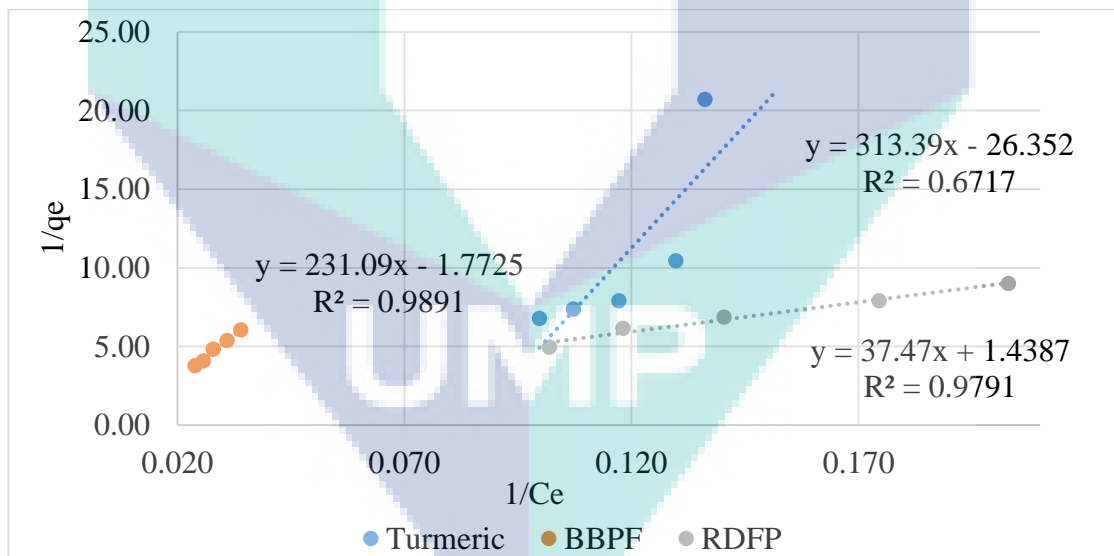


Figure 6.6 Langmuir isotherm on adsorption of colorant pigments onto BY

Table 6.2 Langmuir adsorption isotherm parameters for adsorption of colorant pigments onto BY

Colorant pigments	R <sup>2</sup>	q <sub>max</sub> (mg/g)	K <sub>L</sub> (L/mg)	R <sub>L</sub>
Anthocyanin	0.989	0.564	0.767	0.698
Betacyanin	0.979	0.695	0.038	0.974
Curcumin	0.671	0.038	0.084	0.997

#### 6.4.2 Freundlich isotherm

Another adsorption isotherm, which is the Freundlich isotherm, had been used to describe the interactions that took place between the adsorbate and the adsorbent, where multilayer adsorption took place with non-uniform distribution of adsorption heat and affinities over the heterogeneous surface. As such, Figure 6.7 shows the Freundlich isotherm for adsorption of anthocyanin, betacyanin, and curcumin onto BY. The Freundlich isotherm constants,  $K_F$  and  $n$ , are determined from the slope and the intercept of the line obtained from the plot of  $\log q_e$  versus  $\log C_e$ . Besides, the Freundlich isotherm has a benefit because it is a binding model that can provide accommodation, besides quantifying the heterogeneity, and it is extremely valid in determining heterogeneity. The Freundlich equation is usually measured to be purely empirical in nature, but it has been used widely to designate the adsorption of dye onto adsorbent. The adsorption characteristics for Freundlich models are summarized in Table 6.3, where the results showed that adsorption of anthocyanin and curcumin gave the best fit to adsorption data in the Freundlich isotherm where the R<sup>2</sup> values obtained were 0.986, 0.747, and 0.975 for anthocyanin, betacyanin, and curcumin, respectively. In addition, the magnitude of the exponent  $1/n$  pointed towards favourability of adsorption. Moreover, the value of  $n > 1$  represents favourable adsorption (Shabbir et al., 2016). In this research, the value of  $n$  had been favourable because the value exceeded 1 (1.233) for adsorption of curcumin, but less than 1 for anthocyanin (0.007) and betacyanin (0.329), which suggested unfavourable.

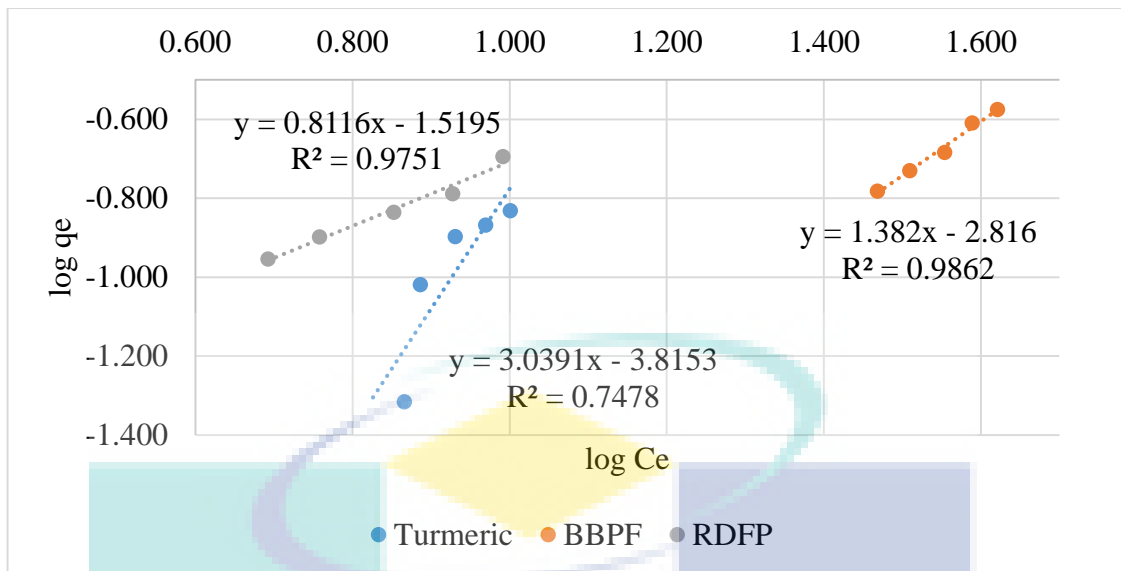


Figure 6.7 Freundlich isotherm for adsorption of colorant pigments onto BY

Table 6.3 Freundlich adsorption isotherm parameters for adsorption of colorant pigments onto BY

Colorant pigments	R <sup>2</sup>	n	K <sub>F</sub> (L/g)
Anthocyanin	0.986	0.007	-1.035
Betacyanin	0.747	0.329	-1.339
Curcumin	0.975	1.233	-0.418

#### 6.4.3 Temkin isotherm

Tempkin and Pyzhev consider the effects of some indirect adsorbate/adsorbate interactions on adsorption isotherms and suggests that due to these interactions, the heat of adsorption of all the molecules in the layer would decrease linearly with coverage. The adsorption data, thus, can be analysed by plotting  $q_e$  versus  $\ln C_e$ . Meanwhile, Figure 6.8 enables the determination of the isotherm constants  $B$  and  $A_T$  from the slope and the intercept, respectively.  $B$  is a constant related to heat of adsorption that could be calculated with Eq. (6.7).

$$B = \frac{RT}{b_T} \quad 6.7$$

The calculated coefficient of determination ( $R^2$ ) showed that the experimental data failed to display a good fit with Temkin isotherm for curcumin alone (Table 6.4). In fact, the low  $b_T$  values indicated that the interaction was purely physisorption.

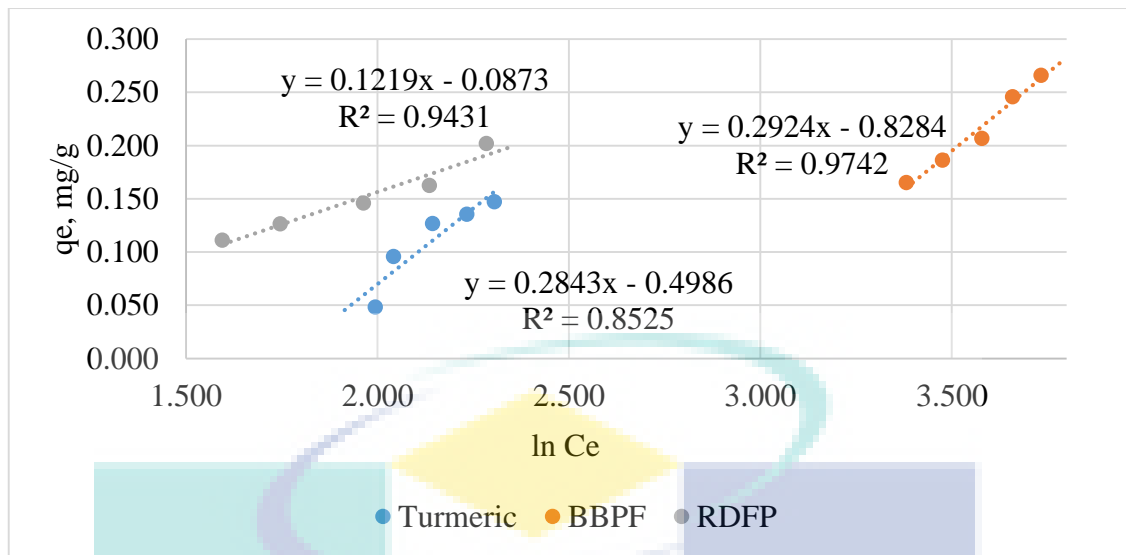


Figure 6.8 Temkin isotherm on adsorption of colorant pigments onto BY (a) Anthocyanin, (b) Betacyanin, and (c) Curcumin

Table 6.4 Temkin adsorption isotherm parameters for adsorption of colorant pigments onto BY

Colorant pigments	R <sup>2</sup>	A <sub>T</sub> (L/mg)	B	b <sub>T</sub> (KJ/mol)
Anthocyanin	0.974	-0.068	3.332	3.878
Betacyanin	0.943	-0.993	7.737	12.479
Curcumin	0.852	-0.219	2.999	3.491

#### 6.4.4 Dubinin-Radushkevich isotherm

By plotting  $\ln q_e$  versus  $\varepsilon^2$ ;  $q_D$  and  $\beta_D$  can be obtained, as depicted in Figure 6.9. The constant  $\beta_D$  gives an idea about the mean free energy,  $E_{DR}$  (kJ/mol), of adsorption per mole of the colorant pigments for anthocyanin, betacyanin, and curcumin when they transfer to the surface of the BY from infinity in the solution. If the adsorbent surface is both heterogeneous and homogeneous, sub regions are considered and the mean free energy value could be calculated using Eq. (6.8) (Dada et al., 2012).

$$E_{DR} = \frac{1}{\sqrt{2\beta_D}} \quad 6.8$$

This parameter is, in fact, useful in estimating the type of adsorption interaction. If the adsorption process is primarily physical in nature, such as Van der Waals forces, the average free energy should typically be in the range of 1-8 kJ/mol. However, if the  $E_{DR}$  is between 8 and 16 kJ/mol, the adsorption process is chemisorption via ion exchange. The Dubinin-Radushkevich isotherm parameters are listed in Table 6.5. All



colorant pigments (anthocyanin and betacyanin), except curcumin, exhibited good agreement with Dubinin-Radushkevich isotherm model, where the values of  $R^2$  (Anthocyanin = 0.985 and betacyanin = 0.973) are close to 1. As for the anthocyanin adsorption onto BY tested, the mean free energy of adsorption calculated for the interaction had been 5.00 kJ/mol, which accounted for physical adsorption. Thus, the Van der Waals forces led to  $E_{DR}$  in the range of 1–8 kJ/mol and the nature of the adsorption was proven by the pseudo-first order kinetic model. On the other hand, for the cases of betacyanin and curcumin, the  $E_{DR}$  obtained were 10.00 and 15.81 kJ/mol, respectively which fall within the range of 8-16 kJ/mol. This indicates that the adsorption is chemical in nature, as well as the electrostatic attraction that took place between the positively-charged BY and the negatively-charged betacyanin and curcumin. This possible nature of adsorption was also proven by the pseudo-second order kinetic model for adsorption of betacyanin and curcumin.

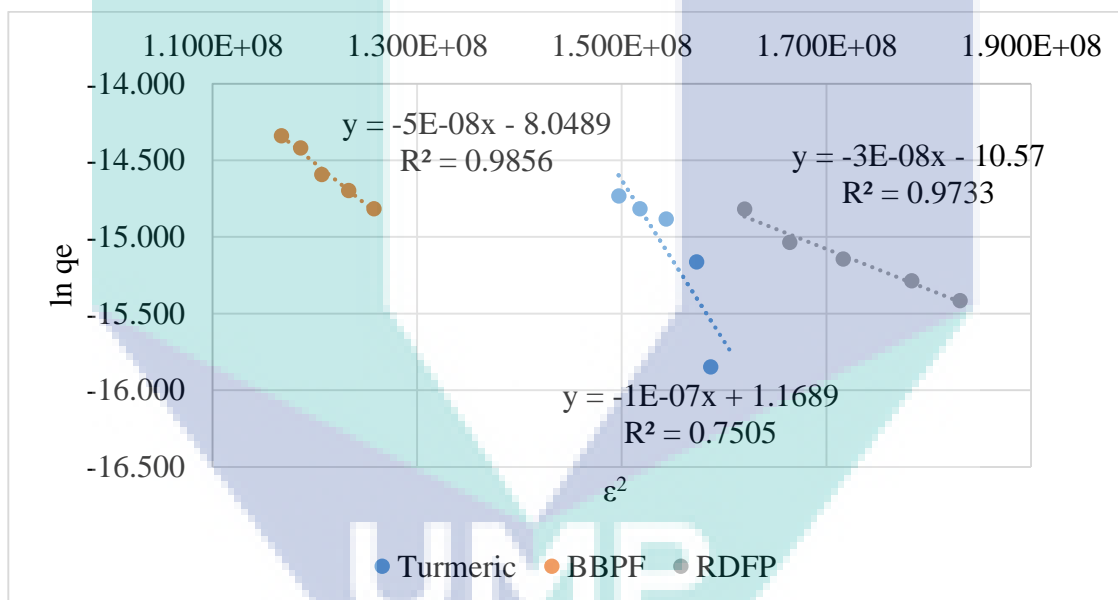


Figure 6.9 Dubinin- Radushkevich isotherm on adsorption of colorant pigments onto BY (a) Anthocyanin, (b) Betacyanin, and (c) Curcumin

Table 6.5 Dubinin-Radushkevich adsorption isotherm parameters for adsorption of colorant pigments onto BY

Colorant pigments	$R^2$	$q_D$ (mol/g)	$\beta_D$ (mol <sup>2</sup> /J <sup>2</sup> )	$E_{DR}$ (kJ/mol)
Anthocyanin	0.985	1.251	2.00E-08	5.00
Betacyanin	0.973	1.524	1.00E-09	10.00
Curcumin	0.750	0.679	5.00E-09	15.81

## 6.5 Error Analysis

In the single-component isotherm studies, the optimization procedure requires an error function to be defined in order to be able to evaluate the fit of the isotherm to the experimental equilibrium data (Ho et al., 2005). In this study, linear coefficients of determination and a non-linear the squares of the errors (SSE), Residual root mean square error (RMSE), Chi- square test,  $\chi^2$  and coefficient of determination,  $R^2$  were used.

### 6.5.1 The Sum of the Squares of the Errors (SSE)

The sum of the squares of the error (SSE) values was evaluated using the Eq. (6.9):

$$\sum_{i=1}^n (q_e - q_{e,m})^2 \quad 6.9$$

### 6.5.2 Residual Root Mean Square Error (RSME)

The residual root mean square error (RMSE) values were evaluated using Eq. (6.10):

$$\sqrt{\sum_{i=1}^n (q_e - q_{e,m})^2} \quad 6.10$$

### 6.5.3 Chi-square ( $\chi^2$ ) Tests

Chi-squares ( $\chi^2$ ) values were evaluated using the Eq. (6.11):

$$\chi^2 = \sum \frac{(q_e - q_{e,m})^2}{q_{e,m}} \quad 6.11$$

Where  $q_{e,m}$  is the equilibrium capacity obtained by calculating from the model (mg/g), and  $q_e$  is experimental data of the equilibrium capacity (mg/g). If data from the model are similar to the experimental data,  $\chi^2$  will be a small number; if they are different,  $\chi^2$  will be a large number. Therefore, it is necessary to also analyse the data set using the Chi-square test to confirm the best- fit isotherm for the adsorption system.

### 6.5.4 Non-linear analysis

The sum of the squares of the errors (SSE), Residual root mean square error (RMSE), Chi- square test,  $\chi^2$  and coefficient of determination,  $R^2$  were obtained and are shown in Table 6.6. By comparing the values of the error functions, the Temkin isotherm

was the best-fitting isotherm for adsorption of Turmeric dye on BY, followed by the Freundlich model for adsorption of RDFP dye onto BY and Langmuir isotherm for adsorption of BBPF onto BY. Similar results reported by Mu et al.,(2016) in which the adsorption isotherm was well fitted to the Langmuir isotherm and suggested that the chemical adsorption contributed to the whole adsorption process of the application of dye on well-defined two-dimensional superparamagnetic clay or polyaniline or Fe<sub>3</sub>O<sub>4</sub> nanocomposite. The models show a high degree of correlation with low squares of the errors (SSE), Residual root mean square error (RMSE) and Chi- square test,  $\chi^2$  values. This is clearly shown in Table 6.6, confirming the good fit of Temkin models for Turmeric dye, Freundlich model for BBPF dye and Langmuir model for RDFP dye with the higher value of coefficient of determination, R<sup>2</sup>. Thus, the non-linear sum of the squares of the errors (SSE), Residual root mean square error (RMSE), Chi- square test,  $\chi^2$  analysis proved that this method of could avoid the errors.



UMP

Table 6.6 Comparison of non-linear regression of the Squares of the errors (SSE), Residual root mean square error (RMSE), Chi-square test,  $\chi^2$  and coefficient of determination,  $R^2$

Natural Dye	Langmuir Equation (2)				Freundlich Equation (4)				Temkin Equation (6)			
	SSE	RMSE	$\chi^2$	$R^2$	SSE	RMSE	$\chi^2$	$R^2$	SSE	RMSE	$\chi^2$	$R^2$
Turneric	645.11300	25.39900	52.05900	0.50355	0.00170	0.04129	0.01784	0.96139	0.00093	0.03057	0.01107	0.97932
BBPF	0.00021	0.01458	0.00118	0.99738	0.00017	0.01287	0.00093	0.99796	0.00029	0.01707	0.00174	0.99638
RDFP	0.00009	0.00967	0.00042	0.99944	0.00010	0.01005	0.00046	0.99940	0.00018	0.01357	0.00088	0.99890

## 6.6 Desorption Study on Dyeing of Natural Dyes onto Bamboo Yarn (BY)

In order to ensure the feasibility of the colorant pigment adsorption, it had been necessary to determine if the colorant pigment adsorbed onto the BY did undergo desorption when soaked in water. Therefore, the BY with the best concentration of dye bath that had been adsorbed onto the BY had undergone this feasibility test. The BY with 3 different dyes prepared in the best dye concentration was soaked in 30 mL of water in test tubes and after 30 minutes, the optical density of the water solution was taken and the reading was recorded. Table 6.7 shows the contents of anthocyanin, betacyanin, and curcumin in water after the desorption process. From the results tabulated in Table 6.7, one can note that betacyanin pigments from the RDFP dye exhibited the highest content desorbed into the 30 mL of water solution in 30 minutes, followed by curcumin extracted from turmeric dye, and then, anthocyanin from BBPF dye. This is because; anthocyanin has the highest ability to retain on the BY, in comparison to curcumin and betacyanin. However, RDFP dye showed the lowest tendency to retain betacyanin dye on BY. Despite all of those, the rate of desorption had been considered low as the amount of colorant pigment contents in the water solution had been deemed as insignificant. Therefore, this experiment is indeed feasible.

Table 6.7 Anthocyanin, betacyanin, and curcumin contents in water after the desorption process

<b>Colorant pigment</b>	<b>Colorant pigment Content (mg/L)</b>
Anthocyanin	0.034
Betacyanin	0.055
Curcumin	0.045

## CHAPTER 7

### CHARACTERIZATION OF MATERIALS

#### 7.1 Introduction

This present study was carried out to study the processes of extraction and dyeing, which involved three selected natural dyes (BBPF, RDFP, and Turmeric) on bamboo yarn (BY). In this chapter, the experimental results of characterization performed upon the samples for extracted natural dyes, BY, DBY, and MBY are presented. The characterization of samples is crucial to determine the functional group for chemical structure of colorant pigment in the natural dyes and to identify the reactions between colorant pigments and cellulose in BY. The sample characterization was determined with FTIR and SEM, where the discussion is elaborated in this chapter.

#### 7.2 Spectral Analysis of Extracted Natural Dyes

##### 7.2.1 BBPF dye

From the FTIR spectrum shown in Figure 7.1, the presence of a broad absorption at  $3237\text{ cm}^{-1}$  displayed a characteristic absorption band of the OH group. The FTIR spectrum also interpreted an aromatic CH absorption at  $2937\text{ cm}^{-1}$ . Besides, the absorption at  $1632\text{ cm}^{-1}$  reflects the stretching of C=C, while the absorption at  $2132\text{ cm}^{-1}$  showed the stretching of C=C bisubstitute for various groups. Next, the absorption at  $1052\text{ cm}^{-1}$  indicated the presence of conjugated aromatic ring. Meanwhile, the weak peaks at  $1403\text{ cm}^{-1}$  and  $1357\text{ cm}^{-1}$  suggested the presence of bending aromatic C=C bond, whereas the peaks at  $1052\text{ cm}^{-1}$  represented C–O bond. The presence of the discussed functional groups confirmed that the extracted colorant pigment from BBPF dye did belong to the anthocyanin group.

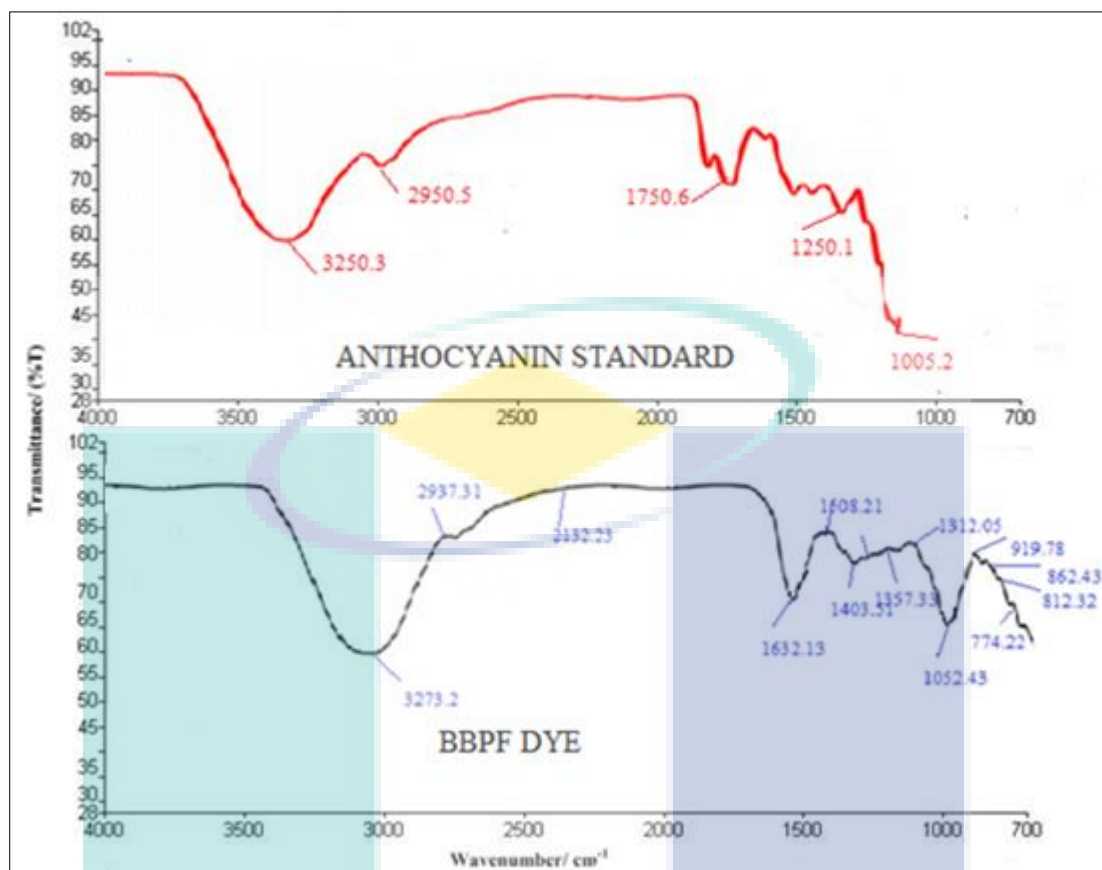


Figure 7.1 FTIR spectra for BBPF dye

### 7.2.2 RDFP dye

The FTIR spectral analysis was performed to identify the major functional groups present in the natural dye extracted from RDFP. The RDFP dye FTIR spectra showed peaks similar to other materials containing betacyanin (Al-Alwani et al., 2015). The FTIR spectrum exhibited in Figure 7.2 shows distinct peaks at 3322, 2945, 2811, 2148, 1633, 1416, 1413, 1061, and 716  $\text{cm}^{-1}$  respectively. The broad and strong band at 3322  $\text{cm}^{-1}$  suggested O-H bond in stretching vibration mode, while the bands at 2945  $\text{cm}^{-1}$  and 2811  $\text{cm}^{-1}$  indicated C-H symmetry in stretching mode. Besides, the wave number at 2148  $\text{cm}^{-1}$  showed the presence of (C $\equiv$ C) in stretching vibration mode respectively, whereas the wave number at 1633  $\text{cm}^{-1}$  confirmed the presence of carbonyl group (C=O) in stretching mode associated with amide bond. Next, the weak peaks at 1416 and 1413  $\text{cm}^{-1}$  suggested the presence of bending aromatic C=C bond. Other than that, the peak at 1061  $\text{cm}^{-1}$  represented the C-O bond and the presence of the amine group N-H was confirmed by the wave number at 716  $\text{cm}^{-1}$  in the spectrum. The presence of amine N-H and carbonyl

C=O, as well as other functional groups, confirmed that the extracted colorant pigment from RDFP dye belonged to the betacyanin group of betalains.

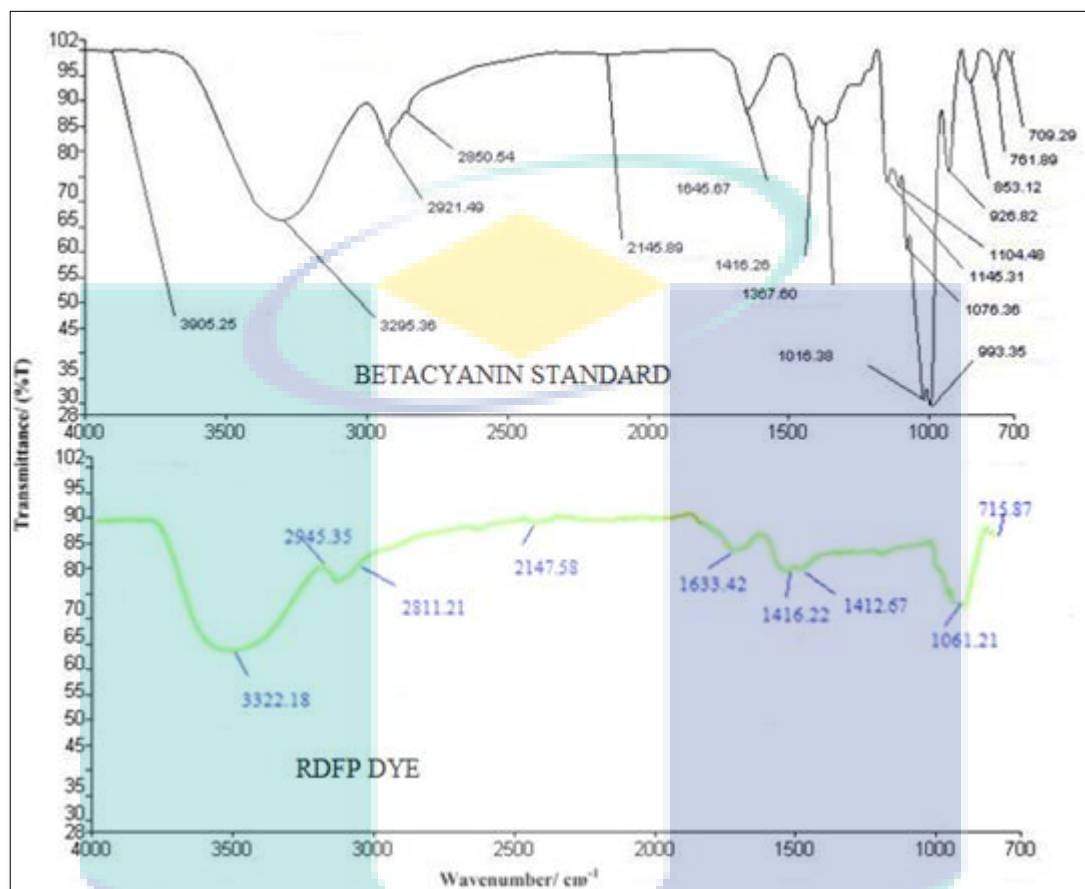


Figure 7.2 FTIR spectra for RDFP dye

### 7.2.3 Turmeric dye

A detailed study on the vibrational FTIR spectra turmeric dye is illustrated in Figure 7.3. The FTIR spectrum of turmeric dye showed a broad peak at  $3395\text{ cm}^{-1}$  and a sharp peak at  $2928\text{ cm}^{-1}$ , which indicated the presence of OH group. The strong peak at  $1726\text{ cm}^{-1}$  displayed a predominantly mixed C=C and C=O character. Another strong band at  $1642\text{ cm}^{-1}$  is attributed to the symmetric aromatic ring stretch vibration C=C ring. Next, the  $1434\text{ cm}^{-1}$ , which corresponded to the vibrational mode of C–O elongation of the alcohol and phenol groups confirmed the extraction of curcumin from turmeric; C–O–C peak. Besides, bands at  $1098$ ,  $852$  and  $504\text{ cm}^{-1}$  are attributed to the bending vibrations of the CH bond of alkene groups ( $\text{RCH}=\text{CH}_2$ ). This is evident of the characteristic FTIR peaks of curcumin in turmeric dye.



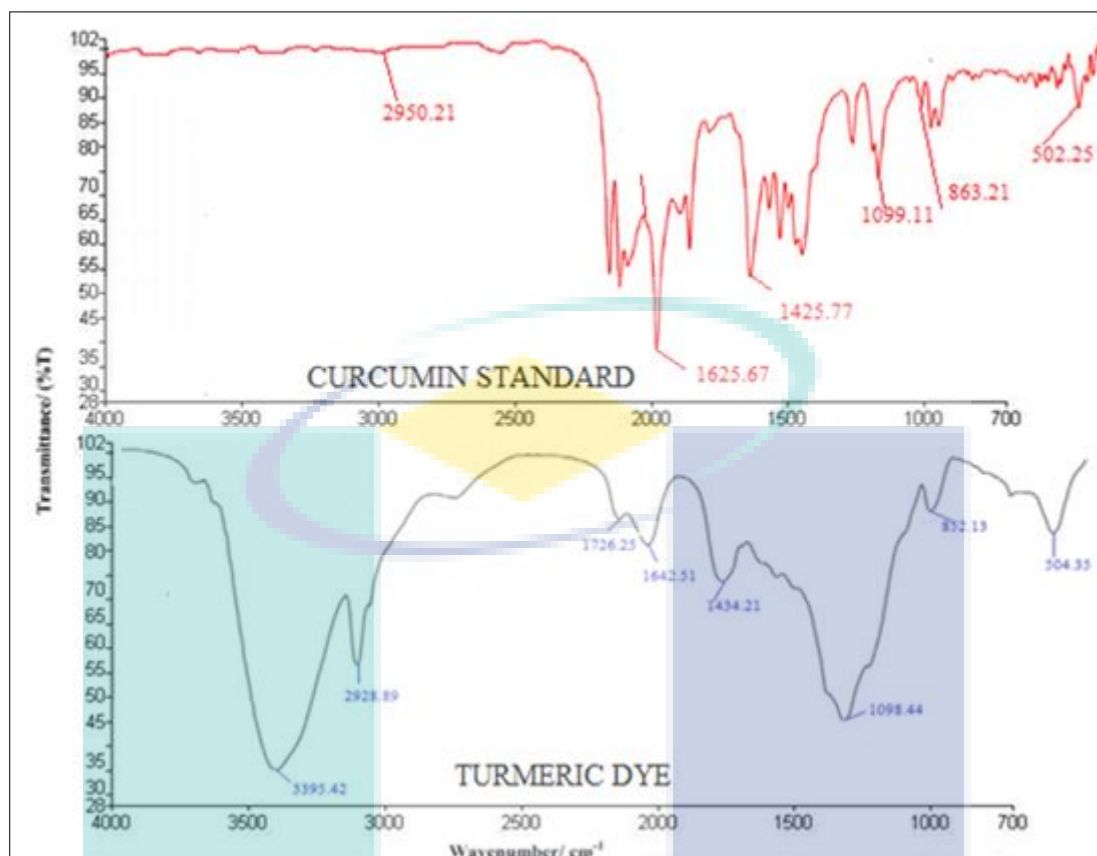
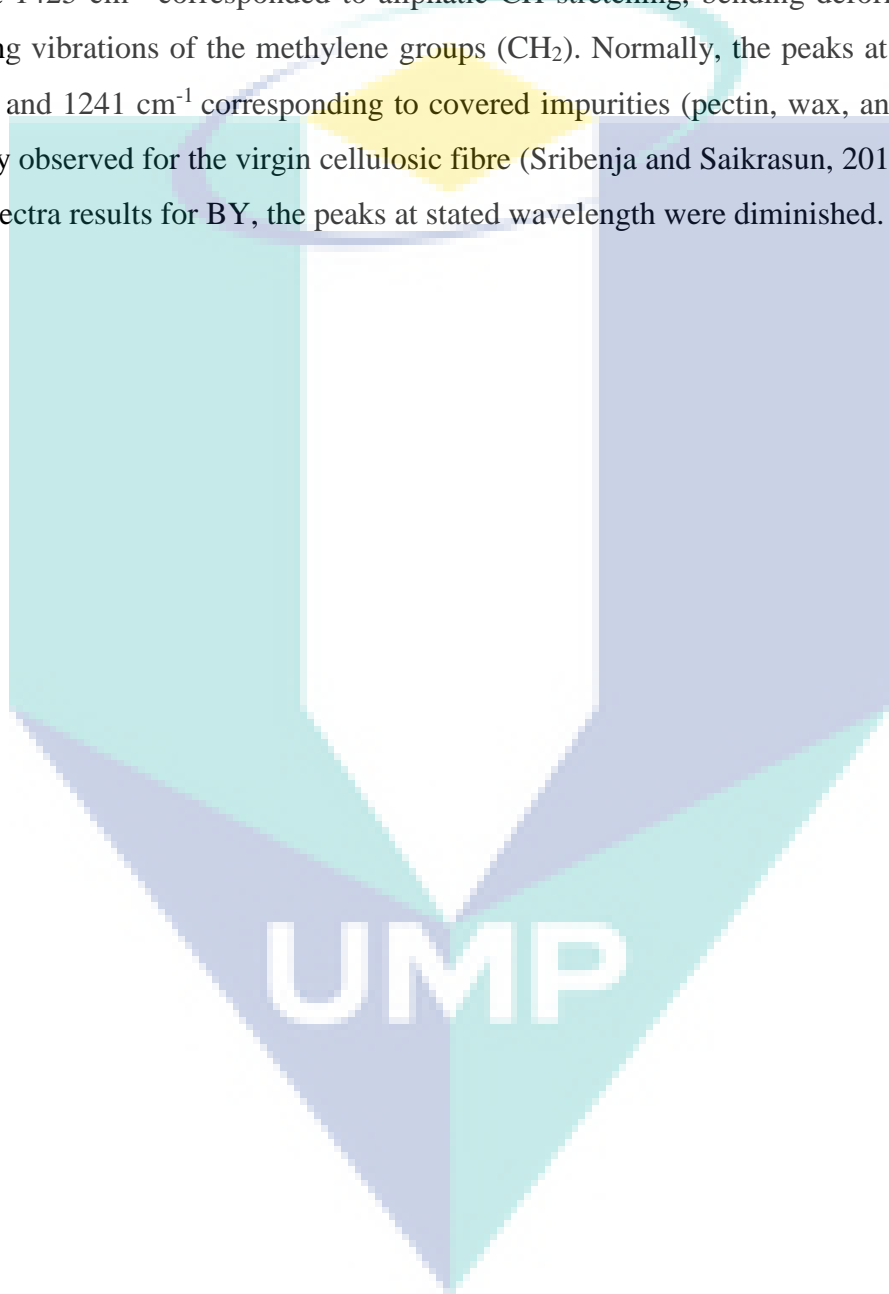


Figure 7.3 FTIR spectra for turmeric dye

### 7.3 Spectral Analysis of Dyeing Natural Dyes on Bamboo Yarn (BY)

The FTIR spectra had been used to identify the presence of functional groups on the solid surface of both untreated and treated BYs (Figure 7.4). It appeared similar to results obtained in previous studies of cotton as expected by Nicholas, (2014) and Sribenja and Saikrasun, (2015). The FTIR spectra for all samples showed the emergence of characteristic cellulose peaks at around  $1000\text{--}1200\text{ cm}^{-1}$  and this spectra was similar studied by Haddar et al., (2014) for cotton fabric. Other characteristic bands related to the chemical structure of cellulose were the hydrogen-bonded OH stretching, where the broad and strong absorption peak could be noted at around  $3354$  and  $3345\text{ cm}^{-1}$  for untreated and treated BYs, respectively. On top of that, C–H stretching was observed at  $2914$  and  $2895\text{ cm}^{-1}$  for untreated and treated BYs respectively, and C–O–C wagging at  $1368\text{ cm}^{-1}$ . The peaks at  $\sim 3354$  and  $2915\text{ cm}^{-1}$  correspond to the hydroxyl group and asymmetric stretching of CH, CH<sub>2</sub> for general cellulose fibre, respectively as stated by Sribenja and Saikrasun, (2015). These results indicated that most of the bands for both untreated and treated BY shared similar base signals and minor changes could be interpreted in the IR spectra. Furthermore, the presence of strong bands at  $1643\text{ cm}^{-1}$

(untreated BY) and  $1644\text{ cm}^{-1}$  (treated BY) confirmed the presence of belongs to the C=O stretching of hemicellulose. Moreover, the bands around  $1368$  and  $1317\text{ cm}^{-1}$  are assigned to  $\text{CH}_2$ -scissoring and OH-bending vibration, respectively. The bands at  $1021\text{ cm}^{-1}$  and  $1023\text{ cm}^{-1}$  for untreated and treated BYs respectively emerged due to C–O and C–C stretching. Furthermore, the splitting distinct bands observed in the spectrum of treated BY at  $1425\text{ cm}^{-1}$  corresponded to aliphatic CH stretching, bending deformations, and rocking vibrations of the methylene groups ( $\text{CH}_2$ ). Normally, the peaks at about  $1730$ ,  $1515$ , and  $1241\text{ cm}^{-1}$  corresponding to covered impurities (pectin, wax, and lignin) are clearly observed for the virgin cellulosic fibre (Sribenja and Saikrasun, 2015). Based on the spectra results for BY, the peaks at stated wavelength were diminished.



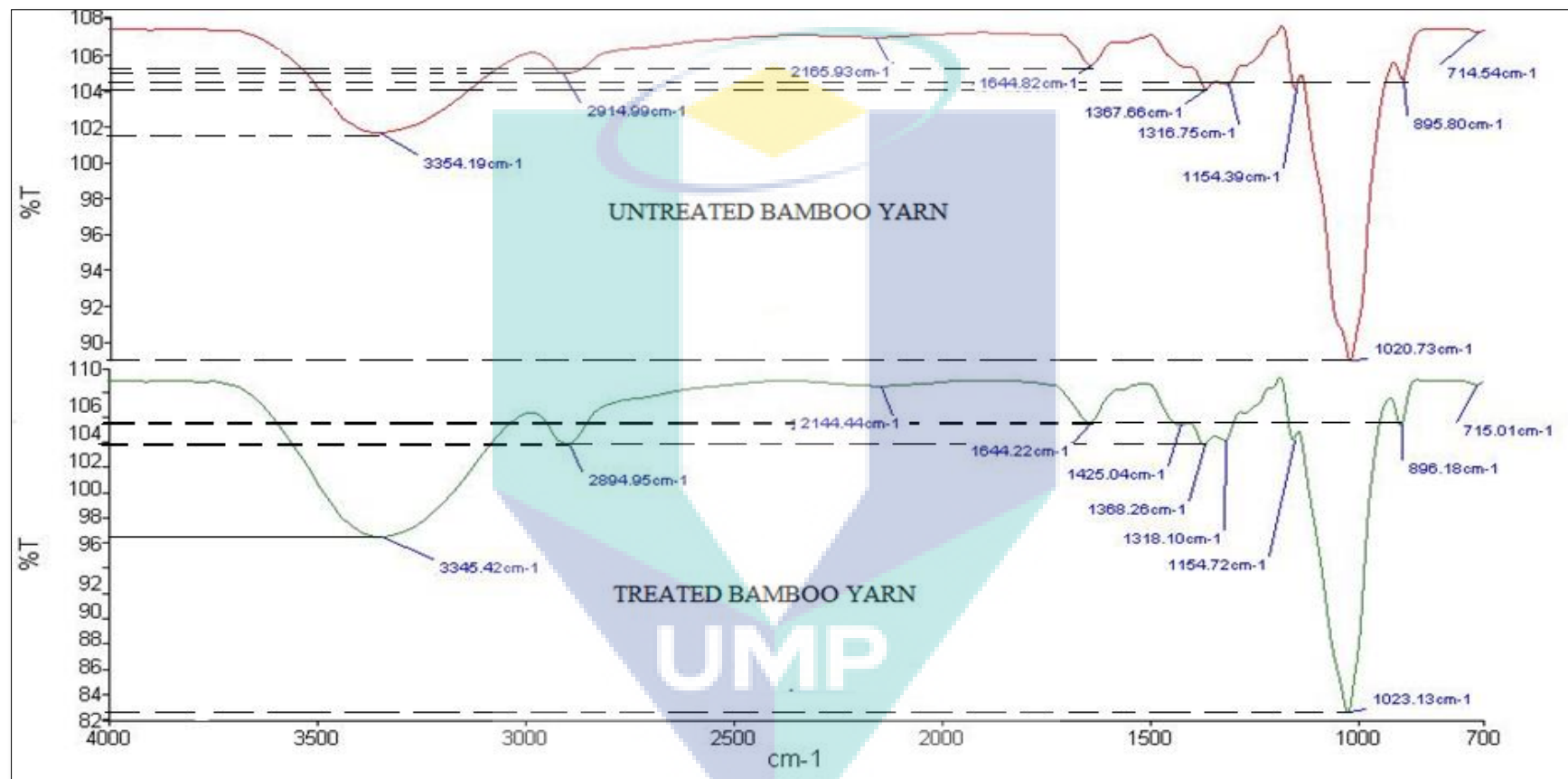


Figure 7.4 The FTIR spectra of untreated BY and treated BY using distilled water

Compared to the undyed BY FTIR spectrum, the blue dyed BY FTIR spectra in Figure 7.5 show a peak shift from  $1644\text{ cm}^{-1}$  to  $1638\text{ cm}^{-1}$ , where the spectrum showed the characteristic of water adsorption. This shift brings the peak to be in line with the  $1632\text{ cm}^{-1}$  peak in the BBPF dye (Figure 7.1). Besides, the  $1630\text{-}1640\text{ cm}^{-1}$  range corresponded to the water in cellulose (Nicholas, 2014). The peak shift at  $1644\text{ cm}^{-1}$  and a new peak observed at  $1798\text{ cm}^{-1}$  caused a slight change in the chemical structure in BY (represented by new peaks or peak shifts) during the dyeing procedure; suggesting the BBPF dye formed minimal chemical bonds with BY. However, as for the pink dyed BY FTIR spectra, where the BY was dyed with RDFP dye, as shown in Figure 7.6, a peak shifted from  $1644\text{ cm}^{-1}$  to  $1641\text{ cm}^{-1}$ . The shift of peak at  $1641\text{ cm}^{-1}$  brought the peak to be more in line with the peak for RDFP dye (Figure 7.2). This shift led to a small modification in the chemical structure of dyed BY with the RDFP dye; suggesting minimal chemical bonds with BY. Nonetheless, no change was noted in peak intensity, new peaks, or peak shifts, as illustrated in Figure 7.7, for BY dyed with turmeric ( $1644\text{ cm}^{-1}$ ), but this peak had been in line with the peak associated to turmeric dye (Figure 7.3). The similar FTIR spectrum studied by Ahamed et al., (2016) of dyeing turmeric dye on spun fibre. Moreover, one should note that strong bonds could form when a dye and a fabric display similar peaks on FTIR spectra. Hence, all the samples of dyed BY demonstrated great affinity towards BBPF, RDFP, and Turmeric dyes, as the dyed BY shared similar peaks with the FTIR spectra for dye.

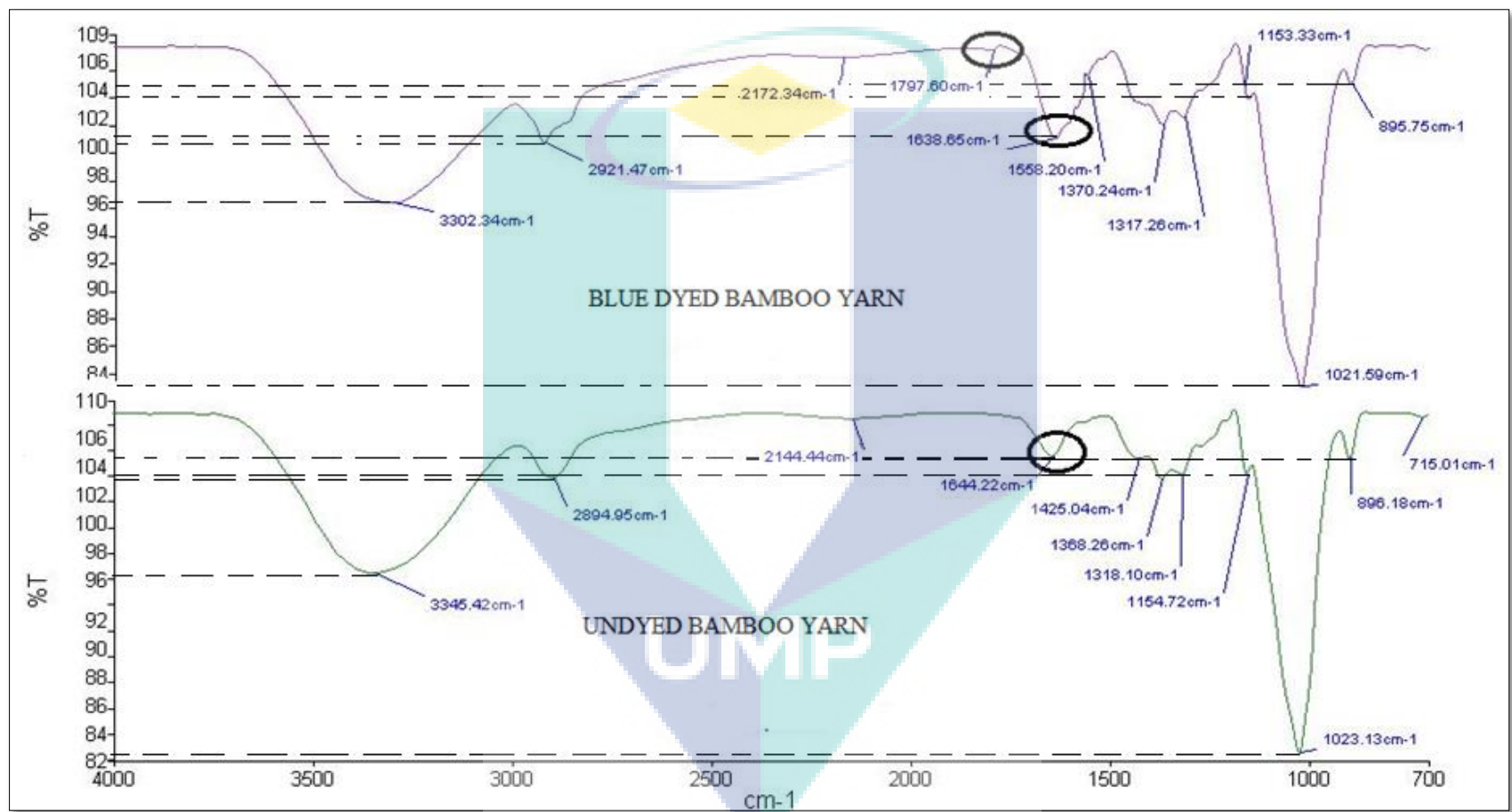


Figure 7.5 The FTIR spectra of blue dyed BY and undyed BY

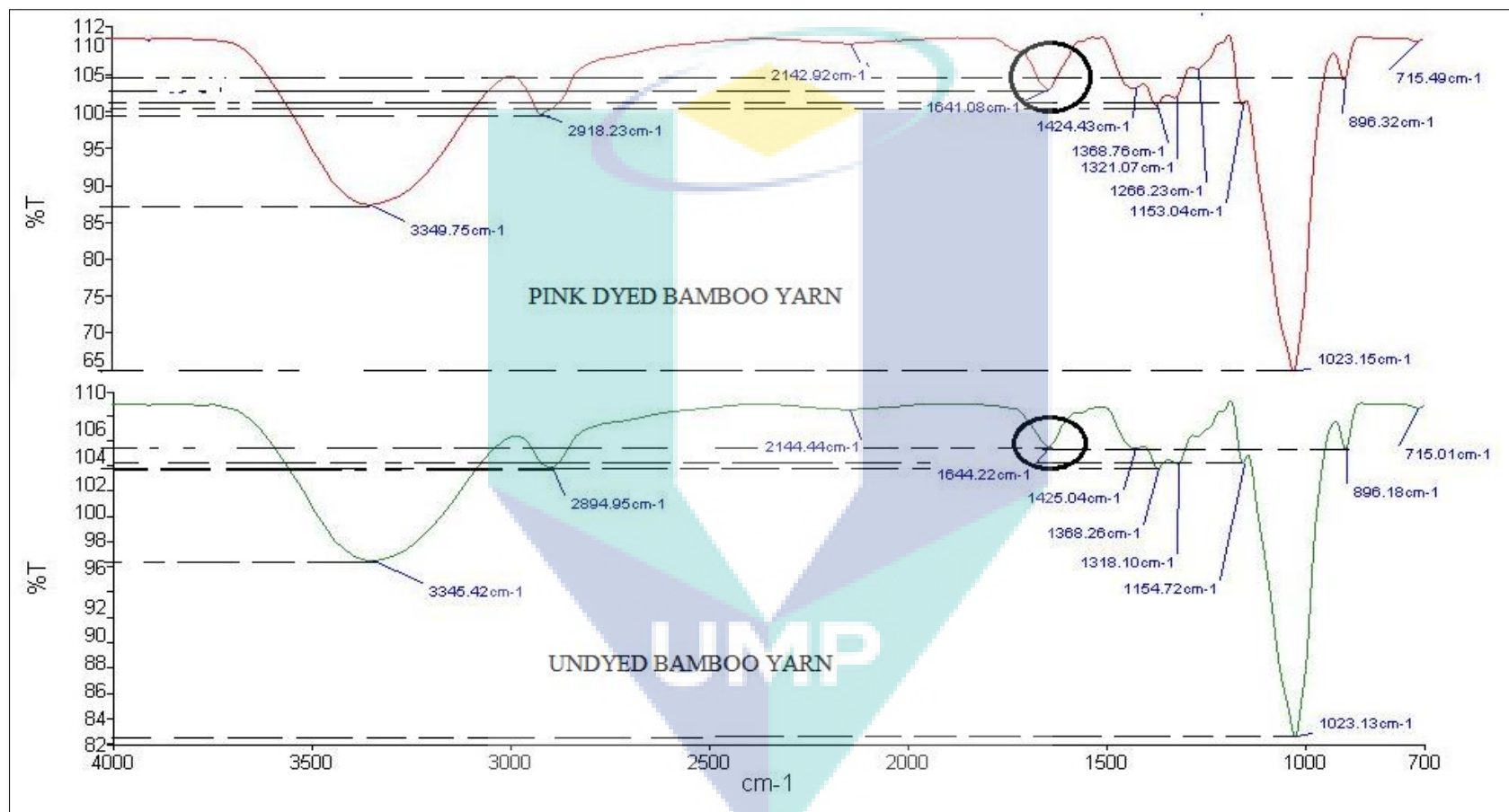


Figure 7.6 The FTIR spectra of pink dyed BY and undyed BY

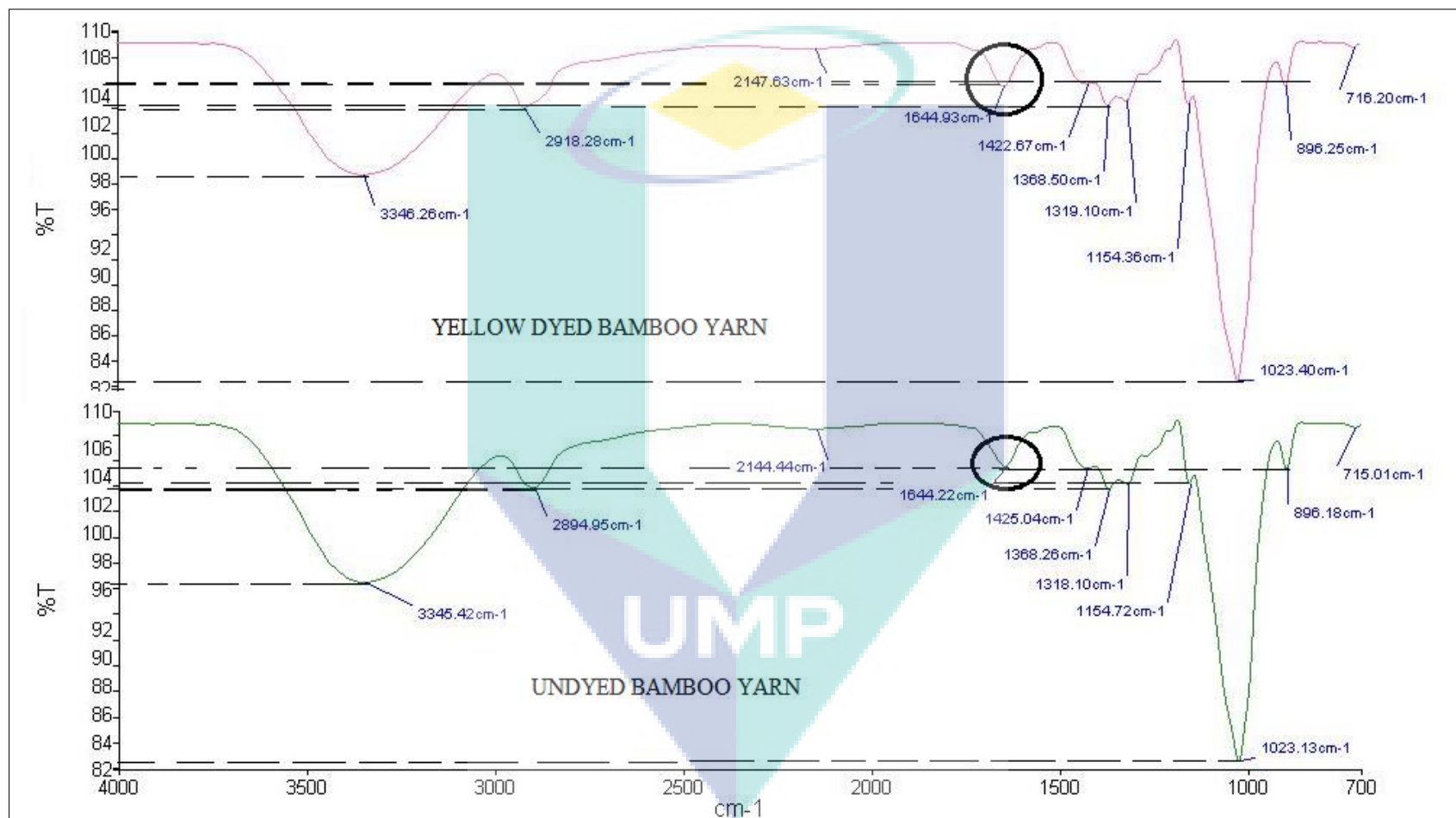


Figure 7.7 The FTIR spectra of yellow dyed BY and undyed BY

Interestingly, the peak at  $1644\text{ cm}^{-1}$  changed its intensity depending on the post-mordanting procedure, as shown in Figures 7.8 until 7.10. The peak intensity in percentage of transmittance on undyed BY was 105 versus 102 on post-mordanted blue dyed BY (Figure 7.8), 104 on post-mordanted pink dyed BY (Figure 7.9), and 103 on post-mordanted yellow dyed BY (Figure 7.10). Furthermore, the decrease in peak intensity for all samples of post-mordanted BY is likely due to natural dyes (BBPF, RDFP, and Turmeric) covering the BY; indicating the presence of a natural dye layer on the surface of the BY. In addition, the increment in peak intensity suggested an increase of water absorbed in BY. This may imply an increased hydrophilicity in BY due to BBPF, RDFP, and Turmeric dyes. However, the discrepancy of hydrophilicity is not clearly understood. Hence, further analysis, including contact angle and surface tension measurements, is warranted for future work to assess the impacts of BBPF, RDFP, and Turmeric dyes upon BY hydrophilicity. Strong bonds could be formed when a dye and a fabric show similar peaks on FTIR spectra. BY displayed peaks at  $1644\text{ cm}^{-1}$ , which corresponded closely to BBPF, RDFP, and Turmeric dyes peaks at  $1632\text{ cm}^{-1}$ ,  $1641\text{ cm}^{-1}$ , and  $1644\text{ cm}^{-1}$ , respectively. This explains that Turmeric dye demonstrated greater affinity to post-mordanted BY compared to BBPF and RDFP, as post-mordanted BY shared similar peaks with the Turmeric dye in FTIR spectra (Figure 7.3).



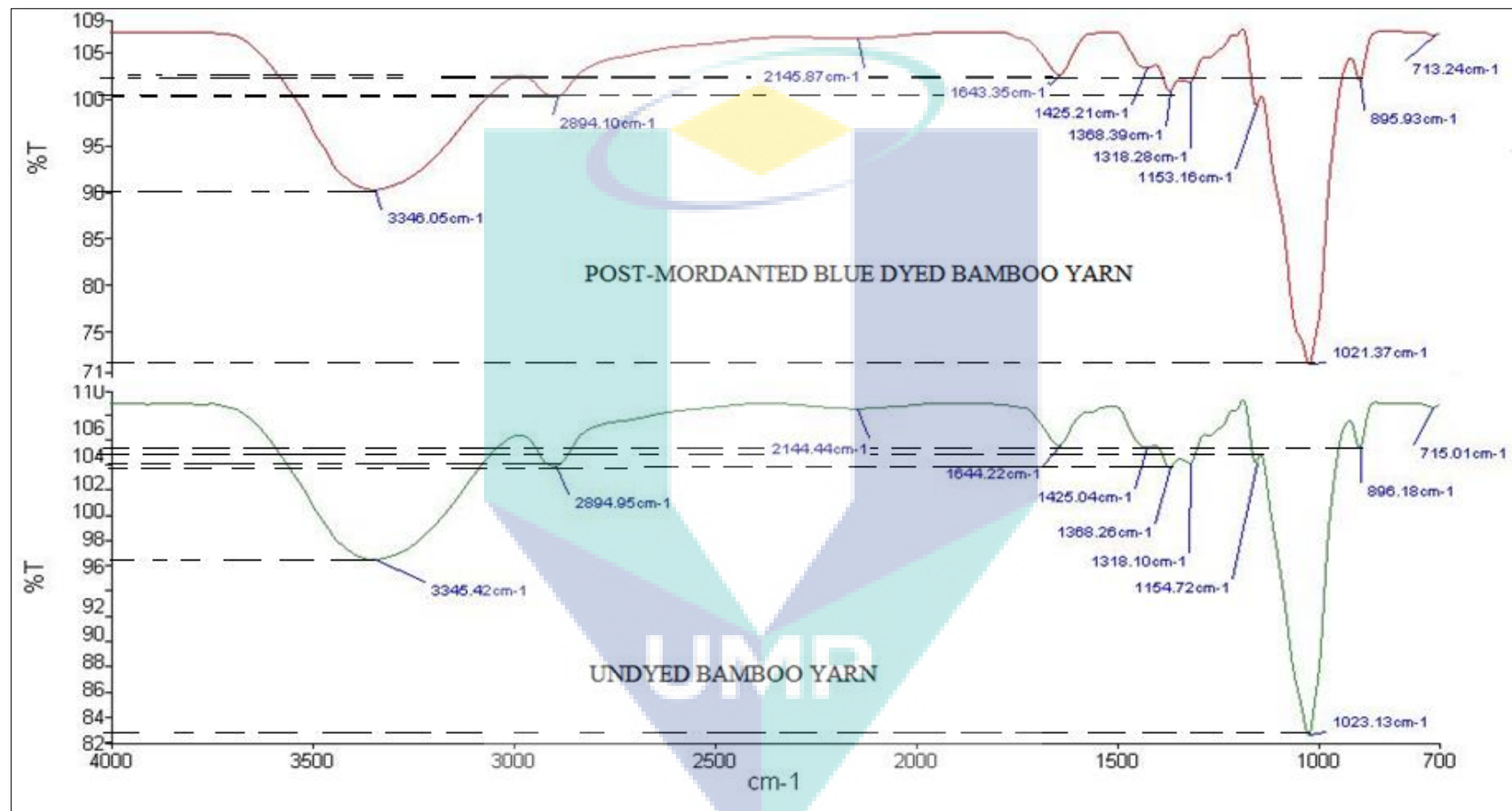


Figure 7.8 The FTIR spectra of post-mordanted blue dyed BY and undyed BY

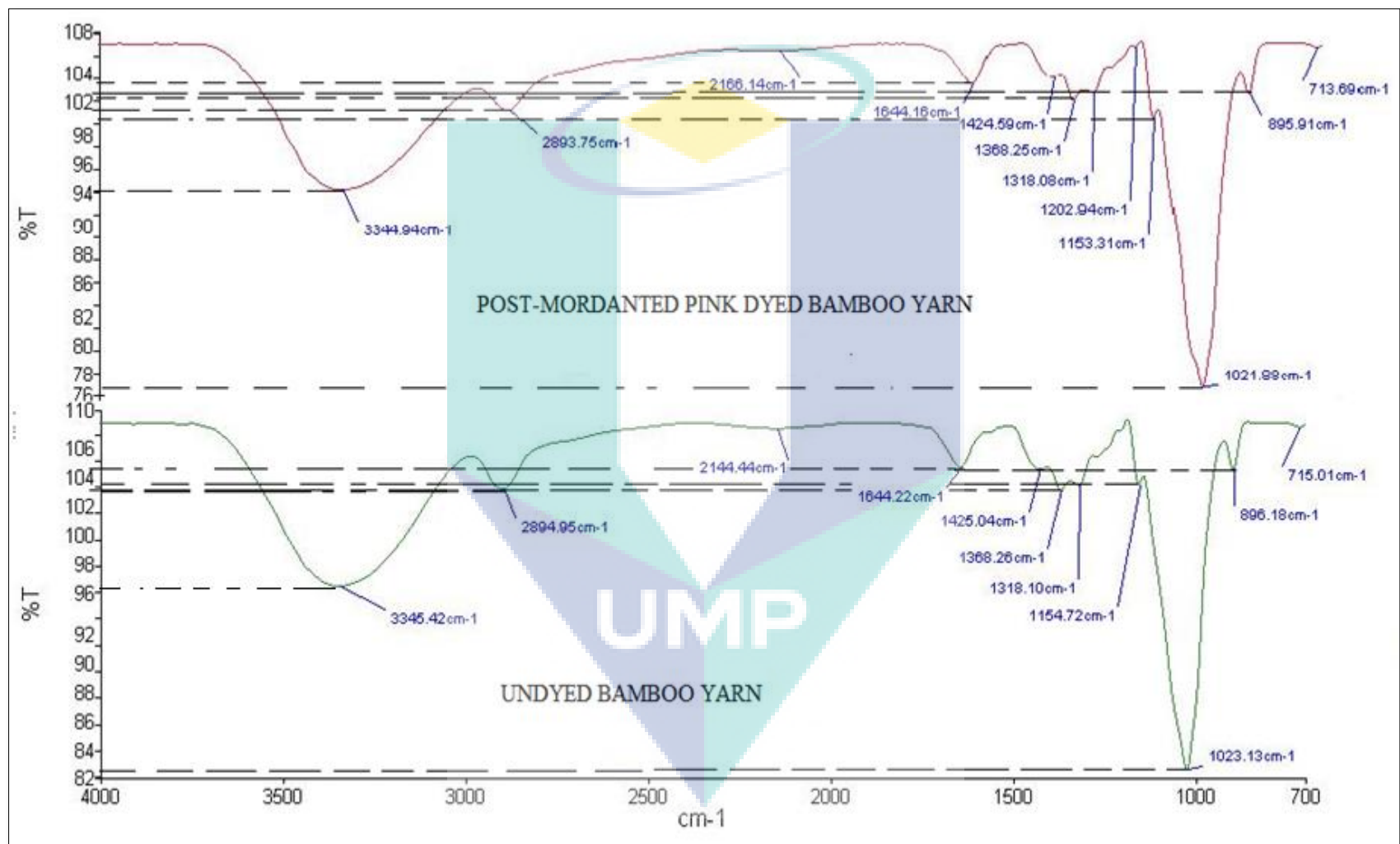


Figure 7.9 The FTIR spectra of post-mordanted pink dyed BY and undyed BY

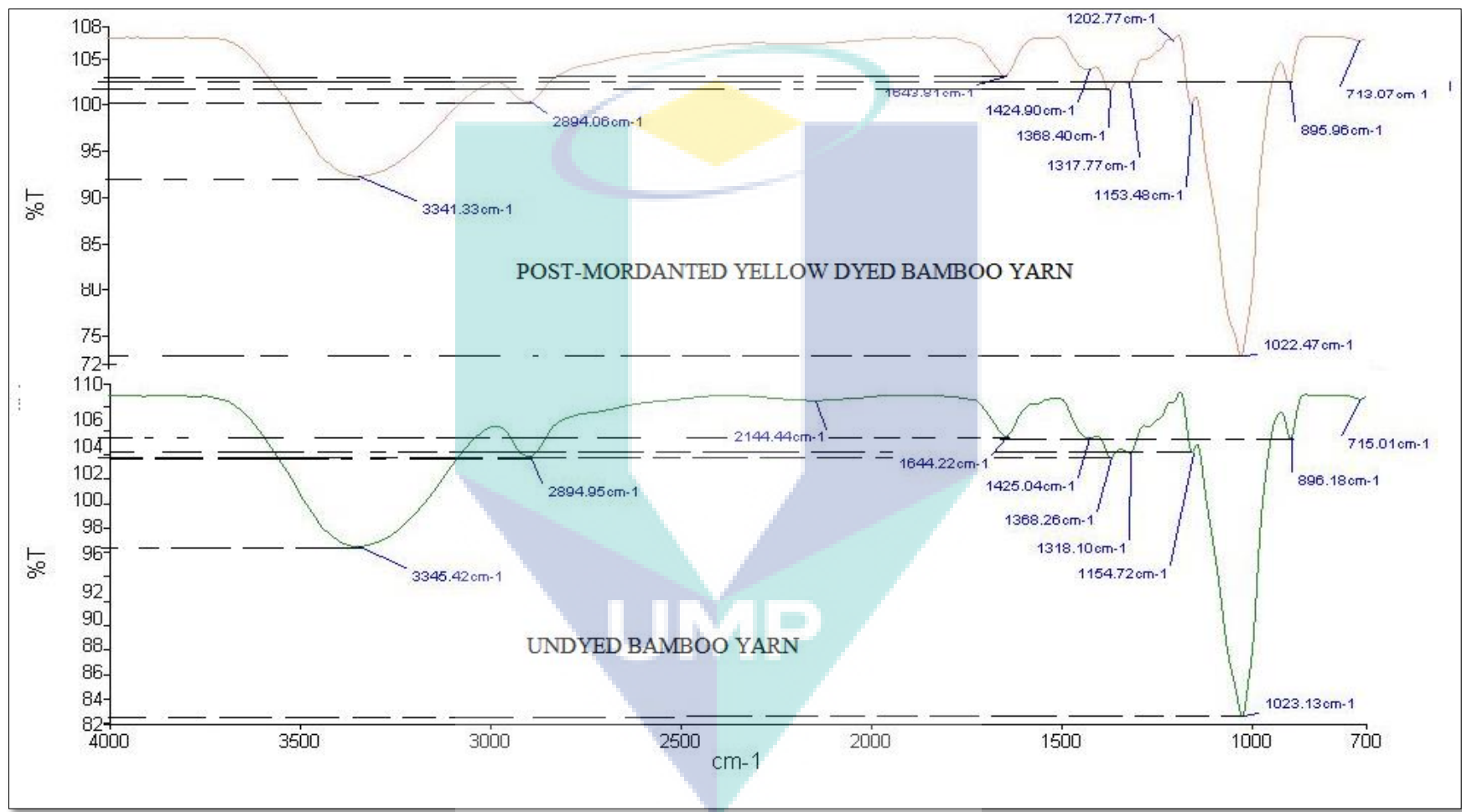


Figure 7.10 The FTIR spectra of post-mordanted yellow dyed BY and undyed BY

## 7.4 Morphology Analysis

SEM operated with the voltage of 10 kV was used for surface morphological characterization. The typical SEM micrographs that display BY surface morphology were presented in Figure 7.11 and Figure 7.12. The diameter of the BY was mostly found in the range of 2-3  $\mu\text{m}$ . For the untreated BY (Figure 7.11(a)), the rough surfaces were clearly observed due to the covered impurities. After washing, the smooth surface of BY is clearly observed (Figure 7.11(b)). The BY was flat with a twisted ribbon-like structure caused by spiralling cellulose fibrils. Figure 7.12 shows the overview of colour images (left column) and the corresponding surface morphology (right column) of the BY before and after dyeing. Before dyeing, white colour with cleaned surfaces are observed (Figure 7.12(1a and 2a)). After dyeing, the colour of the treated BY becomes to a saturated blue (Figure 7.12(1b)), soft pink (Figure 7.12(1c)) and bright yellow (Figure 7.12(1d)) respectively. The results agree well with SEM images (Figure 7.12(2b, 2c and 2d)) that the dyed yarns show a surface roughness due to the dyed adsorbed on the yarn. Sribenja and Saikrasun, (2015) has been reported that the treated bamboo fibres with poly(ethyleneimine) shows relatively higher surface roughness than the controlled one due to the relatively higher amount of dye adsorbed (Lac dye) on the fibre.

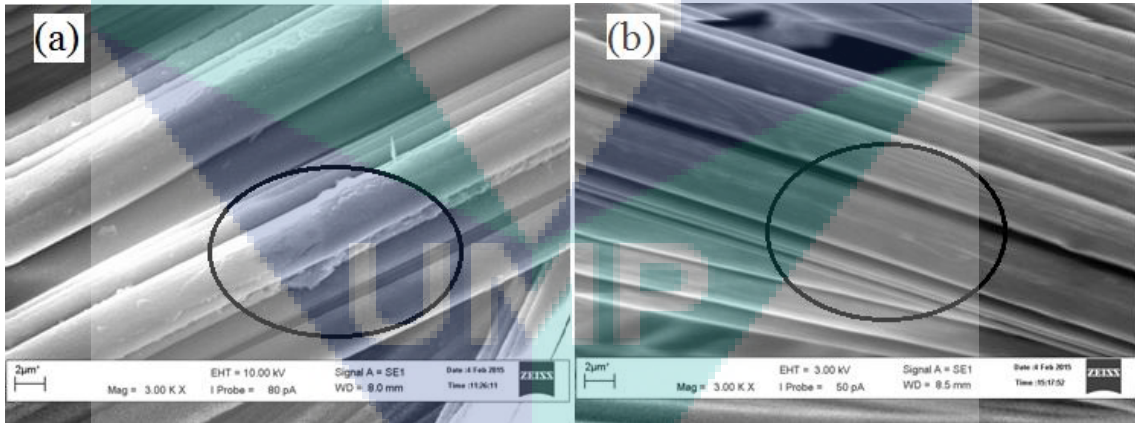


Figure 7.11 SEM images of the samples (a) untreated BY and (b) treated BY

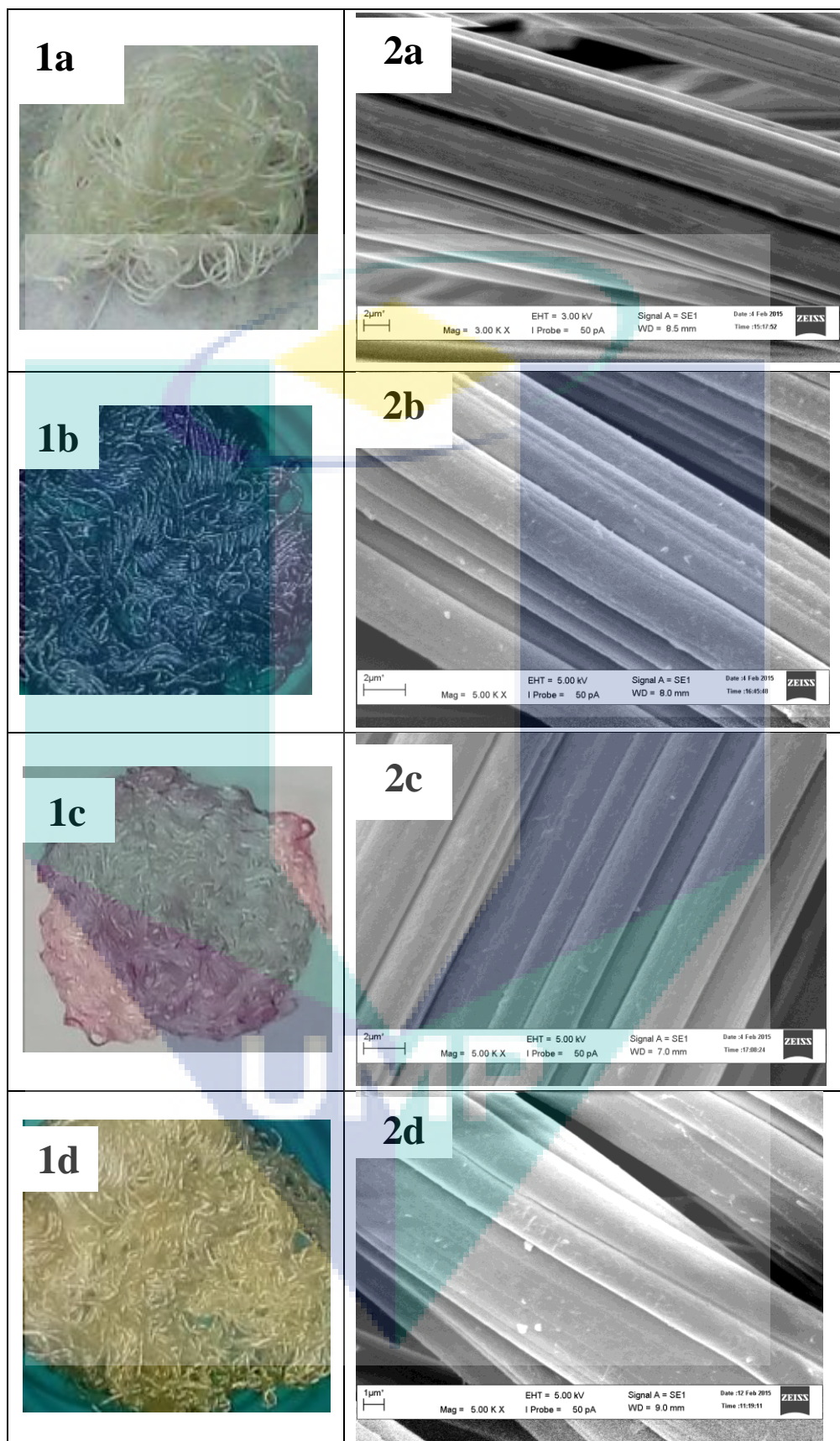


Figure 7.12 Optical images (column 1) and SEM micrographs (column 2) of BY (a) undyed BY, (b) BBPF dye-BY, (c) RDFP dye-BY and (d) Turmeric dye-BY

## CHAPTER 8

### GENERAL CONCLUSIONS AND RECOMMENDATIONS FOR FUTURE WORK

#### 8.1 INTRODUCTION

The current research was carried out to look into the extraction of natural dyes, which were then dyed onto BY. As such, five main phases were incorporated in the process of dyeing the three natural dyes selected in this study on BY. The phases were: i) extraction of natural dyes, ii) dyeing of natural dyes on BY, iii) mordanting and desorption studies, iv) adsorption study of dyeing natural dyes onto BY, and v) characterization of samples. With that, this chapter presents a brief overview of the results and the conclusions that have been described in the preceding chapters of this thesis. The findings of this study demonstrate a promising aspect for future work concerning dyeing of natural dyes on BY. Thus, some recommendations for further study are suggested for extraction of natural dyes from various sources of dyes.

#### 8.2 General Conclusions

This study has two major objectives: i) extraction of natural dyes from BBPF, RDFP, and Turmeric, as well as ii) dyeing of the extracted dyes upon BY. In order to achieve the main objectives of this study, the following four objectives were aimed to elucidate the major objectives. The first objective is to study the effects of temperature, solid liquid ratio (SLR), and time on blue, red, and yellow natural dyes extracted from Blue Butterfly Pea Flower (BBPF), Red Dragon Fruit Peel (RDFP), and Turmeric, as well as to identify the optimal conditions for the extraction of natural dyes. The optimization of extraction conditions led to the production of maximum colorant pigments recovery from the extracted natural dyes. Furthermore, with OFAT and CCD, optimum extraction of BBPF dye for temperature, time, and SLR were determined to be 55 °C, 15 minutes, and 0.10 g/mL respectively while for turmeric dye extraction, 55 °C, 25 minutes, and 0.12 g/mL respectively.

Next, the second objectives are to study the effects of dyeing temperature, dye bath concentration, dye bath pH, and dyeing time to extract dyes from BBPF, RDFP, and Turmeric, as well as to identify the optimal conditions for the dyeing of natural dyes onto Bamboo Yarn (BY). These conditions were analysed via OFAT and CCD, which provided the best conditions for dyeing of selected natural dyes on BY. The optimum conditions of dyeing BY with BBPF dye for dye bath concentration, dyeing time, and dye bath pH had been 0.083 g/mL, 60 minutes, and 6.5, respectively. Meanwhile, the optimized conditions for dyeing of RDFP and Turmeric dyes on BY in terms of dye bath concentration, dyeing time, dye bath pH, and dyeing temperature were 0.10 g/mL and 0.101 g/mL, 90 minutes and 60 minutes, pH 3 and pH 4.1, 70 °C and 67 °C, respectively.

Meanwhile, the third objective is to study the kinetics and the adsorption processes of dyeing natural dyes onto BY with applications of Langmuir, Freundlich, Temkin and Dubinin-Radushkevich isotherm models. The adsorption of the colorant pigments of anthocyanin onto BY adhered to the pseudo-first order model, while the other two colorant pigments of betacyanin and curcumin fitted the pseudo-second order model. In addition, the curcumin pigment displayed greater boundary layer effect than that of anthocyanin, and followed by betacyanin. Besides, the adsorption of BBPF and RDFP dyes onto BY fitted the Langmuir isotherm by comparing the high regression coefficient,  $R^2$  (0.989 and 0.979 respectively). Meanwhile, the adsorption of Turmeric dye onto BY fitted rather well with the Freundlich isotherm with high regression coefficient,  $R^2$ , at 0.975. As for anthocyanin adsorption onto BY, the mean value for free energy of adsorption calculated for the interaction was 5.00 kJ/mol, which accounted for physical adsorption. Thus, led of  $E_{DR}$  in the range of 1–8 kJ/mol indicated that the adsorption mechanism was controlled by van der Waals forces or hydrogen bonding and the nature of adsorption was proven by the pseudo-first order kinetic model. Meanwhile, as for betacyanin and curcumin, the  $E_{DR}$  values were 10.00 and 15.81 kJ/mol, which fall within the range of 8–16 kJ/mol. This indicates that the adsorption is chemical-based and the presences of ionic interaction between the positively-charged BY and the negatively-charged betacyanin and curcumin or covalent bonding. This possible nature of adsorption was also proven by the pseudo-second order kinetic model for adsorption of betacyanin and curcumin.

The last objective of this study is to characterize the structures and the properties of the samples, including the extracted natural dyes, BY, DBY, and MBY. The spectral

analysis of the samples had been analysed by using FTIR, which demonstrated that all the samples of extracted natural dyes contained colorant pigments of anthocyanin, betacyanin, and curcumin in BBPF, RDFP, and Turmeric dyes, respectively. The spectral analysis for untreated and treated BYs indicated that most of the bands had similar base signals, while the minor changes can be interpreted in the IR spectra. Moreover, the samples of dyed BY displayed great affinity towards BBPF, RDFP, and Turmeric dyes, as dyed BY shared similar peaks with the dye FTIR spectra. Other than that, the decrease in peak intensity for all samples of post-mordanted BY had been likely due to the natural dyes (BBPF, RDFP, and Turmeric) covering the BY, indicating the presence of a natural dye layer on the surface of the BY. Additionally, the SEM analysis illustrated the surface morphology of BY samples. As a conclusion, all the objectives outlined in this study have been successfully achieved.

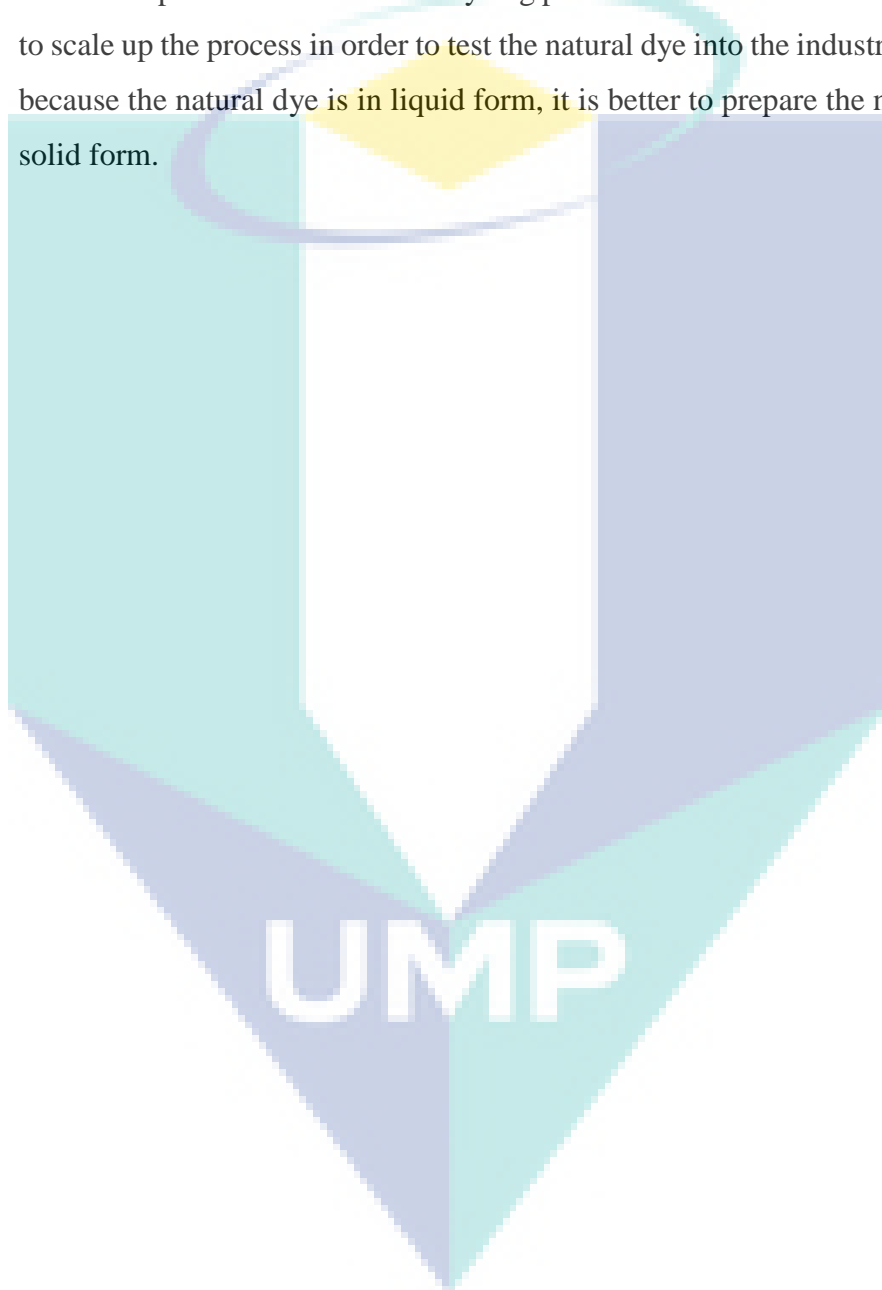
### **8.3 Recommendations for Future Work**

The current study investigated three sources of natural dyes (BBPF, RDFP, and Turmeric) and a natural fibre (BY), whereby the study included the extraction variables of natural dyes, as well as the impact of dyeing variables upon percentage of dye uptake and adsorption of colorant pigments onto BY. Through these experiments, the current study has successfully merits goal of expanding the knowledge pertaining to BBPF, RDFP, and Turmeric dyes, besides providing a foundational dyeing technique on BY. Thus, further studies from different fields are required to promote such research area and to improve the dyeing technique of BY. Hence, the proposed recommendations are listed in the following:

- i. Examination of performances exerted by BBPF, RDFP, and Turmeric dyes upon other cellulosic or protein fibres, like flax, ramie, cotton or silk.
- ii. Dyeing BY with other natural dye sources.
- iii. Inclusion of more chemical structure characterizations, such as X-ray diffraction and contact angle to expand the knowledge of dye adsorption on BY.
- iv. Dyeing carried out at varied pH levels to determine the effects of pH on colour strength, colour appearance, and colourfastness.



- v. An economic feasibility study could help determine if BBPF, RDFP, and Turmeric dyes would be viable for textile production.
- vi. Evaluation of uptake for other dyes onto BY by investigating the effect of mordant type on the dyeing properties.
- vii. Since the optimum conditions for dyeing process had been determined, it is worth to scale up the process in order to test the natural dye into the industrial scale; and because the natural dye is in liquid form, it is better to prepare the natural dye in solid form.



## REFERENCES

- Adeel, S. *et al.* (2017) 'Appraisal of marigold flower based lutein as natural colourant for textile dyeing under the influence of gamma radiations', *Radiation Physics and Chemistry*, 130, pp. 35–39.
- Ahamed, M. I. *et al.* (2016) 'Turmeric/polyvinyl alcohol Th(IV) phosphate electrospun fibers: Synthesis, characterization and antimicrobial studies', *Journal of the Taiwan Institute of Chemical Engineers*.
- Ahmad, A. *et al.* (2009) 'Extraction, Separation and Identification of Chemical Ingredients of *Elephantopus Scaber* L. Using Factorial Design of Experiment', *International Journal of Chemistry*, 1(1), p. p36.
- Ahmad, I. *et al.* (2012) 'Quality Parameters Analysis of Ring Spun Yarns Made From Different Blends of Bamboo and Cotton Fibres', VIII(I), pp. 1–12.
- Al-Alwani, M. A. M. *et al.* (2015) 'Effect of solvents on the extraction of natural pigments and adsorption onto TiO<sub>2</sub> for dye-sensitized solar cell applications', *Spectrochimica Acta Part A: Molecular and Biomolecular Spectroscopy*, 138, pp. 130–137.
- Ali, N. F. and El-Mohamedy, R. S. R. (2011) 'Eco-friendly and protective natural dye from red prickly pear (*Opuntia Lasiacantha Pfeiffer*) plant', *Journal of Saudi Chemical Society*. King Saud University, 15(3), pp. 257–261.
- Ali, S., Hussain, T. and Nawaz, R. (2009) 'Optimization of alkaline extraction of natural dye from Henna leaves and its dyeing on cotton by exhaust method', *Journal of Cleaner Production*, 17(1), pp. 61–66.
- Allen, S. J., McKay, G. and Porter, J. F. (2004) 'Adsorption isotherm models for basic dye adsorption by peat in single and binary component systems.', *Journal of colloid and interface science*, 280(2), pp. 322–33.
- Amalraj, A. *et al.* (2016) 'Biological activities of curcuminoids, other biomolecules from turmeric and their derivatives – A review', *Journal of Traditional and Complementary Medicine*.
- Anusuya, S. and Sathiyabama, M. (2016) 'Effect of chitosan on growth, yield and curcumin content in turmeric under field condition', *Biocatalysis and Agricultural Biotechnology*, 6, pp. 102–106.
- Arici, M. *et al.* (2016) 'Tulip petal as a novel natural food colorant source: Extraction optimization and stability studies', *Industrial Crops & Products*. Elsevier B.V., 91, pp. 215–222.

- B, D. L. R. and Ravi, D. (2013) 'Extraction of Natural Dyes From Selected Plant Sources and Its Application in Fabrics', *International Journal of Textile and Fashion Technology*, 3(2), pp. 53–60.
- Baliarsingh, S. *et al.* (2012) 'Exploring sustainable technique on natural dye extraction from native plants for textile: identification of colourants, colourimetric analysis of dyed yarns and their antimicrobial evaluation', *Journal of Cleaner Production*. Elsevier Ltd, 37, pp. 257–264.
- Benjwal, P., Sharma, R. and Kar, K. K. (2016) 'Effects of surface microstructure and chemical state of featherfiber-derived multidoped carbon fibers on the adsorption of organic water pollutants', *Materials & Design*, 110, pp. 762–774.
- Bhatti, I. A. *et al.* (2013) 'Dyeing of UV irradiated cotton and polyester fabrics with multifunctional Reactive and Disperse dyes', *Journal of Saudi Chemical Society*. King Saud University, 20(2), pp. 178–184.
- Bhuiyan, M. A. R. *et al.* (2017) 'Improving dyeability and antibacterial activity of *Lawsonia inermis* L on jute fabrics by chitosan pretreatment', *Textiles and Clothing Sustainability*. Textiles and Clothing Sustainability, 3(1), p. 1.
- Boonsong, P., Laohakunjit, N. and Kerdchoechuen, O. (2012) 'Natural pigments from six species of Thai plants extracted by water for hair dyeing product application', *Journal of Cleaner Production*, 37, pp. 93–106.
- El Boujaady, H. *et al.* (2013) 'Adsorption/desorption of Direct Yellow 28 on apatitic phosphate: Mechanism, kinetic and thermodynamic studies', *Journal of the Association of Arab Universities for Basic and Applied Sciences*. University of Bahrain.
- Bu, R. *et al.* (2016) 'Adsorption capability for anionic dyes on 2-hydroxyethylammonium acetate-intercalated layered double hydroxide', *Colloids and Surfaces A: Physicochemical and Engineering Aspects*, 511, pp. 312–319.
- Bukhari, M. N. *et al.* (2017) 'Dyeing studies and fastness properties of brown naphthoquinone colorant extracted from *Juglans regia* L on natural protein fiber using different metal salt mordants', *Textiles and Clothing Sustainability*. Textiles and Clothing Sustainability, 3(1), p. 3.
- Carvalho, C. and Santos, G. (2015) 'Global Communities, Biotechnology and Sustainable Design – Natural / Bio Dyes in Textiles', *Procedia Manufacturing*. Elsevier, 3, pp. 6557–6564.
- Celli, G. B. and Brooks, M. S.-L. (2016) 'Impact of extraction and processing conditions on betalains and comparison of properties with anthocyanins — A current review', *Food Research International*.

- Chan, L. S. et al. (2012) 'Error Analysis of Adsorption Isotherm Models for Acid Dyes onto Bamboo Derived Activated Carbon', *Chinese Journal of Chemical Engineering*, 20(3), pp. 535–542.
- Cosentino, H. M., Takinami, P. Y. I. and del Mastro, N. L. (2016) 'Comparison of the ionizing radiation effects on cochineal, annatto and turmeric natural dyes', *Radiation Physics and Chemistry*, 124, pp. 208–211.
- Czitrom, V. (1999) 'One-Factor-at-a-Time Versus Designed Experiments', *American Statistical Association*, 53(2), p. 6.
- Dada, A. . et al. (2012) 'Langmuir , Freundlich , Temkin and Dubinin – Radushkevich Isotherms Studies of Equilibrium Sorption of Zn 2 + Unto Phosphoric Acid Modified Rice Husk', *IOSR Journal of Applied Chemistry*, 3(1), pp. 38–45.
- Debnath, S. et al. (2016) 'Competitive adsorption of ternary dye mixture using pine cone powder modified with  $\beta$ -cyclodextrin', *Journal of Molecular Liquids*.
- Demiroz Gun, A., Unal, C. and Unal, B. T. (2008) 'Dimensional and physical properties of plain knitted fabrics made from 50/50 bamboo/cotton blended yarns', *Fibers and Polymers*, 9(5), pp. 588–592.
- Dranca, F. and Oroian, M. (2016) 'Optimization of ultrasound-assisted extraction of total monomeric anthocyanin (TMA) and total phenolic content (TPC) from eggplant (*Solanum melongena* L.) peel', *Ultrasonics Sonochemistry*, 31, pp. 637–646.
- Erdumlu, N. and Ozipek, B. (2008) 'Investigation of Regenerated Bamboo Fibre and Yarn Characteristics', 16(4), pp. 43–47.
- Fathordoobady, F. et al. (2016) 'Effect of solvent type and ratio on betacyanins and antioxidant activity of extracts from *Hylocereus polyrhizus* flesh and peel by supercritical fluid extraction and solvent extraction', *Food Chemistry*, 202, pp. 70–80.
- Gamal, A. M. et al. (2010) 'Kinetic Study and Equilibrium Isotherm Analysis of Reactive Dyes Adsorption onto Cotton Fiber', *Nature and Science*, 8(11), pp. 95–110.
- Gedik, G. et al. (2014) 'A novel eco-friendly colorant and dyeing method for poly(ethylene terephthalate) substrate', *Fibers and Polymers*, 15(2), pp. 261–272.
- Geelani, S. M. et al. (2017) 'Dyeing and fastness properties of *Quercus robur* with natural mordants on natural fibre', *Textiles and Clothing Sustainability*. Textiles and Clothing Sustainability, 2(1), p. 8.
- Gengatharan, A., Dykes, G. A. and Choo, W. S. (2015) 'Betalains: Natural plant pigments with

- potential application in functional foods', *LWT - Food Science and Technology*, 64(2), pp. 645–649.
- Grover, N. and Patni, V. (2011) 'Extraction and application of natural dye preparations from the floral parts of *Woodfordia fruticosa* ( Linn .) Kurz', 2(December), pp. 403–408.
- Guesmi, A. *et al.* (2012) 'Dyeing properties and colour fastness of wool dyed with indicaxanthin natural dye', *Industrial Crops and Products*, 37(1), pp. 493–499.
- Guesmi, a. *et al.* (2012) 'Dyeing properties and colour fastness of wool dyed with indicaxanthin natural dye', *Industrial Crops and Products*. Elsevier B.V., 37(1), pp. 493–499.
- Haddar, W., Ben Ticha, M., *et al.* (2014) 'A novel approach for a natural dyeing process of cotton fabric with *Hibiscus mutabilis* (Gulzuba): process development and optimization using statistical analysis', *Journal of Cleaner Production*, 68, pp. 114–120.
- Haddar, W., Baaka, N., *et al.* (2014) 'Optimization of an ecofriendly dyeing process using the wastewater of the olive oil industry as natural dyes for acrylic fibres', *Journal of Cleaner Production*. Elsevier Ltd, 66, pp. 546–554.
- Haddar, W., Elksibi, I., *et al.* (2014) 'Valorization of the leaves of fennel (*Foeniculum vulgare*) as natural dyes fixed on modified cotton: A dyeing process optimization based on a response surface methodology', *Industrial Crops and Products*. Elsevier B.V., 52, pp. 588–596.
- Han, H. *et al.* (2016) 'Removal of cationic dyes from aqueous solution by adsorption onto hydrophobic/hydrophilic silica aerogel', *Colloids and Surfaces A: Physicochemical and Engineering Aspects*, 509, pp. 539–549.
- Hmar, B. Z., Kalita, D. and Srivastava, B. (2016) 'Optimization of microwave power and curing time of turmeric rhizome (*Curcuma Longa* L.) based on textural degradation', *LWT - Food Science and Technology*.
- Ho, Y. S., Chiu, W. T. and Wang, C. C. (2005) 'Regression analysis for the sorption isotherms of basic dyes on sugarcane dust', *Bioresource Technology*, 96(11), pp. 1285–1291.
- Jabasingh, S. A., Sahu, P. and Yimam, A. (2016) 'Enviro-friendly biofinishing of cotton fibers using *Aspergillus nidulans* AJSU04 cellulases for enhanced uptake of Myrobalan dye from *Terminalia chebula*', *Dyes and Pigments*. Elsevier Ltd, 129, pp. 129–140.
- John Sushma, N. *et al.* (2015) 'Facile approach to synthesize magnesium oxide nanoparticles by using *Clitoria ternatea*—characterization and in vitro antioxidant studies', *Applied Nanoscience*. Springer Berlin Heidelberg, 6(3), pp. 437–444.

- Kanchana, R. et al. (2013) 'Dyeing of textiles with natural dyes - An eco-friendly approach', *International Journal of ChemTech Research*, 5(5), pp. 2102–2109.
- Kazuma, K., Noda, N. and Suzuki, M. (2003) 'Flavonoid composition related to petal color in different lines of *Clitoria ternatea*', *Phytochemistry*, 64(6), pp. 1133–1139.
- Khan, A. A. et al. (2014) 'Extraction of natural dye from red calico leaves: Gamma ray assisted improvements in colour strength and fastness properties', *Dyes and Pigments*, 103, pp. 50–54.
- Kogawa, K. et al. (2007) 'Biosynthesis of malonylated flavonoid glycosides on the basis of malonyltransferase activity in the petals of *Clitoria ternatea*', *Journal of Plant Physiology*, 164(7), pp. 886–894.
- Kousha, M. et al. (2015) 'Central composite design optimization of Acid Blue 25 dye biosorption using shrimp shell biomass', *Journal of Molecular Liquids*. Elsevier B.V., 207, pp. 266–273.
- Koyuncu, M. (2014) 'Thermodynamic parameters and dyeing kinetics of wool yarn with aqueous extract of *Rubia tinctorum* L', *IIOAB Journal*, 5(2), pp. 12–15.
- Krishnakumar, I. et al. (2015) 'Enhanced absorption and pharmacokinetics of fresh turmeric (*Curcuma Longa* L) derived curcuminoids in comparison with the standard curcumin from dried rhizomes', *Journal of Functional Foods*, 17, pp. 55–65.
- Kulkarni S. S., Bodake U. M., P. G. R. (2011) 'Extraction of Natural Dye from Chili (*Capsicum Annum*) for Textile Coloration', 1, pp. 58–63.
- Kumar, N. et al. (2016) 'Light-weight high-strength hollow glass microspheres and bamboo fiber based hybrid polypropylene composite: A strength analysis and morphological study', *Composites Part B: Engineering*.
- Larik, S. A. et al. (2015) 'Batchwise dyeing of bamboo cellulose fabric with reactive dye using ultrasonic energy', *Ultrasonics Sonochemistry*, 24, pp. 178–183.
- Lee, P. M. and Abdullah, R. (2011) 'Thermal Degradation of Blue Anthocyanin Extract of *Clitoria ternatea* Flower', 7, pp. 49–53.
- Lim, H. K. et al. (2010) 'Chemical composition and DSC thermal properties of two species of *Hylocereus cacti* seed oil: *Hylocereus undatus* and *Hylocereus polyrhizus*', *Food Chemistry*, 119(4), pp. 1326–1331.

- Lin, J. H. et al. (2010) 'Manufacture technique and electrical properties evaluation of bamboo charcoal polyester/stainless steel complex yarn and knitted fabrics', *Fibers and Polymers*, 11(6), pp. 856–860.
- Liu, X.-M., He, D.-Q. and Fang, K.-J. (2015) *Adsorption of cationic copolymer nanoparticles onto bamboo fiber surfaces measured by conductometric titration*, *Chinese Chemical Letters*.
- Lokhande, H. and Dorugade, V. (1999) 'Dyeing nylon with natural dyes', *American dyestuff reporter*, (Fevereiro), pp. 29–34.
- Majumdar, A. and Pol, S. B. (2014) 'Low stress mechanical properties of fabrics woven from bamboo viscose blended yarns', *Fibers and Polymers*, 15(9), pp. 1985–1991.
- Makasana, J. et al. (2016) 'Extractive determination of bioactive flavonoids from butterfly pea (*Clitoria ternatea* Linn.)', *Research on Chemical Intermediates*. Springer Netherlands.
- Malensek, N. (2014) *Colorfastness Properties of Persimmon Dye on Cotton and Wool Substrates*. Colorado State University.
- Maniglia, B. C. et al. (2014) 'Development of bioactive edible film from turmeric dye solvent extraction residue', *LWT - Food Science and Technology*, 56(2), pp. 269–277.
- Maran, J. P., Priya, B. and Nivetha, C. V. (2015) 'Optimization of ultrasound-assisted extraction of natural pigments from *Bougainvillea glabra* flowers', *Industrial Crops and Products*. Elsevier B.V., 63, pp. 182–189.
- Martins, R. M. et al. (2013) 'Curcuminoid content and antioxidant activity in spray dried microparticles containing turmeric extract', *Food Research International*, 50(2), pp. 657–663.
- Meksi, N. et al. (2012) 'Olive mill wastewater: A potential source of natural dyes for textile dyeing', *Industrial Crops and Products*, 40, pp. 103–109.
- Mirjalili, M., Nazarpour, K. and Karimi, L. (2011) 'Eco-friendly dyeing of wool using natural dye from weld as co-partner with synthetic dye', *Journal of Cleaner Production*, 19(9), pp. 1045–1051.
- Monton, C. et al. (2016) 'Quantitation of curcuminoid contents, dissolution profile, and volatile oil content of turmeric capsules produced at some secondary government hospitals', *Journal of Food and Drug Analysis*, 24(3), pp. 493–499.

- Morris, J. B. (2009) 'Characterization of butterfly pea (*Clitoria ternatea* L.) accessions for morphology, phenology, reproduction and potential nutraceutical, pharmaceutical trait utilization', *Genetic Resources and Crop Evolution*, 56(3), pp. 421–427.
- Mu, B. et al. (2016) 'Preparation, characterization and application on dye adsorption of a well-defined two-dimensional superparamagnetic clay/polyaniline/Fe<sub>3</sub>O<sub>4</sub> nanocomposite', *Applied Clay Science*, 132, pp. 7–16.
- Mukherjee, P. K. et al. (2008) 'The Ayurvedic medicine *Clitoria ternatea*—From traditional use to scientific assessment', *Journal of Ethnopharmacology*, 120(3), pp. 291–301.
- Nasirizadeh, N. et al. (2012) 'Optimization of wool dyeing with rutin as natural dye by central composite design method', *Industrial Crops and Products*, 40, pp. 361–366.
- Nayak, L. and Mishra, S. P. (2016) 'Prospect of bamboo as a renewable textile fiber, historical overview, labeling, controversies and regulation', *Fashion and Textiles*. Springer Berlin Heidelberg, 3(1), p. 2.
- Nguyen, T. T. H. et al. (2017) 'Facile preparation of water soluble curcuminoids extracted from turmeric (*Curcuma longa* L.) powder by using steviol glucosides', *Food Chemistry*, 214, pp. 366–373.
- Obenland, D. et al. (2016) 'Impact of storage conditions and variety on quality attributes and aroma volatiles of pitahaya (*Hylocereus spp.*)', *Scientia Horticulturae*, 199, pp. 15–22.
- Osorio-Tobón, J. F. et al. (2014) 'Extraction of curcuminoids from deflavored turmeric (*Curcuma longa* L.) using pressurized liquids: Process integration and economic evaluation', *The Journal of Supercritical Fluids*, 95, pp. 167–174.
- Osorio-Tobón, J. F., Carvalho, P. I. N., Barbero, G. F., et al. (2016) 'Fast analysis of curcuminoids from turmeric (*Curcuma longa* L.) by high-performance liquid chromatography using a fused-core column', *Food Chemistry*, 200, pp. 167–174.
- Osorio-Tobón, J. F., Carvalho, P. I. N., Rostagno, M. A., et al. (2016) 'Process integration for turmeric products extraction using supercritical fluids and pressurized liquids: Economic evaluation', *Food and Bioprocess Processing*, 98, pp. 227–235.
- Pan, Y.-Z. et al. (2014) 'Flavonoid C-glycosides from pigeon pea leaves as color and anthocyanin stabilizing agent in blueberry juice', *Industrial Crops and Products*, 58, pp. 142–147.
- Pasukamonset, P., Kwon, O. and Adisakwattana, S. (2016) 'Alginate-based encapsulation of polyphenols from *Clitoria ternatea* petal flower extract enhances stability and biological activity under simulated gastrointestinal conditions', *Food Hydrocolloids*, 61, pp. 772–779.



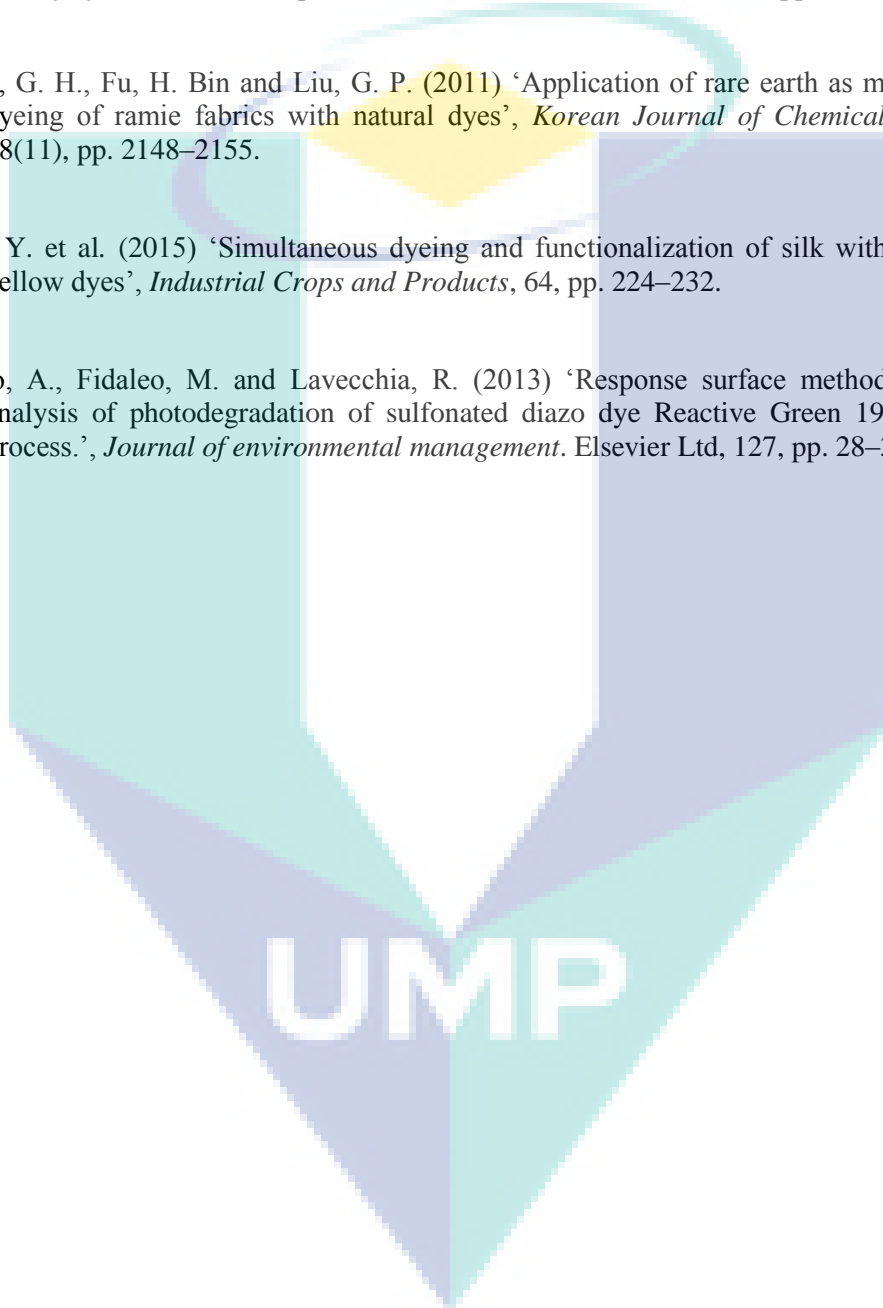
- Pathiraja, I. K. (2014) *Removal of Acid Yellow 25 Dye onto Chitin Extracted from Waste Crab legs and Study of Adsorption Isotherms and Kinetics of AY25 Dye Adsorption*. Southern Illinois University Edwardsville.
- Patil, S. B. et al. (2009) 'Use of flower extract of *Clitoria ternata* L. as a compound indicator', 2(2), pp. 241–242.
- Peng, L. et al. (2016) 'Microwave-assisted deposition of silver nanoparticles on bamboo pulp fabric through dopamine functionalization', *Applied Surface Science*, 386, pp. 151–159.
- Phruksanan, W., Yibchok-anun, S. and Adisakwattana, S. (2014) 'Protection of *Clitoria ternatea* flower petal extract against free radical-induced hemolysis and oxidative damage in canine erythrocytes', *Research in Veterinary Science*, 97(2), pp. 357–363.
- Pinho, E. et al. (2010) 'Development of biofunctional textiles by the application of resveratrol to cotton, bamboo, and silk', *Fibers and Polymers*, 11(2), pp. 271–276.
- Prima, E. C. et al. (2017) 'A combined spectroscopic and TDDFT study of natural dyes extracted from fruit peels of *Citrus reticulata* and *Musa acuminata* for dye-sensitized solar cells', *Spectrochimica Acta Part A: Molecular and Biomolecular Spectroscopy*, 171, pp. 112–125.
- Punrattanasin, N. et al. (2013) 'Silk fabric dyeing with natural dye from mangrove bark (*Rhizophora apiculata* Blume) extract', *Industrial Crops and Products*. Elsevier B.V., 49, pp. 122–129.
- Qu, X. and Wu, C. F. J. (2005) 'One-factor-at-a-time designs of resolution V', *Journal of Statistical Planning and Inference*, 131(2), pp. 407–416.
- Radhakrishnan, S. (2014) *Roadmap to Sustainable Textiles and Clothing*. doi: 10.1007/978-981-287-065-0.
- Raghu, K. S. et al. (2016) 'Age dependent neuroprotective effects of medhya rasayana prepared from *Clitoria ternatea* Linn. in stress induced rat brain', *Journal of Ethnopharmacology*.
- Rahman, N. A. A., Tumin, S. M. and Tajuddin, R. (2013) 'Optimization of Ultrasonic Extraction Method of Natural Dyes from *Xylocarpus Moluccensis*', *International Journal of Bioscience, Biochemistry and Bioinformatics*, 3(1), pp. 53–55.
- Rather, L. J., Shahid-ul-Islam, Khan, M. A., et al. (2016) 'Adsorption and Kinetic studies of *Adhatoda vasica* natural dye onto woolen yarn with evaluations of Colorimetric and Fluorescence Characteristics', *Journal of Environmental Chemical Engineering*, 4(2), pp. 1780–1796.

- Rather, L. J., Shahid-ul-Islam, Shabbir, M., et al. (2016) 'Ecological dyeing of Woolen yarn with *Adhatoda vasica* natural dye in the presence of biomordants as an alternative copartner to metal mordants', *Journal of Environmental Chemical Engineering*, 4(3), pp. 3041–3049.
- Ratnapandian, S., Fergusson, S. M. and Wang, L. (2012) 'Application of Acacia natural dyes on cotton by pad dyeing', *Fibers and Polymers*, 13(2), pp. 206–211.
- Ren, Y. et al. (2016) 'Effect of dye bath pH on dyeing and functional properties of wool fabric dyed with tea extract', *Dyes and Pigments*, 134, pp. 334–341.
- Sachan, K. and Kapoor, V. (2007) 'Optimization of extraction and dyeing conditions for traditional turmeric dye', *Indian Journal of Traditional Knowledge*, 6(April), pp. 270–278. Available at: <http://nopr.niscair.res.in/handle/123456789/918>.
- Samanta, A. K. and Agarwal, P. (2009) 'Application of natural dyes on textiles', *Indian Journal of Fibre & textile Research*, 34(December), pp. 384–399.
- Sathiyabama, M., Bernstein, N. and Anusuya, S. (2016) 'Chitosan elicitation for increased curcumin production and stimulation of defence response in turmeric (*Curcuma longa* L.)', *Industrial Crops and Products*, 89, pp. 87–94.
- Sengupta, S. (2003) 'Natural , “ Green ” Dyes for the Textile', (57).
- Shabbir, M. et al. (2016) 'An eco-friendly dyeing of woolen yarn by *Terminalia chebula* extract with evaluations of kinetic and adsorption characteristics', *Journal of Advanced Research*, 7(3), pp. 473–482.
- Shahid, M. et al. (2017) 'Colourful and antioxidant silk with chlorogenic acid: Process development and optimization by central composite design', *Dyes and Pigments*. Elsevier Ltd, 138, pp. 30–38.
- Shen, J., Gao, P. and Ma, H. (2014) 'The effect of tris(2-carboxyethyl)phosphine on the dyeing of wool fabrics with natural dyes', *Dyes and Pigments*, 108, pp. 70–75.
- Sinha, K., Saha, P. Das and Datta, S. (2012) 'Response surface optimization and artificial neural network modeling of microwave assisted natural dye extraction from pomegranate rind', *Industrial Crops and Products*. Elsevier B.V., 37(1), pp. 408–414.
- Sivakumar, V. et al. (2009) 'Ultrasound assisted enhancement in natural dye extraction from beetroot for industrial applications and natural dyeing of leather', *Ultrasonics Sonochemistry*, 16(6), pp. 782–789.
- Sribenja, S. and Saikrasun, S. (2015) 'Adsorption behavior and kinetics of lac dyeing on poly(ethyleneimine)-treated bamboo fibers', *Fibers and Polymers*, 16(11), pp. 2391–2400.

- Stintzing, F. C., Schieber, A. and Carle, R. (2002) 'Betacyanins in fruits from red-purple pitaya, *Hylocereus polyrhizus* (Weber) Britton & Rose', *Food Chemistry*, 77(1), pp. 101–106..
- Suebkhampet, A. and Sotthibandhu, P. (2012) 'Effect of Using Aqueous Crude Extract From Butterfly Pea Flowers ( *Clitoria Ternatea* L. ) As', 19(1), pp. 15–19.
- Taira, J. et al. (2015) 'Antioxidant capacity of betacyanins as radical scavengers for peroxy radical and nitric oxide', *Food Chemistry*, 166, pp. 531–536.
- Tamil Selvi, a. et al. (2013) 'Studies on the application of natural dye extract from *Bixa orellana* seeds for dyeing and finishing of leather', *Industrial Crops and Products*. Elsevier B.V., 43, pp. 84–86.
- Tao, J. et al. (2014) 'Characterization of genetic relationship of dragon fruit accessions (*Hylocereus spp.*) by morphological traits and ISSR markers', *Scientia Horticulturae*, 170, pp. 82–88.
- Taur, D. J. and Patil, R. Y. (2011) *Evaluation of antiasthmatic activity of Clitoria ternatea L. roots*, *Journal of Ethnopharmacology*.
- Tausif, M. et al. (2015) 'A comparative study of mechanical and comfort properties of bamboo viscose as an eco-friendly alternative to conventional cotton fibre in polyester blended knitted fabrics', *Journal of Cleaner Production*, 89, pp. 110–115.
- Tayade, P. B. and Adivarekar, R. V. (2013) 'Adsorption kinetics and thermodynamic study of *Cuminum cyminum* L. dyeing on silk', *Journal of Environmental Chemical Engineering*, 1(4), pp. 1336–1340.
- Tayebi, H. et al. (2015) 'The Isotherms, Kinetics, and Thermodynamics of Acid Dye on Nylon6 with Different Amounts of Titania and Fiber Cross Sectional Shape', *Journal of Engineered Fibers and Fabrics*, Volume 10(Issue 1), pp. 97–109.
- Tech, I. E. (2012) 'Institutional Engineering and Technology ( IET ) Green Global Foundation ©', 3972.
- Teknologi, J. et al. (2012) 'Ekstraksi Dan Analisis Zat Warna Biru ( Anthosianin ) Dari Bunga Telang ( *Clitoria Ternatea* ) Sebagai Pewarna Alami', 1(1), Pp. 356–365.
- Uddin, M. G. (2015) 'Extraction of eco-friendly natural dyes from mango leaves and their application on silk fabric', *Textiles and Clothing Sustainability*. Textiles and Clothing Sustainability, 1(1), p. 7.

- Valizadeh Kiamahalleh, M. et al. (2016) 'High performance curcumin subcritical water extraction from turmeric (*Curcuma longa* L.)', *Journal of Chromatography B*, 1022, pp. 191–198.
- Vasisht, K. et al. (2016) *Norneolignans from the roots of Clitoria ternatea L.*, *Tetrahedron Letters*.
- Velmurugan, P. et al. (2010) 'Natural pigment extraction from five filamentous fungi for industrial applications and dyeing of leather', *Carbohydrate Polymers*, 79(2), pp. 262–268. doi: 10.1016/j.carbpol.2009.07.058.
- Verma, P. R., Itankar, P. R. and Arora, S. K. (2013) 'Evaluation of antidiabetic antihyperlipidemic and pancreatic regeneration, potential of aerial parts of *Clitoria ternatea*', *Revista Brasileira de Farmacognosia*. Elsevier, 23(5), pp. 819–829.
- Visalakshi, M. and Jawaharlal, M. (2013) 'Research and Reviews : Journal of Agriculture and Allied Sciences Healthy Hues – Status and Implication in Industries – Brief Review .', 2(3), pp. 42–51.
- Voon, H. C., Bhat, R. and Rusul, G. (2012) 'Flower extracts and their essential oils as potential antimicrobial agents for food uses and pharmaceutical applications', *Comprehensive Reviews in Food Science and Food Safety*, 11(1), pp. 34–55.
- Wang, F. et al. (2015) 'The effect of elementary fibre variability on bamboo fibre strength', *Materials & Design*, 75, pp. 136–142.
- Wang, H., Li, P. and Zhou, W. (2014) 'Dyeing of Silk with Anthocyanins Dyes Extract from *Liriope platyphylla* Fruits', *Journal of Textiles*, 2014, pp. 1–9.
- Wongcharee, K., Meeyoo, V. and Chavadej, S. (2007) 'Dye-sensitized solar cell using natural dyes extracted from rosella and blue pea flowers', *Solar Energy Materials and Solar Cells*, 91(7), pp. 566–571.
- Wybraniec, S. et al. (2001) 'Betacyanins from vine cactus *Hylocereus polyrhizus*', *Phytochemistry*, 58(8), pp. 1209–1212.
- Yue, G. G.-L. et al. (2016) 'Combined therapy using bevacizumab and turmeric ethanolic extract (with absorbable curcumin) exhibited beneficial efficacy in colon cancer mice', *Pharmacological Research*, 111, pp. 43–57.
- Zhang, B. et al. (2014) 'Natural dye extracted from Chinese gall – the application of color and antibacterial activity to wool fabric', *Journal of Cleaner Production*, 80, pp. 204–210.

- Zhang, F. et al. (2016) 'High adsorption capability and selectivity of ZnO nanoparticles for dye removal', *Colloids and Surfaces A: Physicochemical and Engineering Aspects*, 509, pp. 474–483.
- Zhang, Y. et al. (2016) 'Adsorption behavior of modified Iron stick yam skin with Polyethyleneimine as a potential biosorbent for the removal of anionic dyes in single and ternary systems at low temperature', *Bioresource Technology*, 222, pp. 285–293.
- Zheng, G. H., Fu, H. Bin and Liu, G. P. (2011) 'Application of rare earth as mordant for the dyeing of ramie fabrics with natural dyes', *Korean Journal of Chemical Engineering*, 28(11), pp. 2148–2155.
- Zhou, Y. et al. (2015) 'Simultaneous dyeing and functionalization of silk with three natural yellow dyes', *Industrial Crops and Products*, 64, pp. 224–232.
- Zuorro, A., Fidaleo, M. and Lavecchia, R. (2013) 'Response surface methodology (RSM) analysis of photodegradation of sulfonated diazo dye Reactive Green 19 by UV/H<sub>2</sub>O<sub>2</sub> process.', *Journal of environmental management*. Elsevier Ltd, 127, pp. 28–35.



**APPENDIX A**  
**LIST OF CHEMICALS AND REAGENTS**

---

**LIST OF CHEMICALS AND REAGENTS**

---

Betacyanin standard

Curcumin Standard

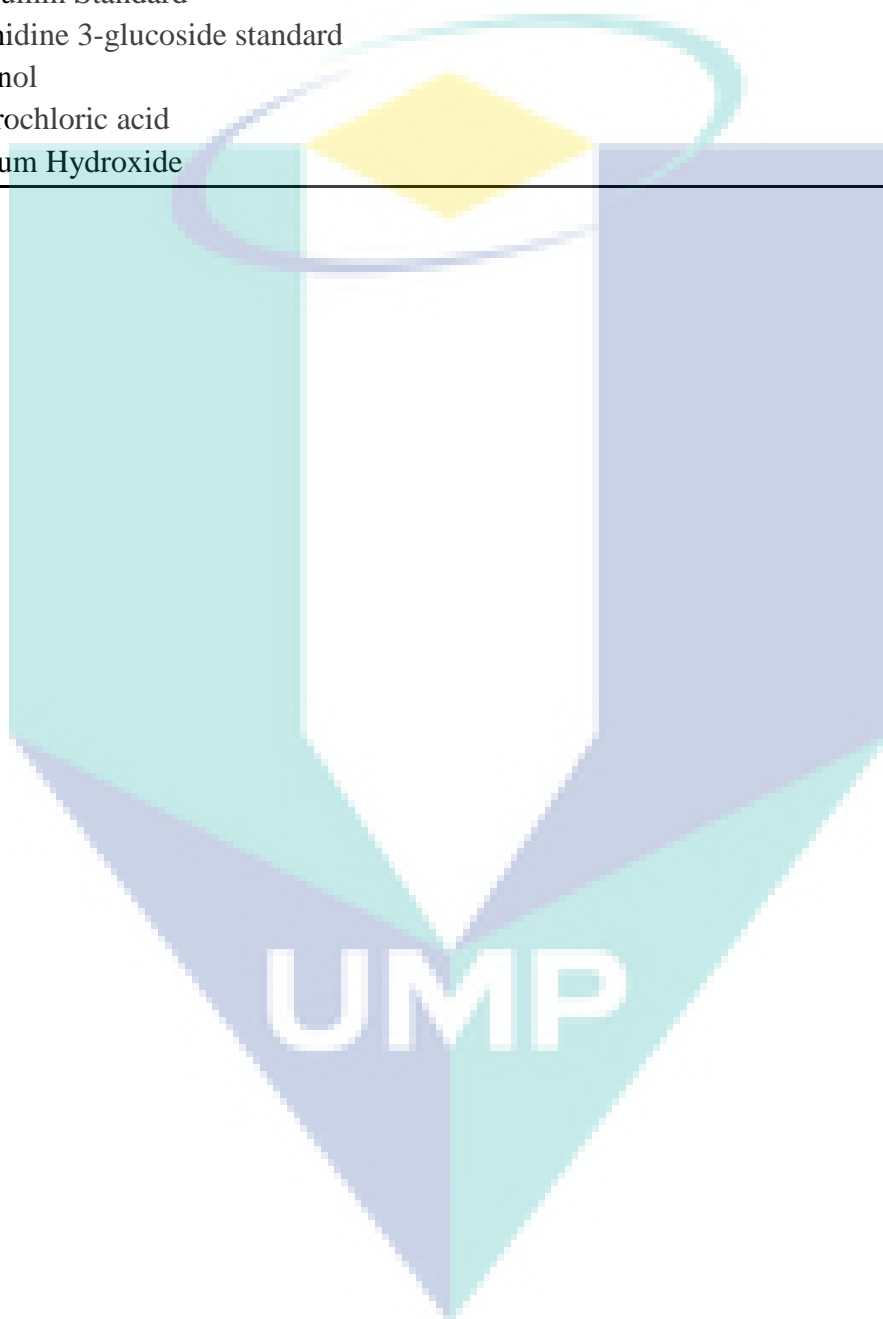
Cyanidine 3-glucoside standard

Ethanol

Hydrochloric acid

Sodium Hydroxide

---

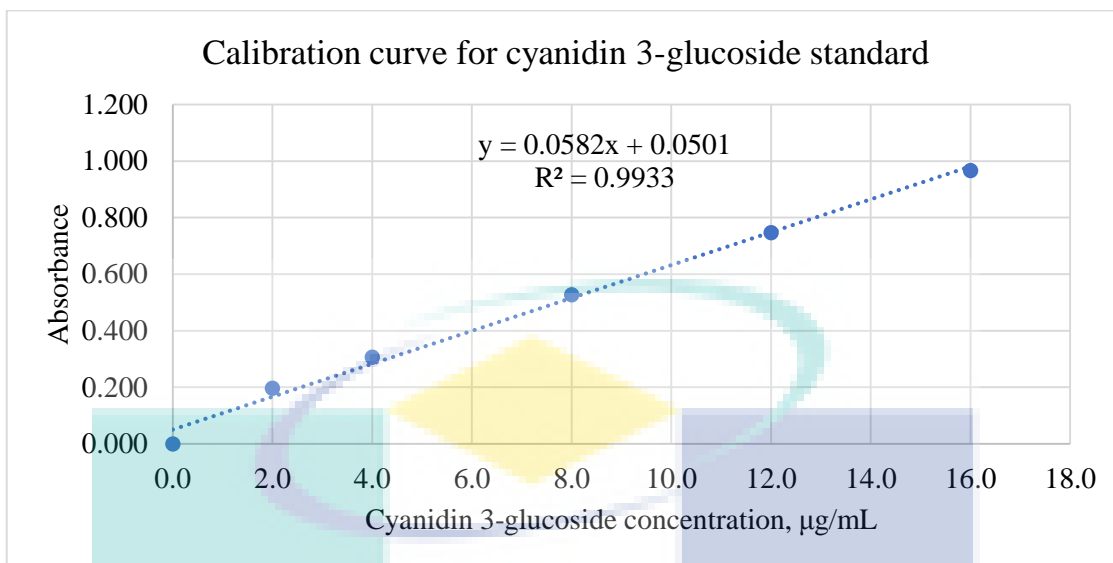


## APPENDIX B CALIBRATION CURVE FOR STANDARD

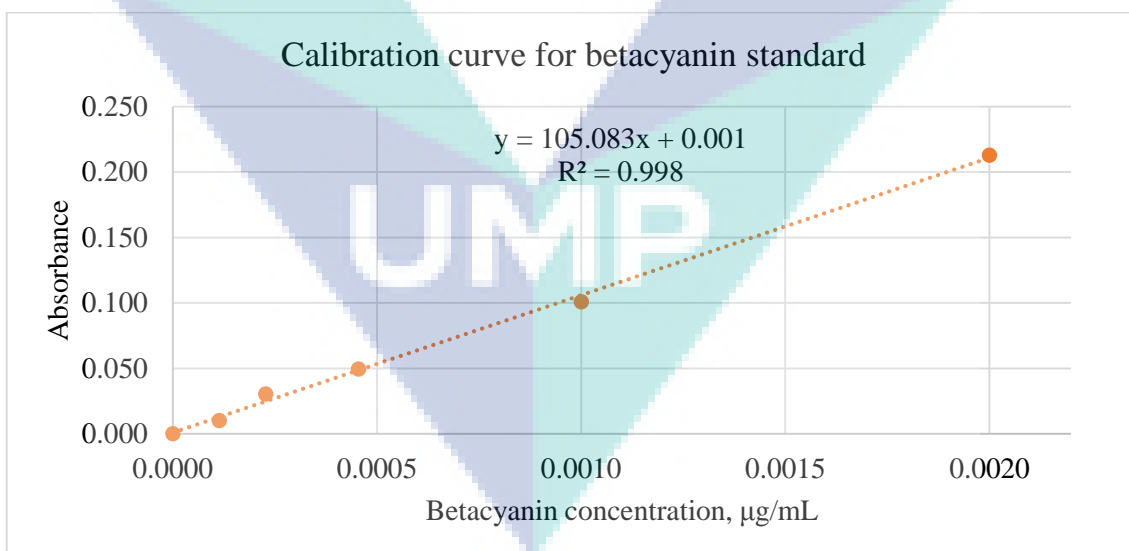
### Construction of calibration curve for standard

Stock solutions for anthocyanin, betacyanin, and curcumin were prepared by dissolving each component in distilled water for both anthocyanin and betacyanin, whereas ethanol for curcumin. Besides, a series of standard solutions had been prepared by sequential dilution with distilled water for both anthocyanin and betacyanin and ethanol for curcumin (the concentrations of anthocyanin, betacyanin, and curcumin being 0, 2, 4, 8, 12, and 16  $\mu\text{g/mL}$ ; 0, 0.0001, 0.0002, 0.0005, 0.0010 and 0.0020; 0, 1.0, 1.5, 2.0, 2.5, 3.0, and 3.5  $\mu\text{g/mL}$ , respectively). Other than that, the absorbance measurements by UV-Vis spectrophotometer for anthocyanin, betacyanin, and curcumin were measured at wavelengths 525, 538, and 419 nm, respectively. The reagent blank used was distilled water for both anthocyanin and betacyanin, whereas ethanol for curcumin. All the measurements were done by triplicate and a standard curve was constructed by plotting the Absorbance against the concentration of the standard. Furthermore, the anthocyanin, betacyanin, and curcumin contents were determined from this standard curve.

Cyanidine 3-glucoside concentration $\mu\text{g ml}^{-1}$	Absorbance
0	0
2	0.197
4	0.307
8	0.527
12	0.747
16	0.967

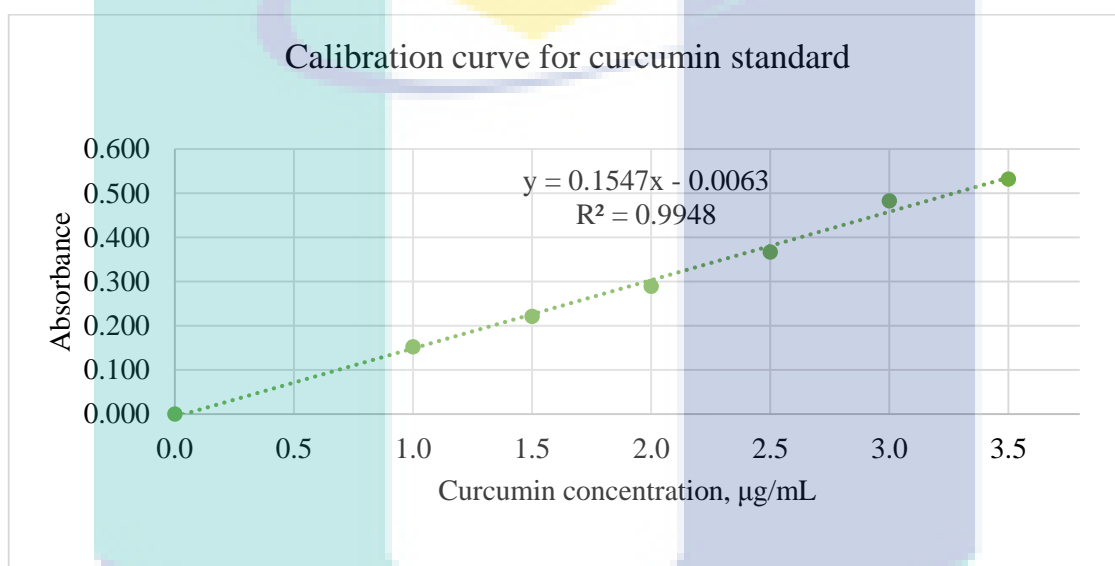


Betacyanin concentration µg ml <sup>-1</sup>	Absorbance
0	0
0.0001	0.0102
0.0002	0.0304
0.0005	0.0494
0.0010	0.1008
0.0020	0.2128



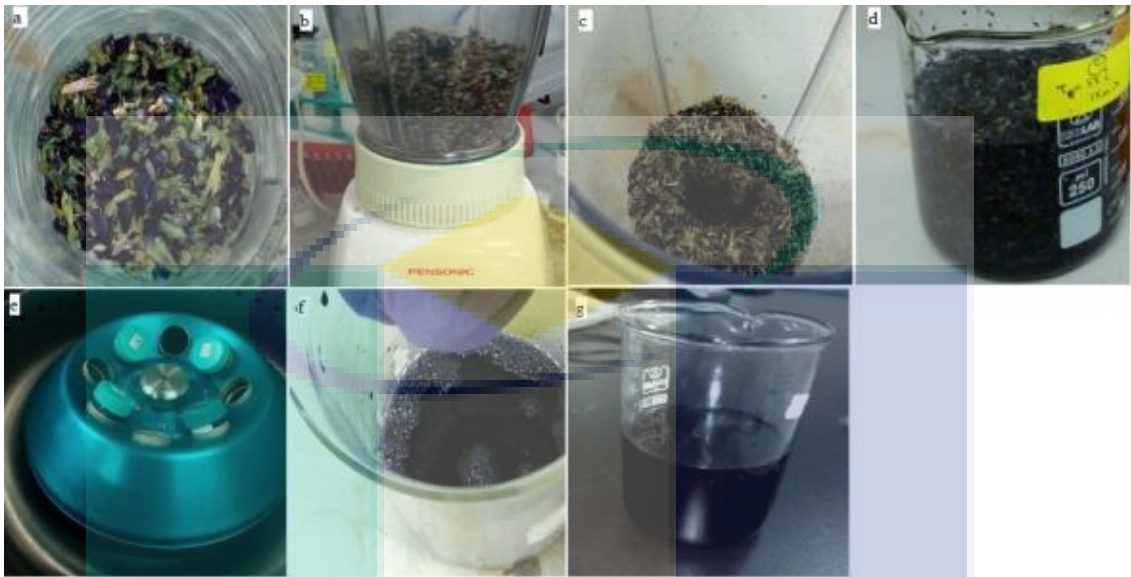


Curcumin concentration $\mu\text{g ml}^{-1}$	Absorbance
0	0
1	0.152
1.5	0.221
2	0.289
2.5	0.367
3	0.483
3.5	0.532

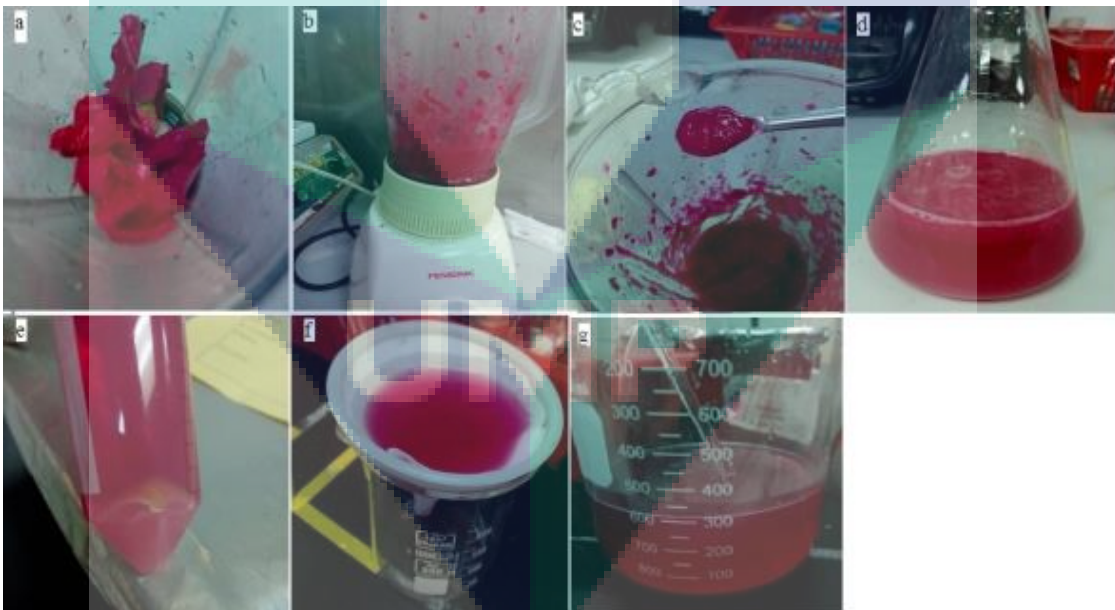


UMP

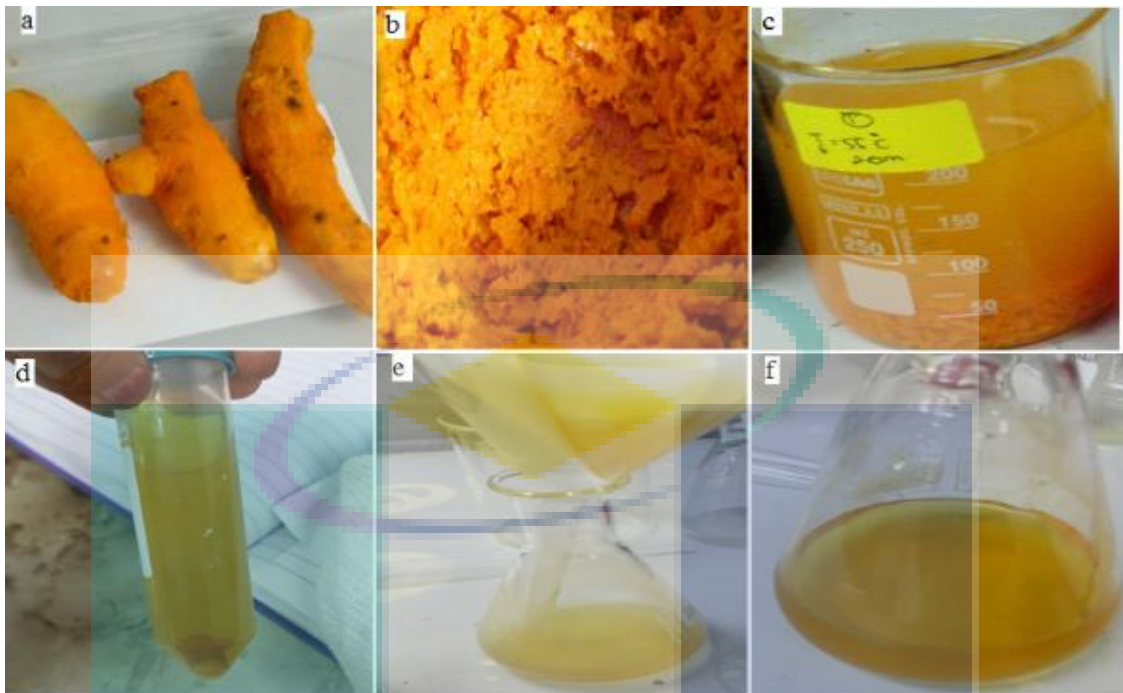
## APPENDIX C EXPERIMENTAL SET UP



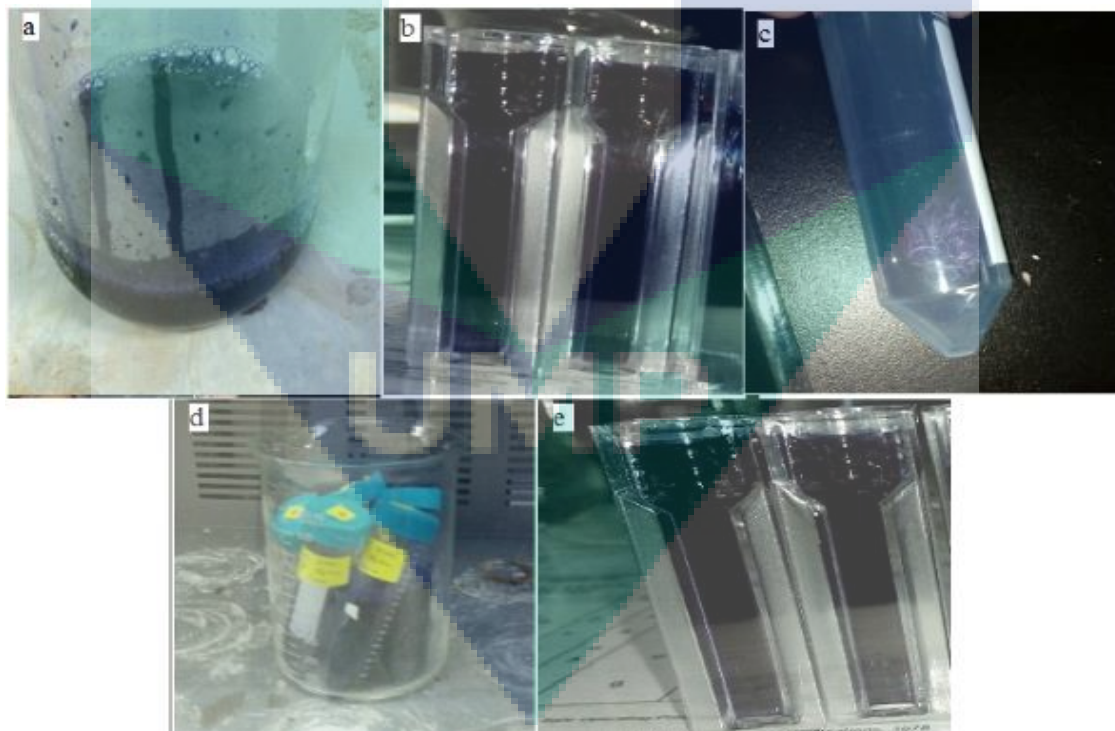
Appendix C 1: (a) The BBPF after being dried in the oven, (b) The BBPF being blended into small pieces, (c) The small pieces of BBPF, (d) The small pieces of BBPF with water being prepared to be centrifuged, (e) BBPF extract in centrifugal, (f) BBPF extracts being filtered, and (g) Blue natural dye from BBPF



Appendix C2: (a) The peel of Dragon fruit, (b) The Dragon fruit peel being blended into small pieces, (c) The Dragon fruit peel after blended, (d) The mixture of Dragon fruit peel with water being prepared to be centrifuged, (e) Dragon fruit peel extract after centrifugation process, (f) Dragon fruit peel extract being filtered, and (g) Red natural dye from dragon fruit peel

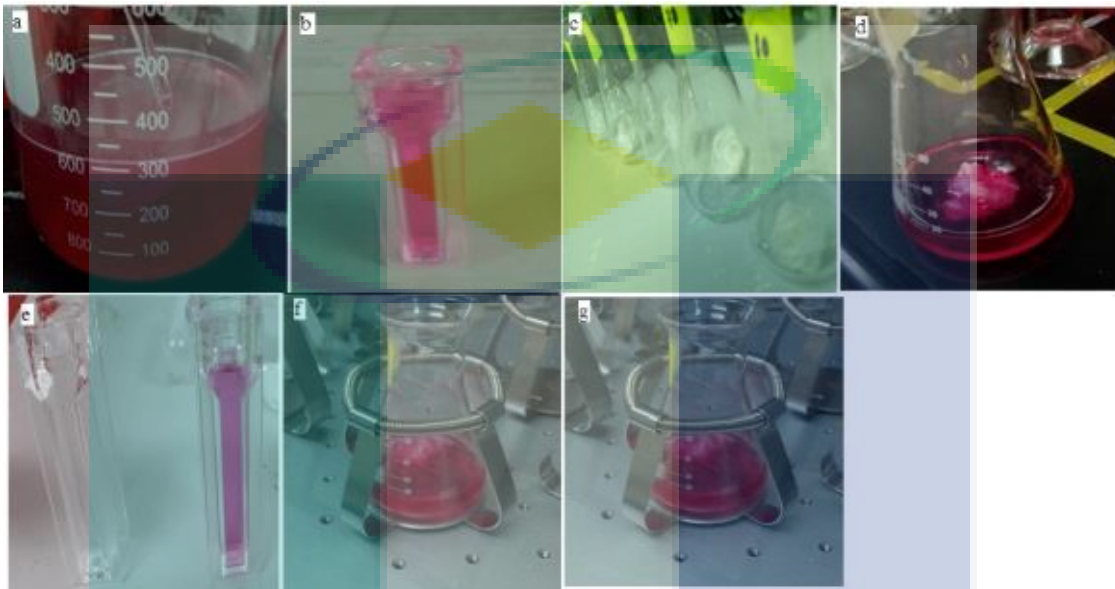


Appendix C 3: (a) The turmeric after the peels were removed, (b) The mixture of turmeric, (c) The mixture of turmeric with water being prepared to be centrifuged, (d) Turmeric extract after centrifugation process, (e) Turmeric extract being filtered, and (f) Yellow natural dye from turmeric.

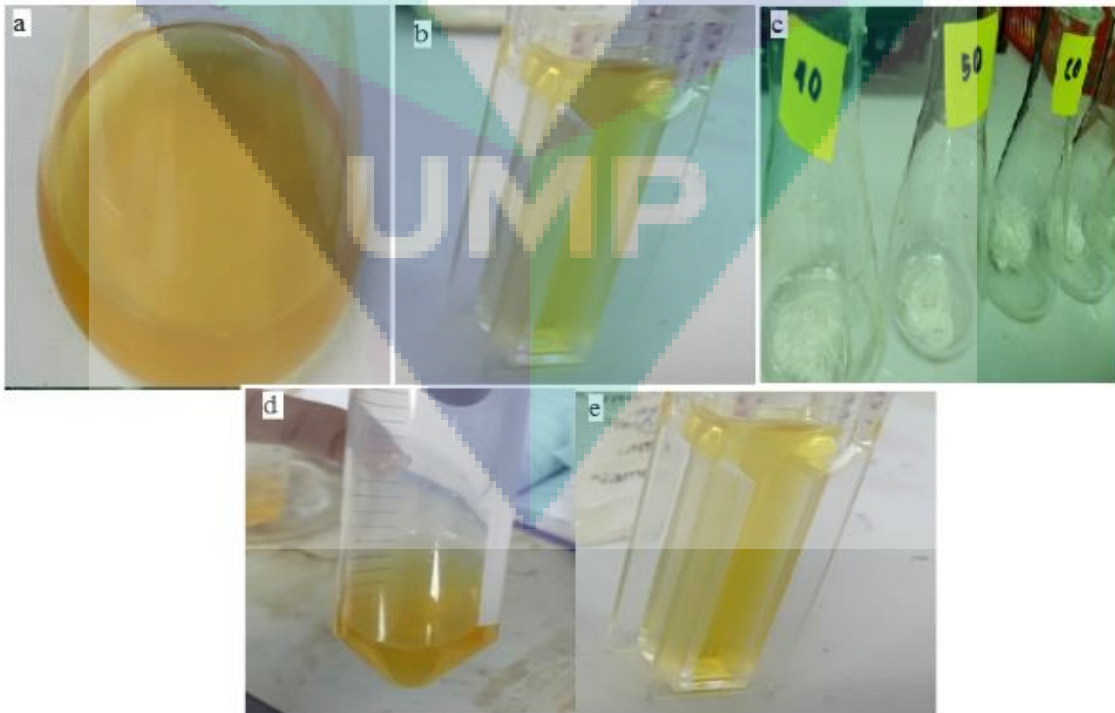


Appendix C 4: (a) Blue Natural Dye from BBPF at Optimum Extraction Conditions, (b) Blue Natural Dye in Cuvette for measuring absorbance before dyeing, (c) BY in Blue Natural Dye Solution, (d) BY in Blue Natural Dye Solution was agitated in

incubator shaker, and (e) Blue Natural Dye in Cuvette for measuring absorbance after dyeing

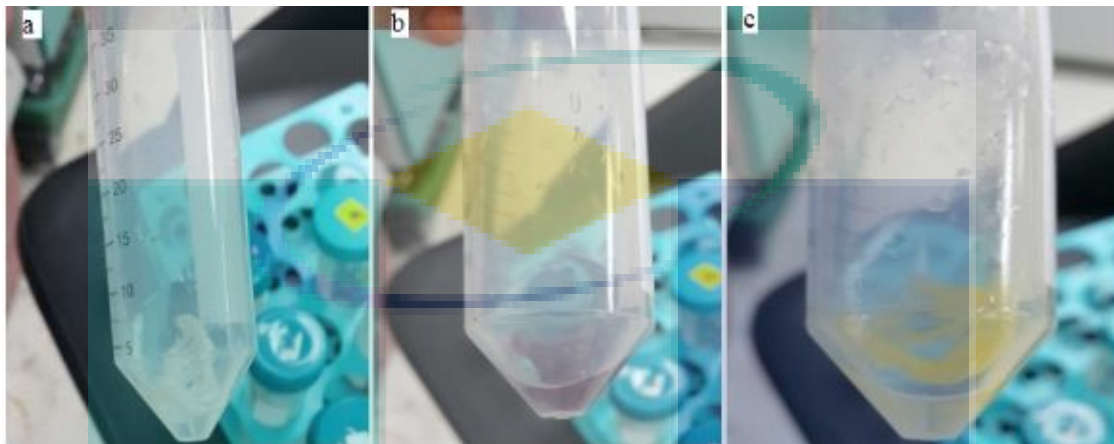


Appendix C 5: (a) Red Natural Dye from RDFP at Optimum Extraction Conditions, (b) Red Natural Dye in Cuvette for measuring absorbance before dyeing, (c) PBY, (d) BY in Red Natural Dye Solution, (e) BY in Red Natural Dye Solution was agitated in incubator shaker, and (f) Red Natural Dye in Cuvette for measuring absorbance after the dyeing process



Appendix C 6: (a) Yellow Natural Dye from Turmeric at Optimum Extraction Conditions, (b) Yellow Natural Dye in Cuvette for measuring absorbance before

dyeing, (c) PBY, (d) BY in Yellow Natural Dye Solution, and (e) Yellow Natural Dye in Cuvette for measuring absorbance after dyeing



Appendix C 7: (a) DBY (Red) was soaked in 25% Alum, (b) DBY (Blue) was soaked in 25% Alum, and (c) DBY (Yellow) was soaked in 25% Alum

UMP